

50 Copies

W

NATIONAL AERONAUTICS AND SPACE ADMINISTRATION

Technical Report 32-1210

Surveyor IV Mission Report
Mission Description and Performance

Prepared by the Surveyor Project Staff

468-10262

FACILITY FORM 602	(ACCESSION NUMBER)	(THRU)
	(PAGES)	(CODE)
	(NASA CR OR TMX OR AD NUMBER)	(CATEGORY)

125
CI-92762
31

JET PROPULSION LABORATORY
CALIFORNIA INSTITUTE OF TECHNOLOGY
PASADENA, CALIFORNIA

January 1, 1968

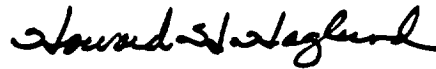
NATIONAL AERONAUTICS AND SPACE ADMINISTRATION

Technical Report 32-1210

Surveyor IV Mission Report
Mission Description and Performance

Prepared by the Surveyor Project Staff

Approved by:



H. H. Haglund
Surveyor Project Manager

J E T P R O P U L S I O N L A B O R A T O R Y
C A L I F O R N I A I N S T I T U T E O F T E C H N O L O G Y
P A S A D E N A , C A L I F O R N I A

January 1, 1968

TECHNICAL REPORT 32-1210

Copyright © 1968
Jet Propulsion Laboratory
California Institute of Technology
Prepared Under Contract No. NAS 7-100
National Aeronautics & Space Administration

Preface

This document constitutes the *Surveyor IV* Mission Report. It describes the fourth in a series of unmanned missions designed to soft-land on the moon and return data from the lunar surface. The report consists of a technical description and an evaluation of engineering results of the systems utilized in the *Surveyor IV* mission. The report is based on data evaluation prior to approximately September 1, 1967, and was compiled using contributions of many individuals in the major systems which support the Project. Some of the information for this report was obtained from other published documents; a list of these documents is contained in a bibliography.

The report for this mission consists of a single volume only. Premature termination of the *Surveyor IV* mission precluded the obtaining of scientific data and results which would normally be presented as separate parts of each Mission Report.

Contents

I. Introduction and Summary	1
A. Surveyor Project Objectives	1
B. Project Description	2
C. Mission Objectives	3
D. Mission Summary	4
II. Space Vehicle Preparations and Launch Operations	7
A. Spacecraft Assembly and Testing	7
B. Combined Systems Test at San Diego	9
C. Launch Operations at AFETR	10
D. Launch Phase Real-Time Mission Analysis	13
III. Launch Vehicle System	17
A. Atlas Stage	17
B. Centaur Stage	18
C. Launch Vehicle/Spacecraft Interface	19
D. Vehicle Flight Sequence of Events	21
E. Performance	23
IV. Surveyor Spacecraft	27
A. Spacecraft System	27
B. Structures and Mechanisms	45
C. Thermal Control	50
D. Electrical Power	52
E. Propulsion	54
F. Flight Control	61
G. Radar	71
H. Telecommunications	76
I. Television	86
J. Soil Mechanics/Surface Sampler	90
V. Tracking and Data System	93
A. Air Force Eastern Test Range	93
B. Goddard Space Flight Center	99
C. Deep Space Network	101

Contents (contd)

VI. Mission Operations System	111
A. Functions and Organization	111
B. Mission-Dependent Equipment	114
C. Mission Operations Chronology	118
VII. Flight Path and Events	123
A. Prelaunch	123
B. Launch Phase	123
C. Cruise Phase	124
D. Midcourse Maneuver Phase	125
E. Terminal Phase	134
F. Landing Site	135
Appendix A. Surveyor IV Mission Events	137
Appendix B. Surveyor IV Spacecraft Configuration	148
Appendix C. Surveyor IV Spacecraft Data Content of Telemetry Modes	151
Appendix D. Surveyor IV Spacecraft Temperature Histories	154
Glossary	163
Bibliography	164

Tables

II-1. Major operations at Cape Kennedy	11
III-1. <i>Atlas</i> propellant residuals	24
III-2. <i>Centaur</i> usable propellant residuals	24
IV-1. Surveyor IV spacecraft telemetry mode summary	33
IV-2. Surveyor IV instrumentation	34
IV-3. Notable differences between <i>Surveyors III</i> and <i>IV</i> : changes incorporated on Surveyor IV	35
IV-4. Surveyor spacecraft subsystem reliability estimates	35
IV-5. Surveyor IV maximum measured peak-to-peak acceleration, compared with data from <i>Surveyors I, II, and III</i>	42
IV-6. Predicted and actual main retro phase events	43
IV-7. Thermal compartment component installation	48
IV-8. Pyrotechnic devices	48

Contents (contd)

Tables (contd)

IV-9. Summary of power subsystem performance	54
IV-10. Vernier thrust levels during midcourse correction	58
IV-11. Flight control modes	62
IV-12. Surveyor IV star map results	64
IV-13. Optical errors	65
IV-14. Comparison of flight control parameters during main retro phase for Surveyor I, III, and IV missions	66
IV-15. Comparative AMR temperatures: Surveyors I, III, and IV	72
IV-16. Typical signal processing parameter values	84
V-1. AFETR configuration	94
V-2. Atlas/Centaur Mark Event readouts	99
V-3. GSFC network configuration	99
V-4. DSN tracking data requirements	102
V-5. Characteristics for S-band tracking systems	103
VI-1. CDC mission-dependent equipment support of Surveyor IV at DSIF stations	115
VI-2. Surveyor IV command activity prior to loss of spacecraft signal	116
VII-1. Surveyor IV encounter conditions based on premidcourse orbit determinations	129
VII-2. Midcourse correction alternatives comparison	135
VII-3. Pre-midcourse and post-midcourse injection and terminal conditions	136
A-1. Mission flight events	141

Figures

I-1. Earth-moon trajectory and nominal events	4
II-1. Surveyor IV undergoing vibration tests	9
II-2. Combined Systems Test Stand at San Diego	10
II-3. Encapsulation of Surveyor IV for J-FACT	11
II-4. Service tower removal prior to launch	14
II-5. Final Surveyor IV launch window design for July 1967	15
III-1. Atlas/Centaur/Surveyor space vehicle configuration	18
III-2. Surveyor/Centaur interface configuration	20
III-3. Launch phase nominal events	22

Contents (contd)

Figures (contd)

IV-1. Surveyor IV spacecraft in cruise mode	28
IV-2. Simplified spacecraft functional block diagram	29
IV-3. Spacecraft coordinates relative to celestial reference	30
IV-4. Surveyor spacecraft system reliability estimates	35
IV-5. Terminal descent nominal events	37
IV-6. Main retro phase sequence	38
IV-7. RADVS beam orientation	39
IV-8. Range-velocity diagram	39
IV-9. Launch-phase accelerometer location	41
IV-10. Landing leg assembly	46
IV-11. Antenna/solar panel configuration	47
IV-12. Thermal switch	49
IV-13. Thermal design	51
IV-14. Simplified electrical power functional block diagram	53
IV-15. Battery energy remaining	54
IV-16. Total battery discharge current	55
IV-17. Vernier propulsion system installation	56
IV-18. Vernier propulsion system schematic showing locations of pressure and temperature sensors	57
IV-19. Vernier engine thrust chamber assembly	58
IV-20. Vernier propulsion subsystem transit temperature ranges	59
IV-21. Main retrorocket motor	59
IV-22. Main retromotor thrust vs time	60
IV-23. Simplified flight control functional diagram	61
IV-24. Gas-jet attitude control system	62
IV-25. Critical flight control signal recordings during main retro phase	67
IV-26. Flight control data (final 6 sec)	69
IV-27. Vernier engine thrust commands during main retro phase (Surveyor III data also shown)	70
IV-28. Altitude marking radar functional diagram	71
IV-29. Simplified RADVS functional block diagram	73
IV-30. Reflectivity of RADVS beams during descent	75
IV-31. Received signal level of RADVS beams during descent	75

Contents (contd)

Figures (contd)

IV-32. RADVS lateral velocity component during descent	76
IV-33. Radio subsystem block diagram	77
IV-34. Omnantenna A/Receiver A signal level during Canopus acquisition roll	78
IV-35. Omnantenna A/Receiver A total received power during transit	79
IV-36. Omnantenna B/Receiver B total received power during transit	80
IV-37. DSIF total received power during transit	82
IV-38. DSS 11 recordings at time of loss of spacecraft signal	83
IV-39. Simplified signal processing functional block diagram	84
IV-40. Survey TV camera	85
IV-41. Simplified survey TV camera functional block diagram	87
IV-42. Camera response functions compared with CIE color matching functions	88
IV-43. TV photometric/colorimetric reference chart	88
IV-44. Surveyor IV camera 600-line light transfer characteristic for center of frame	89
IV-45. Surveyor IV camera 600-line light transfer characteristics at $f/4$ for all filter wheel positions	89
IV-46. Surveyor IV camera 200-line light transfer characteristic for center of frame	89
IV-47. Surveyor IV camera 600-line shading near saturation (diagram measured from Polaroid of composite frame)	90
IV-48. Surveyor IV camera 600-line frequency response for center of frame	90
IV-49. SM/SS deployment envelope	91
V-1. Earth tracks and TDS station coverage for July 14, 1967	94
V-2. AFETR C-band radar coverage: liftoff through Trinidad	96
V-3. AFETR C-band radar coverage: Ascension through Pretoria	96
V-4. AFETR VHF telemetry coverage: liftoff through RIS Coastal Crusader	97
V-5. AFETR VHF telemetry coverage: RIS Coastal Crusader through Pretoria	97
V-6. AFETR S-band telemetry coverage: liftoff through RIS Coastal Crusader	98
V-7. AFETR S-band telemetry coverage: RIS Coastal Crusader through Pretoria	98
V-8. MSFN VHF telemetry coverage	100
V-9. MSFN radar coverage	101
V-10. DSS 72 30-ft antenna system at Ascension	102
V-11. Station tracking periods	105
V-12. DSS received signal level	106
V-13. DSN/GCF communications links	108

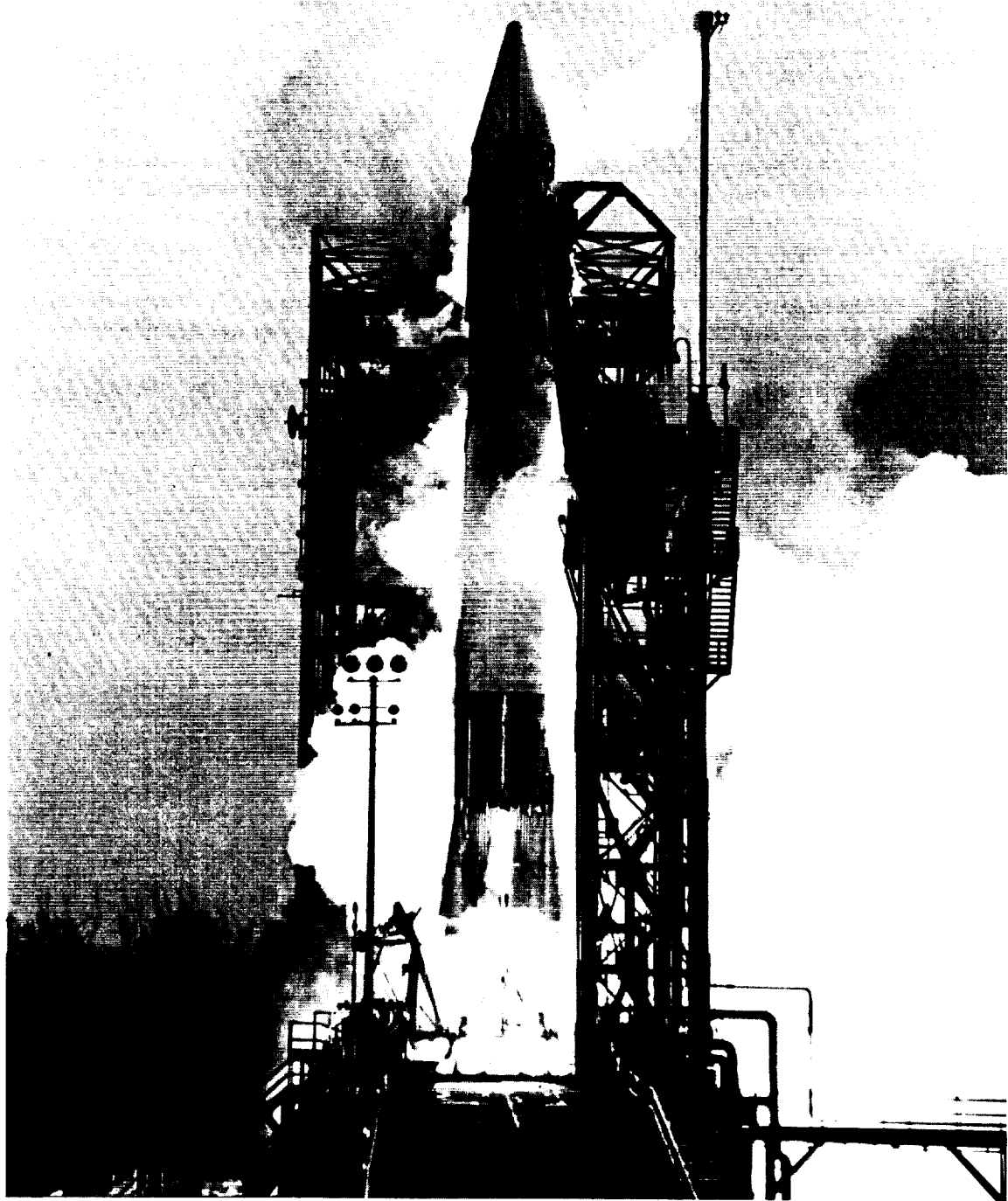
Contents (contd)

Figures (contd)

V-14. General configuration of SFOF data processing system	109
VI-1. Organization of MOS	112
VI-2. Surveyor IV telemetry bit rate/mode profile	119
VII-1. Surveyor IV and Centaur trajectories in earth's equatorial plane	125
VII-2. Surveyor IV earth track	126
VII-3. Surveyor IV target and uncorrected impact points	127
VII-4. Computed Surveyor IV pre-midcourse unbraked impact locations	128
VII-5. Surveyor IV landing location	131
VII-6. Midcourse correction capability contours in B -plane (for a midcourse correction 40 hr after injection)	132
VII-7. Effect of midcourse correction magnitude and execution time on lunar surface miss	133
VII-8. Effect of noncritical velocity component on terminal descent parameters	134
A-1. Operations conducted on July 17, 1967, in the attempt to reacquire Surveyor IV	139
A-2. Operations conducted on July 18, 1967, in the attempt to reacquire Surveyor IV	140
D-1. Landing gear temperatures	155
D-2. Compartment A temperatures	156
D-3. Compartment B temperatures	157
D-4. Vernier propulsion system temperatures	158
D-5. Main retromotor temperatures	160
D-6. Flight control temperatures	160
D-7. Radar temperatures	161
D-8. SM/SS temperatures	162
D-9. Television temperatures	162
D-10. Miscellaneous temperatures	162

Abstract

Surveyor IV, the fourth in a series of seven unmanned spacecraft designed to soft-land on the moon and return engineering and scientific data, was launched from Cape Kennedy, Florida, on July 14, 1967. A nominal launch phase and accurate injection were achieved, followed by a normal transit phase including a successful midcourse maneuver. However, during terminal descent, the *Surveyor IV* radio signal was lost abruptly just prior to expected main retro-motor burnout, only about 2½ min before predicted soft landing. When exhaustive attempts to reestablish radio communications were unsuccessful, the mission was terminated short of the attainment of the flight objectives. A thorough investigation conducted by a formally appointed Technical Review Board was unable to disclose any evidence of the cause for the failure. A technical description of the mission and an evaluation of engineering data obtained are presented herein.



I. Introduction and Summary

Surveyor IV was launched from Cape Kennedy, Florida, at 11:53:29.215 GMT on July 14, 1967. The *Atlas/Centaur* launch vehicle provided a very satisfactory injection into lunar transfer trajectory. A close to nominal mission was achieved through the coast phases, and a successful mid-course correction of 10.27 m/sec was commanded and executed about 38½ hr after launch, during the second Goldstone (California) view period. The automatic terminal descent sequence was initiated on July 17 about 62 hr after launch, and proceeded normally until the *Surveyor IV* radio signal was abruptly lost just prior to main retrorocket burnout when the spacecraft was 49,000 ft from the moon's surface and traveling 1070 ft/sec. Exhaustive attempts to reestablish telecommunications with *Surveyor IV* through July 18, 1967, were unsuccessful. A formally appointed Technical Review Board conducted a detailed examination of the *Surveyor IV* mission, but was unable to find evidence of any single or multiple cause for the failure.

A. Surveyor Project Objectives

The *Surveyor* Project is being conducted to explore the moon with unmanned, automated, soft-landing spacecraft

which are equipped to respond to earth commands and transmit back scientific and engineering data from the lunar surface. The overall objectives of the *Surveyor* Project are:

- (1) To accomplish successful soft landings on the moon as demonstrated by operations of the spacecraft subsequent to landing.
- (2) To provide basic data in support of *Apollo*.
- (3) To perform operations on the lunar surface which will contribute new scientific knowledge about the moon and provide further information in support of *Apollo*.

The first two *Surveyor* spacecraft carried a survey television camera in addition to engineering instrumentation for obtaining in-flight and postlanding data. As an additional instrument, *Surveyors III* and *IV* carried a soil mechanics/surface sampler (SM/SS) device to provide data based on picking, digging, and handling of lunar surface material. A magnet was also attached to one of the footpads of *Surveyor IV* to determine magnetic properties of the soil.

Surveyor I was launched on May 30, 1966, and soft-landed near the western end of the *Apollo* zone of interest at 2.45 deg south latitude and 43.21 deg west longitude (based on *Lunar Orbiter III* data). Operations on the lunar surface were highly successful. In addition to a wide variety of other types of lunar surface data, over 11,000 television pictures were received in the course of operations during the first two lunar days. *Surveyor I* exhibited a remarkable capability to survive eight lunar day and night cycles involving temperature extremes of +250 and -250°F.

Surveyor II was launched on September 20, 1966, and achieved a nominal mission until execution of the mid-course velocity correction. One of the three vernier engines did not fire, causing the spacecraft to tumble. Attempts to stabilize the spacecraft by repeatedly firing the verniers were unsuccessful. When nearly all the spacecraft battery energy had been consumed prior to lunar encounter, the mission was terminated shortly after firing of the main retromotor 45 hr after launch. A thorough investigation by a specially appointed Failure Review Board was unable to disclose the exact cause of failure. A number of recommendations were made to assure against a similar failure and to provide better diagnostic data on future missions.

Surveyor III was launched on April 14, 1967, and achieved a successful soft-landing although the spacecraft lifted off twice after initial touchdown before finally coming to rest. Based on correlation with *Lunar Orbiter III* photographs, the *Surveyor III* landing site is located in the Ocean of Storms at 2.94 deg south latitude and 23.24 deg west longitude, about 625 km east of the *Surveyor I* landing site. Important new data was obtained as a result of extensive postlanding operations with the SM/SS, television, and other spacecraft equipment. The lunar surface characteristics determined by *Surveyor III* confirm the findings of *Surveyor I* and indicate the suitability of an additional site for *Apollo*, which will utilize final descent and landing system technology similar to that of *Surveyor*.

None of the Project Objectives were achieved by the *Surveyor IV* mission, although the mission was very satisfactory until the abrupt and permanent loss of spacecraft signal during terminal descent.

B. Project Description

The *Surveyor* Project is managed by the Jet Propulsion Laboratory for the NASA Office of Space Science and

Applications. The Project is supported by four major administrative and functional elements or systems: Launch Vehicle System, Spacecraft System, Tracking and Data System (TDS), and Mission Operations System (MOS). In addition to overall project management, JPL has been assigned the management responsibility for the Spacecraft, Tracking and Data Acquisition, and Mission Operations Systems. NASA/Lewis Research Center (LeRC) has been assigned responsibility for the *Atlas/Centaur* launch vehicle system.

1. Launch Vehicle System

Atlas/Centaur launch vehicle development began as an Advanced Research Projects Agency program for synchronous-orbit missions. In 1958, General Dynamics/Convair was given the contract to modify the *Atlas* first stage and develop the *Centaur* upper stage; Pratt & Whitney was given the contract to develop the high-impulse LH₂/LO₂ engines for the *Centaur* stage.

The Kennedy Space Center, Unmanned Launch Operations branch, working with LeRC, is assigned the *Centaur* launch operations responsibility. The *Centaur* vehicle utilizes Launch Complex 36, which consists of two launch pads (A and B) connected to a common blockhouse. The blockhouse has separate control consoles for each of the pads. Pad 36A was utilized for the *Surveyor IV* mission.

A total of eight R&D flight tests were conducted in the *Centaur* vehicle program. The launch of *Atlas/Centaur* AC-11 on the *Surveyor IV* mission was the fourth operational use of an *Atlas/Centaur* vehicle. This mission and the first two operational flights (the successful launches of AC-10 and AC-7 on *Surveyors I* and *II*, respectively) utilized the "direct" ascent mode, wherein the *Centaur* second stage provides only one continuous burn to achieve injection into the desired lunar transfer trajectory. For *Surveyor* direct ascent missions, lunar declination must be less than approximately -14 deg, which occurs for a period of only about 8 days per month.

The third *Atlas/Centaur* operational flight (the successful launch of AC-12 on *Surveyor III*) utilized the "parking orbit" mode, which will also be used for the remaining *Surveyor* missions. In the parking orbit or indirect ascent mode, the *Centaur* stage burns twice. The first burn injects the vehicle into a temporary parking orbit with a nominal altitude of 90 nm. After a coast period of up to 25 min, the *Centaur* reignites and provides the additional impulse necessary to achieve a lunar intercept trajectory. The use of the parking orbit ascent mode permits the launching of *Surveyor* missions for all values of lunar declinations. This

allows the design of launch periods which are compatible with favorable postlanding lunar lighting.

2. Spacecraft System

Surveyor is a fully attitude-stabilized spacecraft designed to receive and execute a wide variety of earth commands, as well as perform certain automatic functions including the critical terminal descent and soft-landing sequences. Overall spacecraft dimensions and weight of 2200 to 2300 lb were established in accordance with the *Atlas/Centaur* vehicle capabilities. *Surveyor* has made significant new contributions to spacecraft technology through the development of new and advanced subsystems required for successful soft-landing on the lunar surface. New features which are employed to execute the complex terminal phase of flight include: a solid-propellant main retrorocket with throttlable vernier engines (also used for midcourse velocity correction), extremely sensitive velocity- and altitude-sensing radars, and an automatic closed-loop guidance and control system. The demonstration of these devices on *Surveyor* missions is a direct benefit to the *Apollo* program, which will employ similar techniques. Design, fabrication, and test operations of the *Surveyor* spacecraft are performed by Hughes Aircraft Company under the technical direction of JPL.

3. Tracking and Data System

The TDS system provides the tracking and communications link between the spacecraft and the Mission Operations System. For *Surveyor* missions, the TDS system uses the facilities of (1) the Air Force Eastern Test Range (AFETR) for tracking and telemetry of the spacecraft and vehicle during the launch phase, (2) the Deep Space Network (DSN) for precision tracking communications, data transmission and processing, and computing, and (3) the Manned Space Flight Network (MSFN) and the World-Wide Communications Network (NASCOM), both of which are operated by Goddard Space Flight Center.

The critical flight maneuvers and most television and SM/SS operations on *Surveyor* missions are commanded and recorded by the Deep Space Station (DSS 11) at Goldstone, California, during its view periods. Other stations which provided prime support for the *Surveyor IV* mission were DSS 42, near Canberra, Australia; DSS 51 at Johannesburg, South Africa; DSS 61, near Madrid, Spain; and DSS 72, at Ascension Island, which provided initial two-way acquisition and coverage during the first postinjection pass. Additional support, on a limited basis, was provided by DSS 71 (Cape Kennedy) during the pre-

launch phases, DSS 14 (with a 210-ft antenna at Goldstone) for backup to DSS 11 during the midcourse and terminal descent phases, and DSS 12 (Goldstone) for additional backup to DSS 11 during terminal descent.

4. Mission Operations System

The Mission Operations System essentially controls the spacecraft from launch through termination of the mission. In carrying out this function, the MOS constantly evaluates the spacecraft performance and prepares and issues appropriate commands. The MOS is supported in its activities by the TDS system as well as with special hardware provided exclusively by the *Surveyor* Project and referred to as mission-dependent equipment. Included in this category are the Command and Data Handling Consoles installed at each of the prime DSIF stations and at DSS 71, the Television Ground Data Handling System installed at DSS 11 (TV-11) and the SFOF (TV-1), and other special display equipment.

C. Mission Objectives

The objectives of the *Surveyor IV* mission, established before launch, were as follows:

- (1) Primary flight objectives:
 - (a) Perform a soft-landing on the moon at Sinus Medii,
 - (b) Obtain postlanding television pictures of the lunar surface.
- (2) Secondary flight objectives:
 - (a) Conduct a vernier engine experiment.
 - (b) Manipulate the lunar surface with the surface sampler in the view of the television camera.
 - (c) Obtain touchdown dynamics data.
 - (d) Obtain thermal and radar reflectivity data on the lunar surface.

For the *Surveyor IV* mission, a five-day launch period from July 13 through July 17, 1967, was selected which optimized the postlanding lunar lighting conditions at the selected landing site (within the limitations of launch vehicle capability) and satisfied the other mission constraints.

The launch and transit phases of the *Surveyor IV* mission were carried out as planned, with the full expectation of meeting all of the Flight Objectives. However, none of these objectives were achieved owing to the complete loss of the spacecraft radio signal just prior to

expected main retromotor burnout during terminal descent.

D. Mission Summary

Surveyor IV was launched by the *Atlas/Centaur* AC-11 vehicle on July 14, 1967, the second day of the selected launch period, from Pad 36A at Cape Kennedy. Launch was not attempted on the first day of the period, July 13, because of an electrical connector problem which developed in the *Centaur* propellant utilization system. After a momentary hold called 39 sec before liftoff to complete liquid hydrogen topping, liftoff ($L + 00:00$) occurred at 11:53:29.215 GMT, only 29 sec after opening of the window. All events occurred as planned during the direct-ascent boost on a 103.82-deg azimuth, and the spacecraft was injected into a very accurate lunar transfer trajectory. The uncorrected lunar impact point was approximately 176 km from the targeted point in Sinus Medii. The earth-moon trajectory and major events are depicted in Fig. I-1.

Following spacecraft separation, the *Centaur* performed a required retromaneuver sequence to provide increased separation distance from the spacecraft and to miss the moon. After separation, the spacecraft properly executed the automatic antenna/solar panel positioning and sun acquisition sequences. These sequences established the desired attitude of the spacecraft roll axis and ensured an adequate supply of solar energy during the coast period.

Tracking and telemetry data received in one-way lock by stations of the AFETR, MSFN, and DSIF confirmed a normal mission during the near-earth portion of flight. As planned, DSS 72 was the first station to establish two-way lock and exercise control of the spacecraft by command. Thereafter, the DSIF stations provided nearly continuous two-way coverage of the flight, receiving and recording spacecraft data and transmitting commands.

Spacecraft lock-on with the star Canopus was achieved according to plan about 6 hr after launch. This provided 3-axes attitude reference, which is required before the midcourse and terminal maneuvers can be executed.

Spacecraft system performance during the transit-coast phases was excellent. Additional gyro drift checks were conducted because the indicated gyro drift rates were near the specification limit of 1.0 deg/hr, but this condition had no adverse effect on the flight because the terminal maneuvers were compensated for the measured drift rates.

In order to improve the landing site accuracy, the *Surveyor IV* mission profile was altered from that of previous missions to perform the midcourse correction during the second rather than the first "pass" over DSS 11, Goldstone. A roll-yaw maneuver sequence was conducted in preparation for midcourse velocity correction. Then, about 38½ hr after launch, at 02:30 GMT on July 16, 1967, a velocity correction of 10.27 m/sec was commanded. Shortly after the velocity correction, which corrected the

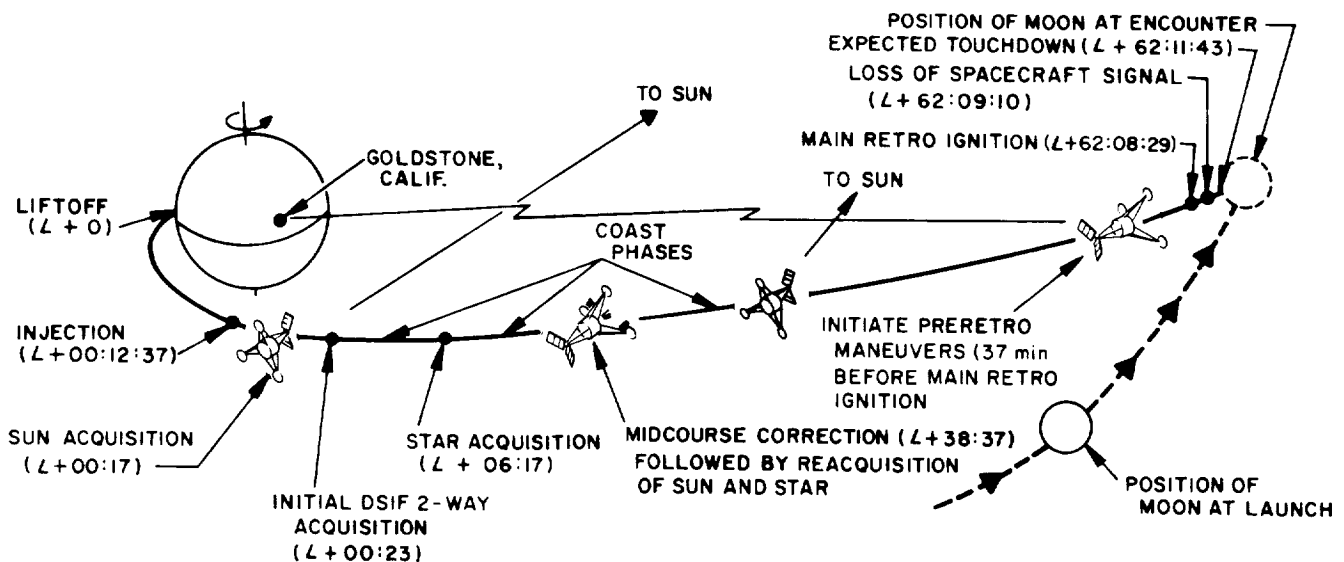


Fig. I-1. Earth-moon trajectory and nominal events

miss distance to within 8.6 km of the aim point, the spacecraft was returned to the coast orientation with sun and Canopus lock by execution of the reverse yaw and roll maneuvers.

In preparation for terminal descent, a roll-yaw-roll maneuver sequence was initiated 38 min before retro ignition. This aligned the retrorocket nozzle and established the desired spacecraft roll attitude, within the RADVS constraints, for postlanding operations. The roll-yaw-roll sequence was selected to optimize telecommunication performance with Omnantenna B.

When the spacecraft was 60 miles slant range from the lunar surface, the automatic descent sequence was initiated successfully by a *mark* signal from the spacecraft altitude marking radar. After a delay of 2.7 sec, the three liquid-propellant vernier engines ignited, followed (after an additional 1.1-sec delay) by ignition of the solid-propellant main retromotor.

The retro descent appeared satisfactory until the spacecraft radio signal was lost abruptly at 02:02:41 GMT on July 17, 1967. The spacecraft signal ceased 41.09 sec after main retromotor ignition or about 1.4 sec before predicted retromotor burnout. At that time the spacecraft

was 49,000 ft above the moon's surface and was traveling 1070 ft/sec. Attempts were made to reestablish radio contact by using every feasible operational technique including commanding the spacecraft to all possible operational modes. This effort was continued until July 18, 1967, when the mission was terminated. The current estimate of the site to which *Surveyor IV* was descending for a soft landing is in Sinus Medii at 0.43 deg north latitude and 1.61 deg west longitude.

A thorough investigation has been conducted by a formally appointed Technical Review Board to identify the cause of the spacecraft malfunction. All possible failure modes were examined. However, with the direct evidence available, the Board has been unable to identify any single or multiple cause for the *Surveyor IV* mission failure. Spacecraft telemetry indicated nominal performance up to the time that carrier, subcarrier, and telemetry signals were abruptly lost. The lack of direct evidence concerning the cause of signal loss is related to the complete absence of spacecraft data following the loss, as well as the inability to extract signal loss transient characteristics that might have provided information pertaining to mechanical or voltage supply transients prior to complete loss of signal. The Board concluded that the *Surveyor IV* failure appeared to be of sufficiently low probability not to warrant any significant spacecraft change.

PRECEDING PAGE BLANK NOT FILMED.

II. Space Vehicle Preparations and Launch Operations

The *Surveyor IV* spacecraft was assembled and system flight-acceptance tests were conducted at the Hughes Aircraft Corporation facility, El Segundo, California. After completion of these tests, the spacecraft was shipped to the Combined System Test Stand (CSTS) at San Diego, on April 13, 1967, for compatibility tests with the *Atlas/Centaur* (AC-11) launch vehicle. Spacecraft/launch vehicle compatibility was verified and the spacecraft was airlifted to the Air Force Eastern Test Range (AFETR), Cape Kennedy, arriving on April 24, 1967. The *Atlas/Centaur* launch vehicle stages arrived at AFETR on April 29 and May 5, 1967, respectively. Prelaunch assembly, checkout, and systems tests were performed successfully at AFETR, and launch was accomplished on July 14, 1967 at 11:53:29.215 GMT, 29.215 sec after opening of the launch window on the second day of the launch period.

A. Spacecraft Assembly and Testing

Tests and operations on each spacecraft are conducted by a test team and data analysis team which work with the spacecraft throughout the period from the beginning of testing until launch. The test equipment used to con-

trol and monitor the spacecraft system performance at all test facilities includes (1) a system test equipment assembly (STEA) containing equipment for testing each of the spacecraft subsystems, (2) a command and data handling console (CDC) similar to the units located at the DSIF stations (see Section VI) for receiving telemetry and TV data and sending commands, and (3) a computer data system (CDS) for automatic monitoring of the spacecraft system. Automatic monitoring capability is necessary because of the large number of telemetered data points and high sampling frequency of most of the *Surveyor* telemetry modes. The CDS provides the following features to aid the data analysis personnel in evaluating the spacecraft performance:

- (1) Digital magnetic tape recording of all input data.
- (2) Suppression of nonchanging data. Only data points which reflect a change are printed on display devices.
- (3) Alarm limit capability. Critical telemetry functions are monitored for out-of-tolerance indications which would be damaging to the spacecraft. An audible alarm sounds if these limits are exceeded.

- (4) Request message. In the event that telemetry data is desired for evaluation, a print of requested data is provided.

1. Spacecraft Ambient Testing

The ambient testing phase consists of initial systems checkout (ISCO) and mission sequence tests. In the initial systems checkout, each subsystem is tested for compatibility and calibration with other subsystems and a systems readiness test is performed for initial systems operational verification. This phase was accomplished by October 10, 1966.

The primary objectives of the mission sequence (MS) tests are to obtain system performance characteristics of the spacecraft under ambient conditions and in the electromagnetic (EM) environment expected on the launch pad and in flight prior to separation from the *Centaur*. First, the *Surveyor IV* spacecraft was commanded through two compressed (32-hr) mission sequence runs without the expected launch pad EM environment. Then, a systems readiness test (SRT) was performed with an EM source to verify functional compatibility of the spacecraft with the expected EM environment. The SRT was followed by a complete "plugs-out" mission sequence approaching flight configuration with simulated EM environment.

The ambient phase of testing was accomplished by October 28, 1966. Anomalies which occurred during this test period included: low current readings from the engineering signal processor (ESP), failure of the auxiliary engineering signal processor (AESP), transmitter degradation, and out-of-tolerance altitude marking radar (AMR) marking accuracy. Radar altimeter and doppler velocity sensor (RADVS) antenna alignment and antenna/solar panel positioner (A/SPP) calibration were performed and the MS/EM anomalies were corrected and verified by retest prior to initiation of solar-thermal-vacuum (STV) testing. In addition, several changes recommended by the *Surveyor II* Failure Review Board were incorporated.

2. Solar-Thermal-Vacuum Testing

The STV testing is performed to verify correct spacecraft functional operations and thermal performance during mission sequences in which the spacecraft is exposed to a range of solar conditions in a simulated STV environment. In these tests as well as in the vibration test phase which follows, the propellant tanks are loaded with "ref-

eree" fluids to simulate flight weight and thermal characteristics. Prior to *Surveyor IV*, STV testing was performed beginning with a low-temperature, nominal-sun-intensity mission sequence phase. In the *Surveyor IV* STV testing which began on December 8, 1966, the order of low- and high-temperature phases was reversed to provide for initial testing of the main battery under high solar intensity.

The first STV mission sequence (Phase A) was performed at 112% of nominal sun (high temperature) and was successful except for a few minor problems: the uplink was intermittent several times using Transponder B and transmitting with low power in telemetry Mode 5 at 550 bit/sec; the AMR electronics temperature ran hotter than predicted (silver flakes in epoxy are believed to have caused shorting to the AMR case); and several TV mirror *close* commands were missed.

Additional problems occurred during the second TV mission sequence (Phase B), which was performed at 87% of nominal sun (low temperature). Transponder B uplink frequency was noted to have a 54-kHz shift from center; vernier engine Line 2 and 3 temperatures were lower than desired; the duty cycle on vernier engine Line 2 heater was higher than predicted; and a transponder out-of-lock problem occurred. Nevertheless, the test was considered successful and the spacecraft was removed from the vacuum chamber for upgrading and correction of the test anomalies. During this period, repeated failures of the auxiliary battery temperature sensor occurred. Grounding of the auxiliary battery box to the spacecraft corrected the problem by preventing discharge of static electricity from the auxiliary battery box to the affected telemetry channel.

Because of the return of *Surveyor III* to El Segundo for retesting, *Surveyor IV* STV Phase C preparations were interrupted on December 29 and the schedule was revised to perform additional upgrading and weight, balance and alignment operations normally conducted after Phase C testing.

Phase C, which was conducted with plugs out at 100% of nominal sun (nominal temperature), was successful, with only the following minor problems: failure of the TV mirrors to respond to several commands; Transmitter B output power drop at elevated temperature; and RADVS Beams 1 and 2 breaklock between 20 to 30 ft during terminal descent. Since the problems were minor and capable of subsequent correction, consent was

granted to proceed with the next test phase. The STV phase was completed on March 1, 1967.

3. System Vibration Testing

Vibration tests are conducted in the three orthogonal axes of the spacecraft to verify proper functional operation during and after exposure to a simulated launch vibration environment. For these tests the spacecraft is placed in the launch configuration, with legs and omniantennas in the folded position (Fig. II-1). In addition, a vernier engine vibration (VEV) test is conducted, with vibration input at the vernier engine mounting points to simulate the environment during the midcourse maneuver and terminal descent phases of flight. These tests verify that the RADVS beams will not produce a false lock as a result of vernier engine vibration. Pre- and post-vibration alignment is performed to verify that spacecraft subsystem alignments are not significantly degraded by exposure to vibration levels. The *Surveyor IV* vibra-



Fig. II-1. *Surveyor IV* undergoing vibration tests

tion test phase began on March 18, 1967, with the Z-axis test and was completed by March 21, 1967. The only significant discrepancy was the excessive phase jitter (52 deg) on Transmitter A when vibration was applied normal to Leg 3. The post-vibration alignment was completed on March 27 with no significant degradation noted. VEV testing was completed on April 7, and after transport preparations, the spacecraft was shipped by van to the Combined System Test Stand in San Diego on April 13, 1967.

B. Combined Systems Test at San Diego

The Combined Systems Test (CST) is performed to demonstrate electrical and mechanical compatibility of the *Surveyor/Atlas/Centaur* and ground support equipment (GSE) during a simulated countdown and flight. The configuration for the tests is shown in Fig. II-2. Following successful completion of factory checkout and acceptance testing of each stage, the *Atlas* was installed in its horizontal test position on December 16, 1966, followed by erection of the *Centaur* in the adjoining test tower on March 13, 1967.

After arrival at the CSTS on April 13, 1967, the *Surveyor IV* spacecraft proceeded through receiving, inspection, assembly and checkout with the STEA with no significant problems. The spacecraft was then mated to the *Centaur* forward adapter and a System Readiness Test (SRT) was performed to verify the integrity of the spacecraft telemetry system prior to encapsulation. On April 19, the spacecraft was encapsulated within the nose fairing, mated to the *Centaur*, and another spacecraft SRT was performed. The CST was performed on April 20, 1967. During the test, there was no indication that the squib mufflers (used to simulate release of the spacecraft omniantennas and landing legs) had been activated by *Centaur* programmer command. An additional *Centaur* programmer test was run, and correct operation of the programmer was verified. After the spacecraft was demated and decapsulated on April 20, the problem was traced to incorrect installation and adjustment of the microswitches which indicate firing of the squib mufflers. Consent to proceed was obtained, and the spacecraft was then prepared for shipment, transported by van to Los Angeles, and airlifted to AFETR, arriving on April 24, 1967.

Minor launch vehicle modifications and replacements were completed and the *Atlas* was shipped by air to AFETR, arriving on April 29, 1967. The nose fairing and interstage adapter arrived on May 1, followed by the *Centaur* on May 5, 1967.

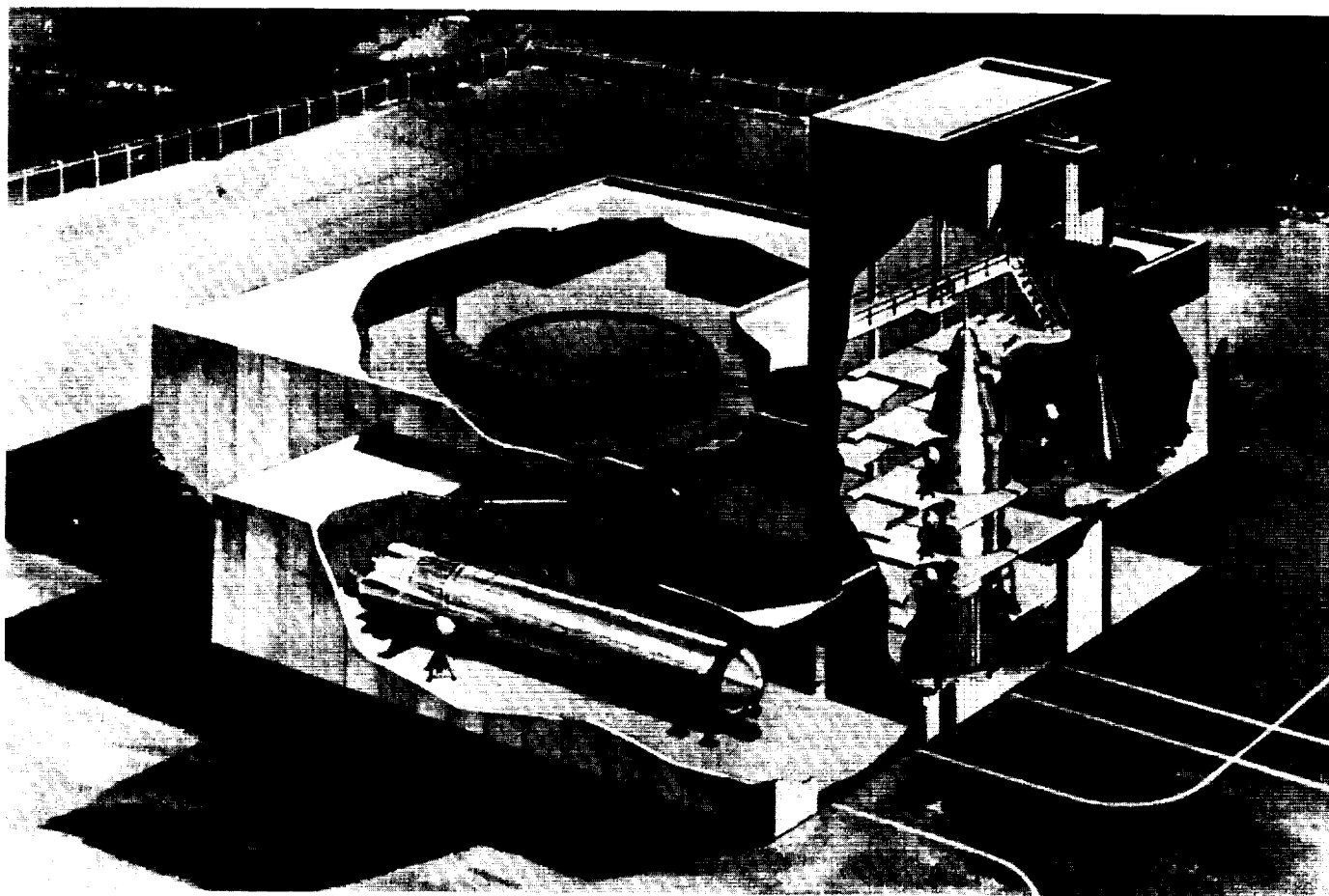


Fig. II-2. Combined Systems Test Stand at San Diego

C. Launch Operations at AFETR

The major operations performed at AFETR, after arrival of the launch vehicle and the spacecraft, are listed in Table II-1.

1. Initial Preparations

The *Atlas* and *Centaur* stages of AC-11 were erected on Launch Pad 36A on May 3 and May 6, 1967, respectively. All required launch vehicle operations preliminary to mating of the spacecraft and performance of the Joint Flight Acceptance Composite Test (J-FACT) were culminated with a successful guidance/autopilot (GAP) test on May 26.

Following receiving, inspection, and assembly of the spacecraft at Hangar AO on April 24, 1967, a series of Performance Verification Tests (PVT 1-4) were performed to check for degradation as a result of shipment. The JPL TV calibration test and soil mechanics/surface

sampler (SM/SS) checkout were also performed in this time period. Many problems with the flight control sensor group (FCSG) during acceptance tests resulted in the unit's being shipped back to El Segundo for repair. This made it necessary to perform the TV verification tests prior to PVT 3 before return of the FCSCG. Another major problem during this test phase was caused by the RADVS Beam 2 noise level being out of specified limits. Because of this, the RADVS antenna was removed and shipped back to Ryan Aeronautical Company for analysis. The problem was found to be due to several bad solder joints. The unit was repaired and reinstalled on the spacecraft.

Following testing at the Hangar AO Spacecraft Checkout Facility (SCF), which was concluded on May 24, the spacecraft was moved to the Explosive Safe Facility (ESF) where it was prepared for J-FACT operations on the launch pad. The spacecraft was built up to a flight configuration except for dummy retromotor, shock absorbers and AMR, referee fluids instead of liquid propellants, and leg and omniantenna deploy squibs in

Table II-1. Major operations at Cape Kennedy

Operation	Location	Date completed, 1967
AC-11 ^a erection (<i>Centaur</i> stage)	Launch Complex 36A	May 6
SC-4 ^b inspection, reassembly, initial checkout	Building AO	May 6
SC-4 vernier engine spacecraft functional test	Building AO	May 9
SC-4 SM/SS tests	Building AO	May 13
SC-4 TV system test and calibration	Building AO	May 14
SC-4 preparations for Joint Flight Acceptance Composite Test (J-FACT)	Explosive Safe Facility (ESF)	May 29
SC-4 mate to <i>Centaur</i>	Launch Complex 36A	May 31
AC-11/SC-4 J-FACT	Launch Complex 36A	June 2
DSS 71/SC-4 compatibility test	Launch Complex 36A	June 3
SC-4 demate	Launch Complex 36A	June 3
SC-4 decapsulation, depressurization, removal of J-FACT items and initial alignment	Explosive Safe Facility	June 9
AC-11 Flight Acceptance Composite Test (FACT) without SC-4 (first)	Launch Complex 36A	June 12
SC-4 Performance Verification Test (PVT) 5 mission sequence	Building AO	June 16
AC-11 propellant tanking test (first)	Launch Complex 36A	June 21
SC-4 vernier system pressure leak test	Explosive Safe Facility	June 21
SC-4 propellant loading	Explosive Safe Facility	June 23
AC-11 propellant tanking test (second)	Launch Complex 36A	June 27
AC-11 FACT without SC-4 (second)	Launch Complex 36A	June 30
SC-4 final weight, balance, and alignment	Explosive Safe Facility	July 1
AC-11 Composite Readiness Test (CRT)	Launch Complex 36A	July 7
SC-4 encapsulation and Systems Readiness Test (SRT)	Explosive Safe Facility	July 8
SC-4 final mate to <i>Centaur</i>	Launch Complex 36A	July 9
Launch	Launch Complex 36A	July 14

^aAtlas/*Centaur* vehicle designation.
^b*Surveyor IV* spacecraft designation.

mufflers. After the spacecraft was mated to the forward adapter, the helium and nitrogen tanks were pressurized to flight-level pressures, the spacecraft was encapsulated (Fig. II-3), and an SRT was performed.

2. Flight Acceptance Composite Tests and Launch Vehicle Propellant Tanking Tests

The *Surveyor IV* spacecraft was transported from the ESF to Launch Pad 36A and mated to the *Centaur* on May 31, 1967, in preparation for the J-FACT. An RF link

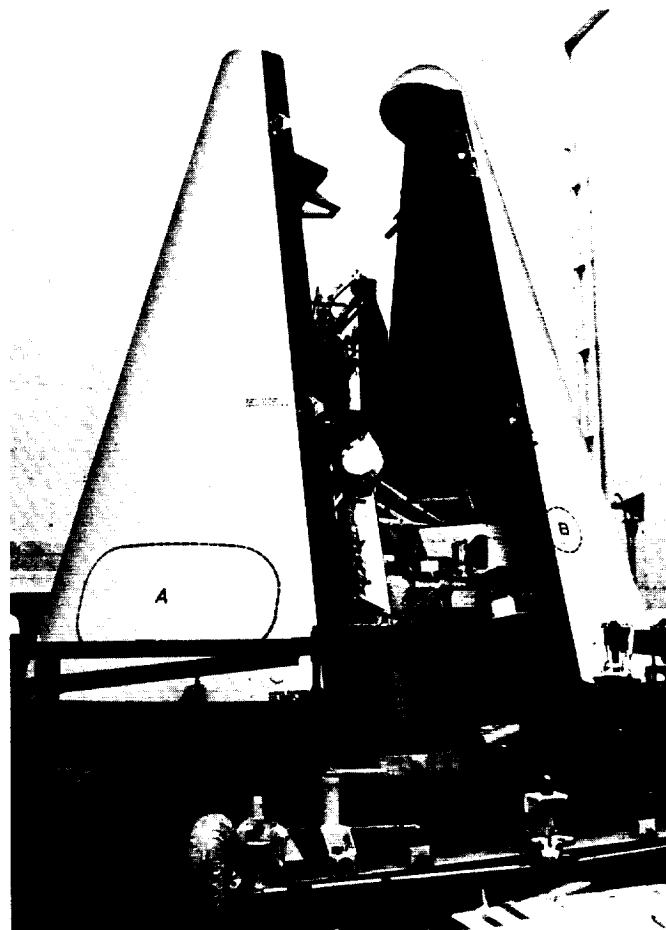


Fig. II-3. Encapsulation of Surveyor IV for J-FACT

optimization test and an SRT were performed, independent of the launch vehicle, after the spacecraft was mated to the *Centaur* to verify proper operation of the spacecraft and GSE. On June 1, an integrated launch control test to check out the vehicle countdown sequence was conducted, followed by a portion of a DSS 71 compatibility test with the spacecraft. The second portion of the DSS 71 compatibility test was performed following J-FACT because of AFETR support commitments. The J-FACT was performed satisfactorily on June 2. This test, involving all systems, covered launch through spacecraft separation and *Centaur* retro maneuver. Spacecraft/*Centaur* separation was simulated by manually disconnecting the adapter field joint electrical connector.

During the J-FACT, between T-120 and T-55 min in the countdown, a launch vehicle electromechanical interference (EMI) test was conducted. The purpose of this test is to verify spacecraft electrical compatibility with the launch complex and vehicle propellant storage and handling systems in lieu of a cryogenic tanking operation.

The EMI test was successfully completed without any observed anomalies or interference with spacecraft telemetry. In addition, *Surveyor* air-conditioning switchover to the standby unit was exercised.

An unprogrammed 12-sec hold occurred at *T*-2 min in the J-FACT countdown, resulting from a delay in receipt of confirmation that the *Surveyor* arm enable was activated. A communications headset failure caused this delay. Another anomaly, a premature launch release indication, was caused by incorrect logic on the second-stage engine control panel. Owing to the premature release indication, the event recorders were not running at a fast speed and some measurement accuracy was sacrificed. The engine panel logic was corrected and verified, and accurate event recorder data was obtained during subsequent tests.

After on-pad calibration of the spacecraft RF system with the service tower in the launch position (removed) and replaced, *Surveyor IV* was demated from the *Centaur* and returned to the ESF on June 3.

Following the J-FACT, two *Atlas/Centaur* Flight Acceptance Composite Tests (FACT) and two vehicle propellant tanking tests were performed without the spacecraft. The first test was a modified FACT performed on June 12 primarily as an overall test of the interface between the computerized controlled launch system (CCLS), located in the blockhouse, and the airborne guidance system. A normal launch release sequence was obtained which verified correction of the engine control panel logic.

Next, the first of two *Atlas/Centaur* flight control and propellant tanking tests was conducted on June 21. Problems encountered during the test included: a nonoperative liquid nitrogen (LN₂) rapid-fill solenoid valve which supplies LN₂ to the *Atlas* booster helium bottle; improper operation of the *Centaur* hydrogen vent valve; indications of erratic outputs from the *Atlas* booster engine pitch channels; and inconsistent radar readouts of the C-band beacon. The defective LN₂ solenoid valve was bypassed for the test and later corrected by repair of a bad wiring splice. The hydrogen vent valve, C-band beacon, and a questionable *Centaur* propellant utilization valve electronics package (PUVEP) were replaced. Several other equipment changes were made prior to the second tanking test including replacement of a leaking *Atlas* liquid oxygen start tank relief valve, repair and recalibration of the flight computer, and replacement of a nonlinear hydrogen tank ullage pressure transducer.

Centaur umbilical P401 was determined to contain moisture which was permitting a voltage leak between the pins. The umbilical cable was replaced and all other umbilicals were examined for moisture and corrective action taken where necessary.

During the second tanking test performed on June 27, a delay occurred when the service tower electrical brake release system malfunctioned during removal. During this test, the C-band beacon readouts were again intermittent. However, the problem was determined to be associated with the radar van location and the antenna pattern. Test results indicated a satisfactory test, and the vehicle was detanked and prepared for the second FACT test, which was successfully performed on June 30.

3. Final Flight Preparations

Following J-FACT, spacecraft operations at the ESF included (1) decapsulation, (2) depressurization, (3) a blowout test of the vernier engine purge plugs, and (4) initial alignment. During depressurization, a calibration was performed on the helium and nitrogen pressure transducers. Vernier propellant Line 2 was inadvertently bent while the main battery was being removed and was replaced. Alignment was completed on June 9, and the spacecraft was transported to the SCF for PVT 5, in which all critical functions are checked in a final spacecraft systems test.

On June 19, the spacecraft was returned to the ESF and placed in the Propellant Loading Building for solvent loading, high-pressure leak check, bladder leak check, and propellant loading. The spacecraft was then transferred to the final assembly building for thermal control coating touch-up, cleaning, weight and balance, and alignment checks. Specific steps of PVT 6 were phased in with the final preparation sequence, which included installation of the main retromotor and pyrotechnic devices.

After the spacecraft was mated to the forward adapter, the helium and nitrogen tanks were pressurized to flight level and the spacecraft was given final inspection and cleaning. The spacecraft was encapsulated within the nose fairing, and an SRT was performed on July 8. During the SRT, the vernier engine strain gage readings did not agree with data from PVT 6 calibration. This anomaly was accepted, as it was determined to have been caused by prestressing of the vernier engine mountings during the purge plug blowout tests. A launch vehicle Composite Readiness Test (CRT) had been run successfully on

July 7 as a final check on vehicle systems, and the spacecraft was moved to the launch pad and mated to the *Centaur* on July 9.

Final spacecraft and launch vehicle checks began immediately after the spacecraft was mated. An RF link optimization, an SRT and practice countdown, and retro-motor safe and arm checks were performed on the spacecraft. The vernier engine strain gage readings still exhibited an apparent shift, and the 200-line TV pictures of the nose fairing test target showed evidence of low-frequency coherent noise modulation. The TV picture noise was traced to two 400-Hz generators in the block-house.

During launch vehicle ordnance installation and loop resistance checks on July 11, the *Atlas* oxidizer tank in-flight pressurization valve was found to have a faulty squib and was replaced with an X-rayed assembly. Also, the *Surveyor* safe and arm device assembly sustained damage during fit checks and was replaced. Following a normal *Atlas* fuel tanking operation on July 11, a manometer leak was discovered and the vehicle was dented to permit installation of a spare manometer system. Retanking was accomplished on July 12. Erratic *Centaur* propellant utilization (PU) valve operation was noted during checks of the PU system. Troubleshooting isolated the problem to a loose connector at the top of the *Centaur* hydrogen tank. Since the connector was inaccessible with the spacecraft mated, it was decided to demate the spacecraft, examine and tighten the connector, and attach a grounding strap. The spacecraft was suspended in the service tower while the corrective action was accomplished, then remated and the interface revalidated. Correction of the *Centaur* PU system problem prevented a launch attempt on the first day of the launch period, and the launch countdown was rescheduled to begin on the evening of July 13, 1967.

4. Countdown and Launch

The final spacecraft SRT began at 23:15 GMT on July 13 at a countdown time of $T-680$ min and was completed at $T-435$ min. The spacecraft joined the launch vehicle countdown during the scheduled 60-min hold, which started at $T-90$ min. Roll-back of the service tower (Fig. II-4) was also completed during the 60-min hold. The countdown then proceeded normally down to the scheduled 15-min hold at $T-5$ min. During the countdown, the following problems occurred but did not require unscheduled holds. A 14-db difference was noted in spacecraft Receiver A signal strength over that obtained during J-FACT; however, a receiver indexing and

no-signal check verified satisfactory receiver sensitivity. A leak was detected in a disconnect cap in the *Centaur* hydrogen peroxide system and the cap was replaced. The GSE coder device for the *Centaur* PU system became erratic because of overheating and was replaced. Also, a GSE problem caused a slight delay in acceptance of the pitch and yaw steering program by the *Centaur* guidance computer.

The countdown was resumed as scheduled at the end of the 15-min hold and proceeded down to $T-39$ sec, when a momentary hold of 29 sec was called to complete liquid hydrogen topping. Liftoff occurred at 11:53:29.215 GMT on July 14, 1967, on a flight azimuth of 103.82 deg.

The countdown included a total of 75 min of planned, built-in holds (the one of 60 min duration at $T-90$ min and the one of 15 min duration at $T-5$ min). A 37-min launch window was available for July 14, extending from 11:53 to 12:30 GMT, 29.315 sec of which was consumed by the unscheduled hold of 29 sec at $T-39$ sec.

All vehicle systems performed satisfactorily throughout the powered phase of flight, and the spacecraft was accurately injected into a lunar transfer trajectory. The *Centaur* burn time was 5 to 6 sec longer than expected, but this was well within tolerance and had no detrimental effect on the mission. Damage to Launch Complex 36A was unusually light. The powered flight sequence of events and launch vehicle performance are described in Section III.

The atmospheric conditions during the launch were favorable, with fair visibility. Surface winds were 6 knots from 200 deg. Surface temperature was 76.6°F, with a relative humidity of 94% and a dewpoint of 75°F. Sea level atmospheric pressure was 1015.4 millibars. The cloud cover was 4/10 stratus at 800 ft, 6/10 altocumulus at 14,000 ft, and 3/10 cirrus at 30,000 ft. The maximum expected wind shear parameter was 11 ft/sec per thousand feet of altitude, occurring between 41,000 and 42,000 ft from 180 deg.

D. Launch Phase Real-Time Mission Analysis

The launch windows which were finally established for the July 1967 launch period are shown in Fig. II-5. Although considerable effort was applied to extending the window length on the first day (July 13) because of its small duration, this day was later scrubbed because of a loose connector in the *Centaur* propellant utilization system.

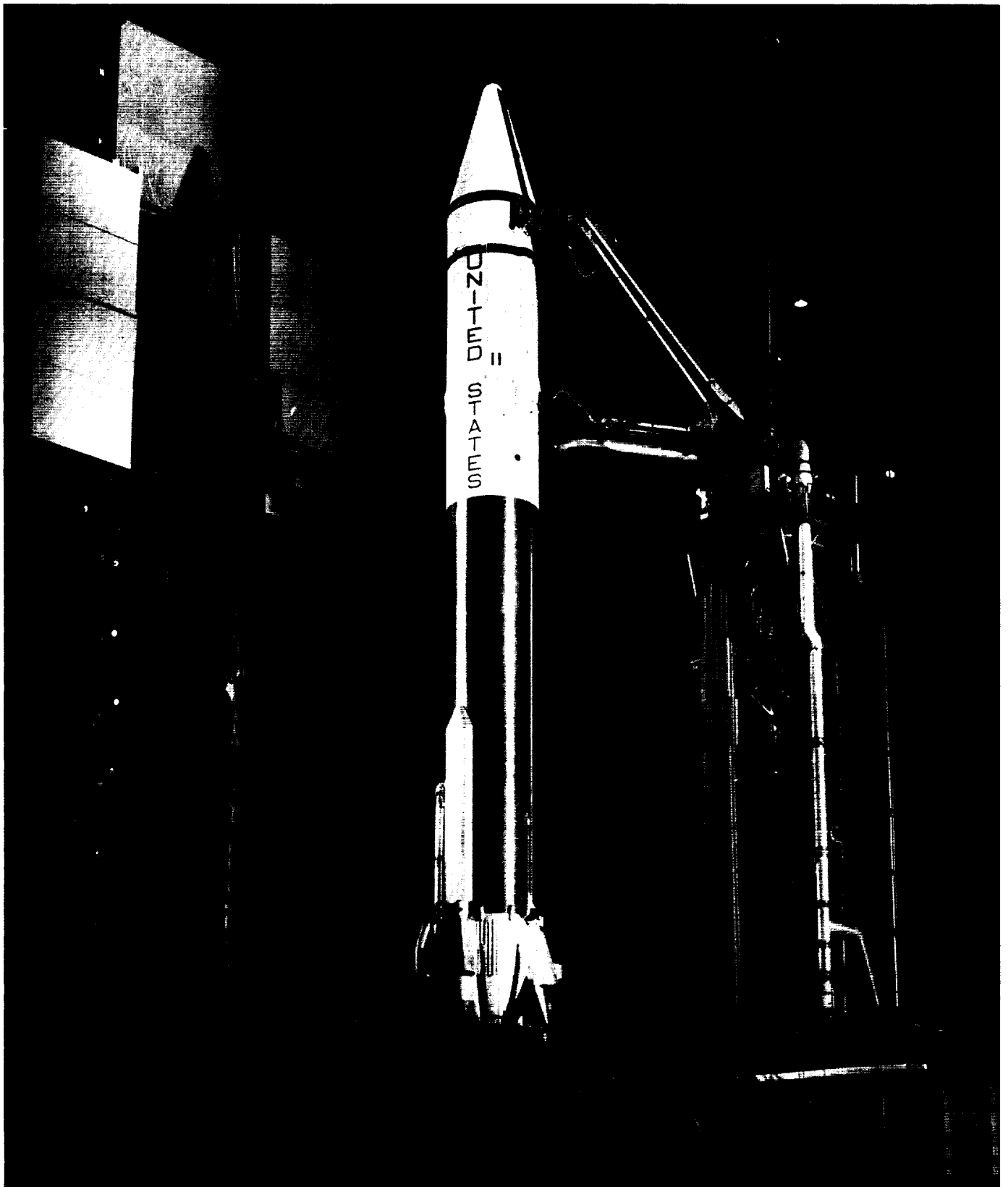


Fig. II-4. Service tower removal prior to launch

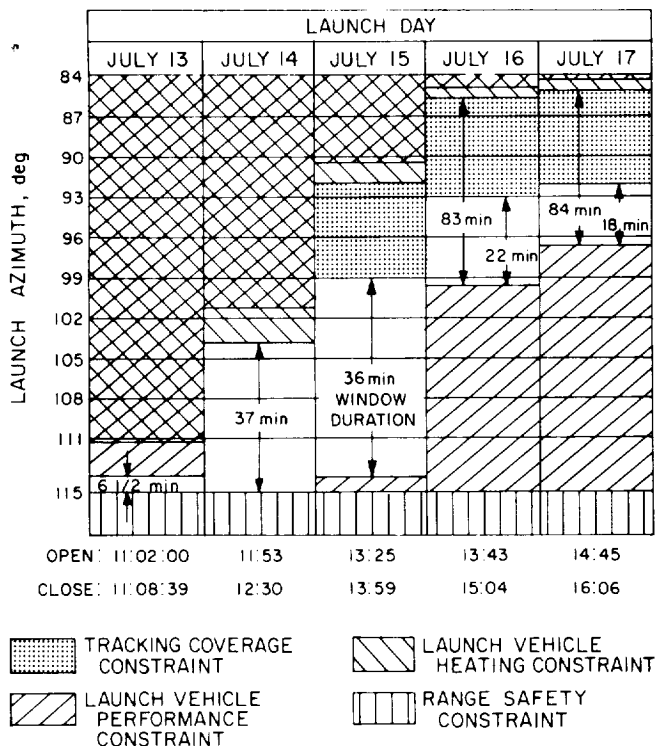


Fig. II-5. Final Surveyor IV launch window design for July 1967

The "launch vehicle performance constraint" on the windows for July 14 through 17 was based upon a requirement that there be a minimum excess *Centaur* propellant weight of 235 lb to cover possible launch vehicle performance dispersions. For July 13, this requirement was reduced to 205 lb to extend the available window on that day only.

The "launch vehicle heating constraint" was based upon a heating rate limitation for the base of the *Atlas* sustainer stage which imposed a restriction on the pitch rate during the *Atlas* powered phase of flight. The *Atlas* pitch rate limitation was specified in terms of inertial flight path angle at *Centaur* main engine cutoff (MECO). For all days except July 13, the flight path angle at MECO could not be more negative than -2 deg. For July 13, the powered flight trajectories were designed to be more lofted, resulting in relaxation of the MECO flight path angle limit to -3.9 deg.

The maximum launch azimuth for which the *Surveyor* Project has approval from Range Safety is 115 deg. Permission was requested to use, if necessary, the azimuth corridor extending down to 120 deg to enlarge the July 13

window only. However, the request was not approved by Range Safety.

The "tracking constraint" resulted from an inability to provide the required 60-sec of C-band tracking subsequent to MECO for northerly azimuths on July 15, 16, and 17. This void in the tracking coverage was created by lack of support by a tracking ship to fill the gap in land station coverage. If the *Surveyor* Project had chosen not to honor the tracking constraint on July 16 and 17, the maximum windows shown in Fig. II-5 would have been available for those dates. (Refer to Section V for discussion of launch phase coverage.)

1. Countdown to Launch

During countdown operations, those factors acting to constrain the launch window or period were continually evaluated by the Launch Phase Mission Analyst. The Mission Director was advised of these evaluations for consideration in the launch or hold decision. In order to provide the Supervisor of Range Operations (SRO) with guidelines for establishing a hold condition related to support of *Surveyor* Project requirements during the final seconds of the countdown, when there would be insufficient time to obtain a decision from the Mission Director, the following automatic hold criteria were established for the first three days of the launch period:

- (1) Commencing at $T-30$ sec and until $T-8$ sec, the SRO shall call a hold if he has positive indication that the required DSN acquisition information cannot be provided by AFETR or that continuous telemetry from launch through *Centaur*/spacecraft separation cannot be received and recorded.
- (2) Commencing at $T-8$ sec (start of automatic sequence), no holds shall be called by the SRO for loss of Project requirements.

Two C-band radars were down during portions of the countdown, but both were considered backup and did not cause a hold condition. The TPQ-18 radar at Grand Bahama was declared in the red at $T-184$ min because of a faulty azimuth servo valve in the hydraulic system and remained down during the entire launch operations because of a lack of spare parts. The TPQ-18 radar on Merritt Island became nonoperational at $T-116$ min owing to problems with the pulse transformer but was repaired and put in operation again at $T-32$ min. The MPS-25 radar at Pretoria, South Africa, was not committed for the mission. However, it did support, and provided postretro tracking data in addition to that obtained

by Ascension. The one Range Instrumentation Ship (RIS) supporting the launch (*Coastal Crusader*) and committed for telemetry coverage between Antigua and Ascension was reported on station.

Countdown operations proceeded normally except for the brief hold called at $T-39$ sec, as described earlier, to complete liquid hydrogen topping of *Centaur*, which delayed liftoff until about 29 sec after opening of the window.

2. Launch to DSIF Acquisition

During the launch, the occurrence of space vehicle Mark Events was reported in near-real-time, followed later with reports of the times at which they occurred. The reported Mark Event times are presented in Table V-2; the times for these events determined by post-flight review are presented in Appendix A, Table A-1. The reported Mark Event times indicated that the near-earth phase of the flight was close to nominal. The only notable deviation in Mark Event times from nominal was the indicated *Centaur* burn duration of about 6 sec longer than expected. However, this was not considered to indicate abnormal performance since the *Centaur* burn duration has averaged about 4.5 sec longer than nominal on previous flights when adjusted for all known biases.

Normality of the launch was also indicated by the following information sources: (1) the running commentary on the "quick-look" analysis of real-time launch vehicle telemetry data, which lasted until after MECO, (2) the reports of uprange tracking station view periods, and (3) a running commentary on the trajectory as it was plotted on the Range Safety charts. Launch vehicle VHF telemetry, including the spacecraft composite signal, was retransmitted via the subcable to Cape Kennedy in real-time from all stations down to Antigua. With RIS *Coastal Crusader* providing telemetry coverage between Antigua

and Ascension, continuous spacecraft telemetry was received either via the *Centaur* link or spacecraft link from launch until loss of lock at Ascension and was transmitted to the SFOF in near-real-time.

The first lunar transfer orbit was computed by the real-time computer system (RTCS) at Cape Kennedy about 4 min after MECO, based upon Antigua tracking data. Although this solution was considered only "fair" by the RTCS because of the low elevation view angle of the Antigua tracking radar, it did indicate that the orbital elements were close to nominal and that the spacecraft would impact the moon without a midcourse correction. The Trinidad radar skin tracked the vehicle subsequent to MECO, but the data was very noisy due to the low elevation view angle of the station and was not used by the RTCS for transfer orbit computations.

Based on the initial RTCS transfer orbit computations, acquisition predicts were generated and transmitted for DSS 72, 61, and 51. Owing to the short interval between MECO and DSS 72 rise (about 4 min), the predicts arrived after DSS 72 acquisition, which was achieved in one-way about 1 min after station rise.

Additional RTCS computations based upon DSS 72 and 51 data also resulted in satisfactory transfer orbits. Transfer orbit elements were also computed by the RTCS based upon the *Centaur* guidance vector obtained from telemetry data. Although the first guidance telemetry vector was not usable, the second vector obtained was used to generate transfer orbit elements which confirmed an accurate injection. Using post-retro tracking data from Ascension and Pretoria, the *Centaur* stage orbit was also computed by the RTCS. This orbit was considered to have a good fit and indicated that a satisfactory retro maneuver had been performed. (Also refer to Section VII for discussion of orbit determinations.)

III. Launch Vehicle System

The *Surveyor IV* spacecraft was accurately injected into the desired lunar transit trajectory by a General Dynamics *Atlas/Centaur* launch vehicle (AC-11). The vehicle was launched July 14, 1967, at 11:53:29.215 GMT on a "direct ascent" powered flight from Launch Complex 36A of the AFETR at Cape Kennedy, Florida. This was the fourth operational flight of an *Atlas/Centaur* vehicle and the third and last *Surveyor* mission to utilize the "direct ascent" mode wherein the *Centaur* stage burns only once. The remaining three *Surveyor* missions will be launched via the "parking orbit" ascent mode which was used for *Surveyor III* with AC-12. AC-11 was identical in all essential respects to AC-7, the previous direct ascent vehicle used for the *Surveyor II* mission.

The *Atlas/Centaur* vehicle with the *Surveyor* spacecraft encapsulated in the nose fairing is 113 ft long and weighs 303,000 lb at liftoff (2-in. rise). The basic diameter of the vehicle is a constant 10 ft from the aft end to the base of the conical section of the nose fairing. The configuration of the completely assembled vehicle is illustrated in Fig. III-1. Both the *Atlas* first stage and *Centaur* second stage utilize thin-wall, pressurized, main propellant tank sections of monocoque construction to provide primary structural integrity and support for all vehicle systems. The first and second stages are joined by an

interstage adapter section of conventional sheet and stringer design. The clamshell nose fairing is constructed of laminated fiberglass over a fiberglass honeycomb core and attaches to the forward end of the *Centaur* cylindrical tank section.

A. *Atlas* Stage

The first stage of the *Atlas/Centaur* vehicle is a modified version of the *Atlas D* used on many previous NASA and Air Force missions such as *Ranger*, *Mariner*, and *OGO*. The *Atlas* utilizes the Rocketdyne MA-5 propulsion system, which burns RP-1 kerosene and liquid oxygen in each of its five engines to provide a total liftoff thrust of approximately 387,000 lb. The individual sea-level thrust ratings of the engines are: two booster engines at 165,000 lb each, one sustainer engine at 57,000 lb, and two vernier engines at 670 lb each. The *Atlas* can be considered a 1½-stage vehicle because the "booster section," weighing 6000 lb and consisting of the two booster engines together with the booster turbopumps and other equipment located in the aft section, is jettisoned after about 2.4 min of flight. The sustainer and vernier engine continue to burn until propellant depletion. A mercury manometer propellant utilization system is used to control mixture ratio for the purpose of minimizing propellant residuals at *Atlas* burnout.

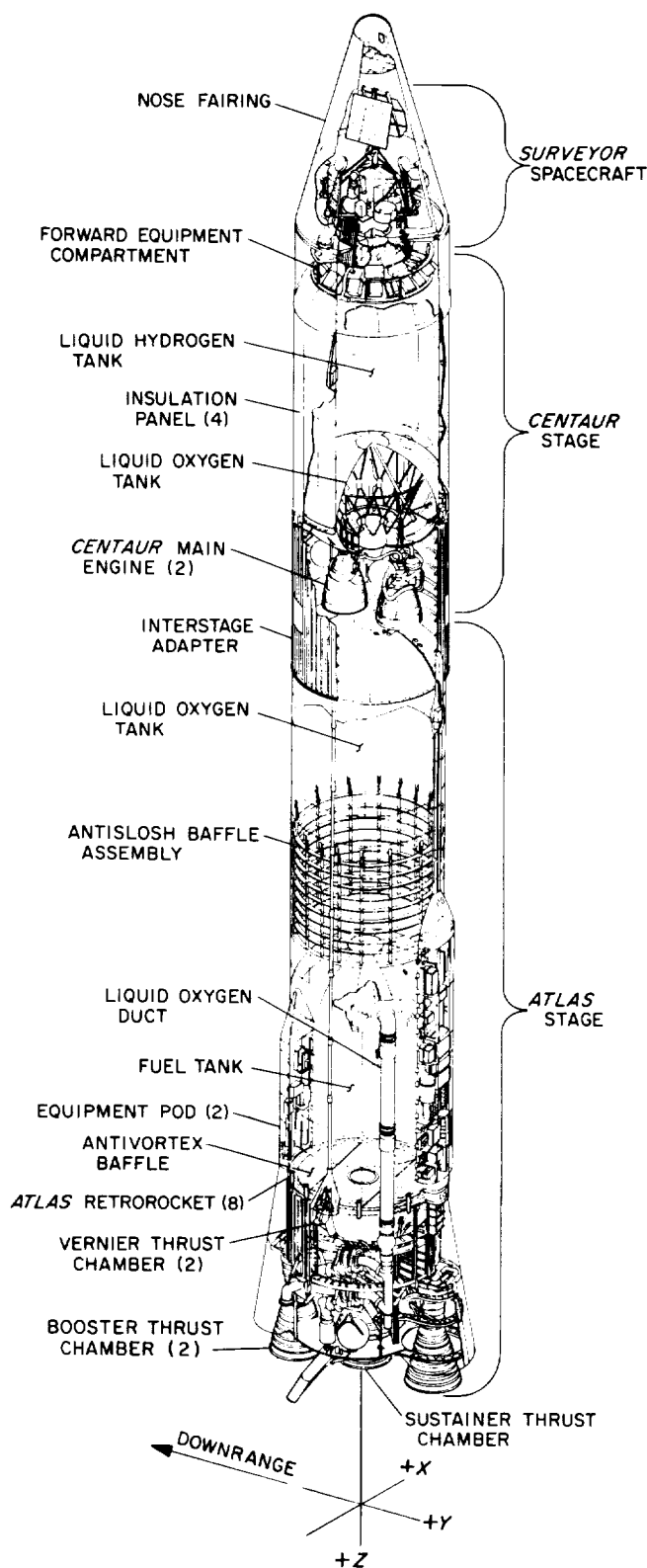


Fig. III-1. Atlas/Centaur/Surveyor space vehicle configuration

Flight control of the first stage is accomplished by the *Atlas* autopilot, which contains displacement gyros for attitude reference, rate gyros for response damping, and a programmer to control flight sequencing until *Atlas/Centaur* separation. After booster jettison, the *Atlas* autopilot also is fed steering commands from the all-inertial guidance set located in the *Centaur* stage. Vehicle attitude and steering control are achieved by the coordinated gimbaling of the five thrust chambers in response to autopilot signals.

The *Atlas* contains a single VHF telemetry system which transmits data well beyond *Atlas/Centaur* separation. The system operates on a frequency of 229.9 MHz over two antennas mounted on opposite sides of the vehicle at the forward ends of the equipment pods. On the AC-11 flight, 97 *Atlas* measurements were telemetered. Redundant range-safety command receivers and a single destructor unit are employed on the *Atlas* to provide the Range Safety Officer with means of terminating the flight by initiating engine cutoff and destroying the vehicle. The *Atlas* destruct system is inactive after normal *Atlas/Centaur* staging occurs.

B. Centaur Stage

The *Centaur* second stage is the first vehicle to utilize liquid hydrogen/liquid oxygen, high-specific-impulse propellants. The cryogenic propellants require special insulation to be used for the forward, aft, and intermediate bulkheads as well as the cylindrical walls of the tanks. The cylindrical tank section is thermally insulated by four jettisonable insulation panels having built-in fairings to accommodate antennas, conduits, and other tank protrusions. Most of the *Centaur* electronic equipment packages are mounted on the forward tank bulkhead in a compartment which is air-conditioned prior to liftoff.

The *Centaur* is powered by two Pratt & Whitney constant-thrust engines rated at 15,000 lb thrust each in vacuum. Each engine can be gimballed to provide control in pitch, yaw, and roll. Propellant is fed from each of the tanks to the engines by boost pumps driven by hydrogen peroxide turbines. In addition, each engine contains integral "boot-strap" turbopumps driven by hydrogen propellant. Hydrogen propellant is also used for regenerative cooling of the thrust chambers. The AC-11 *Centaur* stage utilized RL10A-3-1 engines which were similar to the engines used for other direct-ascent flights. (RL10A-3-3 engines which have improved performance are used for the *Surveyor* parking orbit missions.)

A propellant utilization system is used on the *Centaur* stage to achieve minimum residual of one propellant at depletion of the other. The system controls the mixture ratio valves as a continuous function of propellant in the tanks by means of capacitive-type tank probes and an error ratio detector. The nominal oxygen-hydrogen mixture ratio is 5:1 by weight.

The second stage utilizes a Minneapolis-Honeywell all-inertial guidance system containing an on-board computer which provides a pitch and yaw corrective program for wind shear relief during *Atlas* booster phase and vehicle steering commands after jettison of the *Atlas* booster section. The *Centaur* guidance signals are fed to the *Atlas* autopilot until *Atlas* sustainer engine cutoff and to the *Centaur* autopilot after *Centaur* main engine ignition. During flight, platform gyro drifts are compensated for analytically by the guidance system computer rather than by applying corrective gyro torquing signals. The *Centaur* autopilot system provides the primary control functions required for vehicle stabilization during powered flight, execution of guidance system steering commands, and attitude orientation following the powered phase of flight. In addition, the autopilot system employs an electromechanical timer to control the sequence of programmed events during the *Centaur* phase of flight, including a series of commands required to be sent to the spacecraft prior to spacecraft separation.

The *Centaur* reaction control system provides thrust to control the vehicle after powered flight. For small corrections in yaw, pitch, and roll attitude control, the system utilizes six individually controlled, fixed-axes, constant-thrust, hydrogen peroxide reaction engines. These engines are mounted in clusters of three, 180 deg apart, near the periphery of the main propellant tanks just aft of the interstage adapter separation plane. Each cluster contains one 6-lb-thrust engine for pitch control and two 3.5-lb-thrust engines for yaw and roll control. In addition, four 50-lb-thrust hydrogen peroxide engines are installed on the aft bulkhead, with thrust axes parallel with the vehicle axis. These engines are used to achieve initial separation of the *Centaur* from the spacecraft prior to retromaneuver blowdown and to execute larger attitude corrections if necessary. (Four axially oriented 3-lb-thrust engines are installed on dual-burn vehicles only for use in achieving propellant control during parking orbit coast.)

The *Centaur* stage utilizes a VHF telemetry system with a single antenna transmitting through the nose fairing cylindrical section on a frequency of 225.7 MHz. The

telemetry system provides data from transducers located throughout the second stage and spacecraft interface area as well as a spacecraft composite signal from the spacecraft central signal processor. On the AC-11 flight, 141 vehicle measurements were transmitted by the *Centaur* telemetry system.

Redundant range safety command receivers are employed on the *Centaur*, together with shaped-charge destruct units for the second stage and spacecraft. This provides the Range Safety Officer with means to terminate the flight by initiating *Centaur* main engine cutoff and destroying the vehicle and spacecraft retrorocket. The system can be safed by ground command, which is normally transmitted by the Range Safety Officer when the vehicle has reached orbital energy.

A C-band tracking system is contained on the *Centaur* which includes a light-weight transponder, circulator, power divider, and two antennas located under the insulation panels. The C-band radar transponder provides real-time position and velocity data for the range safety instantaneous impact predictor as well as data for early orbit determination and postflight guidance and trajectory analysis.

C. Launch Vehicle/Spacecraft Interface

The general arrangement of the *Surveyor/Centaur* interface is illustrated in Fig. III-2. The spacecraft is completely encapsulated within a nose fairing/adapter system in the final assembly bay of the Explosive Safe Facility at AFETR prior to being moved to the launch pad. This encapsulation provides protection for the spacecraft from the environment before launch as well as from aerodynamic loads and heating during ascent. An ablative-type coating (Thermolag) is applied over the nose fairing and *Centaur* insulation panels to provide added thermal protection.

The spacecraft is first attached to the forward section of a two-piece, conical adapter system of aluminum sheet and stringer design by means of three latch mechanisms, each containing a dual-squib pin puller. The following equipment is located on the forward adapter: three separation spring assemblies each containing a linear potentiometer for monitoring separation; a 52-pin electrical connector with a pyrotechnic separation mechanism; three pedestals for the spacecraft-mounted separation sensing and arming devices; a shaped-charge destruct assembly directed toward the spacecraft retromotor; an accelerometer for monitoring lateral vibration at the

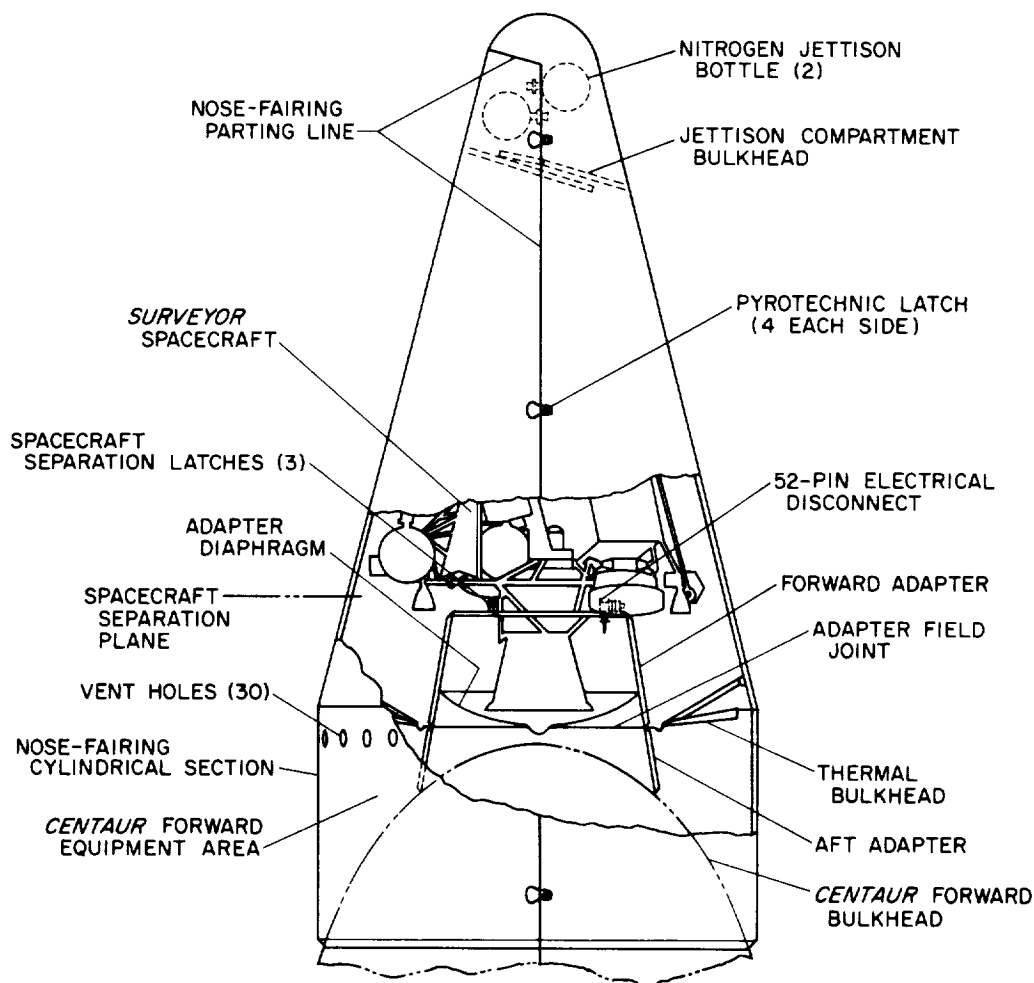


Fig. III-2. Surveyor/Centaur interface configuration

separation plane (four additional accelerometers are located on the spacecraft side of the separation plane as shown in Fig. IV-8); and a diaphragm to provide a thermal seal and to prevent contamination from passing to the spacecraft compartment from the *Centaur* forward equipment compartment.

The low-drag nose fairing is an RF-transparent, clam-shell configuration consisting of four sections fabricated of laminated fiberglass cloth faces and honeycomb fiberglass core material. Two half-cone forward sections are brought together over the spacecraft mounted on the forward adapter. An annular thermal bulkhead between the adapter and base of the conical section completes encapsulation of the spacecraft.

The encapsulated assembly is mated to the *Centaur* with the forward adapter section attaching to the aft adapter section at a flange field joint requiring 72 bolts.

The conical portion of the nose fairing is bolted to the cylindrical portion of the fairing, the two halves of which are attached to the forward end of the *Centaur* tank around the equipment compartment prior to mating of the spacecraft. Doors in the cylindrical sections provide access to the adapter field joint. The electrical leads from the forward adapter are carried through three field connectors and routed across the aft adapter to the *Centaur* umbilical connectors and to the *Centaur* programmer and telemetry units.

Special distribution ducts are built into the nose fairing and forward adapter to provide air conditioning of the spacecraft cavity after encapsulation and until liftoff. Seals are provided at the joints to prevent shroud leakage except out through vent holes in the cylindrical section. Prior to launch, the shroud cavity is monitored for possible spacecraft propellant leakage by means of a toxic gas detector tube which disconnects at liftoff. Tubes

are also inserted into each of the vernier engine combustion chambers to permit nitrogen purging for humidity control and leak detection until manual removal before the service tower is rolled away.

The entire nose fairing is designed to be ejected by separation of two clamshell pieces, each consisting of a conical and cylindrical section. Four pyrotechnic pin-puller latches are used on each side of the nose fairing to carry the tension loads between the fairing halves. Nose fairing loads are transmitted to the *Centaur* tank through a bolted joint which also attaches to the forward end of the *Centaur* insulation panels and contains a flexible linear shaped charge for insulation panel and nose fairing separation. A nitrogen bottle is mounted in each half of the nose fairing near the forward end to supply gas for cold gas jets to force the panels apart. Hinge fittings are located at the base of each fairing half to control ejection, which occurs under vehicle acceleration of approximately 1 g during the *Atlas* sustainer phase of flight.

D. Vehicle Flight Sequence of Events

All vehicle flight events occurred satisfactorily at near nominal times. Predicted and actual times for the vehicle flight sequence of events are included in Table A-1 of Appendix A. Figure III-3 illustrates the major nominal events. Following is a brief description of the vehicle flight sequence of events, with all times referenced to liftoff (2-in. rise) unless otherwise noted. (Refer to Section II-C for a description of the countdown.)

1. *Atlas* Booster Phase of Flight

Hypergolic ignition of all five *Atlas* engines was initiated about 2 sec before liftoff. Vehicle liftoff occurred 29.215 sec after opening of the launch window on the second day of the launch period at 11:53:29.215 GMT, July 14, 1967. This was the first attempt to launch this vehicle. The launcher mechanism is designed to begin a controlled release of the vehicle when all engines have reached nearly full thrust. At 2 sec after liftoff, the vehicle began a 13-sec programmed roll from the fixed launcher azimuth setting of 105 deg to the desired launch azimuth of 103.82 deg. The programmed pitchover of the vehicle, including pitch and yaw corrective programs for wind shear relief, began 15 sec after liftoff and lasted until booster engine cutoff (BECO).

The vehicle reached Mach 1 at 58 sec and maximum aerodynamic pressure occurred at 79 sec. During the booster phase of flight the booster engines were gim-

balled for pitch, yaw, and roll control, and the vernier engines were active in roll control only while the sustainer engine was centered.

At 141.9 sec, BECO was initiated by a signal from the *Centaur* guidance system when vehicle acceleration equalled 5.69 g (expected value: 5.7 ± 0.08 g). At 3.1 sec after BECO, with the booster and sustainer engines centered, the booster section was jettisoned by release of pneumatically operated latches.

2. *Atlas* Sustainer Phase of Flight

At BECO + 8 sec, the *Centaur* guidance system was enabled to provide steering commands for the *Atlas* sustainer phase of flight. During this phase the sustainer engine was gimballing for pitch and yaw control, while the verniers were active in roll. The *Centaur* insulation panels were jettisoned by firing shaped charges at 175.8 sec at an altitude of approximately 48.9 nm, where the aerodynamic heating rate was rapidly decreasing. At 202.1 sec, squibs were fired to unlatch the clamshell nose fairing, which was jettisoned 0.5 sec later by means of nitrogen gas thruster jets activated by pyrotechnic valves.

Other programmed events which occurred during the sustainer phase of flight were: the unlocking of the *Centaur* hydrogen tank vent valve to permit venting as required to relieve hydrogen boiloff pressure; starting of the *Centaur* boost pumps 47 sec prior to *Centaur* main engine start (MES); and locking of the *Centaur* oxidizer tank vent valve followed by "burp" pressurization of the tank.

Sustainer and vernier engine cutoff (SECO and VECO) occurred simultaneously at 239.35 sec as a result of oxidizer depletion, which was the expected cutoff mode. Shutdown began with an exponential thrust decay phase of about 1-sec duration due to low oxidizer inlet pressure to the turbopump and resulting loss in turbopump performance. Then final fast shutdown by propellant valve closure was initiated by actuation of a switch when fuel manifold pressure dropped to 650 ± 50 psi. Also, at the SECO event, the *Centaur* hydrogen tank vent valve was locked and burp pressurization of the tank was begun.

Separation of the *Atlas* from the *Centaur* occurred 1.9 sec after SECO by firing of shaped charges at the forward end of the interstage adapter. This was followed by ignition of eight retrorockets located at the aft end of the *Atlas* tank section to back the *Atlas*, together with the interstage adapter, away from the *Centaur*.

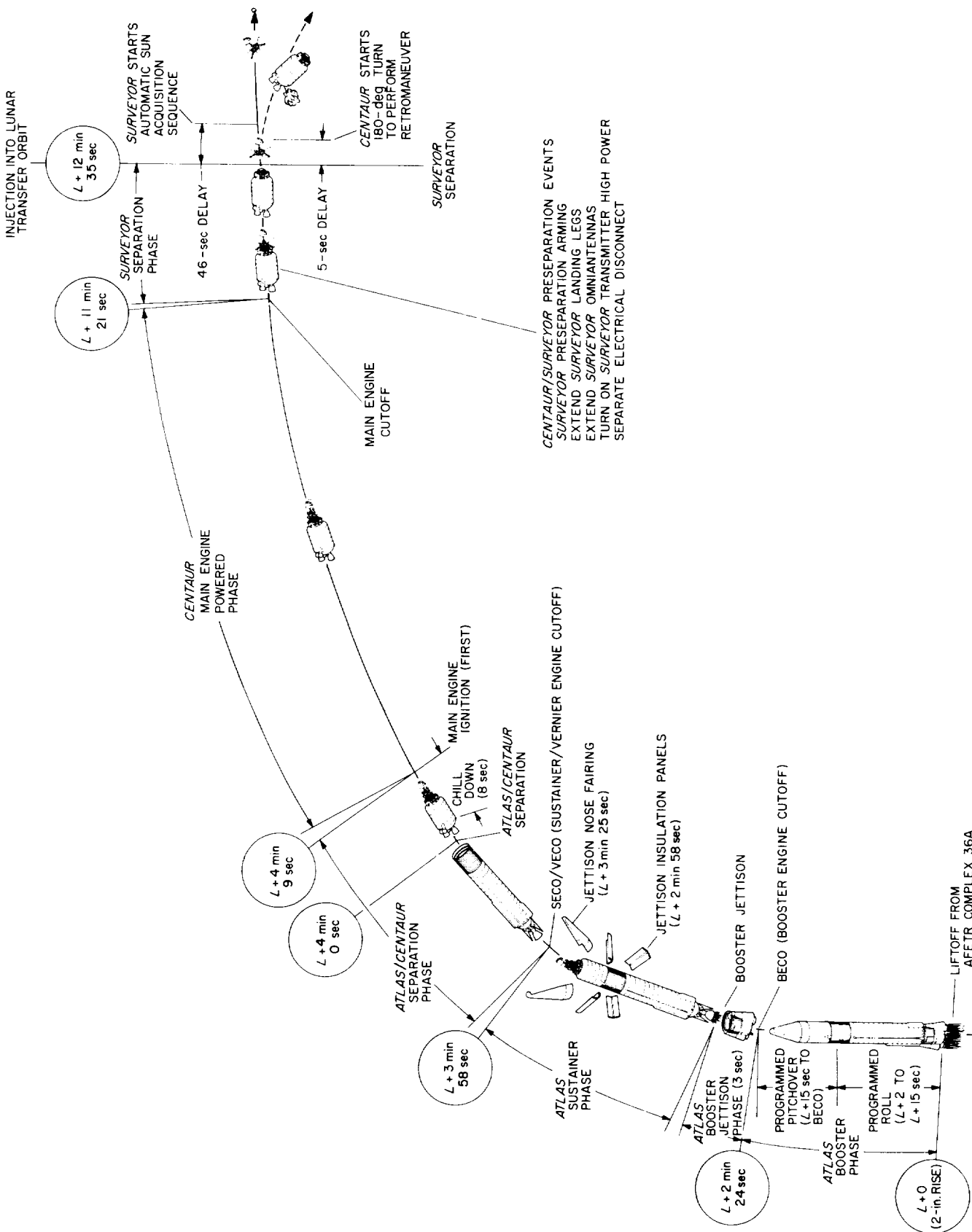


Fig. III-3. Launch phase nominal events

3. Centaur Phase of Flight Through Spacecraft Separation

The *Centaur* prestart sequence for providing chilldown of the propulsion system was initiated 8 sec before ignition of the *Centaur* main engines (MES). MES was commanded 11.5 sec after SECO at 250.8 sec. *Centaur* guidance was reenabled 4 sec after MES to provide steering commands during *Centaur* powered flight. After a burn duration of 437.0 sec, main engine cutoff (MECO) was commanded by guidance at 687.8 sec, when sufficient impulse had been delivered for injection into the desired lunar transfer trajectory. The *Centaur* burn duration was about 5.2 sec longer than predicted for the actual launch conditions. At main engine cutoff, the hydrogen peroxide engines were enabled again for attitude stabilization.

During the 69.1-sec period between MECO and spacecraft separation, the following signals were transmitted to the spacecraft from the *Centaur* programmer: *extend spacecraft landing gear*, *unlock spacecraft omniantennas*, and *turn on spacecraft transmitter high power*. An arming signal also was provided by the *Centaur* during this period to enable the spacecraft to act on the preseparation commands.

The *Centaur* commanded separation of the spacecraft electrical disconnect 5.5 sec before spacecraft separation, which was initiated at 756.9 sec. The *Centaur* attitude-control engines were disabled for 5 sec during spacecraft separation in order to minimize vehicle turning moments.

4. Centaur Retromaneuver Phase of Flight

At 5 sec after spacecraft separation, the *Centaur* began a turnaround maneuver using the attitude-control engines to point the aft end of the stage in the direction of the flight path. About 40 sec after beginning the turn, which required approximately 108 sec to complete, two of the 50-lb-thrust hydrogen peroxide engines were fired for a period of 20 sec while the *Centaur* continued the turn. This provided initial lateral separation of the *Centaur* from the spacecraft.

About 240 sec after spacecraft separation, the propellant blowdown phase of the *Centaur* retromaneuver was initiated by opening the hydrogen and oxygen prestart (chilldown) valves. Oxygen was vented through the engine nozzles while hydrogen discharged directly from the chilldown valves. Liquid hydrogen depletion occurred approximately 52 sec after start of blowdown, after which time only gaseous hydrogen was exhausted. Transition from liquid to gaseous oxygen flow occurred about 156 sec after start of blowdown. Propellant blow-

down was terminated after 250 sec by energizing the *Centaur* power changeover switch at 1246.9 sec, which turned off all power except telemetry and the C-band beacon.

E. Performance

The *Atlas/Centaur* AC-11 vehicle performance was very near nominal, providing a very satisfactory powered flight phase and accurate injection of the *Surveyor IV* spacecraft into the prescribed lunar transfer trajectory.

1. Guidance and Flight Control

The guidance system performed well throughout the flight. The spacecraft was injected on a lunar transfer trajectory which would have resulted in an uncorrected impact only 176 km from the prelaunch target point. (Refer to Section VII for a presentation of vehicle guidance accuracy results in terms of equivalent midcourse velocity correction.)

The guidance system discrete commands (BECO, SECO backup, and MECO) were generated as planned. When guidance steering was enabled from BECO + 8 sec until SECO and again from MES + 4 sec until MECO, the initial attitude errors (maximum 8.5 deg nose down and 4.5 deg nose right) were quickly nulled. After correction of the initial errors, the vehicle was held in close alignment with the commanded steering vector.

Autopilot performance was satisfactory throughout the flight with proper initiation of programmed events and control of vehicle stability. Vehicle disturbances during the *Atlas* phase of flight were at or below the expected levels based on previous flights and were quickly damped following *Atlas* autopilot activation at 42-in. motion. Between SECO and MES, disturbing torques occurred as expected due to boost pump exhaust and main engine chilldown venting. Vehicle disturbances during the *Centaur* powered phase, including the MECO transient, were also similar to previous flights and were easily handled by the vehicle control system. During the *Centaur* phase of flight, the vehicle is rate-stabilized in roll rather than roll-position-stabilized. Analysis indicates about 25 deg of counterclockwise roll had occurred at MECO relative to the local vertical. Following MECO, the roll rate indicated a decreasing duty cycle until the start of *Centaur* turnaround.

The *Centaur* reaction control system performed properly, maintaining desired vehicle attitude following

Centaur powered flight and providing the necessary low level axial thrust for initial lateral separation from the spacecraft. No attitude control engines were fired in the pitch and yaw planes during the period between MECO and spacecraft separation. However, several short firings occurred in roll as on previous flights. About 0.2 sec after the spacecraft separation command, disturbing torques were noted in both pitch and yaw which resulted in *Centaur* vehicle rates of about 0.25 deg/sec in each plane. Spacecraft separation did not appear to be affected by these unexplained vehicle disturbances. The vehicle rate gyros indicate a brief (0.8-sec) loss of thrust from the attitude control engines 1.5 sec after start of *Centaur* turnaround. A similar occurrence was observed on the AC-12 flight (*Surveyor III*) and was attributed to gas bubbles in the hydrogen peroxide line.

2. Propulsion and Propellant Utilization

Atlas propulsion system performance was very satisfactory. All engine parameters were close to nominal except for an 8% high chamber pressure on one vernier engine which did not affect engine performance. Normal sustainer cutoff characteristics were exhibited following oxidizer depletion, which had been predicted. Performance of the *Atlas* propellant utilization (PU) system was also satisfactory. The predicted *Atlas* residuals (propellant above pump) are compared in Table III-1 with preliminary actual values computed from flight data.

Table III-1. *Atlas* propellant residuals, lb

	Actual	Predicted
Oxidizer	390	229
Fuel	307	215

The *Centaur* propulsion system performed well over the entire burn period, which was about 5.2 sec longer than predicted but well within the estimated 3σ tolerance. A longer than predicted *Centaur* burn duration has occurred on each of the previous *Surveyor* missions, but the specific cause is not known. Performance of the *Centaur* PU system was very close to optimum. Preliminary values of the predicted and computed actual *Centaur* usable residuals after MECO are compared in Table III-2.

Table III-2. *Centaur* usable propellant residuals, lb

	Actual	Predicted
Oxidizer	300	257
Fuel	76.3	66

The usable residuals would have provided 5.2 sec additional burn time before theoretical oxidizer depletion, with an ultimate fuel residual of approximately 16.5 lb. Comparing this to the predicted value of 15 lb residual hydrogen indicates a *Centaur* PU system error of only 1.5 lb excess hydrogen.

3. Pneumatic, Hydraulic, and Electrical Power Systems

Operation of the *Atlas* pneumatic system including the programmed tank pressurization and pneumatic control functions was properly accomplished throughout the flight. Both *Centaur* propellant tanks were maintained at satisfactory levels during all phases of flight, with normal occurrence of the "burp" pressurization sequences and hydrogen tank venting. The *Centaur* engines' control regulator outlet pressure indicated an abnormal increase to the relief valve setting during the *Atlas* powered phase of flight. At SECO, a sudden pressure decay occurred, after which the normal operating level was maintained. Abnormal pressure increases also occurred on the AC-9 and AC-12 flights and were attributed to excessive regulator leakage. This anomaly has had no apparent effect on system performance.

Performance of the vehicle hydraulic and electrical power systems was satisfactory throughout the flight.

4. Telemetry, Tracking, and Range Safety Command

The *Atlas* and *Centaur* instrumentation and telemetry systems functioned well, with only minor measurement anomalies. For the first time on an *Atlas/Centaur* flight, usable data was obtained from all of the vehicle transducers.

The *Centaur* C-band radar apparently operated normally to provide good tracking data. An evaluation of the system can only be made on the basis of received tracking data and station operator logs because the airborne system is not instrumented. (See also Section V.)

The *Atlas* and *Centaur* range safety command systems performed satisfactorily. About 3 sec after MECO, a range safety command to disable the destruct systems was sent from Antigua and properly executed.

5. Vehicle Loads and Environment

Vehicle loads and thermal environment were within expected ranges throughout the flight. Maximum axial accelerations were 5.69 g at BECO during the booster

phase and 1.80 g about 1.7 sec before SECO during the sustainer phase. Longitudinal oscillations during launch reached a maximum (0.72 g peak-to-peak at 6.1 Hz) at 0.4 sec and damped out by 15 sec.

The five accelerometers installed in the vicinity of the *Centaur*/*Surveyor* interface indicated expected steady-state vibration levels of less than 1 g (rms), which agrees closely with measured data from previous flights. Shocks of 600–700 Hz for a duration of less than 5 msec were observed in response to shaped charge firings at insulation panel jettison and *Atlas*/*Centaur* separation, but as observed on previous flights, the magnitudes exceeded the range (20 g peak-to-peak) of the telemetry channel. Several vibration transients were observed which were not associated with any discrete flight events. The two most severe transients occurred at 532.6 and 683.5 sec after liftoff and had magnitudes of approximately 8 g and 4.5 g (peak-to-peak), respectively, at a frequency of 1400 to 1600 kHz. Transients having similar spectra but of lower amplitude have been observed on previous *Centaur* flights. The exact cause of these transients has not been determined, but the results of an investigation indicate the shocks may be due to a combination of dynamic and thermal loads in the area of the *Centaur* forward bulkhead and adapter structure. (Also see Section IV-A for a discussion of spacecraft launch phase vibration environment.)

The *Surveyor* compartment thermal and pressure environments were normal throughout flight. The ambient temperature within the compartment was 84°F at liftoff and gradually decreased to 74°F by 86 sec as a result of expansion during ascent. The ambient pressure decayed characteristically to essentially zero prior to nose fairing jettison.

6. Separation and Retro Maneuver Systems

All vehicle separation systems functioned normally. Booster section jettison occurred as planned, with resulting vehicle rates comparable to previous flights.

Satisfactory insulation panel jettison was confirmed by normal transient effects on vehicle rates, axial acceleration, vibration, etc. The times of 35-deg rotation of the four insulation panels during jettison are provided by a breakwire at one hinge arm of each panel. The average panel rotation rates derived from the breakwire instrumentation are comparable to values obtained on earlier flights.

Normal separation of the nose fairing was verified by indications of 3-deg rotation from disconnect wires which are incorporated in the pullaway electrical connectors of each fairing half.

Atlas/*Centaur* separation occurred as planned. Displacement data obtained with respect to time is in close agreement with expected values and indicates successful *Atlas* retrorocket operation. Only a very small angular motion occurred between stages before the *Atlas* cleared the *Centaur*.

At spacecraft separation, first motion of all three springs occurred simultaneously within the accuracy of the extensometer (linear potentiometer) data. Spring extension to the full 1-in. position was normal and nearly identical, producing a spacecraft separation rate of approximately 1 ft/sec. The spacecraft angular rates resulting from the separation event were small and well within the specified maximum acceptable rate of 3.0 deg/sec. The spacecraft separation event did not appear to be affected by *Centaur* disturbing torques, which were noted beginning 0.2 sec after the separation command. (Refer to Section IV-F for discussion of angular separation rates as determined from spacecraft gyro data.)

All phases of the *Centaur* retromaneuver were executed as planned. Five hours after spacecraft separation, the *Centaur*/*Surveyor* separation distance was computed to be about 1150 km, which is well in excess of the required minimum distance of 336 km at that time. The *Centaur* closest approach to the moon was computed to be 22,500 km and occurred at about 10:00 GMT, July 17, 1967.

IV. Surveyor Spacecraft

The basic objectives of the *Surveyor IV* spacecraft system were: (1) accomplish a soft landing on the moon at a new site within the *Apollo* zone of interest; (2) demonstrate spacecraft capability to soft-land on the moon with an unbraked, off-vertical approach angle not greater than 45 deg; (3) obtain postlanding television pictures; (4) obtain data on the mechanical properties of the lunar surface using the soil mechanics/surface sampler (SM/SS); and (5) obtain data on radar reflectivity, thermal characteristics, touchdown dynamics, and other measurements of the lunar surface through the use of various spacecraft equipment. Except for the different landing sites, the *Surveyor IV* mission objectives were very similar to those of *Surveyor III*. However, owing to premature termination of the mission just prior to touchdown, *Surveyor IV* was unable to meet its objectives.

Liftoff occurred at 11:53:29.215 GMT on July 14, 1967. Injection of the spacecraft occurred at 12:06:06 GMT on a trajectory that would have provided, with no midcourse correction, a total miss of approximately 110 miles from the target landing site within Sinus Medii (Central Bay). The mission was normal in all respects until terminal descent. All contact was lost with the spacecraft at

$L + 62:09:12$, less than 2 sec before the expected retro engine burnout and only about $2\frac{1}{2}$ min prior to predicted touchdown. Efforts to reestablish contact with the spacecraft were unsuccessful. Up to this point, the spacecraft had performed almost flawlessly and had responded to approximately 322 commands.

A formally appointed Technical Review Board conducted a thorough investigation of the *Surveyor IV* failure but was unable to find evidence which would indicate the cause.

A. Spacecraft System

In the *Surveyor* spacecraft design, the primary objective was to maximize the probability of successful spacecraft operation within the basic limitations imposed by launch vehicle capabilities, the extent of knowledge of transit and lunar environments, and the current technological state of the art. In keeping with this primary objective, design policies were established which (1) minimized spacecraft complexity by placing responsibility for mission control and decision-making on earth-based equipment wherever possible, (2) provided the capability

of transmitting a large number of different data channels from the spacecraft, (3) included provisions for accommodating a large number of individual commands from the earth, and (4) made all subsystems as autonomous as practicable.

Figure IV-1 illustrates the *Surveyor* spacecraft in the cruise mode and identifies many of the major components. A simplified functional block diagram of the spacecraft system is shown in Fig. IV-2. The spacecraft design is discussed briefly in this section and in greater detail

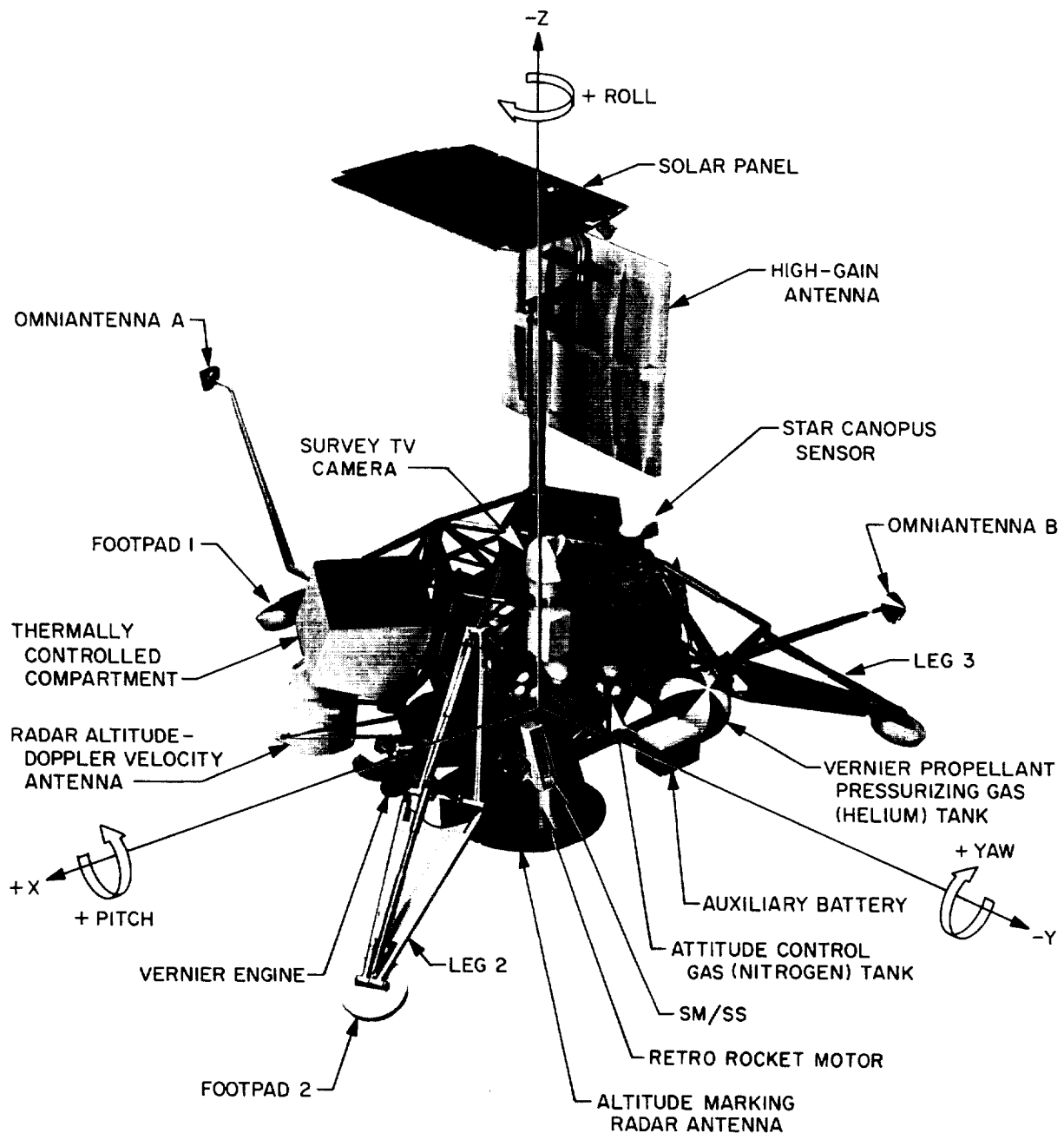


Fig. IV-1. *Surveyor IV* spacecraft in cruise mode

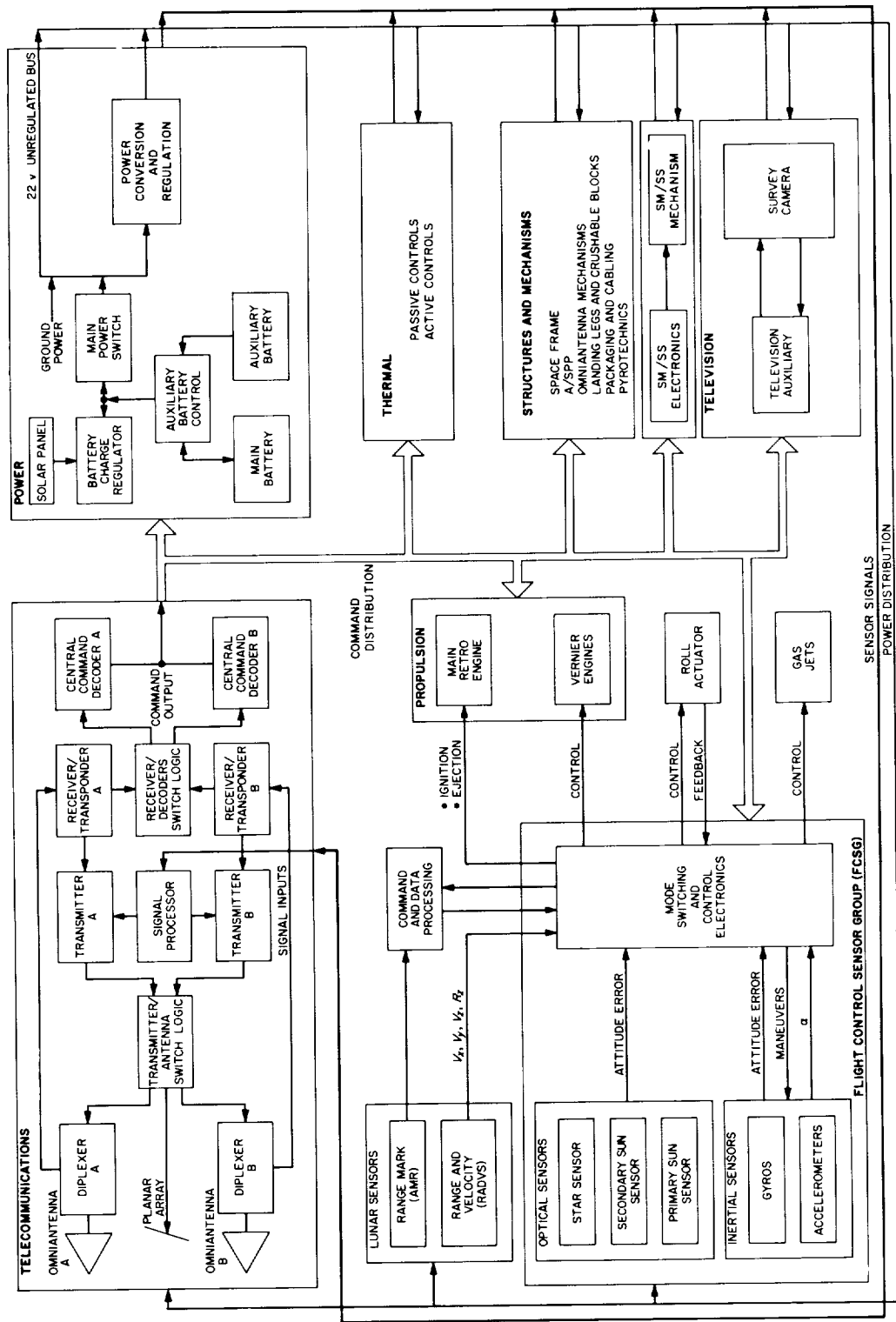


Fig. IV-2. Simplified spacecraft functional block diagram

in the subsystem sections which follow. A detailed configuration drawing of the spacecraft is contained in Appendix B.

1. Spacecraft Coordinate System

The spacecraft coordinate system is an orthogonal, right-hand Cartesian system. Figure IV-3 shows the spacecraft motion about its coordinate axes relative to the celestial references. The cone angle of the earth is the angle between the sun vector and the earth vector as seen from the spacecraft. The clock angle of the earth is measured in a plane perpendicular to the sun vector from the projection of the star Canopus vector to the projection of the earth vector in the plane. The spacecraft coordinate system may be related to the cone and clock angle coordinate system, provided sun and Canopus lock-on has been achieved. In this case, the spacecraft minus Z-axis is directed toward the sun, and the minus X-axis is coincident with the projection of the Canopus vector in the plane perpendicular to the direction of the sun. The spacecraft +Z-axis is in the direction of the retro motor thrust vector, and Leg 1 lies in the X-Y plane.

2. Spacecraft Mass Properties

The *Surveyor IV* spacecraft weighed 2295 lb at separation. Center of gravity of the vehicle is kept low to obtain stability over a wide range of landing conditions. Center-of-gravity limits after *Surveyor/Centaur* separation for midcourse and retro maneuvers are constrained by the attitude correction capabilities of the flight control and vernier engine subsystems during retrorocket burning. Limits of travel of the vertical center of gravity in the touchdown configuration are designed to landing site assumptions and approach angle requirements so that the spacecraft will not topple when landing.

3. Vehicle Structures and Mechanisms

The vehicle structures and mechanisms subsystem provides support, alignment, thermal protection, electrical interconnection, mechanical actuation, and touchdown stabilization for the spacecraft. The subsystem consists of the basic spaceframe, landing gear, crushable blocks, omnidirectional antenna mechanisms, antenna solar panel positioner (A/SPP), pyrotechnic devices, electrical cabling, thermal compartments, and separation sensing and arming devices.

The spaceframe is the basic structure of the spacecraft and provides a rigid mount for all components of the spacecraft and mounting surfaces and attachments for

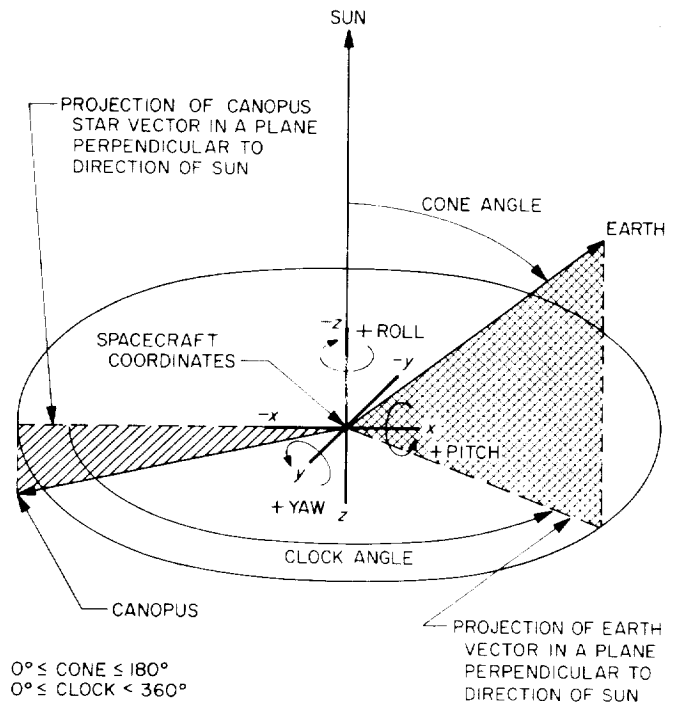


Fig. IV-3. Spacecraft coordinates relative to celestial references

connecting to *Centaur*. The tripodic landing gear and crushable blocks stabilize the spacecraft and absorb impact energy during touchdown. The omniantenna mechanisms provide for omniantenna deployment. The A/SPP supports and positions (around four independent axes) the planar array antenna and solar panel. The pyrotechnic devices mechanically actuate mechanisms, switches, and valves. The electrical cabling interconnects the spacecraft subsystems and components. The thermal compartments provide thermal control for temperature-sensitive components. The separation sensing and arming devices ensure that certain critical squib firing circuits will remain disabled until after *Centaur* separation.

4. Thermal Control

Thermal control of equipment over the extreme temperature range of the lunar surface (+260 to -260°F) is accomplished by a combination of passive, semipassive, and active methods including the use of heaters controlled by ground command. The design represents the latest state of the art in the application of thermal design principles to lightweight spacecraft. The spacecraft thermal design includes "passive" controls such as superinsulation and special surface finishes, "active" heater systems, and "semiactive" thermal switches.

5. Electrical Power

The electrical power subsystem generates, stores, converts, and controls electrical power for distribution to the spacecraft subsystems. Most of the power required by the spacecraft is supplied by the solar panel, which converts solar energy into electrical power. Excess electrical power from the solar panel is stored in the main rechargeable battery and is delivered during peak periods of demand when the solar panel output cannot meet such demands by itself. Thus the main battery augments the solar panel during peak power periods. An auxiliary non-rechargeable battery provides a backup power source for the main battery and solar panel. The electrical power subsystem also contains an engineering mechanisms auxiliary that provides a constant current source for the operation of pyrotechnic devices.

A single solar panel is utilized which is capable of generating continuous unregulated power at 90 to 55 W, depending upon environmental temperature and incidence angle of solar radiation. Peak unregulated power capability is limited to 1000 W by the two spacecraft batteries (main and auxiliary). The initial energy storage of the subsystem is 4400 W-hr. Only one battery, the main battery, can be recharged, to an energy storage of 3520 W-hr. The batteries determine the unregulated power voltage and are designed to sustain a voltage between 17.5 and 27.5 V, with a nominal value of 22 V. The unregulated power is distributed to the loads via an unregulated bus.

Regulated power is provided by a boost regulator at 29 V, controlled to 1% for the flight control and "non-essential" loads and to 2% for the "essential" loads. The maximum regulated power capability of the boost regulator is 270 W.

6. Propulsion

The propulsion subsystem provides thrust during the midcourse correction and terminal descent phases. The propulsion subsystem, consisting of a bipropellant vernier engine system and a solid-propellant main retrorocket motor, is controlled by the flight control system through preprogrammed maneuvers, commands from earth, and maneuvers initiated by flight control sensor signals.

The three thrust chambers of the vernier engine subsystem provide the thrust for midcourse velocity vector correction, attitude control during main retrorocket burning, and velocity vector and attitude control during ter-

минаl descent. Thrust Chamber 1 can be swiveled to provide a thrust vector about the roll axis. Thrust Chambers 2 and 3 are stationary and provide thrust parallel to the roll axis for pitch and yaw control. The thrust of each engine can be differentially throttled over a range of 30 to 104 lb to provide attitude control in pitch and yaw.

The main retro motor is utilized to remove the major portion of the spacecraft approach velocity during terminal descent. It is a spherical solid-propellant motor with a partially submerged nozzle to minimize overall length. The motor provides a thrust of 8,000 to 10,000 lb for a duration of about 41 sec.

7. Flight Control

The flight control subsystem provides spacecraft velocity and attitude control during transit and terminal descent and includes the following spacecraft elements: flight control sensor group (FCSG), attitude control jets, attitude control gas supply, and Vernier Engine 1 roll actuator.

The FCSG contains inertial (gyros), optical (Canopus sensor, acquisition sun sensor, primary sun sensor), and acceleration sensors and flight control electronics. The outputs of each of these sensors and radar sensors are utilized by analog electronics to provide commands for operation of attitude gas jets and the spacecraft vernier and main retro propulsion systems. Flight control requires ground commands for initiation of various sequences and performance of "manual" operations. Flight control programming initiates and controls other sequences.

The celestial sensors allow the spacecraft to be locked to a specific orientation defined by the vectors to the sun and the star Canopus and the angle between them. Initial search and acquisition of the sun are accomplished by the secondary sun sensor. The primary sun sensor then maintains the orientation with the sun line.

Of the inertial sensors, integrating gyros are used to maintain spacecraft orientation inertially when the celestial references are not available. Accelerometers measure the thrust levels of the spacecraft propulsion system during midcourse correction and terminal descent phases.

A pair of attitude jets is located on each of the three legs of the spacecraft. The attitude jets provide for angular rate stabilization after spacecraft separation from the

Centaur, attitude orientation for sun and Canopus acquisition, attitude control during coast phases, and attitude orientation for midcourse correction and terminal descent. The attitude control gas supply provides nitrogen under regulated pressure from a supply tank to the attitude jets.

The three vernier engines are controlled to provide thrust (which can be varied over a wide range) for midcourse correction of the spacecraft velocity vector and controlled descent to the lunar surface. Commands to the vernier roll actuator tilt the thrust axis of Vernier Engine 1 away from the spacecraft roll axis for attitude and roll control during thrust phases of flight when the attitude gas jets are not effective.

8. Radar

Two radar systems are employed by the *Surveyor* spacecraft. An altitude marking radar (AMR) provides a *mark* signal to initiate the main retro sequence. In addition, a radar altimeter and doppler velocity sensor (RADVS) functions in the flight control subsystem to provide three-axes velocity, range, and altitude *mark* signals for flight control during the main retro and vernier phases of terminal descent. The RADVS consists of a doppler velocity sensor, which computes velocity along each of the spacecraft X, Y, and Z axes, and a radar altimeter, which computes slant range from 50,000 ft to 14 ft and generates 1000-ft *mark* and 14-ft *mark* signals.

9. Telecommunications

The spacecraft telecommunications subsystem provides for (1) receiving and processing commands from earth, (2) providing angle tracking and one- or two-way doppler data for orbit determination, and (3) processing and transmitting spacecraft telemetry data.

Continuous command capability is assured by two identical receivers which remain on throughout the life of the spacecraft and operate in conjunction with two omniantennas and two command decoders through switching logic.

Operation of a receiver in conjunction with a transmitter through a transponder interconnection provides a phase-coherent system for doppler tracking of the spacecraft during transit and after touchdown. Two identical transponder interconnections (Receiver/Transponder A and Receiver/Transponder B) are provided for redundancy. Transmitter B with Receiver/Transponder B is the transponder system normally operated during transit.

Data signals from transducers located throughout the spacecraft are received and prepared for telemetry transmission by signal-processing equipment which performs commutation, analog-to-digital conversion, and pulse-code and amplitude-to-frequency modulation functions. Most of the data signals are divided into six groups (commutator modes) for commutation by two commutators located within the telecommunications signal processor. (An additional commutator is located within the television auxiliary for processing television-frame identification data.) The content of each commutator mode has been selected to provide essential data during particular phases of the mission (Table IV-1 and Appendix C). Other signals (such as strain gage data, which is required continuously over brief intervals) are applied directly to sub-carrier oscillators.

Summing amplifiers are used to combine the output of any one commutator mode with continuous data. The composite signal from the signal processor, or television data from the television auxiliary, is sent over one of the two spacecraft transmitters. The commutators can be operated at five different rates (4400, 1100, 550, 137.5, and 17.2 bit/sec) and the transmitters at two different power levels (10 W or 100 mW). In addition, switching permits each of the transmitters to be operated with any one of the three spacecraft antennas (two omniantennas and a planar array) at either the high or low power level. Selection of data mode(s), data rate, transmitter power, and transmitter-antenna combination is made by ground command. A data rate is selected for each mission phase which will provide sufficient signal strength at the DSIF station to maintain the telemetry error rate within satisfactory limits. The high-gain antenna (planar array) is utilized for efficient transmission of video data.

10. Television

The *Surveyor* television subsystem includes a survey camera and a television auxiliary for final decoding of commands and processing of video and frame identification data for transmission by either of the spacecraft transmitters.

The survey camera is designed for postlanding operation by earth commands to provide photographs of the lunar surface panorama, portions of the spacecraft, and the lunar sky. Photographs may be obtained in either of two modes: a 200-line mode for relatively slow (61.8 sec/frame) transmission over an omniantenna or a 600-line mode for a more efficient and rapid (3.6 sec/frame) transmission over the planar array.

Table IV-1. Surveyor IV spacecraft telemetry mode summary

	Data mode	Method of transmission	Data rate	Number of signals		Signals emphasized	Primary use
				Analog	Digital		
Engineering commutator	1	PCM/FM/PM	All	41	40	Flight control, propulsion	Canopus acquisition midcourse maneuver
Engineering commutator	2	PCM/FM/PM	All	78	59	Flight control, propulsion AMR, RADVS	Transit interrogations, backup for main retro phase
Engineering commutator	3	PCM/FM/PM	All	17	39	Inertial guidance, AMR, RADVS, vernier engines	Backup for vernier descent phase
Engineering commutator	4	PCM/FM/PM	All	72	30	Temperatures, power status, telecommunications	Transit interrogations, lunar operations
Engineering commutator	5	PCM/FM/PM	All	108	50	Flight control, power status, temperature	Midcourse and terminal attitude maneuvers, launch and primary cruise data, lunar interrogations
Engineering commutator	6	PCM/FM/PM	All	47	74	Flight control, power status, AMR, RADVS, vernier engine conditions	Terminal descent thrust phase
Television commutator	7	PCM/FM	Only 4400 bit/sec	13		TV survey camera	TV camera interrogation, TV camera operation
Shock absorber strain gages		FM/PM	Continuous	3		Strain gages	Touchdown force on spacecraft legs
Gyro speed		FM/PM	50 Hz	3		Inertial guidance unit	Verify gyro sync
Accelerometers		(a) Centaur VHF (b) FM/FM	Continuous	(a) 4 (b) 4		Launch phase accelerometers	(a) Launch phase vibration (b) Not used

The camera is identical with the TV camera carried aboard previous *Surveyors* except for a new square hood that protects the reflecting mirror mounted in the camera turret from stray light reflections. The camera is mounted about 16 deg from vertical and is pointed upward toward a mirror mounted in the camera hood. The mirror together with the hood can be rotated 360 deg and the mirror can be tilted in steps for horizontal and vertical scanning, respectively. Special mirrors are mounted on the spacecraft frame to provide additional camera coverage of areas of interest under the spacecraft.

The camera can be focused over a range from 4 ft to infinity and can be zoomed to obtain photos in a narrow-angle (6.4-deg) or a wide-angle (25.4-deg) field of view. A lens iris provides a stop range from $f/4$ to $f/22$. The camera is equipped with a focal plane shutter which normally provides an exposure time of 150 msec but can be commanded to remain open for time exposures. A sensing device, attached to the shutter, will keep it from

opening if the light level is too strong. The same device automatically controls the iris setting. This device can be overridden by ground command. A filter wheel assembly between the lens and mirror contains three colored (red, green, and blue) filters and one clear filter.

11. Soil Mechanics/Surface Sampler (SM/SS) and Magnet Instruments

The SM/SS consists of extendable tongs and a scoop with associated electronics. The instrument is designed for postlanding operation and is capable of digging, picking, scratching, and manipulating the lunar surface. The tongs can be extended 64 in. and can be moved 54 deg in vertical motion and 112 deg in azimuth motion. The results of SM/SS operations are obtained primarily through TV pictures. The only telemetry measurements obtained on the instrument itself are current measurements of the four drive motors from which approximate force information may be derived.

The soil magnet experiment consists of one magnet and one unmagnetized control bar, both mounted on Footpad 2 in view of the camera. Televised pictures of lunar surface material in the proximity of the magnet and control bar are used to assess magnetic properties of the lunar surface.

12. Instrumentation

Transducers are located throughout the spacecraft system to provide signals that are relayed to the DSIF stations by the telecommunication subsystem. These signals are used primarily to assess the condition and performance of the spacecraft. Some of the measurements also provide data useful in deriving knowledge of certain characteristics of the lunar surface. In most cases the individual subsystems provide the transducers and basic signal conditioning required for signals provided for data related to their equipment. All the instrumentation signals provided for the *Surveyor IV* spacecraft are summarized by category and responsible subsystem in Table IV-2.

All of the temperature transducers are resistance-type units except for two microdiode bridge amplifier assemblies used in the television subsystem. The voltage (sig-

nals) and position (electronic switches) measurements consist largely of signals from the command and control circuits. A strain gage is mounted on each of the vernier engine brackets to measure thrust and on each of the three landing leg shock absorbers to monitor touchdown dynamics.

The flight control accelerometer is mounted on the retro motor case to verify motor ignition and provide gross retro performance data. Of the remaining eight accelerometers, four are designed to provide data on the vibration environment during launch phase and four are designed to provide data on the dynamic response of spacecraft elements to flight events which occur after spacecraft separation. Only data from the retro motor accelerometer and launch phase accelerometers has been telemetered on *Surveyor* missions to date.

Additional discussion of instrumentation is included with the individual subsystem descriptions.

13. Design Changes

Table IV-3 presents a summary of notable differences in design between the *Surveyor III* and *IV* spacecraft.

Table IV-2. *Surveyor IV* instrumentation

Sensor type	Subsystem location										
	Structures, mechanisms, and thermal control	Electrical power	Propulsion	Flight control	Radar	Telecommunications		SM/SS	Television	Total	
						Signal processing	Radio and command decoding				
Temperature (thermistors)	32	5	16	9	7	3	2	2	2	75	
Temperature (bridges)									2	2	
Pressure		1	2	1						4	
Position (potentiometers)	7								6	13	
Position (mechanical switches)	10	1		1						12	
Position (electrical switches)	1	2		33	15			8	2	4	68
Current		13							1		14
Voltage (power)		6									6
Voltage (signals)				14	7			6			27
Strain gages	3		3								6
Accelerometers	8			1						9	
Inertial sensors (gyro speed)				3						3	
RF power							2			2	
Optical				9						9	
Calibration				1		10			1	12	
Totals	61	28	21	72	29	13	18	5	15	262	

Table IV-3. Notable differences between Surveyors III and IV: changes incorporated on Surveyor IV

Item	Description
RADYS cross-coupled sidelobe logic (CCSLL) for all beams	CCSLL was incorporated for all RADYS beams to reduce probability of reacquiring on a cross-coupled sidelobe if loss of lock should occur during terminal descent. This also removed a previous operational constraint on spacecraft roll attitude during initial acquisition.
RADYS CCSLL disable altitude	RADYS was modified to disable CCSLL below 1000 ft altitude to prevent recurrence of a Surveyor III problem in which CCSLL caused loss of lock at low altitude, preventing the 14-ft mark from being generated. CCSLL is most effective at higher altitudes and may produce erroneous outputs near the lunar surface.
RADYS conditional reliable logic (CRODVS)	RADYS was modified to extend CRODVS enable to 1000 ft altitude to ensure proper steering signals for reacquisition of main lobe in the event main lobe rejection should occur before spacecraft is in essentially vertical descent.
Flight control unregulated current sensor	A new shunt (EP-40) was added for measuring all flight-control unregulated current (roll actuator, gas jets, gyro thermal control, and gyro heaters), which was formerly measured together with other unregulated current loads on a single shunt (EP-4). This will make possible better analysis of individual loads.
SM/SS temperature sensor	A new sensor (SS-13) was added on the SM/SS for more accurate measurement of mechanism temperature to ensure against SM/SS motor operation below -4°F , where excessive torque may occur.
RF transfer switch	As a result of microswitch failures in test, the RF transfer switch circuitry was modified to handle the coil current interrupting function with existing circuitry in the transmitters instead of with microswitches, which are now utilized for switch position indication only.
Optimum charge regulator (OCR)	The OCR trickle charge voltage was reduced to a range of 27.1 to 27.3 V to avoid excessive gas generation which had occurred with a previous value of 27.5 V. There is no significant effect on total stored battery energy. The OCR was also redesigned to increase the efficiency from 77 to 80%.
Soil magnet instrument	An 80- to 100-gauss magnet and an unmagnetized bar were added to the side of Footpad 2 in view of the camera and in range of the SM/SS to investigate the magnetic properties of the lunar soil.
Camera motors	The elevation and azimuth drive motors of the TV camera mirror were improved by making several mechanical changes.
Thermal switches	A special process was introduced to vacuum-bake the thermal switch contact coatings at 300°F to drive off volatile constituents which were found to contribute to the problem of the switches sticking closed, as occurred on the Surveyor I and III missions after sunset.

Item	Description
Propellant tank superinsulation	A conductive mesh was incorporated in the outer surface of the superinsulation blanket and grounded to the spaceframe to eliminate static charge buildup in accordance with Range Safety requirements.
Footpad paint patterns	Special paint patterns were applied to Footpads 2 and 3 to enhance television camera coverage.

14. Spacecraft Reliability

The prelaunch reliability estimate for the *Surveyor IV* spacecraft was 0.65 at 50% confidence level for the flight through landing phases of the mission, assuming successful injection. The reliability estimates for the *Surveyor IV* spacecraft vs systems test experience are shown in Fig. IV-4. Table IV-4 lists the prelaunch reliability estimates for each subsystem. For comparative purposes,

Table IV-4. Surveyor spacecraft subsystem reliability estimates

	Surveyor I	Surveyor II	Surveyor III	Surveyor IV
Subsystem				
Telecommunication	0.925	0.944	0.965	0.929
Vehicle and mechanisms	0.816	0.868	0.907	0.854
Propulsion	0.991	0.991	0.968	0.947
Electrical power	0.869	0.958	0.935	0.953
Flight control	0.952	0.889	0.971	0.931
Systems interaction factor	0.736	0.949	0.967	0.978
Overall spacecraft system	0.456	0.658	0.745	0.653

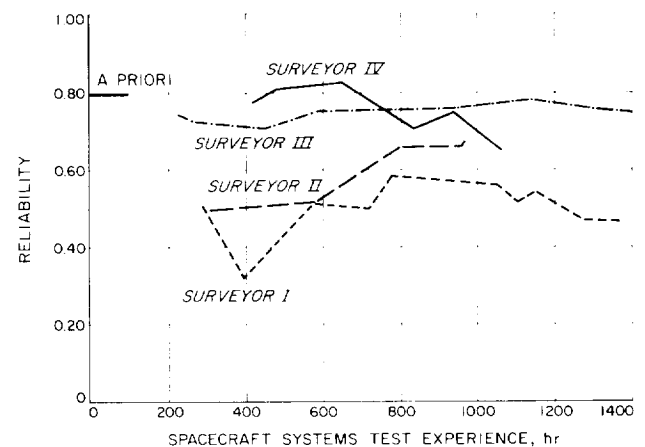


Fig. IV-4. Surveyor spacecraft system reliability estimates

Surveyor I, II, and III estimates are also shown. The primary source of data for these reliability estimates is the time and cycle information experienced by spacecraft units during systems tests. Data from *Surveyor I, II, and III* test and flight experience was included where there were no significant design differences between the units. In general, a failure is considered relevant if it could occur during a mission. Relevance of failures is based on a joint reliability/systems engineering decision.

Owing to the number of unit changes on the spacecraft, the reliability estimate is considered generic to *Surveyor IV* rather than descriptive of the exact *Surveyor IV* spacecraft configuration. At the 80% confidence level, *Surveyor IV* reliability was 0.62. This value was based upon application of the binomial distribution.

15. Functional Description of Spacecraft Automatic Flight Sequences

The *Surveyor* spacecraft system has been designed for automatic operation in the following flight sequences:

a. Solar panel deployment and sun acquisition. Immediately upon separation from the *Centaur*, the spacecraft automatically deploys the solar panel to the transit position in a two-step sequence. First, the A/SPP solar panel axis is unlocked and the solar panel is rotated 56 deg from the stowed position to an orientation normal to the spacecraft Z-axis. When this position is reached, the solar panel axis is locked and the A/SPP roll axis is unlocked. The antenna/solar panel combination is then rotated 60 deg about the roll axis and locked in the transit position.

Also upon separation from the *Centaur*, the spacecraft flight control system operates the attitude control jets in a rate-stabilization mode to reduce angular motion imparted to the spacecraft to within deadband limits of ± 0.1 deg/sec. After a 51-sec delay following electrical disconnect, which allows time for the spacecraft to reduce the angular motion, a sun acquisition sequence is automatically initiated. First, flight control commands a roll maneuver which permits the sun to be acquired by the acquisition sun sensor, which has a 10-deg-wide by 196-deg-fan-shaped field of view that is centered about the spacecraft minus Z-axis. Upon initial sun acquisition, the roll is stopped and a positive yaw maneuver is initiated to permit the narrow-view primary sun sensor to acquire and lock-on the sun. A secondary sun sensor is mounted on the solar panel to provide a means of sun acquisition by ground command if the automatic sequence fails.

Upon completion of the solar panel deployment and sun acquisition sequences, the spacecraft coasts with its roll axis (and the active face of the solar panel) held positioned toward the sun by maintaining the sun within the field of view of the center cell of the primary sun sensor. The other axes are held inertially fixed by means of the roll gyro.

b. Canopus acquisition. Some time after sun acquisition, a roll maneuver is initiated by ground command for star verification and Canopus acquisition. As the spacecraft rolls about its Z-axis, the Canopus sensor provides intensity signals of objects which pass through its field of view and have intensities in the sensitivity range of the sensor. Comparison of a map constructed from these signals and a map previously prepared based on predictions permits identification of Canopus from among the signals. After sufficient spacecraft roll to permit Canopus verification, the spacecraft is switched to *star acquisition* mode by ground command to permit the spacecraft to lock-on Canopus automatically the next time Canopus passes through the sensor field of view. Canopus acquisition establishes three-axes attitude reference, which is required before the midcourse and terminal maneuvers can be performed.

c. Midcourse velocity correction. The spacecraft executes each of the desired midcourse attitude maneuvers (roll, pitch, or yaw) upon initiation by ground command. The spacecraft automatically terminates each maneuver when the desired magnitude (previously transmitted by ground command and stored in the flight control programmer) of turn has been accomplished. The maneuvers must be accomplished serially since the flight control programmer can store only one magnitude at a time.

The magnitude of the desired vernier thrust time for midcourse velocity correction is also transmitted to the spacecraft, verified, and stored by the flight control. During the midcourse thrusting phase, the three vernier engines provide a constant spacecraft acceleration of about 0.1 earth *g* until cutoff is commanded by flight control. During thrusting, the vernier engines are differentially throttled and the roll actuator is controlled to achieve attitude stabilization.

d. Terminal descent sequence. The terminal phase begins with the preretro attitude maneuvers (Fig. IV-5). These maneuvers are commanded from earth in a manner similar to the midcourse maneuvers to reposition the attitude of the spacecraft from the coast phase sun-star reference such that (1) the expected direction of the retro

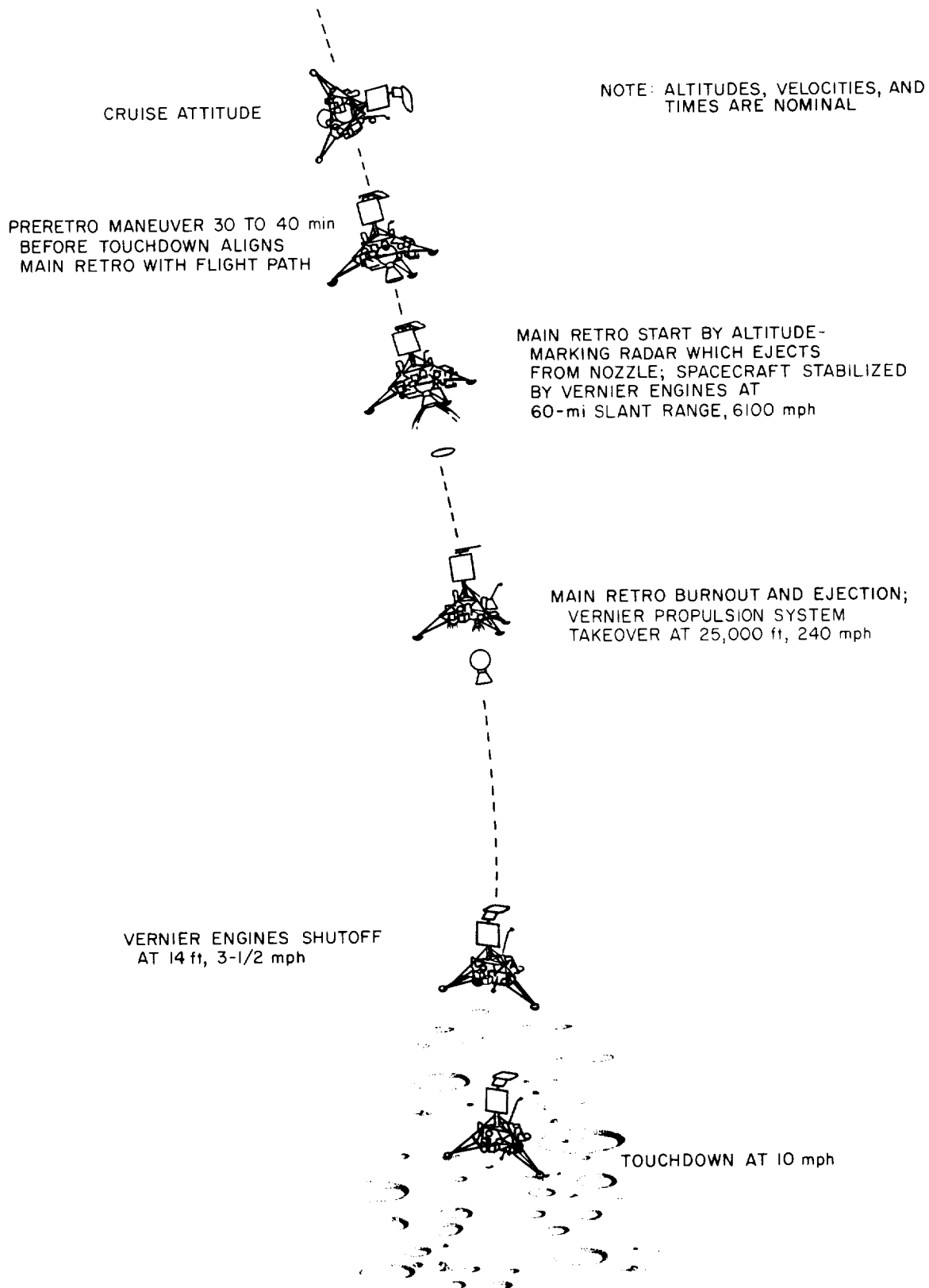


Fig. IV-5. Terminal descent nominal events

thrust vector will be aligned with respect to the spacecraft velocity vector, and (2) the spacecraft roll attitude will provide the most desirable landed orientation for lunar operations within the RADVS and telecommunications descent constraints. Following completion of the attitude maneuvers, the AMR is activated. It has been preset to generate a *mark* signal when the slant range to the lunar surface is 60 miles nominal. A backup *mark* signal, delayed a short interval after the AMR *mark* should occur, is transmitted to the spacecraft to initiate the automatic sequence in the event the AMR *mark* is not generated. A delay between the *altitude mark* and main retro motor ignition has been preset in the flight control programmer by ground command. Vernier engine ignition is automatically initiated 1.1 sec prior to main retro ignition. The main retro phase sequence is illustrated in Fig. IV-6.

During the main retro phase, spacecraft attitude is maintained in the inertial direction established at the end of the preretro maneuvers by differential throttle control of the vernier engines while maintaining the total vernier thrust at the midthrust level. The main retro burns at essentially constant thrust for about 40 sec, after which the thrust starts to decay. This tailoff is detected by an inertial switch which increases vernier thrust to the high level and initiates a programmed time delay of about 12 sec, after which the main retro motor case is ejected. The main retro phase removes more than 95% of the spacecraft velocity and puts the spacecraft position, ve-

locity, and attitude relative to the lunar surface within the capability of the final, vernier phase.

The vernier phase generally begins at altitudes between 10,000 and 50,000 ft and velocities in the range of 100 to 700 ft/sec. This wide range of vernier-phase initial conditions exists because of statistical variations in parameters which affect main retro burnout. About 2 sec after separation of the main retro case, vernier thrust is reduced and controlled to produce a constant spacecraft deceleration of 0.9 lunar g , as sensed by an axially oriented accelerometer. The spacecraft attitude is held in the preretro position until the doppler velocity sensor locks onto the lunar surface (Fig. IV-7). The thrust axis is then aligned and maintained to the spacecraft velocity vector throughout the remainder of the descent until the terminal sequence is initiated (when the attitude is again held inertially fixed). With the thrust axis maintained in alignment with the velocity vector, the spacecraft makes a "gravity turn," wherein gravity tends to force the flight path toward the vertical as the spacecraft decelerates.

The vehicle descends at 0.9 lunar g until the radars sense that the "descent contour" has been reached (Fig. IV-8). This contour corresponds, in the vertical case, to descent at a constant deceleration. The vernier thrust is commanded such that the vehicle follows the descent contour until shortly before touchdown, when the terminal sequence is initiated. Nominally, the terminal sequence consists of a constant-velocity descent from

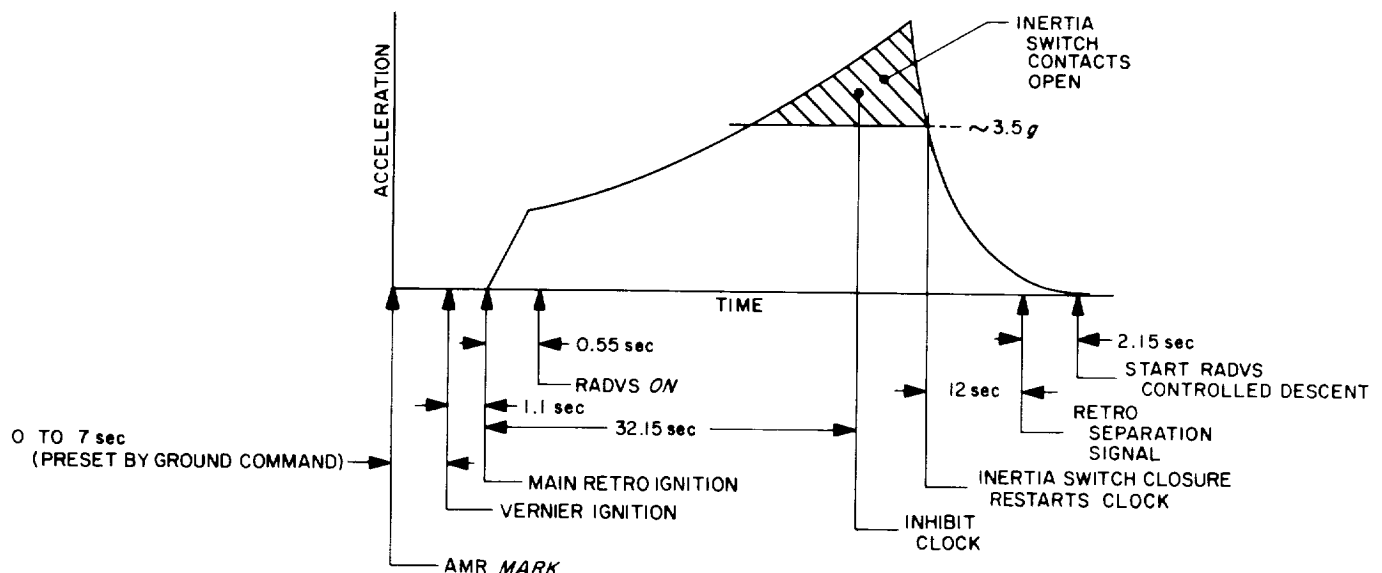


Fig. IV-6. Main retro phase sequence

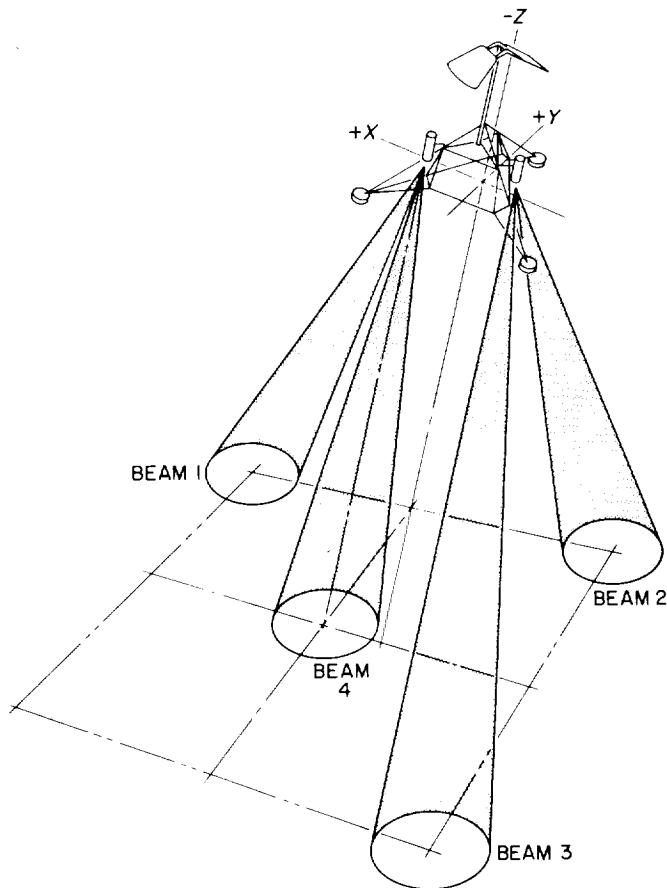


Fig. IV-7. RADVS beam orientation

40 to 14 ft at 5 ft/sec, followed by a free fall from 14 ft, resulting in touchdown at approximately 13 ft/sec.

Constraints on the allowable main retro motor burnout conditions are of major importance in *Surveyor* terminal descent design.

RADVS operational limitations contribute to constraints on the main retro burnout conditions. Linear operation of the doppler velocity sensor is expected for slant ranges below 50,000 ft and for velocities below 700 ft/sec. The altimeter limit is between 30,000 and 40,000 ft, depending on velocity. These constraints are illustrated in the range-velocity plane of Fig. IV-8.

The allowable main retro burnout region is further restricted by the maximum thrust capability of the vernier engine system. To accurately control the final descent, the minimum thrust must be less than the least possible landed weight (lunar gravity) of the vehicle. The result is a minimum thrust of 90 lb. This in turn constrains the

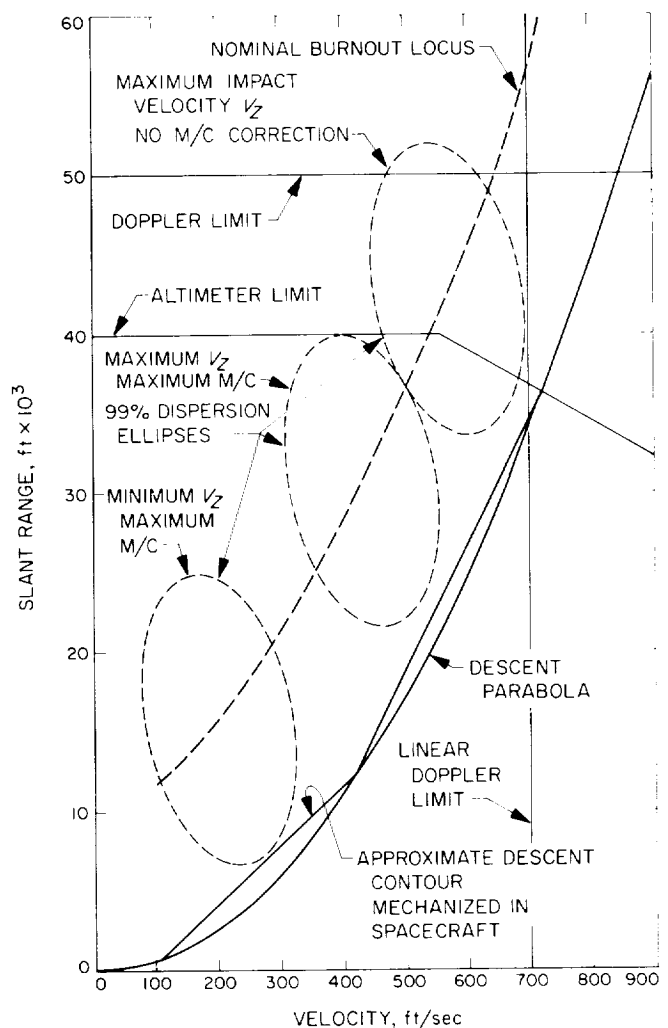


Fig. IV-8. Range-velocity diagram

maximum vernier thrust to 312 lb because of the limited range of throttle control which is possible.

Descent at the maximum thrust to touchdown defines a curve in the range-velocity plane below which main retro burnout cannot be allowed to occur. Actually, since the vernier engines are also used for attitude stabilization by differential thrust control, it is necessary to allow some margin from the maximum thrust level. Furthermore, since it is more convenient to sense deceleration than thrust, the vernier phase of terminal descent is performed at nearly constant deceleration rather than at constant thrust. Therefore, maximum thrust will be utilized only at the start of the vernier phase.

The maximum vernier phase deceleration defines a parabola in the altitude-velocity plane. For vertical

descents at least, this curve defines the minimum altitude at which main retro burnout is permitted to occur with a resulting soft landing. This parabola is indicated in Fig. IV-8. (For ease of spacecraft mechanization, the parabola is approximated by a descent contour consisting of straight-line segments.)

Main retro burnout must occur sufficiently above the descent contour to allow time to align the thrust axis with the velocity vector before the trajectory intersects the contour. Thus, a "nominal burnout locus" (also shown in Fig. IV-8) is established which allows for altitude dispersions plus an alignment time which depends on the maximum angle between the flight path and roll axis at burnout.

The allowable burnout region having been defined, the size of the main retro motor and ignition altitude are determined such that burnout will occur within that region.

In order to establish the maximum propellant requirements for the vernier system, it is necessary to consider dispersions in main retro burnout conditions as well as midcourse maneuver fuel expenditures. The principal sources of main retro burnout velocity dispersion are the imperfect alignment of the vehicle prior to main retro ignition and the variability of the total impulse. In the case of a vertical descent, these variations cause dispersions of the type shown in Fig. IV-8, where the ellipse defines a region within which burnout will occur with probability 0.99. The design chosen provides enough fuel so that, given a maximum midcourse correction, the probability of not running out is at least 0.99.

The spacecraft landing gear is designed to withstand a horizontal component of the landing velocity. The horizontal component of the landing velocity is nominally zero. However, dispersions arise primarily because of the following two factors:

- (1) Measurement error in the doppler system resulting in a velocity error normal to the thrust axis.
- (2) Nonvertical attitude due to: (a) termination of the "gravity turn" at a finite velocity, and (b) attitude control system noise sources.

Since the attitude at the beginning of the constant-velocity descent is inertially held until vernier engine cutoff, these errors give rise to a significant lateral velocity at touchdown.

16. Spacecraft System Performance

A summary of *Surveyor IV* spacecraft system performance is presented below by mission phases. Also refer to Sections IV-B through IV-J for spacecraft subsystem performance; Section VI-C presents a chronology of mission operations.

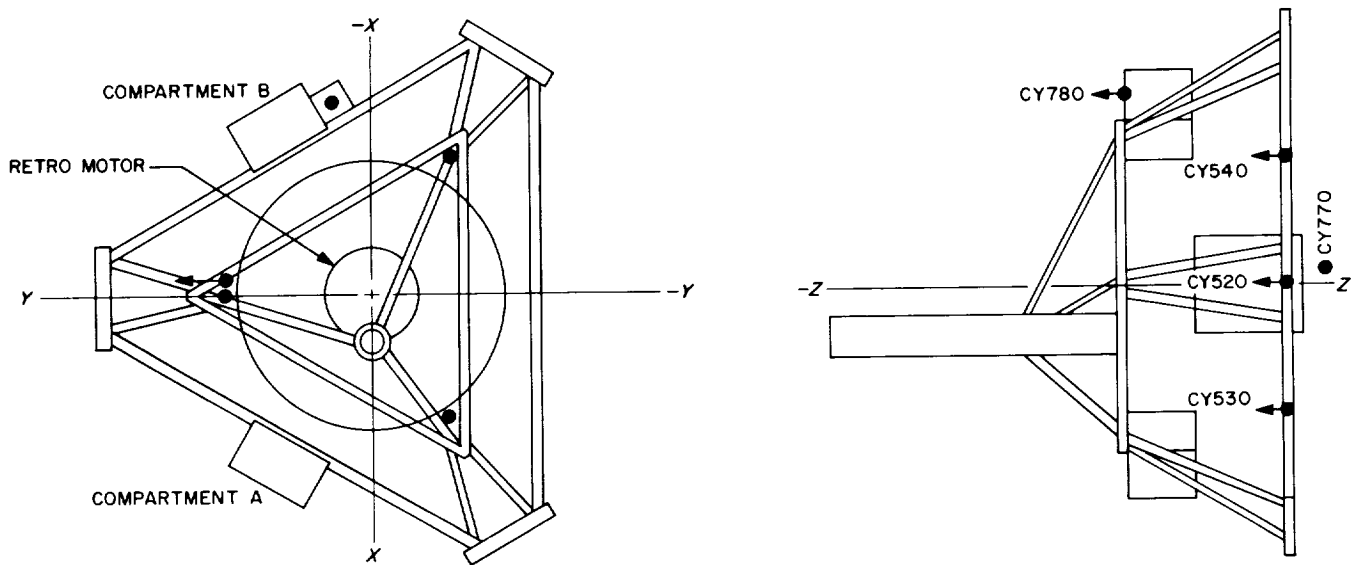
a. Countdown and launch phase performance. The spacecraft proceeded smoothly through the countdown with only one anomaly occurring. The AGC signal from spacecraft Receiver A indicated a signal level about 14 db lower than the level observed during the corresponding period of J-FACT (Joint Flight Acceptance Composite Test). Tests were conducted to check the AGC reading at which indexing occurred, as well as the indication for a no-signal condition. Results of these checks led to the conclusion that receiver performance was satisfactory and that the signal level difference was probably due to difficulty in providing identical air link conditions during the J-FACT and launch operations.

Liftoff occurred at 11:53:29.215 GMT on July 14, 1967, with the spacecraft in the standard launch configuration (transmitter low power on, launch phase accelerometer amplifier on, legs and omniantennas folded, solar panel and planar array stowed and locked, etc.). Performance during the direct-ascent launch phase was as expected.

During the boost phase of flight, the *Surveyor* spacecraft is subjected to a variable vibration environment consisting of acoustically induced random vibration and the transient response to discrete flight events. The *Surveyor IV* space vehicle was instrumented with five accelerometers in order to obtain information on this vibration environment. The location and orientation of these accelerometers in the launch vehicle/spacecraft interface are shown in Fig. IV-9. Output of the Z-axis accelerometer, CY520, was telemetered continuously; outputs of the other four accelerometers were telemetered on a commutated channel.

Typical *Surveyor IV* accelerometer data is shown in Table IV-5 for those events which were recorded and is comparable, in general, to the *Surveyor I, II, and III* flight data, which is also shown. The 95th percentile (approximately 1.64σ) estimate of the acceleration spectral density (over the frequency bandwidth of 100–500 Hz) at *Surveyor IV* liftoff is $0.011 g^2/\text{Hz}$. The specification value is $0.0145 g^2/\text{Hz}$.

On this flight there were several transients which cannot be attributed to any discrete spacecraft or booster



TRANSDUCER	LOCATION	RANGE, g	FREQUENCY RANGE, Hz	REMARKS
CY520	SPACECRAFT, NEAR ADAPTER ATTACH POINT 1	± 10	2-2500	CONTINUOUS
CY530	SPACECRAFT, NEAR ADAPTER ATTACH POINT 2	± 10	2-1260	COMMUTATED
CY540	SPACECRAFT, NEAR ADAPTER ATTACH POINT 3	± 10	2-1260	COMMUTATED
CY770	ADAPTER, NEAR SPACECRAFT ATTACH POINT 1	± 10	2-1260	COMMUTATED
CY780	SPACECRAFT, IN FCSG	± 10	2-1260	COMMUTATED

Fig. IV-9. Launch-phase accelerometer location

event. These transients have been seen on other flights, but on this mission they were of a higher magnitude (up to 4 g , zero-to-peak, at a predominant frequency of 1400 Hz). The levels indicated, however, are well below the vibration levels to which the flight spacecraft was acceptance-tested before launch. The most likely source for these transients is believed to be the thermal expansion and contraction of the launch vehicle structural elements during flight.

The spacecraft properly executed all preseparation events initiated by the *Centaur* programmer, which included turning on the transmitter high power, extending the landing legs, and extending the omniantennas. Spacecraft separation from the *Centaur* was also accomplished as desired. The automatic solar panel and A/SPP roll-axis stepping sequence was initiated by spacecraft separation

and occurred normally. The solar panel was unlocked and required about 350 sec to step through -56 deg to its transit position, where it was locked. Upon locking of the solar panel, the A/SPP was unlocked and rolled $+60$ deg in a period of about 240 sec to its desired transit position, where it was locked.

Spacecraft separation also enabled the cold-gas attitude control system, and the small angular rates which had been imparted to the spacecraft were reduced to 0.1 deg/sec in less than 13 sec. After the built-in time delay from electrical disconnect, the sun acquisition sequence occurred properly, beginning with a negative roll through about 59 deg, which was terminated upon illumination of the acquisition sun sensor. Then followed a positive yaw turn through about 46 deg, which was terminated upon illumination of the primary sun sensor center cell.

**Table IV-5. Surveyor IV maximum measured peak-to-peak acceleration, g,
compared with data from Surveyors I, II, and III**

		Accelerometer						Accelerometer					
		CY520	CY530	CY540	CY770	CY780		CY520	CY530	CY540	CY770	CY780	
Liftoff	I	3	4	4	12	2	Main engine	I	1	1	c	c	c
	II	a	a	3	a	3	start 1	II	a	a	c	a	c
	III	4.8	a	4.1	16.6	3.1		III	1.4	a	c	c	c
	IV	4	4	5	7	2		IV	1	c	c	c	c
Maximum	I	b	b	b	b	b	Main engine	I	4.5	c	c	4.5	c
aerodynamic	II	b	b	b	b	b	cutoff 1	II	a	a	c	a	c
loading	III	2.4	a	2.2	5.7	1.64		III	3.3	a	c	3.3	c
	IV	2.7	2.1	2.8	4.7	0.8		IV	3.3	2	c	c	c
Booster	I	3	c	c	c	c	Main engine	I	c	c	c	c	c
engine	II	a	a	c	a	3	start 2	II	c	c	c	c	c
cutoff	III	3.3	a	c	3.7	1.3		III	2.0	a	c	c	c
	IV	3	2	c	c	c		IV	c	c	c	c	c
Insulation	I	> 20 ^d	c	c	> 20 ^d	c	Main engine	I	c	c	c	c	c
panel	II	a	a	c	a	c	cutoff 2	II	c	c	c	c	c
jettison	III	> 20 ^d	a	c	c	c		III	0.45	a	c	c	c
	IV	> 20 ^d	c	c	> 20 ^d	c		IV	c	c	c	c	c
Shroud	I	3	c	c	a	c	Legs extend	I	20	c	10	c	c
separation	II	a	a	c	a	2.6		II	a	a	c	a	c
	III	4.3	a	c	c	c		III	18	a	c	13	c
	IV	4	c	c	8	c		IV	18	12	c	c	c
Sustainer	I	1	c	1	c	c	Omniantennas	I	20	c	12	c	c
engine	II	a	a	c	a	c	deploy	II	a	a	c	a	c
cutoff	III	1.2	a	1.3	c	c		III	16	a	c	c	c
	IV	2	2	c	c	c		IV	18	c	c	c	c
Atlas/Centaur	I	> 20 ^d	> 20 ^d	c	c	c							
separation	II	a	a	c	a	c							
	III	> 20 ^d	a	c	c	c							
	IV	> 20 ^d	c	c	c	c							

^aThese transducers were inoperative.

^bData not available.

^cCommuted channel. This transducer was not being monitored at this event.

^dExceeded bandwidth of channel.

^eNot applicable.

b. Coast phase performance. Initial DSIF acquisition was performed by DSS 72. After achieving initial phase lock, Receiver B dropped phase lock owing to a DSIF servo system problem which caused the transmitting antenna to slew 15 deg off the spacecraft.

After two-way acquisition had been reestablished by DSS 72 about 28 min after liftoff, an initial assessment was made in the transmitter high-power mode. Following this assessment, which indicated all systems to be normal, the spacecraft responded correctly to an initial sequence of commands to place the spacecraft in the cruise configuration. In the cruise configuration, the launch phase accelerometer power was off and the transmitter was operated on low-power at 1100 bit/sec with the coast phase commutator on. The commanding of flight

control to *cruise* mode was delayed owing to a high-intensity signal from the Canopus sensor, which indicated the presence of the earth in the field of view. About 3½ hr after launch, the signal intensity had decreased, indicating that the earth had left the field of view, and the spacecraft was commanded to *cruise* mode, which insured that the flight control system would revert to *inertial* mode if sun lock was lost.

Automatic Canopus lock-on occurred successfully almost 6½ hr after launch, when acquisition was attempted after an initial roll to generate a star map. The total spacecraft roll was 565 deg. Signals from at least three objects were noted which did not appear on the predicted star map. It was concluded that the objects were particles which passed through the field of view during

the rotation. The Canopus sensor performance was excellent. The ratio of measured to predicted Canopus intensity was approximately 1.16.

The number of gyro drift checks conducted during the coast phases was larger than normal because of indications that drift rates were near the specification value of 1.0 deg/hr. The drift rates were not of serious concern because the terminal maneuvers were compensated for the final drift rates, which were computed to be -0.5 deg/hr roll, -1.0 deg/hr pitch, and $+0.5$ deg/hr yaw.

A total of twelve standard engineering interrogations were conducted during the coast phases. Spacecraft data at all times indicated that all subsystems were performing normally and within predicted operational limits.

Performance of the thermal control system was excellent, with all temperatures near predictions. Only two minor thermal control anomalies occurred: a sudden unexplained rise of 5°F in the temperature of one oxidizer tank; and the fact that the attitude jet temperature did not reflect an expected effect from the new paint pattern. Curves of temperature histories of spacecraft components during transit are contained in Appendix D.

Telecommunications system performance was satisfactory throughout the flight until abrupt loss of signal prior to touchdown. Deviations from the predicted received signal levels were noted on both the up-link and down-link. However, gyro drift checks performed during the coast periods account for some omniantenna gain variations that were not taken into consideration when the predictions were generated. Allowing for the gyro checks, Receiver B received signal level was lower than that expected during the flight phases, indicating that a minus 5-db bias existed in the receiver performance or calibration data.

Power subsystem operation was normal throughout transit, with telemetered parameters close to predictions. Overall optimum charge regulator efficiency was approximately 79%, and main battery energy remaining at loss of signal was about 2250 W-hr.

c. Midcourse correction performance. For this mission it was decided to conduct the midcourse correction during the second Goldstone view period rather than during the first pass as on previous missions. The maneuver was conducted later to obtain better landing site accuracy, which was possible as a result of improved pre-midcourse

orbit determination and reduced effect of execution errors on landing site dispersion.

Each of the midcourse maneuvers was initiated when the respective attitude control loop limit cycle error was as near to a null as possible to reduce the expected attitude error. After the pre-midcourse attitude maneuvers had been accomplished, vernier engine ignition was commanded on about $38\frac{1}{2}$ hr after liftoff for a 10.5-sec period to provide a 10.3-m/sec velocity correction. Ignition was smooth, with small pitch and yaw attitude changes. It is estimated that the midcourse maneuver corrected the miss distance to within 8.6 km of the final aim point.

The peak gyro angles were less than 1 deg after vernier engine shutdown, which was well within the minimum gyro gimbal range of ± 10 deg. Inertial reference was therefore retained, and reacquisition of the sun and Canopus was accomplished via the standard reverse maneuver sequence.

d. Terminal maneuver and descent performance. The spacecraft properly executed the commanded terminal maneuvers, which were initiated about 38 min prior to retro ignition. As in the case of the pre-midcourse maneuvers, the terminal maneuvers were initiated as near as possible to the attitude control limit cycle null positions.

The automatic descent sequence was initiated by the altitude marking radar *mark* signal. The predicted and actual event times for the terminal descent are presented in Table IV-6. Ignition of the vernier engines and main retromotor was smooth, with only very small changes in

Table IV-6. Predicted and actual main retro phase events (GMT July 17, 1967, at the spacecraft)

Event	Predicted ^a	Actual (best estimate)
AMR mark	02:01:53.992	02:01:54.784
Vernier ignition	02:01:56.723	02:01:57.493
Main retro ignition	02:01:57.823	02:01:58.602
RADVS power on	02:01 58.373	02:01:59.464
RODYS signal		02:02:30.167
Loss of spacecraft signal		02:02:39.696
Inertia switch open (3.5-g level)	02:02:39.823	—
Retro case eject	02:02:51.823	—
Vernier phase start (RADVS control)	02:02:54.723	—
10-ft/sec mark	02:05:04.131	—
14-ft mark	02 05:09.631	—
Touchdown (initial)	02:05:11.331	—

^aBased upon the final post-midcourse computer run of the Terminal Guidance Program completed approximately 3 hr before retro ignition.

spacecraft attitude. RADVS turn-on occurred at the expected time, and all three velocity beams acquired lock about 32 sec after main retro ignition. The spacecraft radio signal was abruptly lost about 41.1 sec after main retro ignition, only 1.5 sec before predicted retro burnout and about 2½ min before expected touchdown. The signal loss occurred within less than a millisecond and there was no evidence of subcarrier loss before carrier loss. Exhaustive efforts to regain radio contact with *Surveyor IV* were unsuccessful.

At the time of signal loss, the spacecraft was about 49,000 ft above the lunar surface, and its velocity was 1070 ft/sec. The final data received indicated that the spacecraft condition was completely satisfactory. The only significant anomaly which had appeared during the main retro phase was greater-than-normal modulation of the thrust commands to Vernier Engines 1 and 2, which had not occurred during midcourse thrusting.

17. Technical Review Board Conclusions and Recommendations

Based on detailed examination of the telemetry records and other evidence, including the results of the working analysis groups, the Technical Review Board has been unable to identify any single or multiple cause for the failure of the *Surveyor IV* mission. The Board did conclude that the failure was in the spacecraft itself and could not be attributed to either the ground system (telemetry, tracking, or command links) or to human error. Many failure modes can be postulated, but it is not possible from the direct evidence available to pinpoint any one mode or combination of modes as a reason for the failure. The Board considers the following to be the most likely of the possible failure modes:

- (1) Breakage of critical power lead in wiring harness, or failure of connector or solder joint.

Comment: Abrupt and nearly simultaneous (within 0.25 msec) loss of carrier, subcarrier, and data was verified, and reacquisition after telemetry loss was unsuccessful. Problems have been encountered with manufacturing and reworking small-gage (22) wire to connectors and providing appropriate strain relief to multiwire harnesses.

- (2) Main retromotor case rupture.

Comment: The motor still contained about 70 lb of propellant and was 1.4 sec from the end of burn. This time corresponds to reaching zero propellant web, and excessive case heating at this point is possible. X-rays of other motors indicate the possibility

of liner separation, which can be contributory to a failure.

- (3) Failure in transmitter that caused its power to drop to zero, or value below required carrier strength, and subsequent failure of spacecraft upon its landing in Sinus Medii area.

Comment: There have been instances of loss of transmitter high power on SC-1 and SC-6.* The SC-6 anomaly, although different in character from the *Surveyor IV* signal loss, is still not resolved. Sinus Medii is considerably more hostile than the *Surveyor I* and *III* sites, and inability to reacquire telemetry could be due to damage on landing.

- (4) Failure of pressure vessel—helium tank, nitrogen tank, shock absorber, or propellant tank.

Comment: These units represent a large source of stored energy which could cause substantial fragmentation. Imperfect welds, scratches, or local defects can cause rupture of a pressure vessel a significant time after a sustained stress is applied.

The Board has concluded that any of the above failure modes is a relatively low probability occurrence, and cannot single out any one as being more likely than another. Spacecraft telemetry indicated nominal performance up to the time that carrier, subcarrier, and telemetry signals were abruptly lost. Detailed examination of the telemetry dropout from the predetection tapes at DSS 11 and 14 did not give any further insight into the nature of the failure. The only two apparent anomalies which were considered significant prior to signal dropout are:

- (1) A thrust modulation in Vernier Engines 1 and 2, indicating a relatively small moment disturbance of 300 to 500 in.-lb about Leg 3 between a frequency of 5 to 25 Hz not evidenced in previous missions.
- (2) Several sharp accelerations (up to 8 g peak-to-peak measured) at the spacecraft attach ring during *Atlas* and *Centaur* burns.

No reasonable correlation has been found between these and other less significant anomalies. Moreover, it is the Board's conclusion that the two main anomalies, thrust modulation and shocks during launch, did not cause the signal dropout.

*SC-1 through SC-7 are the serial designations of the spacecraft for the successive *Surveyor* missions beginning with *Surveyor I*.

Because of the inability to identify a specific cause and the technical impracticability of conducting an extensive ground test program to duplicate the failure, it is the Board's recommendation not to introduce any significant spacecraft change, because a change might itself be the source of some unforeseen future problem. In view of the available evidence and in view of the two previous successes (*Surveyor I* and *III* missions), it appears that the *Surveyor IV* failure was of sufficiently low probability that change in the current program is unwarranted.

However, there are certain actions that the Board has recommended. They are of three general types: (1) increasing the confidence of spacecraft preflight readiness, (2) providing some insight into the *Surveyor IV* failure, and (3) enhancing in-flight data retrieval for future missions.

The recommendations are summarized below:

- (1) Determine whether there are additional inspection techniques, particularly at AFETR, that might be employed to assure integrity of wiring terminations—especially of those wires that could cause signal loss if broken.
- (2) Determine whether there are additional inspection techniques, particularly at AFETR, that might be employed to ensure integrity of critical structural components such as the compartment thermal isolators, and to detect defects in pressure vessels.
- (3) With the participation of expert personnel not previously connected with *Surveyor*, review the inspection techniques and inspection records from all retrorockets in the program and review the processing procedures with consideration of specific questions related to detecting or preventing anomalies in the motors and providing a reproducible product.
- (4) Reverify analytically and/or by test the existence of vernier thrust command under worst-case conditions of structural resonances and stiffness, flight control and vernier engine transfer functions, propellant gas saturation, retro input, and any other pertinent parameters. The unexpected appearance of the vernier thrust command oscillation ("buzz") during the *Surveyor IV* retro phase resulted in concern by the Board that the buzz characteristics of the system are not completely understood and that on a future *Surveyor* mission the loop might be unstable.

- (5) Consider several methods suggested by the Board whereby additional data might be derived from future *Surveyor* flights in the event of abrupt signal loss.
- (6) Continue investigation of the apparent *Surveyor IV* anomalies so long as further investigation appears fruitful.
- (7) Obtain *Lunar Orbiter V* photographs of the *Surveyor IV* landing area to establish, if possible whether the spacecraft impacted the moon ballistically or whether it landed intact.
- (8) Attempt to "cover" critical phases of future *Surveyor* missions with large optical telescopes to aid in the diagnosis of certain types of failures if such should occur in the future.

B. Structures and Mechanisms

The vehicle and mechanisms subsystem provides support, alignment, thermal protection, electrical interconnection, mechanical actuation, and touchdown stabilization for the spacecraft and its components. The subsystem includes the basic spaceframe, landing gear mechanism, crushable blocks, omnidirectional antenna mechanisms, antenna/solar panel positioner (A SPP), pyrotechnic devices, electronic packaging and cabling, thermal compartments, thermal switches, and separation sensing and arming device.

1. Spaceframe and Substructure

The spaceframe, constructed of thin-wall aluminum tubing, is the basic structure of the spacecraft. The landing legs and crushable blocks, the retrorocket motor, the *Centaur* interconnect structure, the vernier propulsion engines and tanks, and the A/SPP attach directly to the spaceframe. Substructures are used to provide attachment between the spaceframe and the following subsystems: the thermal compartments, TV, SM SS, RADVS antennas, flight control sensor group, attitude control nitrogen tank, and the vernier system helium tank.

During the *Surveyor IV* mission, there was no indication of any failures or anomalies due to structural malfunctions.

Since all flight loads and vibration data indicate that the environment was significantly less severe than flight acceptance test levels, it seems extremely unlikely that any structural failure occurred on the *Surveyor IV* mission.

2. Landing Gear

The landing gear consists of three landing leg assemblies and three crushable honeycomb blocks attached to the spaceframe (Fig. IV-10). The leg assemblies are made up of a tubular inverted tripod structure, an A-frame, a lock strut, and a honeycomb footpad.

During launch, the legs are folded for stowage under the shroud. Shortly before spacecraft separation, upon command from the *Centaur* programmer, the legs are released by squib-actuated pin pullers and are extended automatically by torsion springs located at the leg hinge axes. After extension, the leg positions are measured by three potentiometers which are also located near the hinge axes.

Upon landing, each leg pivots about its hinge axis. Landing loads are absorbed by compression of the upper member of the tripod, which is a combined shock absorber and spring assembly. The shock absorber columns are instrumented with strain gages. Axial loads measured by the strain gages are telemetered to provide continuous analog traces during the terminal descent and touch-down phase.

For a vertical landing on a hard, level surface at a velocity in excess of about 8.5 ft/sec, the crushable blocks will contact the surface. Energy will then be dissipated if the blocks penetrate the surface or by crushing of the blocks if the surface bearing strength exceeds 40 psi.

Crushing of the honeycomb footpads is not expected for landing velocities below about 11.5 ft/sec or for surface bearing strength less than about 10 psi.

On the *Surveyor IV* mission, landing gear deployment was normal.

3. Omnidirectional Antennas

The omnidirectional antennas are mounted on the ends of folding booms hinged to the spaceframe. Pins retain the booms in the stowed position during launch. Squib-actuated pin pullers release the booms upon command from the *Centaur* shortly before spacecraft separation. A leaf-type kickout spring on each omniantenna boom initiates movement. Torsion springs continue the movement to the fully deployed positions, where the booms are automatically locked.

The *Surveyor IV* omniantenna booms were extended by *Centaur* command, and both antennas were locked in the landing or transit position as indicated by the telemetry.

4. Antenna and Solar Panel Positioner

The A/SPP supports and positions the high-gain planar array antenna and solar panel. The planar array antenna and solar panel have four axes of rotation: roll, polar, solar, and elevation (Fig. IV-11). Stepping motors rotate the axes in either direction in response to commands

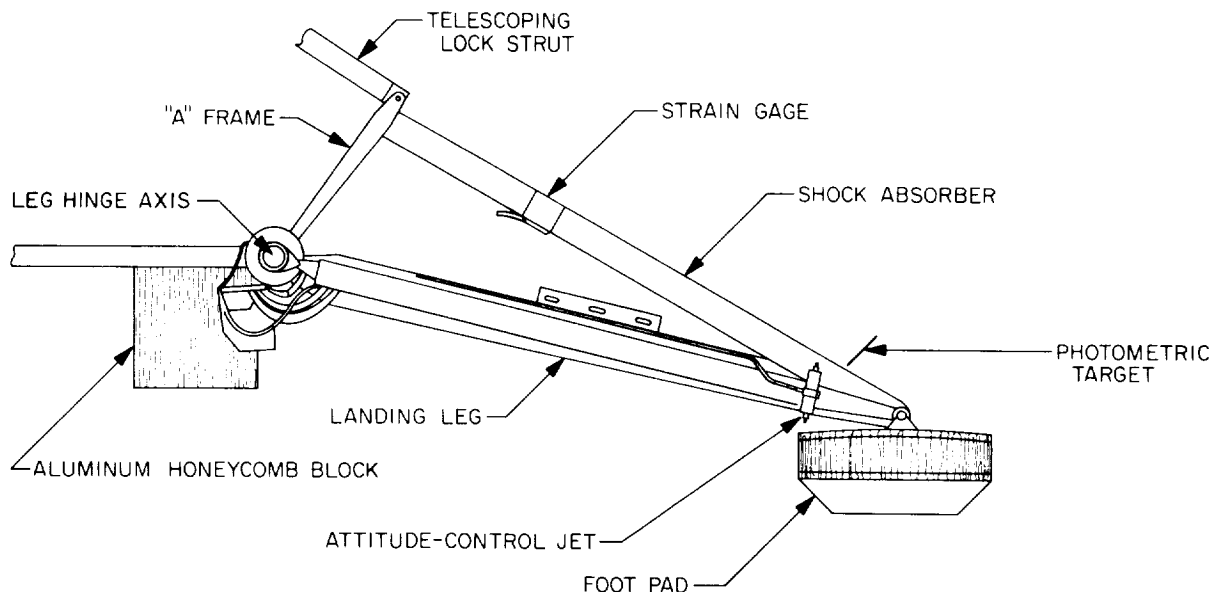


Fig. IV-10. Landing leg assembly

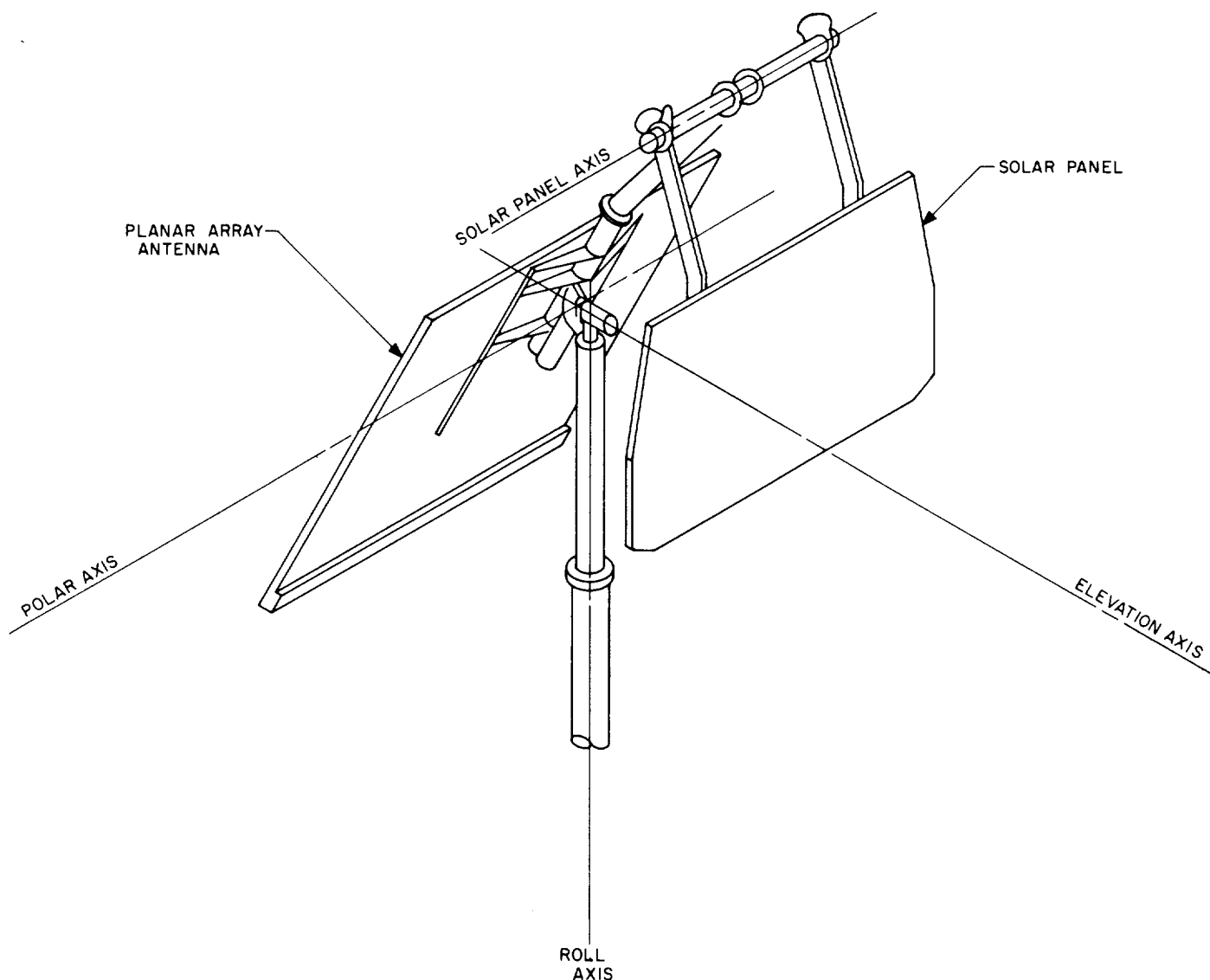


Fig. IV-11. Antenna/solar panel configuration

from earth or during automatic deployment following *Centaur*/spacecraft separation. This freedom of movement permits orienting the planar array antenna toward the earth and the solar panel toward the sun.

The solar axis is locked in a vertical position for stowage in the nose fairing. After spacecraft separation, the solar panel is positioned parallel to the spacecraft X-axis. The A/SPP remains locked in this position until after touchdown, at which time the roll, solar, and elevation axes are released. Potentiometers on each axis indicate A/SPP orientation. Each command from earth gives $\frac{1}{8}$ deg of rotation in the roll, solar, and elevation axes and $\frac{1}{16}$ deg in the polar axis.

The A/SPP operated as expected during the *Surveyor IV* mission. After spacecraft separation, the roll and solar axes moved to their transit positions.

5. Thermal Compartments

Two thermal compartments (A and B) house thermally sensitive electronic items. Equipment in the compartments is mounted on thermal trays that distribute heat throughout the compartments. An insulating blanket, consisting of 75 sheets of 0.25-mil-thick aluminized mylar, is installed between the inner shell and the outer protective cover of the compartments. Each compartment employs

thermal switches (9 on Compartment A and 6 on Compartment B) which are capable of varying the thermal conductance between the inner compartment and the external radiating surface. The thermal switches maintain thermal tray temperature below $+125^{\circ}\text{F}$. Each compartment contains a thermal control and heater assembly to maintain the temperature of the thermal tray above a specified temperature (above 40°F for Compartment A and above 0°F for Compartment B). The thermal control and heater assembly is capable of automatic operation, or may be turned on or off by earth command. Components located within the compartments are identified in Table IV-7.

6. Thermal Switch

The thermal switch is a thermal-mechanical device which varies the conductive path between an external

radiation surface and the top of the compartment (Fig. IV-12). The switch is made up of two contact surfaces which are ground to within one wavelength of being optically flat. One surface is then coated with a conforming substance to form an intimate contact with the mating surface. The contact actuation is accomplished by four bimetallic elements located at the base of the switch. These elements are connected mechanically to the top of the compartment so that the compartment temperature controls the switch actuation. The switches are identical, and were adjusted to open at a temperature of $35 \pm 10^{\circ}\text{F}$ on the *Surveyor IV* mission.

The external radiator surface is such that it absorbs only 12% of the solar energy incident on it and radiates 74% of the heat energy conducted to its surface. When the switch is closed and the compartment is hot, the switch loses its heat energy to space. When the compartment gets cold, the switch contacts open about 0.020 in., thereby opening the heat-conductive path to the radiator and thus reducing the heat loss through the switch to almost zero. Three of the switches on each compartment are instrumented with temperature sensors attached to the radiators. The temperature sensors provide an indication of switch actuation for those switches which are monitored.

On the *Surveyor I* and *III* missions, thermal compartment cooling rates after sunset indicated that some switches had stuck in the closed position. Special tests were conducted to investigate this problem, the results of which led to a special process that was used first for the *Surveyor IV* switches. This process consisted of vacuum-backing the contact coating at 300°F to drive off

Table IV-7. Thermal compartment component installation

Compartment A	Compartment B
Receivers (2)	Central command decoder
Transmitters (2)	Boost regulator
Main battery	Central signal processor
Battery charge regulator	Signal processing auxiliary
Engineering mechanisms auxiliary	Engineering signal processor
Television auxiliary	Low data rate auxiliary
Thermal control and heater assembly	Thermal control and heater assembly
Auxiliary battery control	Auxiliary engineering signal processor

Table IV-8. Pyrotechnic devices

Type	Location and use	Quantity of devices	Quantity of squibs	Command source
Pin pullers	Lock and release Omnantennas A and B	2	2	<i>Centaur</i> programmer
Pin pullers	Lock and release landing legs	3	3	<i>Centaur</i> programmer
Pin pullers	Lock and release planar antennas and solar panel	7	7	Separation sensing and arming device and ground station
Pin puller	Lock and release Vernier Engine 1	1	1	Ground station
Pin puller	SM/SS unlatch mechanism	1	1	Ground station
Separation nuts	Retro rocket attach and release	3	6	Flight control subsystem
Valve	Helium gas release and dump	1	2	Ground station
Pyro switches	EMA Board 4, RADVS power on and off	4	4	Ground station and flight control subsystem
Initiator squibs	Safe and arm assembly retrorocket initiators	1	2	Flight control subsystem
Locking plungers	Landing leg, shock absorber locks	3	3	Ground station
		26	31	

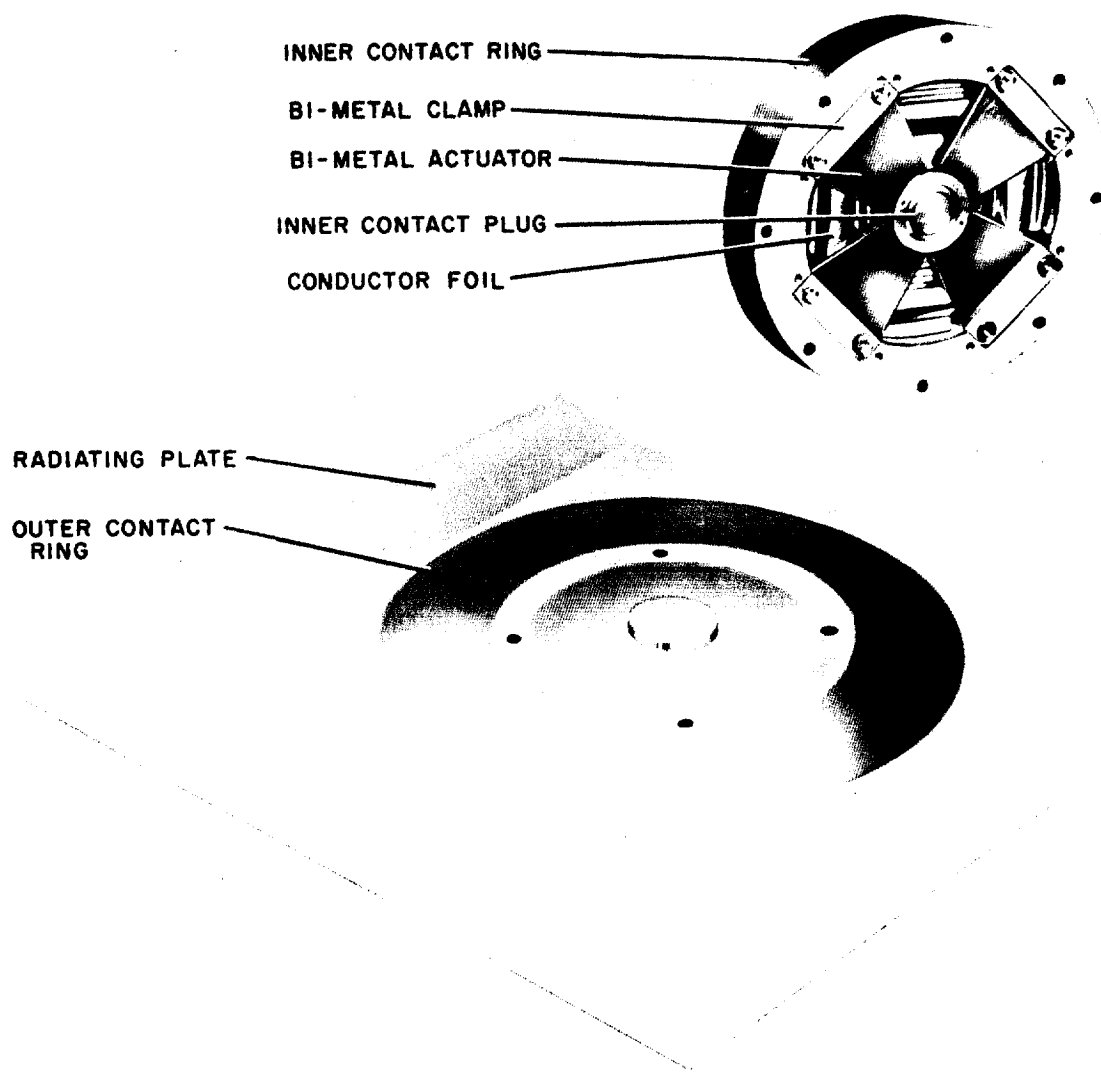


Fig. IV-12. Thermal switch

the volatile materials which had been found to contribute to the sticking.

On the *Surveyor IV* mission, the thermal switches were closed during flight and kept the electronics at or below the maximum allowable temperature at all times.

7. Pyrotechnic Devices

The pyrotechnic devices installed on *Surveyor IV* are indicated in Table IV-8. All the squibs used in these devices are electrically initiated, hot-bridgewire, gas-generating devices. Qualification tests for flight squibs

included demonstration of reliability at a firing current level of 4 or 4.5 A. "No Fire" tests were conducted at a 1-A or 1-W level for 5 min. Electrical power required to initiate pyrotechnic devices is furnished by the spacecraft main battery. Power distribution is through 19.0- and 9.5-A constant-current generators in the engineering mechanism auxiliary (EMA).

All pyrotechnic devices functioned normally upon command. Mechanical operation of locks, valves, switches, and plunger, actuated by squibs, was indicated on telemetry signals as part of the spacecraft engineering measurement data.

8. Electronic Packaging and Cabling

The electronic assemblies provide mechanical support for electronic components in order to insure proper operation throughout the various environmental conditions to which they are exposed during a mission. The assemblies (or control items) are constructed utilizing sheet metal structure, sandwich-type etched circuit board chassis with two-sided circuitry, plated through holes, and/or bifurcated terminals. Each control item, in general, consists of only a single functional subsystem and is located either in or out of the two thermally controlled compartments, depending on the temperature sensitivity of the particular subsystem. Electrical interconnection is accomplished primarily through the main spacecraft harness. The cabling system is constructed utilizing a light-weight, minimum-bulk, and abrasion-resistant wire which is an extruded teflon having a dip coating of modified polyamide.

C. Thermal Control

The thermal control subsystem is designed to provide acceptable thermal environments for all components during all phases of spacecraft operation. Spacecraft items with close temperature tolerances were grouped together in thermally controlled compartments. Those items with wide temperature tolerances were thermally decoupled from the compartments. The thermal design fits the "basic bus" concept in that the design was conceived to require minimum thermal design changes for future missions. Monitoring of the performance of the spacecraft thermal design is done by 77 engineering temperature sensors which are distributed throughout the spacecraft as follows:

Flight control	9
Mechanisms	3
Radar	7
Electrical power	5
Transmitters	2
Survey TV	4
Vehicle structure	30
Propulsion	16
SM/SS electronics	1

The spacecraft thermal control subsystem is designed to function in the space environment, both in transit and on the lunar surface. Extremes in the environment as well

as mission requirements on various pieces of the spacecraft have led to a variety of methods of thermal control. The spacecraft thermal control design is based upon the absorption, generation, conduction, and radiation of heat.

The radiative properties of the external surfaces of major items are controlled by using paints, by polishing, and by using various other surface treatments. Reflecting mirrors are used to direct sunlight to certain components. In cases where the required radiative isolation cannot be achieved by surface finishes or treatments, the major item is covered with an insulating blanket composed of multiple-sheet aluminized mylar. This type of thermal control is called "passive" control.

The major items whose survival or operating temperature requirements cannot be achieved by surface finishing or insulation alone use heaters that are located within the unit. These heaters can be operated by external command, thermostatic actuation, or both. The thermal control design of those units using auxiliary heaters also includes the use of surface finishing and insulating blankets to optimize heater effectiveness and to minimize the electrical energy required. Heaters are considered "active" control.

Items of electronic equipment whose temperature requirements cannot be met by the above techniques are located in thermally controlled compartments (A and B). Each compartment is enclosed by a shell covering the bottom and four sides and contains a structural tray on which the electronic equipment is mounted. The top of each compartment is equipped with a number of temperature-actuated switches (9 in Compartment A and 6 in Compartment B). These switches, which are attached to the top of the tray, vary the thermal conductance between the tray and the outer radiator surfaces, thereby varying the heat-dissipation capability of the compartments. When the tray temperature increases, heat transfer across the switch increases. During the lunar night, the switch opens, decreasing the conductance between the tray and the radiators to a very low value in order to conserve heat. When dissipation of heat from the electronic equipment is not sufficient to maintain the required minimum tray temperature, a heater on the tray supplies the necessary heat. The switches are considered "semi-active."

Examples of units which are controlled by active, semi-active, or passive means are shown in Fig. IV-13.

The thermal performance of the spacecraft was nominal up to the time of signal loss except for two minor

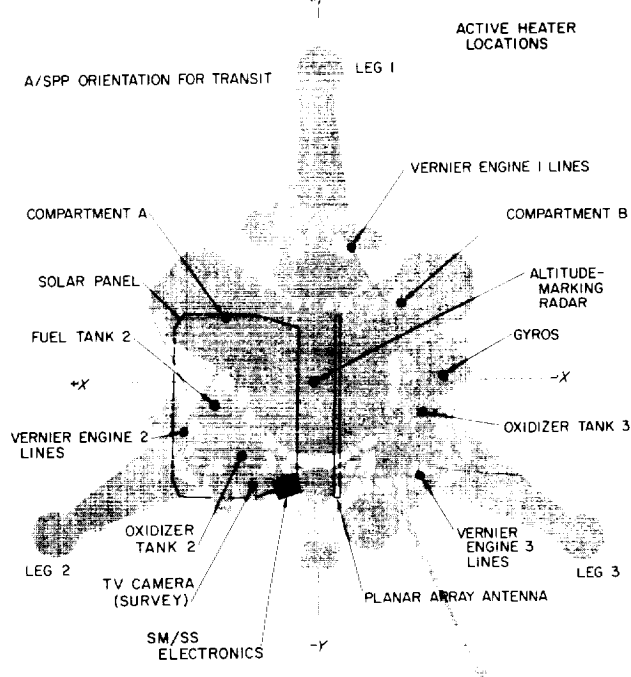
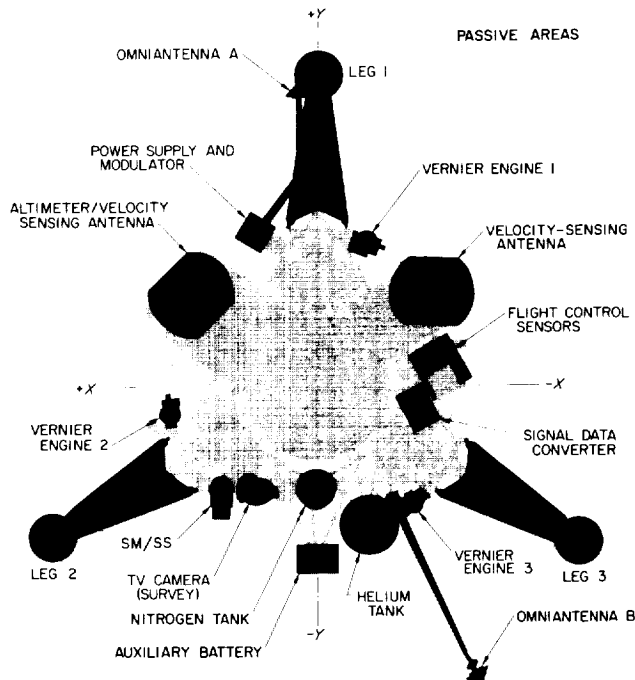
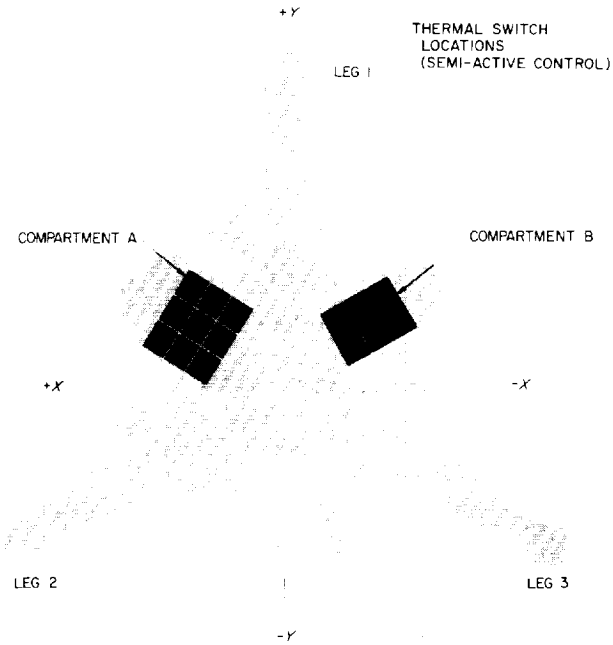
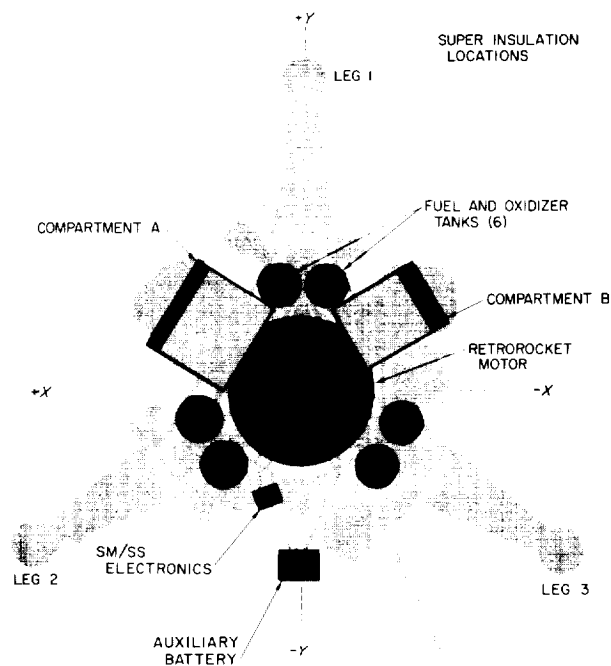


Fig. IV-13. Thermal design

anomalies which were noted during the flight. An expected increase in attitude jet temperature due to the grey stripes on the footpad did not occur and the jet temperature was the same as on the previous mission. A sudden increase of 5°F in Oxidizer Tank 1 temperature at $L + 30$ hr was noted. The temperature rise occurred after the end of one of the gyro drift checks, although this drift check was not different from the other 12 checks made during the mission. Subsequent performance of the vernier propulsion system was nominal.

Thermal data during retro-fire was as expected, with nothing to indicate any failures.

Appendix D contains plots of the transit temperatures.

D. Electrical Power

The electrical power subsystem is designed to generate, store, convert, and distribute electrical energy. A block diagram of the subsystem is shown in Fig. IV-14. The subsystem derives its energy from the solar panel and the spacecraft battery system. The solar panel converts solar radiation energy into electrical energy. Solar panel power capability is affected by temperature and the incidence of solar radiation and varies from 90 to 55 W.

The spacecraft battery system consists of a main battery and an auxiliary battery. The main battery is a secondary or rechargeable battery; the auxiliary battery is a primary or nonrechargeable battery.

The batteries provide about 1690 W-hr during transit, the balance of the energy being supplied by the solar panel. The maximum storage capacity of the main battery is 165 A-hr; that of the auxiliary battery is 50 A-hr. The selection of battery operation mode is determined by the auxiliary battery control (ABC). There are three modes of battery operation: *main battery* mode, *auxiliary battery* mode, and *high-current* mode. In the *main battery* mode only the main battery is connected to the unregulated bus. This is the nominal configuration. In the *auxiliary battery* mode, the main battery is connected to the unregulated bus through a series diode, while the auxiliary battery is directly connected. In the *high-current* mode, both the main and auxiliary batteries are connected to the unregulated bus without the series diode. The battery modes are changed by earth commands except that the ABC automatically switches to *auxiliary battery* mode from *main battery* mode in case of main battery failure. This automatic function can be disabled by earth command.

The four modes of solar panel operation are controlled by the battery charge regulator (BCR). In the *on* mode, the optimum charge regulator (OCR) tracks the volt/ampere characteristic curve of the solar panel and hunts about the maximum power point. In the OCR *off* mode, the solar panel output is switched off. This mode is intended to prevent overcharging of the main battery by the solar panel. In the OCR *bypass* mode, the solar panel is connected directly to the unregulated bus. This mode is used in case of OCR failure. In the *trickle charge* mode, the main battery charging current is controlled by its terminal voltage. All of the BCR modes except the *trickle charge* mode are controlled by earth commands.

The OCR *off* and *trickle charge* modes are automatically controlled by the battery charge logic (BCL) circuitry. When the main battery terminal voltage exceeds 27.5 V or its manifold pressure exceeds 65 psia, the BCR goes automatically to the *off* mode. The *trickle charge* mode is automatically enabled when the main battery terminal voltage reaches 27.23 V. The BCL can be disabled by earth command.

Current from the BCR and spacecraft batteries is distributed to the unregulated loads and the boost regulator (BR) via the unregulated bus. The voltage on the unregulated bus can vary between 17.5 and 27.5 V, with a nominal value of 22 V. The BR converts the unregulated bus voltage to $29.0 \text{ V} \pm 1\%$ and supplies the regulated loads. The preregulator supplies a regulated $30.4 \text{ V} \pm 1\%$ to the preregulated bus. The essential loads are fed by the preregulated bus through two diodes in series. The diodes drop the preregulated bus voltage of 30.4 V to the essential bus voltage of 29.0 V. The preregulated bus also feeds the flight control regulator and the nonessential regulator, which in turn feed the flight control and nonessential busses, respectively. These regulators can be turned on and off by earth commands. The nonessential regulator has a *bypass* mode of operation which connects the preregulated bus directly to the nonessential bus. This mode is used if the nonessential regulator fails.

The power subsystem operated normally throughout the mission. The data presented in Table IV-9 verifies that telemetered parameters were in close agreement with the predicted values during transit. The average solar panel output current was 1.80 A at an average voltage of 48.8 V. Average OCR output current was 3.2 A, which agrees with the test data. Overall OCR efficiency was about 79%.

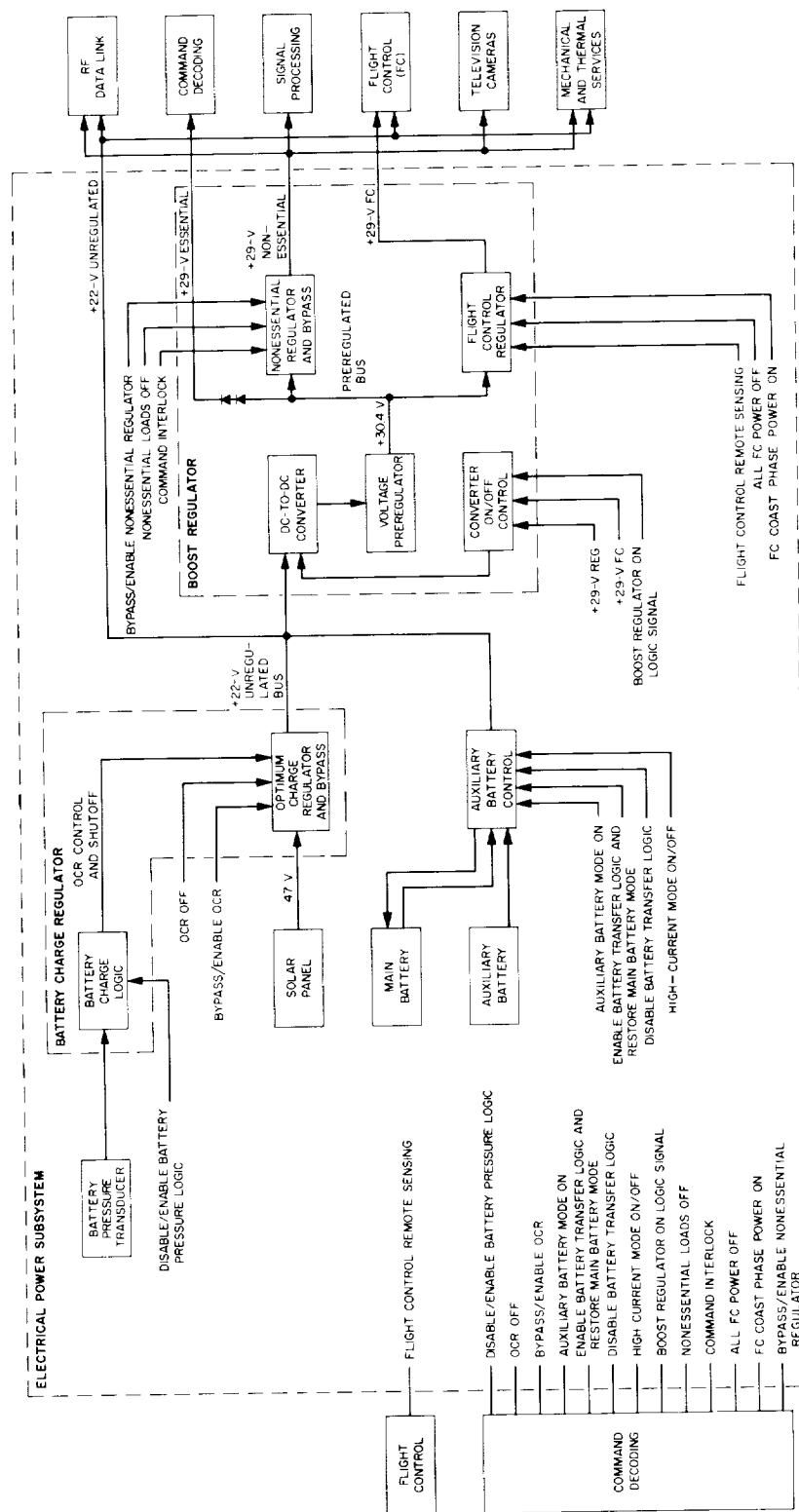


Fig. IV-14. Simplified electrical power functional block diagram

Table IV-9. Summary of power subsystem performance

Parameter	Time from liftoff	Predicted	Actual
Solar panel power, W	Throughout transit	85	86
Optimum charge regulator (OCR) power output, W	Throughout transit	70	71
Main battery stored energy, A-hr	0 hr	165	165
	22	139	143
	40	118	123
	50	111	116
	60	106	111
	62	102	104
Auxiliary battery stored energy, A-hr	0	45	45
	44	45	45
	55	39	40
	62	30	29
Average OCR efficiency, %	Throughout transit	78	79
Average boost regulator efficiency, %	Throughout transit	77	77.6
Battery discharge current, A	{ High-power periods	4.35	4.45
	{ Low-power periods	0.73	0.88
Regulated current, A	{ High-power periods	3.90	3.94
	{ Low-power periods	1.72	1.72
OCR output current, A	{ High-power periods	3.28	3.2
	{ Low-power periods	3.28	3.2
Unregulated current, A (EP4 and EP40)	{ High-power periods	1.10	1.14
	{ Low-power periods	1.10	1.14

The main and auxiliary battery energy levels at liftoff were 3608 and 1150 W-hr, respectively. In transit, the solar panel supplied an average of 78.3% of the total system electrical loads during low-power periods and 41.7% during high-power periods. The spacecraft batteries provided the balance of electrical power required. Profiles of stored battery energy during transit are shown in Fig. IV-15. The profiles closely follow the power management program curve. Total battery discharge current is shown in Fig. IV-16.

The main battery pressure stabilized during transit to 13.2 psia at a steady-state battery temperature of 76°F, both measurements falling well within the normal safe operating limits. During the last part of the transit phase, the auxiliary battery temperature was raised by operating in auxiliary battery mode to insure adequate voltage. This mode of operation also allowed the main battery to retain a greater amount of energy for posttouchdown operations. The main battery energy at time of loss of data was estimated to be 2250 W-hr.

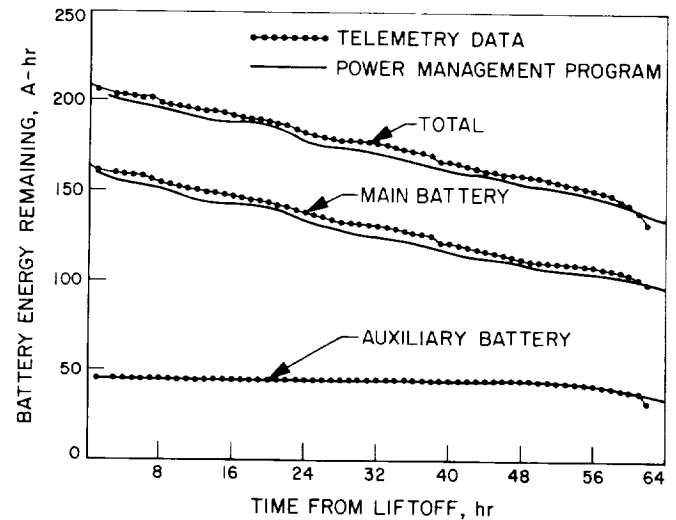


Fig. IV-15. Battery energy remaining

The power subsystem telemetry data prior to loss of the spacecraft signal was completely normal and gave no indication of the cause of failure of the *Surveyor IV* mission.

E. Propulsion

The propulsion subsystem supplies thrust force during the midcourse correction and terminal descent phases of the mission. The propulsion subsystem consists of a vernier engine system and a solid-propellant main retro-rocket motor. The propulsion subsystem is controlled by the flight control system through preprogrammed maneuvers, commands from earth, and maneuvers initiated by flight control sensor signals.

1. Vernier Propulsion

The vernier propulsion subsystem supplies the thrust forces for midcourse maneuver velocity vector correction, attitude control during main retrorocket motor burning, and velocity vector and attitude control during terminal descent. The vernier engine system consists of three thrust chamber assemblies and a propellant feed system. The feed system is composed of three fuel tanks, three oxidizer tanks, a high-pressure helium tank, propellant lines, and valves for system arming, operation, and deactivation.

Fuel and oxidizer are contained in six tanks of equal volume, with one pair of tanks for each engine. Each tank contains a teflon expulsion bladder to permit complete and positive expulsion and to assure propellant

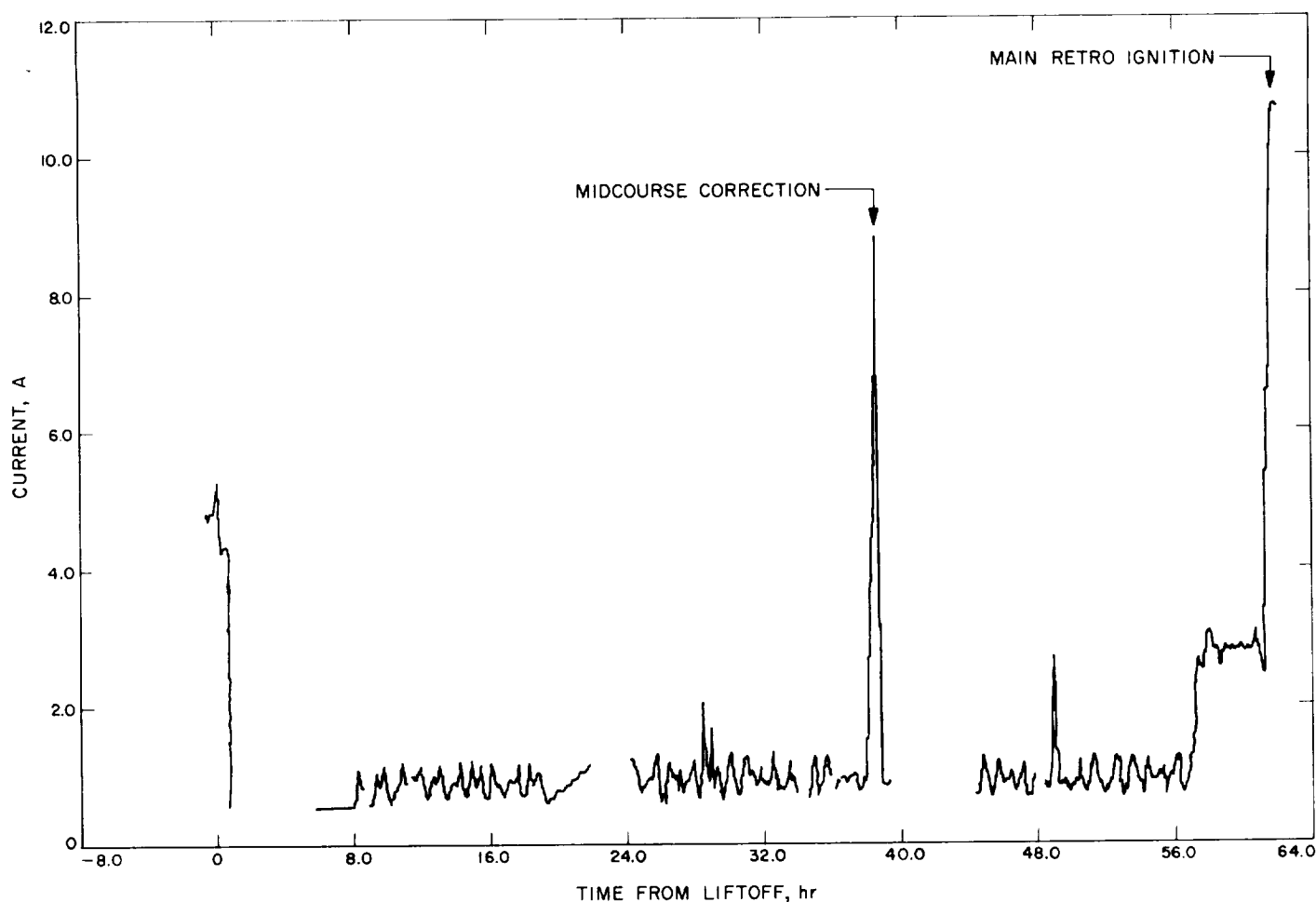


Fig. IV-16. Total battery discharge current

control under zero-g conditions. The oxidizer is nitrogen tetroxide (N_2O_4) with 10% by weight nitric oxide (NO) to depress the freezing point. The fuel is monomethyl hydrazine monohydrate ($MMH \cdot H_2O$). Fuel and oxidizer ignite hypergolically when mixed in the thrust chamber. The total minimum usable propellant load is 178.3 lb. The arrangement of the tanks on the spaceframe is illustrated in Fig. IV-17. Propellant freezing or overheating is prevented by a combination of active and passive thermal controls, utilizing surface coatings, multilayered blankets, and electrical and solar heating. The propellant tanks are thermally isolated to insure that the spacecraft structure will not function as a heat source or heat sink.

Propellant tank pressurization is provided by the helium tank and valve assembly as shown in the vernier propulsion system schematic of Fig. IV-18. The high-pressure helium is released to the propellant tanks by activating a squib-actuated helium release valve. A single-stage regulator maintains the propellant tank pressure at 730 psi.

Helium relief valves relieve excess pressure from the propellant tanks in the event of a helium pressure regulator malfunction.

The thrust chambers (Fig. IV-19) are located near the hinge points of the three landing legs on the bottom of the main spaceframe. The moment arm of each engine is about 38 in. Engine 1 can be rotated ± 6 deg about an axis in the spacecraft X-Y plane for spacecraft roll control. The Engine 1 roll actuator is unlocked by the same command that actuates the helium release valve.

Engines 2 and 3 are not movable. The thrust of each engine (which is monitored by strain gages installed on each engine mounting bracket) can be throttled over a range of 30 to 104 lb. The specific impulse varies with engine thrust.

Based on available data on the *Surveyor IV* mission, the vernier propulsion subsystem remained well within

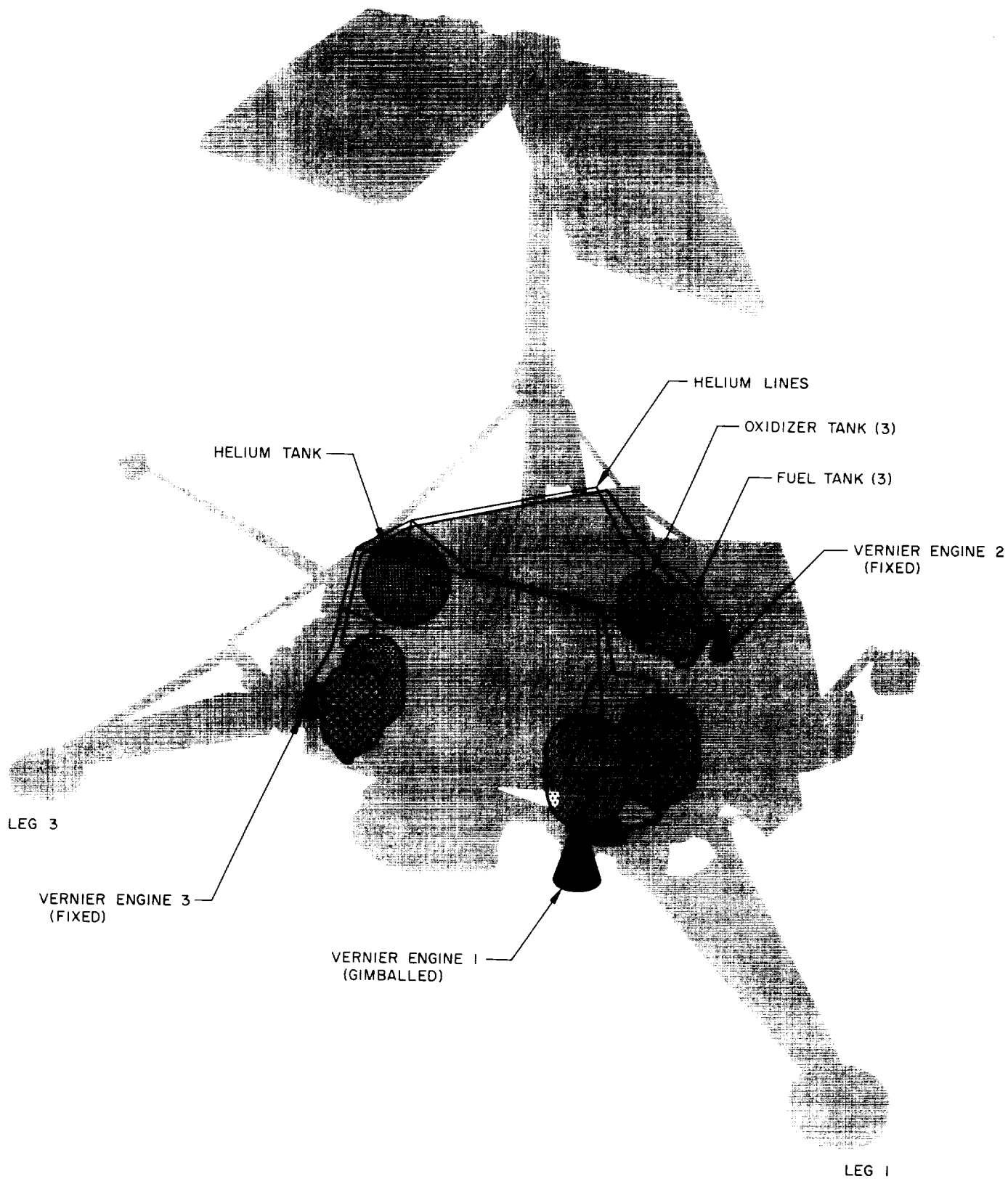


Fig. IV-17. Vernier propulsion system installation

performed in a nominal fashion with no anomalies or errors apparent. The desired thrust duration of 10.5 sec was established by previous ground command stored in the flight control. The difference between the actual firing

Table IV-10. Vernier thrust levels during midcourse correction, lb

Engine	Average thrust command (last 5 sec of midcourse)	Thrust command offset before ignition	Corrected average thrust command	Predicted thrust	Error
1	78.0	2.7	75.3	75.3	0
2	76.3	2.5	73.8	76.9	-3.1
3	81.6	1.6	80.0	77.2	2.8
			229.1	229.4	-0.3

duration and the commanded duration was less than the resolution level of the telemetry system. The predicted and actual average thrust levels during the last 5 sec of midcourse correction are presented in Table IV-10. The shutdown impulse provided by the engines was between 0.0 and 0.175 lb-sec.

Following midcourse, during the second cruise portion of the mission, the propulsion subsystem parameters maintained nominal levels.

At 02:01:55 GMT on July 17, 1967, the terminal descent sequence was initiated by the generation of an electrical signal from the spacecraft altitude marking radar. Approximately 2.75 sec later, vernier ignition occurred; after

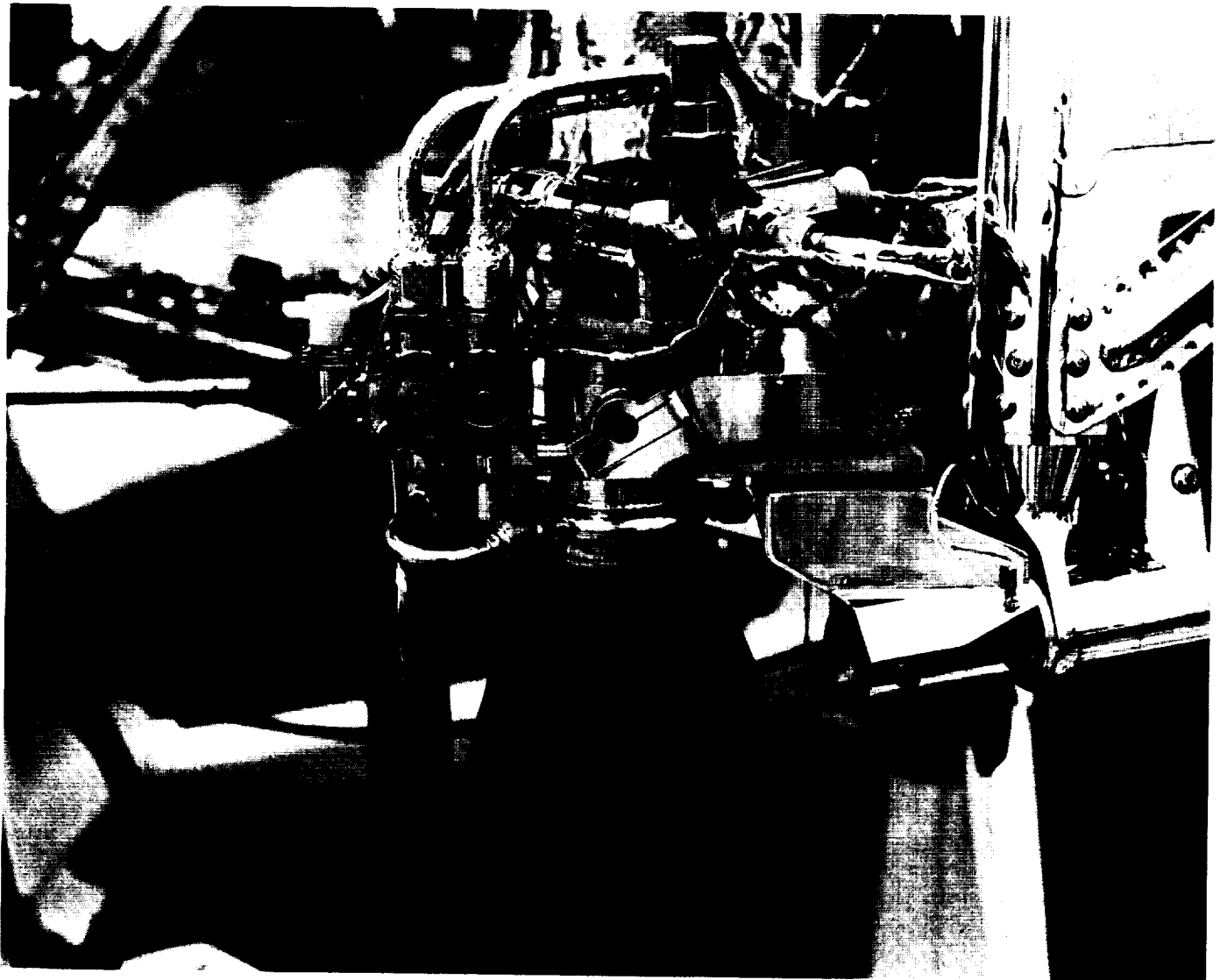


Fig. IV-19. Vernier engine thrust chamber assembly

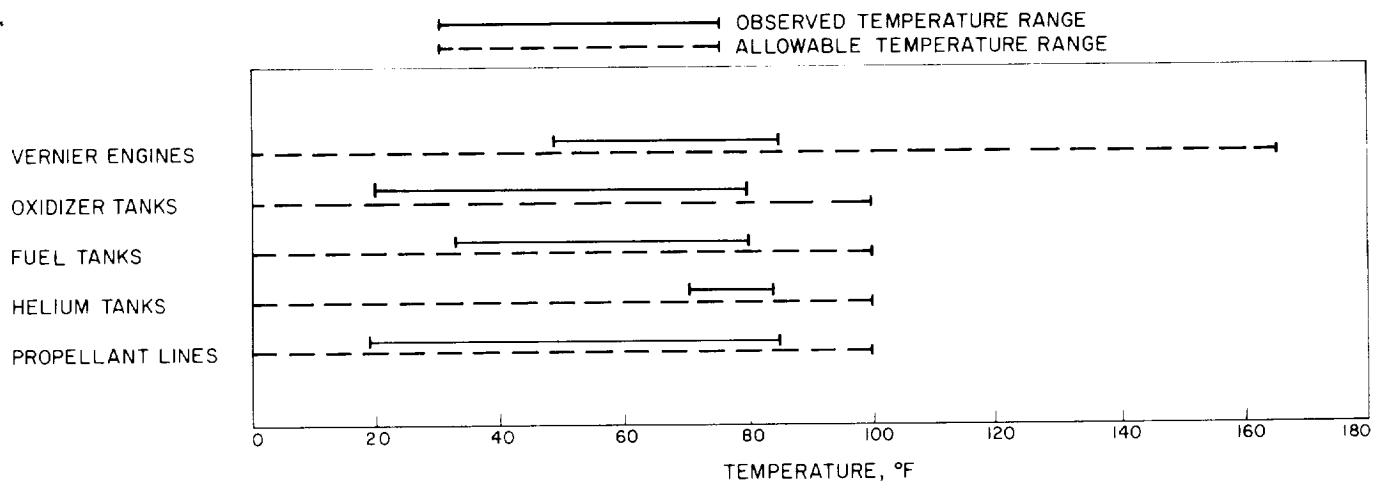


Fig. IV-20. Vernier propulsion subsystem transit temperature ranges

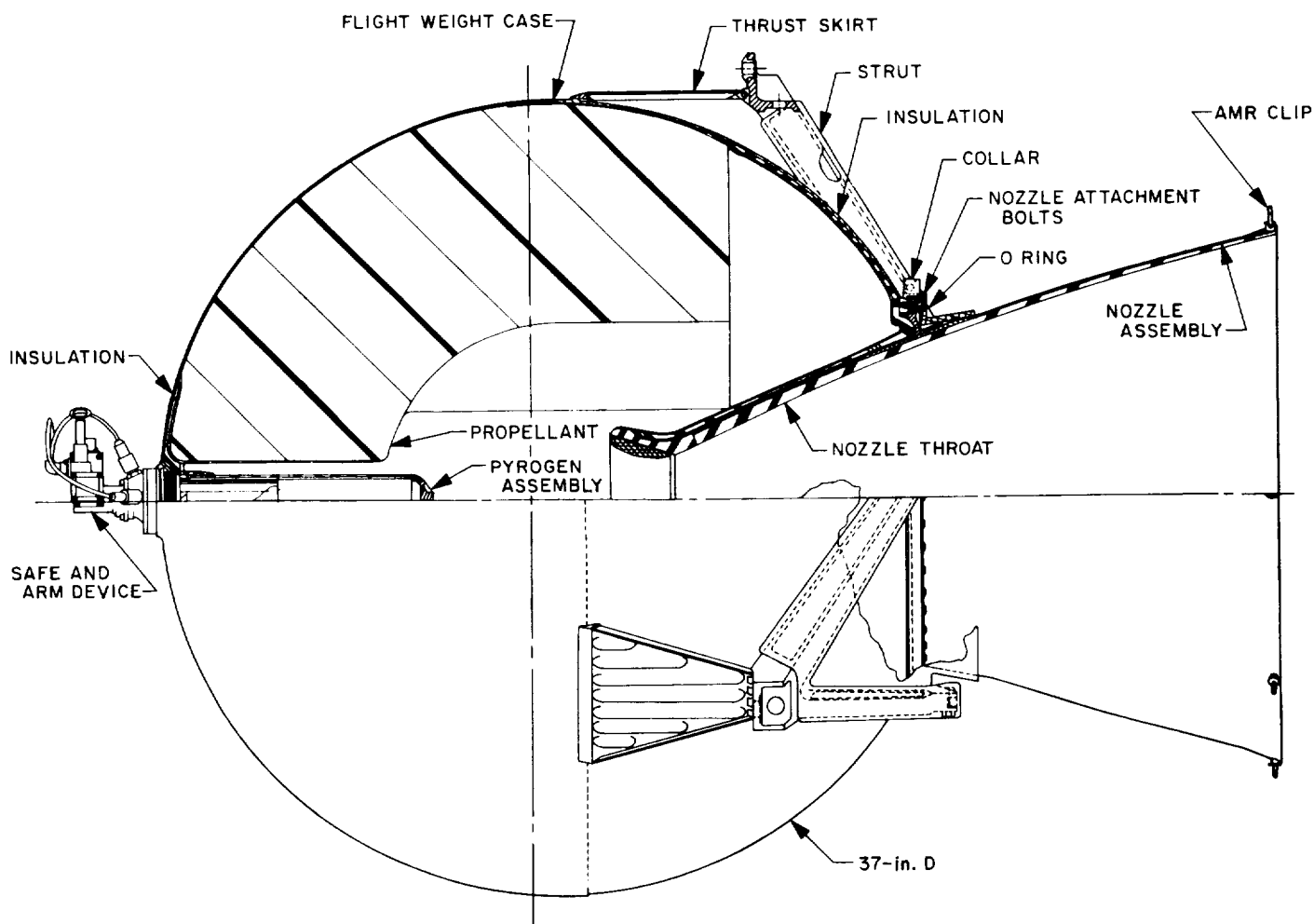


Fig. IV-21. Main retrorocket motor

an additional programmed interval of 1.1 sec, ignition of the main retromotor took place. At approximately 02:02:41 GMT the spacecraft RF signal was abruptly lost by the DSIF.

Prior to the loss of signal, all vernier propulsion system parameters were normal and at or near their predicted levels with only one anomaly. The observed anomaly was modulation of the thrust commands to Engines 1 and 2 during the retro period (see Section IV-F—Spacecraft Flight Control). Thrust commands to Engine 3 were not modulated during this period, and no modulation in the commands to the engines occurred during the midcourse correction. The peak-to-peak modulation of Engines 1 and 2 thrust commands was 3 to 6 lb compared to an engine throttling range of ± 37 lb. The average values of Engines 1 and 2 thrust were near the expected mid-thrust level of 66.7 lb. The modulation at no time threatened the ability of the vernier engines to control the attitude of the spacecraft since the amplitude of the modulation was much less than the throttling range of the engines. It does not appear that this anomaly is symptomatic of a failure which could have caused the loss of signal from the spacecraft.

2. Main Retrorocket

The main retrorocket, which performs the major portion of the deceleration of the spacecraft during terminal descent, is a spherical, solid-propellant unit with a partially submerged nozzle to minimize overall length (Fig. IV-21). The motor utilizes a carboxyl-terminated polyhydrocarbon, composite-type propellant and conventional grain geometry.

The motor case is attached at three points on the main spaceframe near the landing leg hinges, with explosive nut disconnects for postburnout ejection. Friction clips around the nozzle flange provide attachment points for the altitude marking radar (AMR). The *Surveyor IV* retrorocket, including the thermal insulating blankets, weighed approximately 1445 lb. This total included about 1300 lb of propellant. The thermal control design of the retrorocket motor is completely passive, depending on its own thermal capacity and insulating blanket (21 layers of aluminized mylar plus a cover of aluminized teflon). The prelaunch temperature of the unit is $70 \pm 5^\circ\text{F}$. At terminal maneuver, when the motor is ignited, the propellant will have cooled to a thermal gradient with a bulk average temperature of about 50 to 55°F .

The AMR normally triggers the terminal maneuver sequence. When the retro firing sequence is initiated,

the retrorocket gas pressure ejects the AMR. The motor operates at a thrust level of 8,000 to 10,000 lb for approximately 42.5 sec at an average propellant temperature of 55°F .

Beginning at a launch bulk average temperature of approximately 72°F , the retro cooled at the predicted rate to an average temperature of 55°F at the time of ignition. At this temperature the burn time was predicted to be 42.53 sec.

The main retro ignited as programmed and burned normally until the loss of all spacecraft telemetered data. Abrupt loss of all spacecraft data occurred 41.1 sec after main retro ignition. The retromotor had passed its peak pressure and was just beginning its thrust tailoff. This point corresponds to "100% web point," where the only unconsumed propellant is in the form of propellant slivers. It is estimated that at this time the chamber pressure was 475 psi and that approximately 70 lb of propellant was in the case.

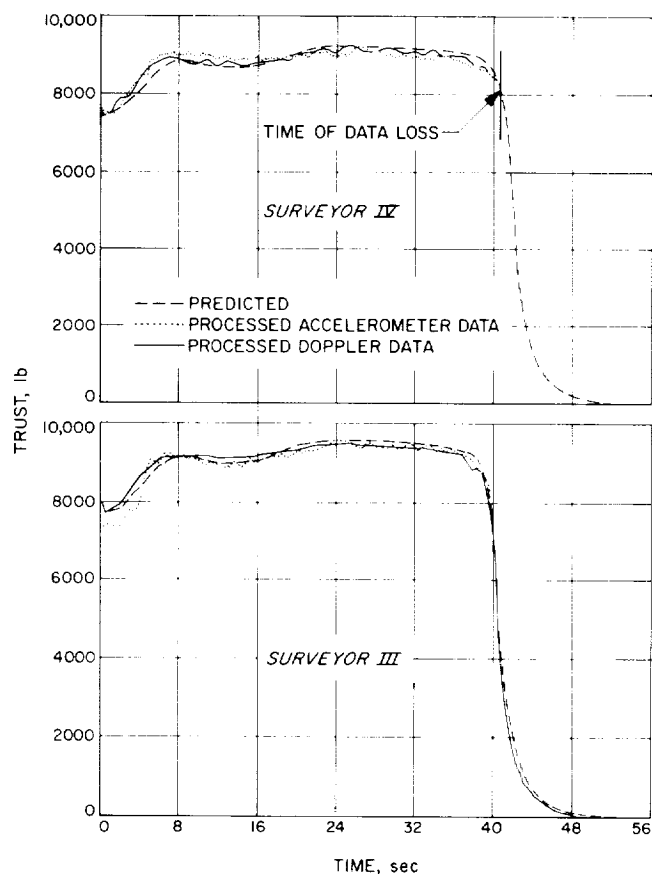


Fig. IV-22. Main retromotor thrust vs time

Main retro thrust vs time curves reconstructed from the doppler and accelerometer data are shown in Fig. IV-22. The actual thrust vs time curves show good agreement with the predicted curve up to loss of transmitted data. (Curves for the successful *Surveyor III* mission are also shown for reference.) For the main retro thrust period to the point of spacecraft signal loss, the actual and predicted changes in velocity were calculated to be 7705 and 7747 ft/sec, respectively. This amounts to only 0.55% low, compared to $\pm 1\%$ allowed deviation from the nominal. The low value is conservative since the total velocity difference is actually due to a number of sources in addition to the main retro and the fact that the retro had not completely burned out. The maximum retro thrust was calculated to be 9200 lb, compared to a predicted value of 9250 lb. There was no indication of any abnormal retro operation prior to the loss of the spacecraft signal.

The modulation of Vernier Engines 1 and 2 thrust commands during main retro burning was such that it is not possible to compute meaningful pitch, yaw, or roll moment data. In addition, since the spacecraft telemetry signal was lost prior to retro burnout, no data is available

on retro burn time or retro separation from the spacecraft.

F. Flight Control

The flight control subsystem provides spacecraft velocity and attitude control during transit from the time of spacecraft separation from the *Centaur* vehicle to spacecraft touchdown on the lunar surface. The basic flight control functions include:

- (1) Attitude stabilization and orientation during transit.
- (2) Midcourse velocity correction based on ground commands.
- (3) Retro ignition and ejection and vernier descent control for soft-landing of the spacecraft.

1. Flight Control Description

The flight control subsystem consists of reference sensing elements, flight control and mode control electronics, and vehicle control elements functionally arranged as shown in Fig. IV-23.

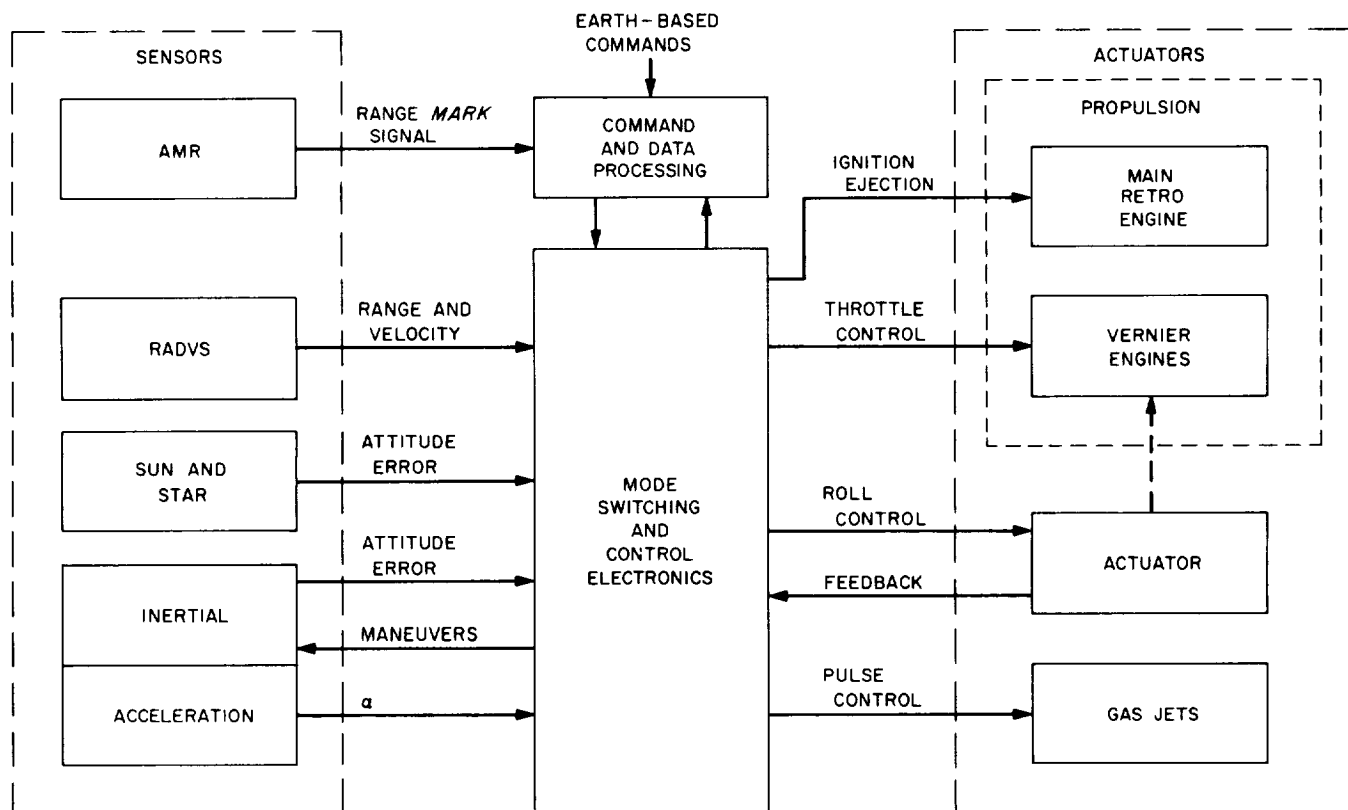


Fig. IV-23. Simplified flight control functional diagram

The principal references used by the spacecraft are inertial, celestial, and lunar; each is sensed respectively by inertial, optional, and radar sensors. The control electronics process the reference sensor outputs, earth-based commands, and the flight control programmer and decoder outputs to generate the necessary control signals for use by the vehicle control elements. The vehicle control elements consist of the attitude-control cold-gas-jet activation valves and gas supply system, the vernier engine throttlable thrust valves and controllable gimbal actuator, and the main retro igniter and retro case separation pyrotechnics.

The gas-jet attitude control system is a cold gas system using nitrogen as a propellant. This system consists of a gas supply system and three pairs of solenoid-valve-operated gas jets interconnected with tubing (see Fig. IV-24). The nitrogen supply tank is initially charged to a nominal pressure of 4600 psia. Pressure to the gas jets is controlled to 40 ± 2 psia by a regulator.

Vehicle response in attitude, acceleration, and velocity is controlled as needed by various "control loops" throughout the coast and thrust phases of flight, as shown in Table IV-11. Upon separation of the spacecraft from the *Centaur*, stabilization of the spacecraft tipoff rates is achieved through activation of the gas jet system and use of rate feedback gyro control (rate mode). After rate capture, inertial mode is achieved by switching to position feedback gyro control.

Because of the long duration of the transit phase and the small unavoidable drift error of the gyros, celestial references are used to provide the desired attitude of the spacecraft. Following a 51-sec delay after electrical dis-

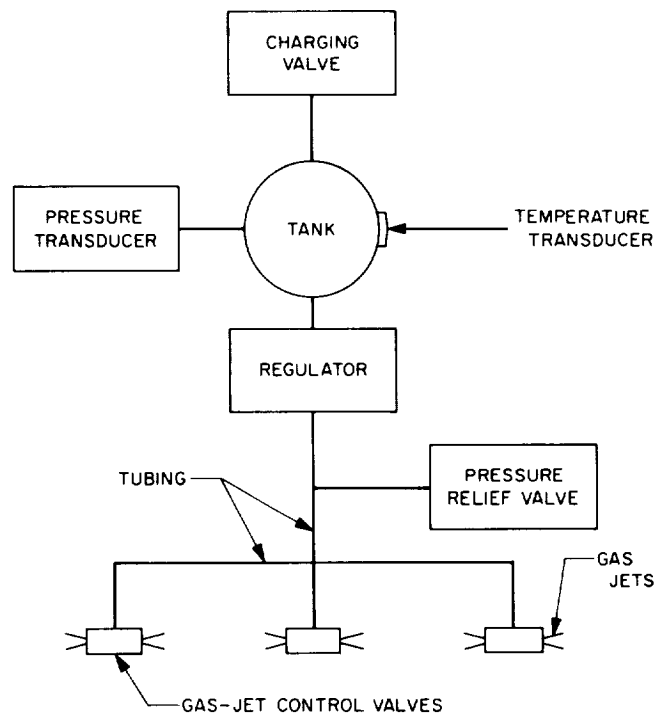


Fig. IV-24. Gas-jet attitude control system

Table IV-11. Flight control modes

Control loop	Flight phase	Modes	Remarks
Attitude control loop			
Pitch and yaw	Coast	Rate Inertial Celestial	Gas jet matrix signals
	Thrust	Inertial Lunar radar	Vernier engine matrix signals
Roll	Coast	Rate Inertial Celestial	Leg 1 gas jet signals
	Thrust	Inertial	Vernier Engine 1 gimbal command
Acceleration control loop			
Thrust axis	Thrust (midcourse) Thrust (terminal descent)	Inertial (with accelerometer) Inertial (with accelerometer)	Nominal 3.22 ft/sec ² Minimum 4.77 ft/sec ² Maximum 12.56 ft/sec ²
Velocity control loop			
Thrust axis	Thrust	Lunar radar	Command segment signals to 43-ft altitude Constant 5-ft/sec velocity signals to 14-ft altitude
Lateral axis	Thrust	Lunar radar	Lateral/angular conversion signals

connect from the *Centaur*, a flight control timer automatically initiates the sun acquisition sequence by commanding a negative roll maneuver. The sun is first acquired by the acquisition sun sensor which has a 10-deg-wide by 196-deg-fan-shaped field of view that includes the spacecraft Z-axis and is centered about the minus X-axis. The roll command is terminated after initial sun acquisition, and a positive yaw command is automatically initiated which allows the narrow-view primary sun sensor to acquire and lock-on the sun. A secondary sun sensor, mounted on the solar panel, provides a backup for manual acquisition of the sun if the automatic sequence fails.

Automatic Canopus acquisition and lock-on are normally achieved after initiation of a roll by command from earth. This occurs because the Canopus sensor angle is preset with respect to the primary sun sensor prior to launch for each mission. Star mapping for Canopus verification is achieved by commanding the spacecraft to roll while the spacecraft maintains sun lock.

The transit phase is performed with the spacecraft in the celestial-referenced mode except during initial rate-stabilization, midcourse, and terminal descent maneuvers and gyro drift checks, when the inertial mode is used.

Midcourse velocity correction capability is provided by means of the vernier engine throttle valves, a precision timer, and an accurate acceleration sensing device. The difference between the command acceleration level and the output from the accelerometer provides an error signal which is used to command the throttle valves for the required thrust level. The timer provides capability to perform velocity corrections of 0 to 50 m/sec with automatic shutdown.

The terminal maneuver descent sequence has been described in detail in Section IV-A-15. The flight control subsystem provides initial orientation of the main retro-motor thrust axis and automatic sequencing after the lunar reference is first established by a signal from the AMR. Most of the approach velocity is removed by the solid propellant retromotor during the initial phase of terminal descent. Spacecraft attitude during this phase is inertially stabilized using the gyros and differential throttling of the vernier engines.

During the vernier phase of descent, which follows main retro burnout and ejection, a sophisticated flight control technique is utilized which includes the use of radars to obtain range and velocities. The range information is used by the flight control subsystem during the

vernier phase of descent to compute longitudinal velocity commands for controlling the total vernier engine thrust to achieve the desired descent profile (approximately constant acceleration). The velocity data is applied to the attitude control loop to produce a near-gravity turn during descent by aligning the spacecraft thrust axis with the velocity vector. The velocity data is also used to generate error signals for the velocity control loop.

2. Flight Control Performance

Flight control performance was completely normal during the mission except for a low-level vernier thrust modulation anomaly which appeared after retro ignition. The induced loads on the spacecraft as a result of this anomaly were well below the structural and flight control capability of the spacecraft.

a. Spacecraft/Centaur separation. The spacecraft gyro data indicated the following maximum angular rates (in deg/sec) occurred as a result of the spacecraft separation sequence: pitch, -0.42 ; yaw, $+0.16$; roll, 0.0 . Tipoff rates well within the specification limit of 3.0 deg/sec were confirmed by *Centaur* data which indicated virtually simultaneous extension of the three separation springs. The spacecraft reduced angular motion about each of the axes to ≤ 0.1 deg/sec in less than 13 sec.

b. Sun acquisition. A very nominal sun acquisition sequence was automatically executed. The acquisition sun sensor was illuminated after a negative roll of 59.4 deg. This was followed by a positive yaw turn of 45.6 deg which established primary sun sensor lock-on. The *sun-lock* signal was generated at a primary sun sensor pitch error of approximately -3.0 deg and a yaw error of -12.6 deg, which is within the expected lock-on field-of-view range of the sensor. The sun acquisition sequence required only about $3\frac{1}{2}$ min.

c. Star (Canopus) acquisition. During star mapping and Canopus acquisition roll, the moon was expected to pass approximately 2.0 deg outside the field of view and the earth was expected to pass approximately 11 deg outside the field of view. Since large-area bright objects within approximately 35 deg of the sensor's line of sight will reflect light into the sensor from baffles in the sensor's light shield, it was expected that some *star intensity* signal would result when the sensor was rolling past both the moon and the earth. The analog recorder traces of *star angle* and *star intensity* indicated four clearly distinguishable stars plus a 20 -deg-wide low-intensity signal and a 45 -deg-wide high-intensity signal. The angular spacing of these signals was compared with previously

calculated star, earth, and moon angles, thus permitting positive identification of Canopus, Eta U Majoris, Delta Velorum, Gamma Cassiopeiae, the moon, and earth. The results of the star map analysis are shown in Table IV-12.

One unexpected object appeared in the field of view during the first 360 deg of roll, and two unexpected objects appeared during the remaining roll. Both of these objects produce telemetry signals shaped like celestial body responses, but they remained in the field of view for a shorter time. It was concluded that these objects were particles moving in space with a roll velocity component somewhat faster than the spacecraft roll rate of 0.5 deg/sec.

For the *Surveyor IV* mission, the sun filter value was calibrated at the same level ($0.8 \times$ Canopus) as for the *Surveyor III* mission. The ratio of measured to predicted Canopus intensity was approximately 1.16, and it can be concluded that either the effective gain is 16% high, or the predicted value is low, or both factors are present to some degree.

Owing to the fact that *lock-on* signals were received when the earth was in the field of view, it was decided to send the *sun and star* command after the earth had passed the field of view for the second time. Thus, the spacecraft was commanded to the *sun and star* mode at 495 deg of roll or 75 deg before the second appearance of Canopus. The *lock-on* signal occurred at 565 deg of roll and, with the *star angle* signal now acting as the *roll*

error signal, spacecraft roll motion was damped out to the optical deadband limit in approximately 60 sec. *Cruise mode on* was commanded at $L + 06:19$.

d. Gyro drift measurements. Twelve gyro drift checks were made during the mission. Two were roll-axis-only checks and ten were checks of drift about all three axes. Although eight gyro drift checks were made prior to the midcourse velocity correction, the pre-midcourse attitude maneuver magnitudes were not compensated for drift because of the negligible effect on pointing accuracy. The terminal attitude maneuvers were compensated for the following gyro drift rates (in deg/hr): roll, -0.5 ; pitch, -1.0 ; yaw, $+0.15$. The gyro drift values selected for preterminal maneuver compensation were based essentially upon an average of all measurements made during the mission.

e. Pre-midcourse attitude maneuvers. The maneuver combination selected to orient the spacecraft in the desired direction for the midcourse velocity correction consisted of a $+72.5$ -deg roll maneuver followed by a -64.3 -deg yaw maneuver. For the first time, an attempt was made to reduce the pointing errors by initiating the pre-midcourse attitude maneuvers at the null point in the optical mode limit cycle. The technique was successful in that all maneuvers were initiated at a time when the optical mode limit cycle errors were not at a peak. Table IV-13 indicates the optical errors that existed at the start of each maneuver.

Table IV-12. *Surveyor IV* star map results

GMT, hr:min:sec	Roll angle, deg	Source	Angle from Canopus, deg		Peak intensity, V	
			Indicated	Predicted	Measured	Predicted
17:51:27.5	0	(Start of roll)	-210.6			
17:53:31.4	62.0	Eta U Majoris	-148.6	-148.7	0.71	0.57
17:55:15.6	114.1	Moon	-96.5	-97.0	0.88	
17:56:18.5	145.5	Particle	-65.1		0.63	
17:57:46.2	189.4	Delta Velorum	-21.3	-21.1	0.65	0.49
17:58:28.7	210.6	Canopus			4.32	4.11
18:01:57.6	315.1	Earth	104.5	103.0	4.42	
18:03:06.8	349.7	Gamma Cassiopeiae	139.2	139.2	0.64	0.47
18:05:08.5	410.5	Particle	199.9		0.60	
18:05:30.9	421.7	Eta U Majoris	211.1	211.3	0.75	0.57
18:07:15.8	474.2	Moon	263.5	263	0.86	
18:08:01.5	497.0	Particle	286.4		1.22	
18:09:45.9	549.2	Delta Velorum	338.6	338.9	0.69	0.49
		Canopus			4.68 ^a	4.42 ^a
		No star			0.51 ^a	0.37 ^a

^aAt zero roll rate.

Table IV-13. Optical errors

Maneuver	Error, deg	Limit cycle peak, deg
Roll	+0.066	± 0.3
Yaw	-0.06 pitch	± 0.23
	-0.10 yaw	± 0.27

As can be seen, the roll and pitch optical errors were close to the null point, while the yaw optical error was closer to its limit cycle peak than its null.

f. Midcourse velocity correction. The midcourse velocity correction was successfully executed starting at about $L + 38:36$. Based on orbit determination, the actual magnitude of velocity change was 10.132 m/sec compared to a commanded value of 10.305 m/sec, and the midcourse thrust vector pointing error was within the accuracy of the two-way doppler tracking system (<0.2 deg). Based on prelaunch alignment and flight data, the preignition pointing error was calculated to be 0.19 deg.

Vernier ignition was smooth, followed by a nominal thrusting phase. The small gyro errors (<0.18 deg) produced by the ignition transient were reduced to zero within 2 sec. The peak gyro errors resulting from vernier engine shutdown were less than 1.2 deg. The vernier engine shutdown dispersions (relative to mean impulse of the three engines) were estimated to be (in lb-sec): Engine 1, -0.18 ; Engine 2, $+0.03$; Engine 3, $+0.15$. These values are well within the specification limit of ± 0.63 lb-sec.

Reverse maneuvers were successfully used to reacquire the sun and Canopus following the velocity correction since the peak gyro errors caused by vernier engine shutdown were sufficiently small (approximately 1 deg maximum) to prevent the gyros from hitting their travel limit stops (± 10 deg), which would have resulted in a loss of inertial reference.

g. Nitrogen gas consumption. The calculated weight of on-board nitrogen at launch was 4.56 lb based on a telemetered tank pressure of 4568 psi at a tank temperature of 75.8°F . This agreed closely with the best estimate of 4.6 lb of nitrogen loaded. All subsequent nitrogen weight estimates were corrected for this 0.04-lb difference.

The expected nitrogen usage up until the terminal maneuvers was 0.45 ± 0.22 lb for the *Surveyor IV* mission, not allowing for the gyro drift checks. Including the gyro drift checks, the predicted usage was calculated to be 0.63 ± 0.22 lb.

The actual nitrogen consumption for the mission prior to the terminal maneuvers was 0.64 lb, which compares favorably with predicted usage when the gyro drift lock-on transients are accounted for. Nitrogen usage was determined from telemetered supply tank pressure and temperature.

h. Terminal maneuvers. The first attitude maneuver was initiated 37 min 13 sec before retro ignition. Normally, the time constraint on break of optical lock is 33 min, based on an allowable 1-deg/hr gyro drift contribution to the pointing error. Since the attitude maneuvers were compensated for gyro drift, the earlier maneuver time was acceptable.

As in the case of the pre-midcourse maneuvers, an attempt was made to initiate the maneuvers at the limit cycle null points. The first maneuver ($+80.9$ deg roll) was initiated within approximately -0.05 deg of null while the pitch and yaw optical errors at the start of the second maneuver ($+92.7$ deg yaw) were -0.07 and -0.14 deg, respectively. A third maneuver (-25.3 deg roll) was also performed to achieve the desired roll attitude to provide the preferred landed roll orientation while satisfying the RADVS constraints.

i. Terminal descent. The telemetry data confirmed that the true AMR mark signal occurred prior to emergency mark. Other retro phase events through loss of signal occurred as expected, confirming satisfactory performance of the magnitude register and programmer.

Traces of the critical flight control parameters during the retro phase through loss of spacecraft signal are shown in Fig. IV-25. The only significant anomaly apparent in the flight control system during the retro phase was a considerable degree of modulation of Vernier Engines 1 and 2 thrust commands. Other parameters were quite normal, as indicated by key values presented in Table IV-14 for comparison of *Surveyor IV* with *Surveyor I* and *III* missions.

Ignition of the vernier engines on *Surveyor IV* was executed smoothly, with impulse dispersions between engines well within specification values. Shortly after retro ignition, maximum control torque equivalent to 14 ft-lb was produced by differential throttling of the vernier engines. This is equivalent to a very small center-of-gravity offset of 0.016 in. (specification limit, 0.18 in.). However, the average values of the engine thrust commands in the last 15 sec of the main retro burn period indicate a static moment that cannot be accounted for by normal center-of-gravity and thrust vector variations.

Table IV-14. Comparison of flight control parameters during main retro phase for Surveyor I, III, and IV missions

	Surveyor I	Surveyor III	Surveyor IV
Acceleration, g			
Main retro ignition	4.1	3.4	3.3
Peak	10.5	9.5	8.3
Acceleration error, telemetry, V	1.8	1.82	1.70
Pitch gyro error, deg			
Max or min	-0.13	-0.22	-0.12
Steady-state	+0.02	-0.08	+0.06
Yaw gyro error, deg			
Max or min	-0.891	+0.157	-0.375
Steady-state	+0.015	0	-0.250
Roll gyro error, deg			
Max or min	+0.2	-0.35	-0.5
Steady-state	+0.1	+0.165	0
Engine 1 thrust command, lb			
Max or min	87.5	75.5	77.0
Steady-state	66.1	69.0	71.2
Engine 2 thrust command, lb			
Max or min	67.5	58.7	65.6
Steady-state	66.7	64.0	69.0
Engine 3 thrust command, lb			
Max or min	66.6	65.3	64.4
Steady-state	67.6	68.0	66.4
Total thrust command, lb			
Steady-state	200.4	201.0	206.6
Roll actuator position, deg			
Max or min	-0.4	+0.97	+0.57
Steady-state	-0.2	+0.21	0
Engine 1 strain gauge			
Max or min, V	1.0	0.93	0.95
Max or min, lb	(Calibration uncertain)	60.9	55.5
Engine 2 strain gauge			
Max or min, V	1.44	1.60	1.60
Max or min, lb	79.6	59.8	63.0
Engine 3 strain gauge			
Max or min, V	1.58	1.54	1.45
Max or min, lb	88.77	58.8	58.3

Peak pitch and yaw inertial attitude errors, as indicated by the gyro error signals (Fig. IV-25), occurred at vernier ignition and amounted to -0.35 and -0.09 deg, respectively. Roll inertial attitude error was less than 0.05 deg throughout the main retro phase. Therefore, each gyro was exercised less than 10% of the allowable travel range of more than ± 10 deg.

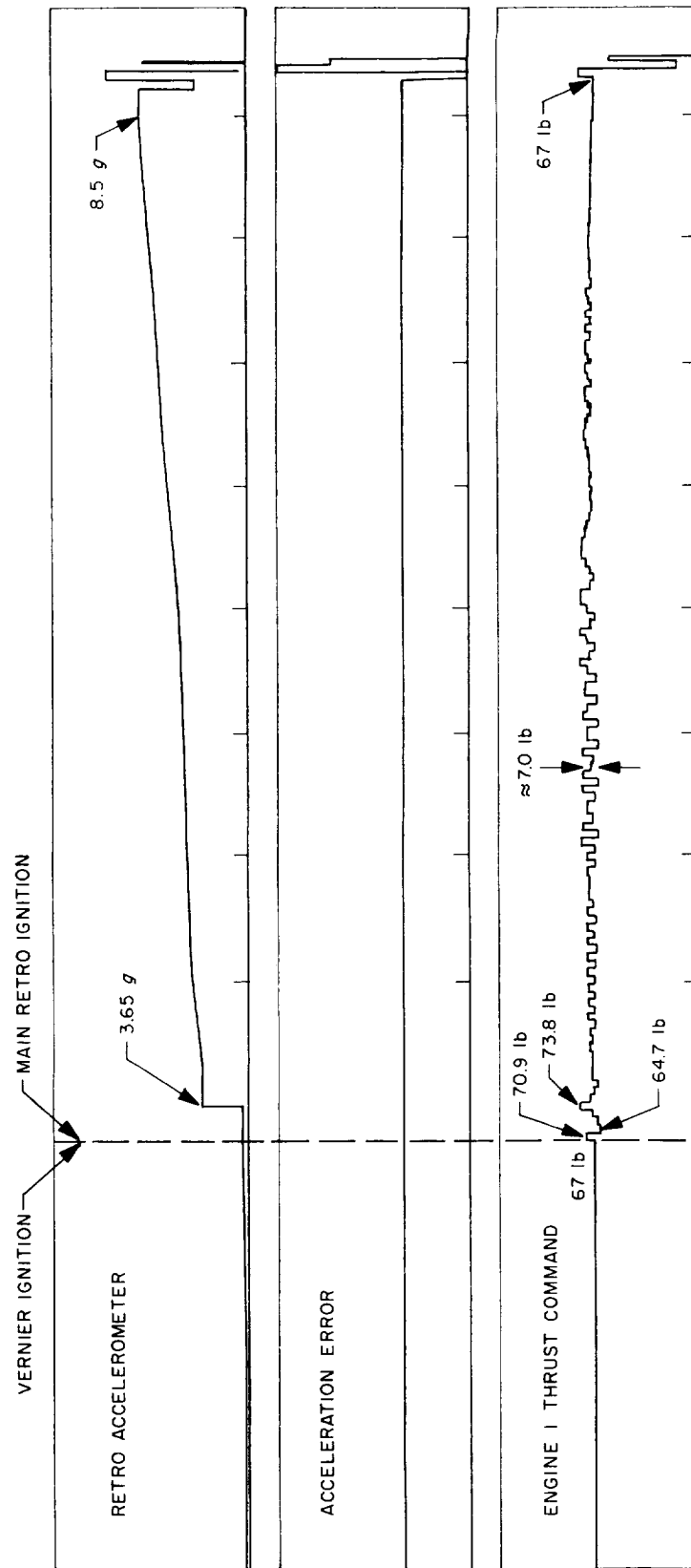
Among the other telemetry data shown in Fig. IV-25, the signals from the three strain gages attached to the vernier engine brackets indicate engine thrust magnitude but are of quite limited resolution. Outputs of the strain gages are sensitive to vehicle acceleration and local heat-

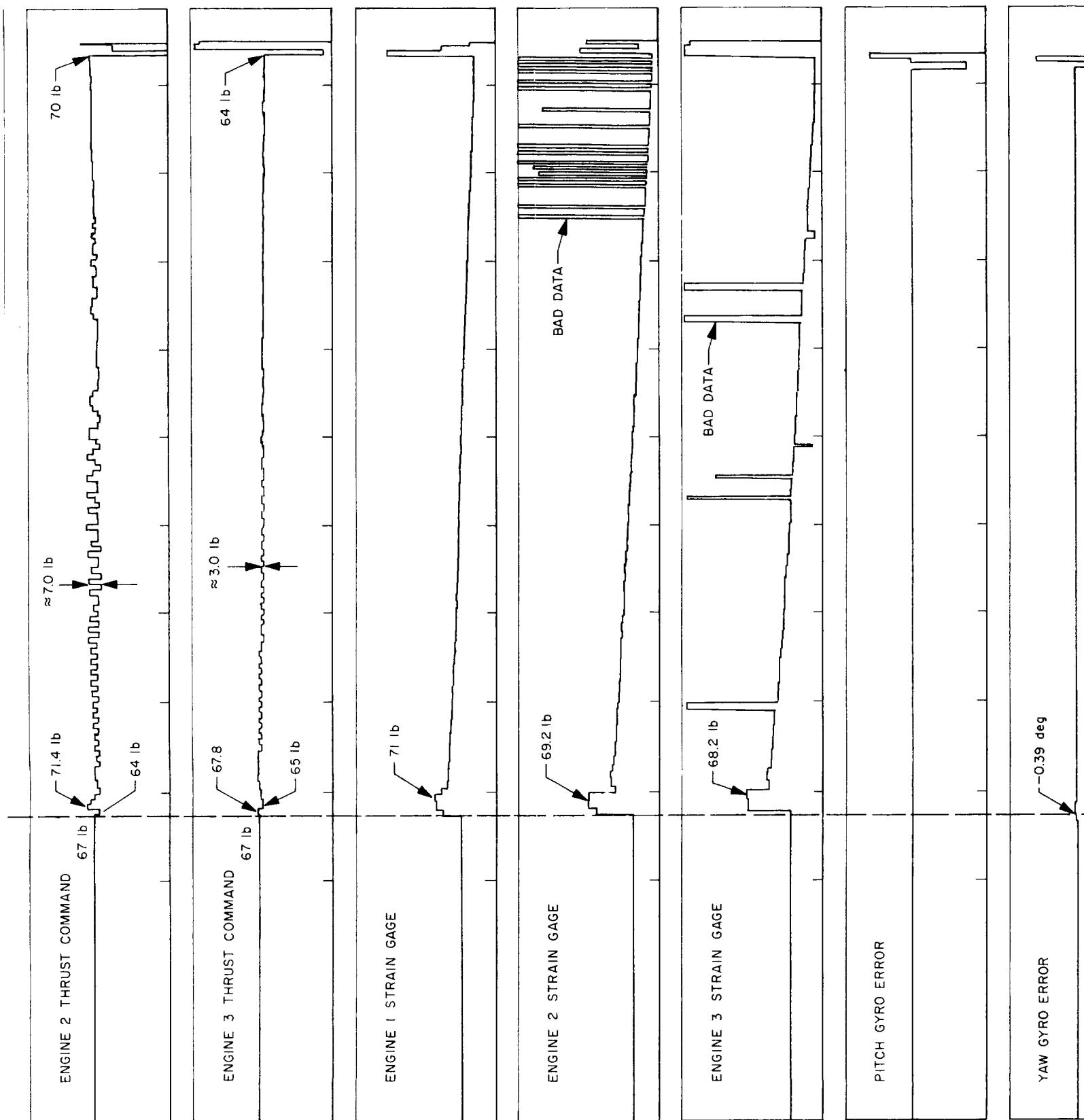
ing, which accounts for the descending slope of the traces during the burn. The roll actuator position signal, which indicates angular displacement of Engine 1 for roll control, appears normal. Variations in this signal are due to engine thrust level changes and roll disturbances caused by changes in acceleration forces. The output of the retro accelerometer indicates a normal retro burn within the accuracy of the device. The lateral (V_x and V_y) and longitudinal (V_z) velocity outputs of the RADVS exhibit a change about 33 sec after ignition due to lock-on of Beams 1, 2, and 3, and subsequent generation of reliable 3-axes velocity information. The RADVS range output indicates only the search pattern influenced by acquisition by the velocity beams.

In an attempt to check for evidence relative to the loss of spacecraft signal, the final 6 sec of data on the key flight control data channels was plotted (Fig. IV-26) and carefully examined. No evidence exists to explain the loss of data from the spacecraft, nor is there any change in the data indicative of a spacecraft disturbance or anomaly. The spacecraft attitude and thrust control loop time constants are such that any disturbance starting more than 0.2 sec before loss of signal would have been evident in the data. Any disturbance starting within 0.1 sec of signal loss would probably not be indicated.

The vernier engine thrust commands during the retro phase are presented in Fig. IV-27, with an expanded scale to illustrate the abnormal modulation. Data for the Surveyor III mission is also plotted for comparison. On Surveyor IV, as much as 7-lb peak-to-peak modulation was indicated on the commands to Engines 1 and 2. Examination of the individual thrust commands reveals that the commands to Engines 1 and 2 were usually in-phase, which implies a varying total thrust. The Engine 3 command modulation was of much smaller amplitude and usually out of phase with Engine 1 commands. The attitude control system mixing networks are designed such that, in the absence of engine thrust saturation, this type of modulation is impossible. The Engine 1 strain gage signal appears to have responded out-of-phase with the Engine 1 thrust commands. However, Engine 2 strain gage and thrust command signals were in-phase. Engine 3 modulation was too small to make a comparison.

An intensive investigation was conducted to determine the actual frequency, phasing, and amplitude of the modulation which are masked by telemetry signal processing effects. From tests including the sampling of both digital and analog data, it has been determined that erroneous thrust command data can result from the commutation





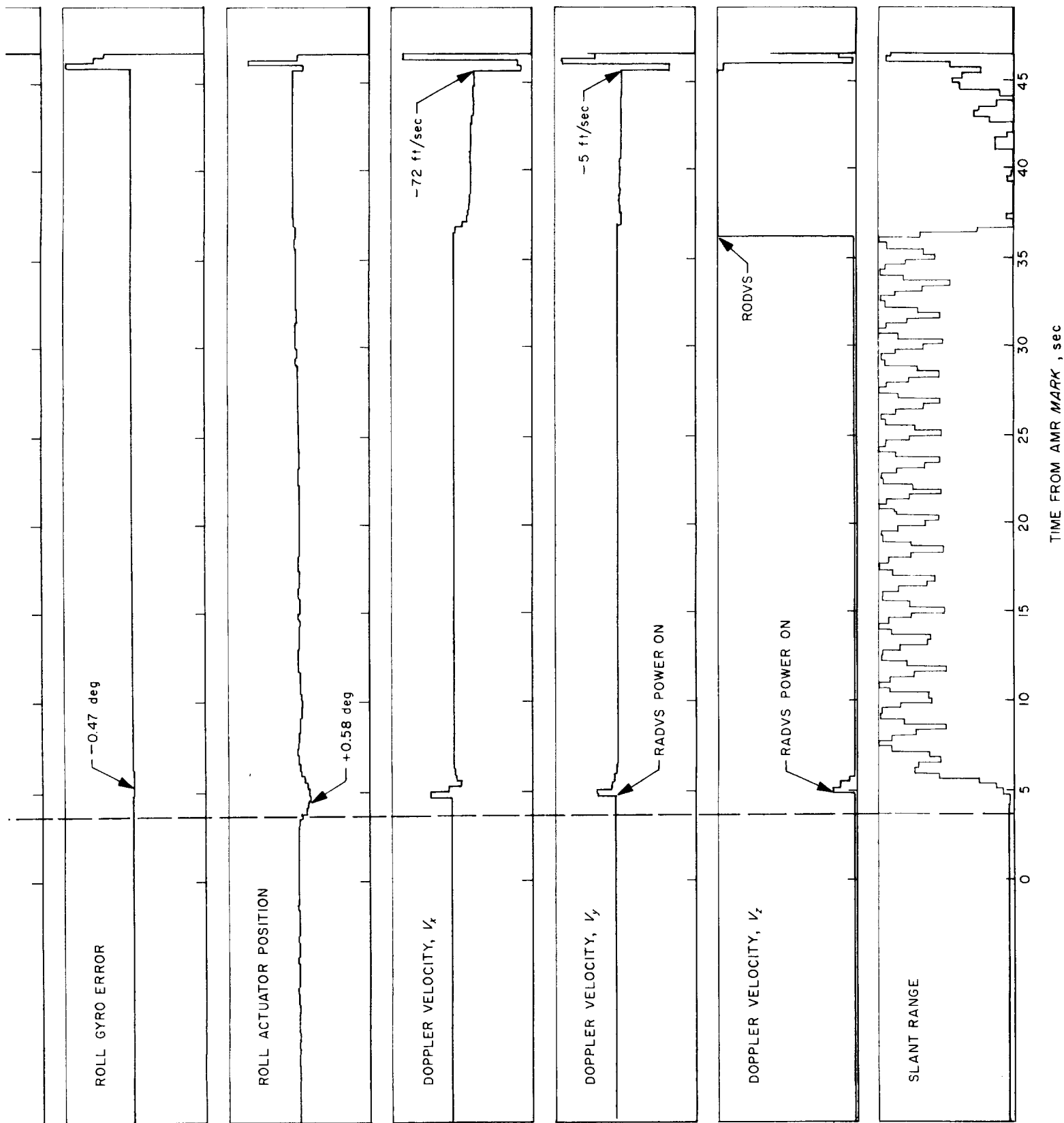


Fig. IV-25. Critical flight control signal recordings during main retro phase

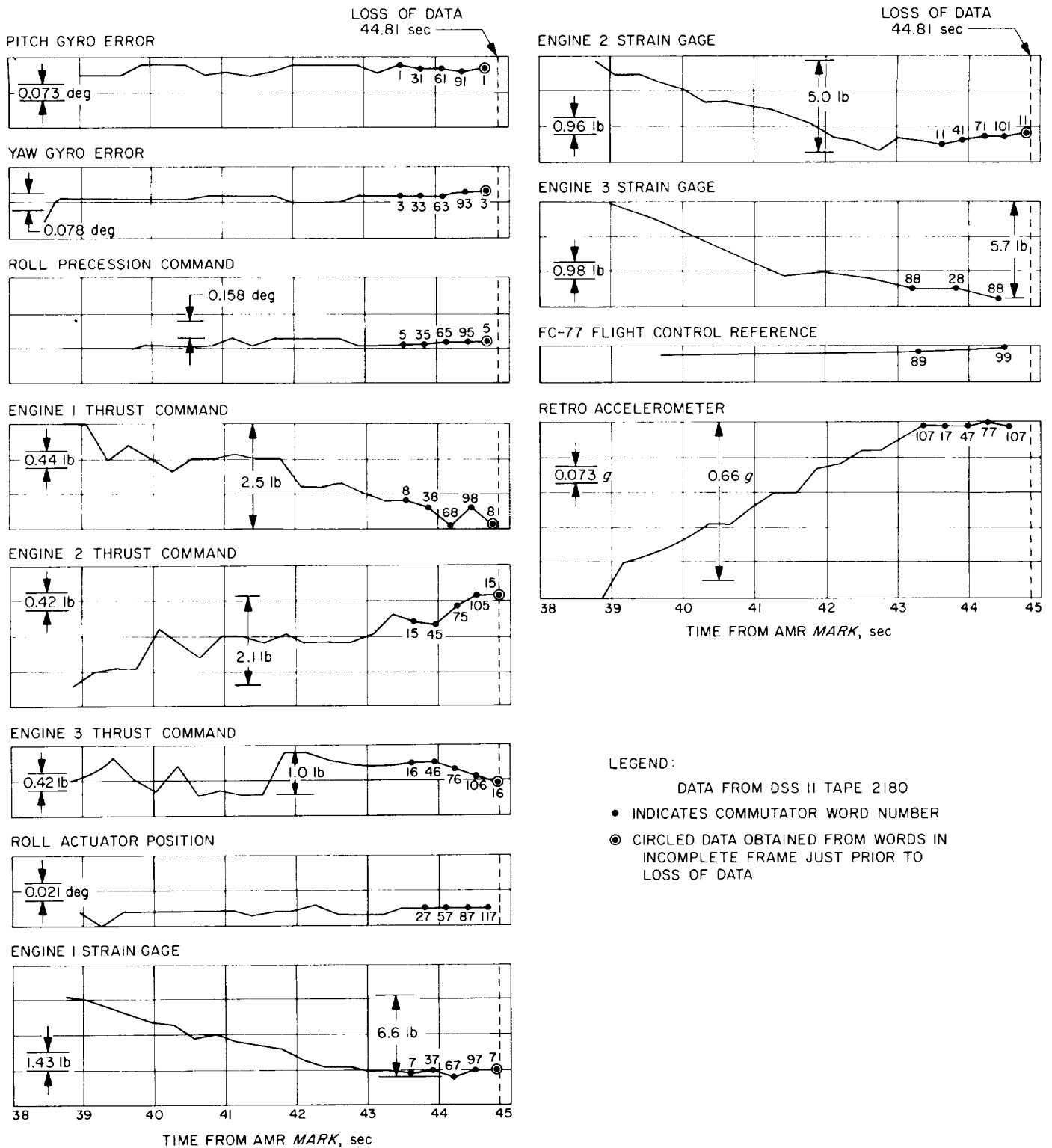


Fig. IV-26. Flight control data (final 6 sec)

of a rapidly varying signal. It is presumed, therefore, that Engines 1 and 2 were actually throttled out-of-phase. It should be noted that the total thrust command during

the final 7 sec stabilized at the correct midthrust value, leading to the conclusion that the thrust commands in that period were as indicated by the data.

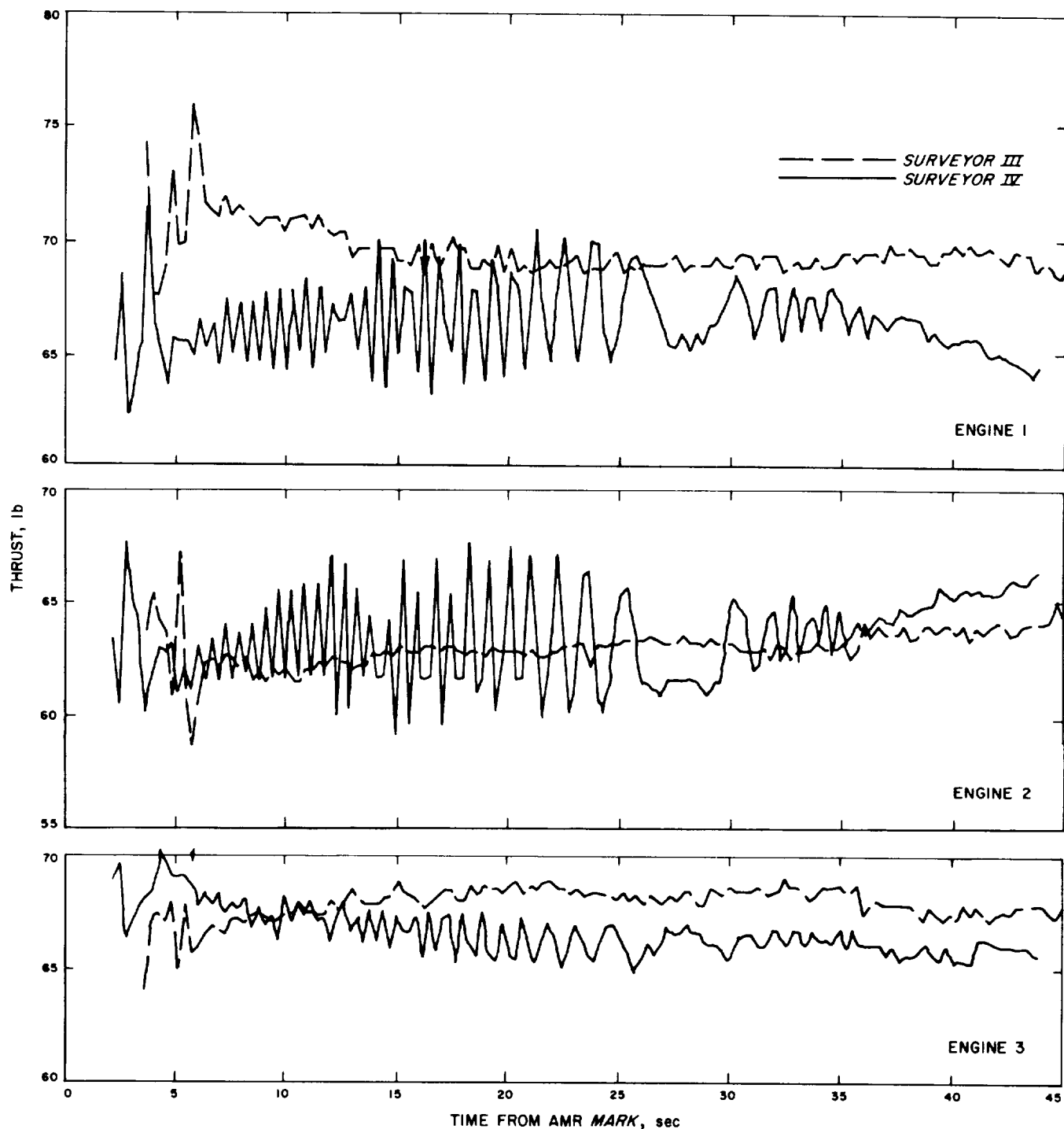


Fig. IV-27. Vernier engine thrust commands during main retro phase (Surveyor III data also shown)

Results of the investigation thus far indicate that the frequency of the modulation was in the region of 5–25 Hz. If the modulation was a result of a control system oscillation, it appears unlikely that the induced loads would have been of sufficient magnitude to cause failure of any space-

craft element. If the modulation is associated with the spacecraft failure, it is concluded that the most probable mechanism is a control system oscillation resulting from a large spacecraft assembly having a lower-than-normal resonant frequency, possibly due to a structural failure.

A secondary possibility is that modulation of the main retro thrust occurred in direction or magnitude, although no known mechanism appears to fit the data. It should be noted that no abnormal disturbances were indicated during the midcourse velocity correction, when the attitude control system configuration is identical to that which exists during the retro phase except that an accelerometer is not in the loop.

G. Radar

Two radar devices, the altitude marking radar (AMR) and the radar altimeter and doppler velocity sensor (RADVS), are employed on the *Surveyor* spacecraft for use during the terminal descent phase.

1. Altitude Marking Radar

The AMR (Fig. IV-28) is a conventional noncoherent radar, employing a pulsed magnetron, single antenna, duplexed mixer, crystal-controlled solid-state local oscillator,

wideband intermediate frequency (IF) amplifier, noncoherent detector, and video processing circuitry. Dynamic range is extended by AGC of the IF amplifier; AGC voltage is telemetered and provides an indication of received signal power. The video circuitry is of special design to provide a *mark* signal with high accuracy and reliability at a slant range from the lunar surface that can be preset between 52 and 70 miles (60 miles for *Surveyor IV*). Two fixed, adjacent range gates continuously examine the video signal. Their outputs are continuously summed and differenced. When the sum exceeds a fixed threshold and the difference simultaneously crosses zero with positive slope, the *mark* signal is generated. The sum threshold is set for an extremely low probability of marking on noise (false *mark*) throughout the operating time, while video integration plus a very substantial radar gain margin ensures a high probability of marking successfully.

Two separate ground commands, whose timing is controlled, are required to fully activate the AMR. The first signal, called simply *AMR on*, commands on the primary

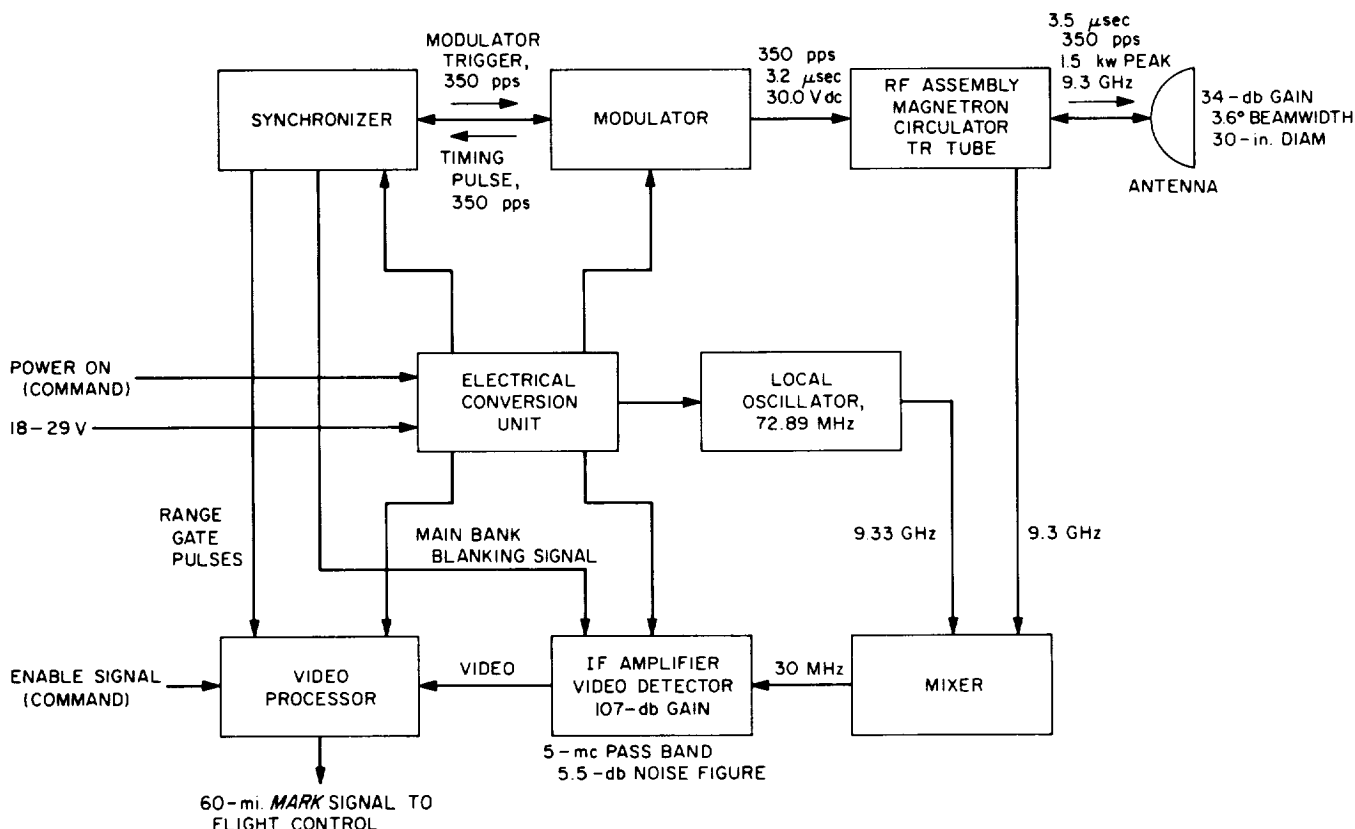


Fig. IV-28. Altitude marking radar functional diagram

power to the AMR, which includes all internal power except high voltage to the transmitter. The video signal is inhibited from reaching the marking circuits until the second command, thus eliminating any residual probability of false marking on noise during this warmup interval. The second signal, called *AMR enable*, commands on the transmitter high voltage and also removes the video inhibit. This enabling function is timed not only for favorable thermal conditions at the expected marking time but also to preclude premature marking on second-round echoes at much longer ranges.

AMR signals which are telemetered include three digital signals and three analog signals plus analog temperature data. The three digital signals (R-1, R-11, FC-64) are confirmations of on-board discrete events; they confirm, respectively, that prime power has been applied (*AMR on*), that high voltage and video enabling have been applied (*AMR enable*), and that the self-generated slant range trigger (*AMR mark*) has occurred. The three analog signals (besides temperature) are magnetron current (R-12), AGC voltage level (R-14), and late-gate detected video voltage level (R-29). The AGC not only confirms receiver response to RF return, but is also useful in evaluating terrain reflectivity. The magnetron current confirms pulsing of the magnetron after *enable*, and is useful primarily as a transmitter failure mode indication. The late-gate signal, primarily a receiver failure mode indication, normally confirms the presence of a gated video signal rising quickly to a peak at the time of *mark* and decaying quickly thereafter.

The AMR mounts in the retro rocket nozzle and is retained by friction clasps around the nozzle flange, with spring washers between the AMR and the flange. When the retro rocket is ignited, the gas generated by the ignitor develops sufficient pressure to eject the AMR from the nozzle. The AMR draws 22 V power through a break-away plug that also carries input commands, the output *mark* signal, and telemetry information.

On *Surveyor IV*, the AMR operated satisfactorily during the period it performed during terminal descent. AGC voltage increased normally and smoothly as expected up to and including *AMR mark* and until AMR ejection. The AMR AGC quiescent level (prior to *enable*) was somewhat higher than experienced in testing or in previous missions, but there was no effect upon the mission and no correlation with loss of the spacecraft signal could be found. Telemetry indication of late-gate signal was normal, indicating a lunar return in the dual-channel video gate at the expected time.

AGC return followed within 2.5 db of the predicted return signal power. The predictions were based upon a lunar return reflection coefficient of -11.05 db at an approach angle θ of 31.5 deg. The received pulse was approximately 20 sec in width, and the received power at *mark* was -78.8 dbm.

AMR power output as measured by magnetron input current was normal and steady at 2 W average.

The last of the AMR temperatures telemetered on *Surveyor IV* were within the expected range and compared favorably with those encountered on the *Surveyor I* and *III* missions as shown in Table IV-15.

**Table IV-15. Comparative AMR temperatures:
Surveyors I, III, IV**

	Surveyor I, °F	Surveyor III, °F	Surveyor IV, °F
Antenna, edge	-187	-200	-182
Antenna, inside rear	-12	0	-5
AMR electronics	+16	+17.5	+14

2. Radar Altimeter and Doppler Velocity Sensor

The RADVS (Fig. IV-29) functions in the flight control subsystem to provide three-axes velocity, range, and altitude *mark* signals for flight control during the main retro and vernier phases of terminal descent. The RADVS consists of a doppler velocity sensor (DVS), which computes velocity along with spacecraft X, Y, and Z axes, and a radar altimeter (RA), which computes slant range from 40,000 to 14 ft and generates 1000-ft and 14-ft *mark* signals. The RADVS comprises five assemblies: (1) klystron power supply/modulator (KPSM), which contains the RA and DVS klystrons, klystron power supplies, and altimeter modulator, (2) altimeter/velocity sensor antenna, which contains Beams 1 and 4 transmitting and receiving antennas and preamplifiers, (3) velocity sensing antenna, which contains Beams 2 and 3 transmitting antennas and preamplifiers, (4) RADVS signal data converter, which consists of the electronics to convert doppler shift signals into dc analog signals, and (5) interconnecting waveguide. The RADVS is turned on at about 50 miles above the lunar surface and is turned off at about 13 ft.

a. Doppler velocity sensor. The doppler velocity sensor (DVS) operates on the principle that a reflected signal has a doppler frequency shift proportional to the approaching velocity. The reflected signal frequency is higher than the transmitted frequency for the closing condition. Three beams directed toward the lunar surface

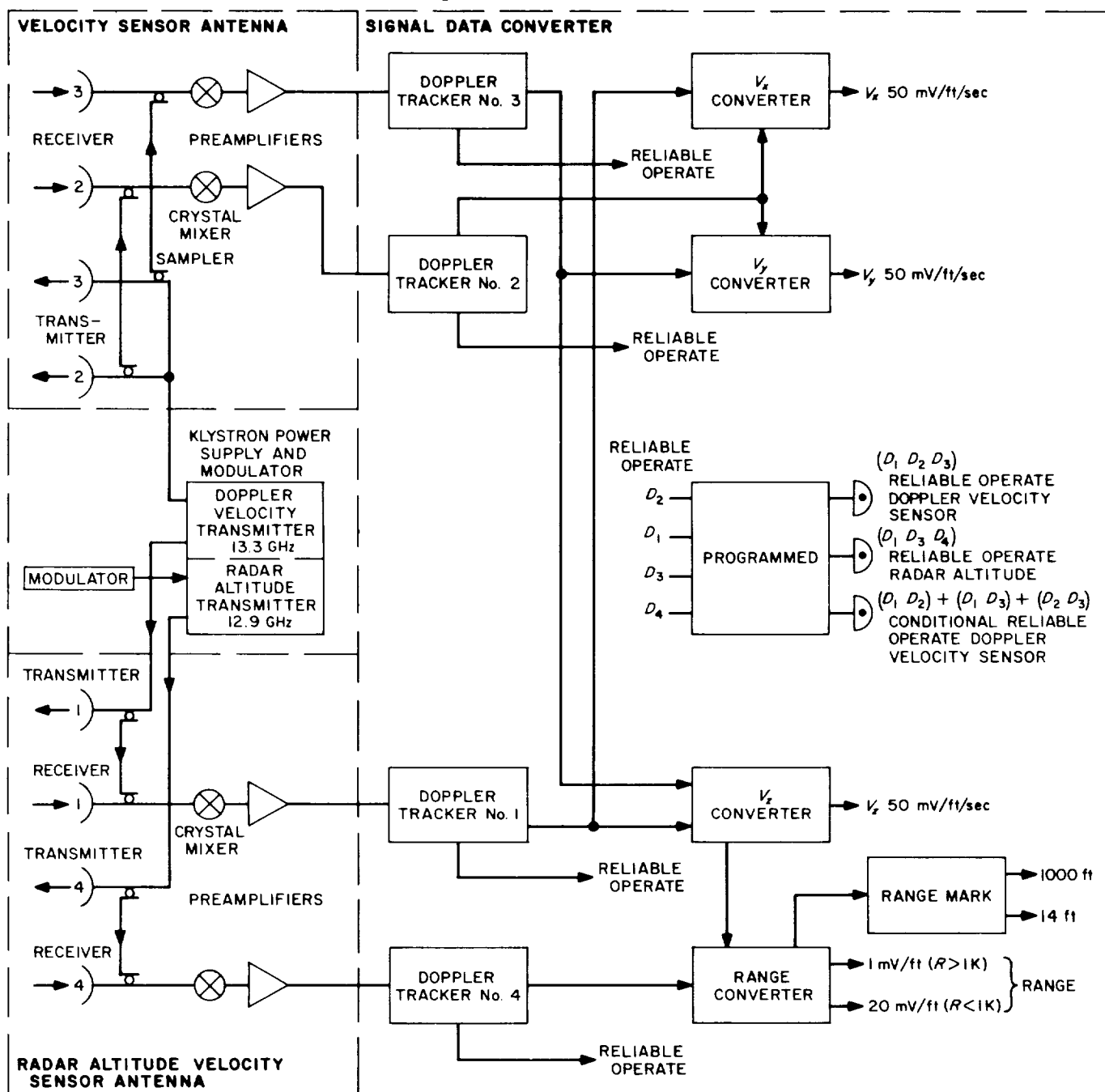


Fig. IV-29. Simplified RADVS functional block diagram

enable velocities in an orthogonal coordinate system to be determined.

The KPSM provides an unmodulated DVS klystron output at a frequency of 13.3 GHz. This output is fed equally to the DVS 1, DVS 2, and DVS 3 antennas. The RADVS velocity sensor antenna unit and the altimeter velocity sensor antenna unit provide both transmitting and receiving antennas for all three beams. The reflected signals are mixed with a small portion of the transmitted frequency at two points $\frac{3}{4}$ wavelength apart for phase determination, detected, and amplified by variable-gain amplifiers providing 40, 65, or 90 db of amplification, depending on received signal strength. The preamp output signals consist of two doppler frequencies, shifted by $\frac{3}{4}$ transmitted wavelength, and preamp gain-state signals for each beam. The signals are routed to the trackers in the RADVS signal data converter.

The D1 through D3 trackers in the signal data converter are similar in their operation. Each provides an output which is 600 kHz plus the doppler frequency for approaching doppler shifts. If no doppler signal is present, the tracker will operate in search mode, scanning frequencies between 82 kHz and 800 Hz before retro burnout, or between 22 kHz and 800 Hz after retro burnout. When a doppler shift is obtained, the tracker will operate as described above and initiate a lock-on signal. The tracker also determines amplitude of the reflected signal and routes this information to the signal processing electronics for telemetry.

The velocity converter combines tracker output signals D_1 through D_3 to obtain dc analog signals corresponding to the spacecraft X, Y, and Z velocities; $D_1 + D_3$ is also sent to the altimeter converter to compute range.

Reliability and reference circuits produce a *reliable operate doppler velocity sensor* (RODVS) signal if D_1 through D_3 lock-on signals are present beginning about 3 sec after main retro burnout. The RODVS signal is routed to the flight control electronics and to the signal processing electronics telemetry. The system is designed to produce a *conditional reliable operate doppler velocity sensor* (CRODVS) signal if only one or two, rather than all three, of the DVS beams are in lock. If the CRODVS signal occurs, the spacecraft will steer into the unlocked beams to achieve lock-on of all beams and generation of RODVS.

During the *Surveyor III* mission, about 5 sec before touchdown at an altitude of about 37 feet, Beam 3 lost lock and did not regain lock because the low spacecraft velocity of approximately 5 ft/sec was outside the sweep

range. To ensure against loss of lock on *Surveyor IV* and future missions, the cross-coupled sidelobe logic was disabled below 1000 ft. The isolation between beam cross coupling was increased to permit use of CRODVS down to 1000 ft altitude, thus facilitating landings at increased approach angles. On the *Surveyor III* mission, CRODVS was disabled 1 sec after the three velocity trackers had achieved lock. If CRODVS is inhibited, the spacecraft switches to inertial attitude hold when beam lock is lost. Availability of CRODVS to 1000 ft altitude allows spacecraft maneuvering to reacquire lock, thus assuring greater probability of maintaining the programmed descent profile.

b. Radar altimeter. Slant range is determined by measuring the reflection time delay between the transmitted and received signals. The transmitted signal is frequency-modulated at a changing rate so that return signals can be identified.

The RF signal is radiated, and the reflected signal is received by the altimeter/velocity sensor antenna. The received signal is mixed with two samples of transmitted energy $\frac{3}{4}$ wavelength apart, detected, and amplified by 40, 60, or 80 db in the altimeter preamp, depending on signal strength. The signals produced are difference frequencies resulting from the time lag between transmitted and received signals of a known shift rate, coupled with an additional doppler frequency shift because of the spacecraft velocity.

The altimeter tracker in the signal data converter accepts doppler shift signals and gain-state signals from the altimeter/velocity sensor antenna and converts these into a signal which is 600 kHz plus the range frequency plus the doppler frequency. This signal is routed to the altimeter converter for range dc analog signal generation.

The range mark, reliability, and reference circuits produce the 1000-ft *mark* signal and the 14-ft *mark* signal from the *range* signal generated by the altimeter converter where the doppler velocity V_z is subtracted giving the true range.

The *range mark* and *reliable* signals are routed to flight control electronics. The signals are used to rescale the *range* signal for vernier engine shutoff and to indicate whether or not the *range* signal is reliable. The *reliable operate* signal is also routed to signal processing for transmission to DSIF.

c. RADVS performance. On the *Surveyor IV* mission, the RADVS performed as planned and all events occurred as predicted from RADVS on to loss of communications,

which occurred at about $1\frac{1}{2}$ sec before predicted retro burnout. The loss of all data occurred abruptly, and the evidence does not indicate a radar failure as a primary cause of spacecraft failure. There was a possible confirmation of a small spacecraft attitude oscillation in the few seconds after the RADVS signal.

Figure IV-30 shows received signal levels (reflectivity) at the IF output in terms of db below telemetry saturation. Time in the figure is taken from time of main retro ignition. Before beam lock (during sweep for acquisition), noise level is indicated, with an occasional peak due to a received signal, if the sampling time happens to correspond to the time when the received signal is in the IF bandwidth. The noise level is high at this point compared to the level at the detector because of the wide bandwidth.

Figure IV-31 shows the received signal level at the antenna feedhorns in dbm. The predicted values are based on expected signal levels for predicted flight altitude and

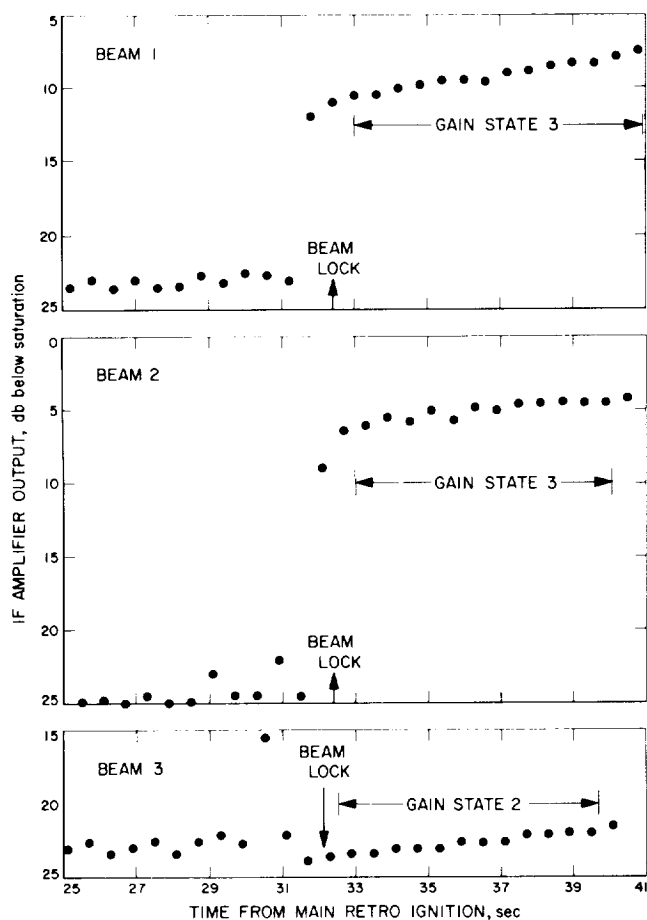


Fig. IV-30. Reflectivity of RADVS beams during descent

attitude. A nominal reflectivity was assumed corresponding to values obtained from earth-based radar observations. It was anticipated early in the *Surveyor IV* program that a variation of ± 6 db might occur in local areas. Nominal values were used for antenna gain (60 db, two-way) and for beam power output (2.45 W).

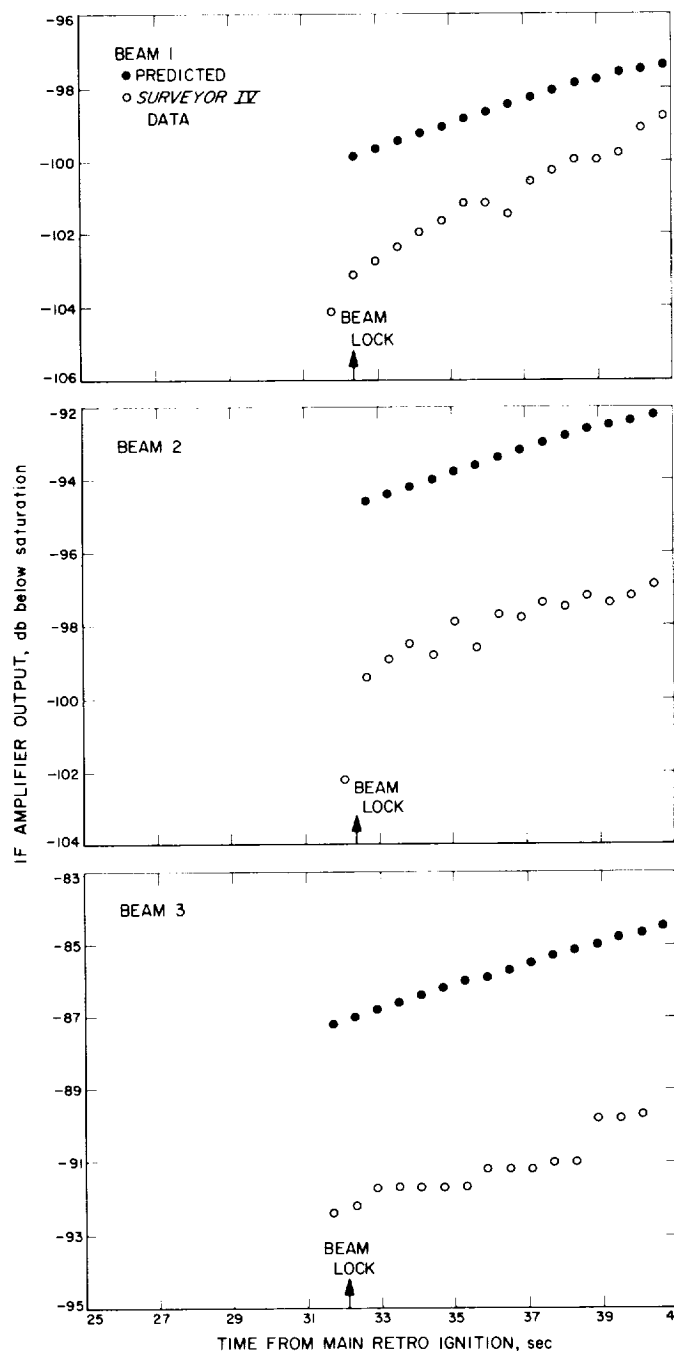


Fig. IV-31. Received signal level of RADVS beams during descent

All three velocity beams acquired lock in the same data sampling interval. While the beams were locked, the reflectivity signals followed their predicted values but were 3 to 4 db low. This is attributed to terrain reflectivity uncertainty and, possibly, to minor calibration errors. Beam 1 was the weakest received beam as was expected, owing to approach and roll angles. This beam was received at a level of -103 dbm (at the antenna feedhorn) at acquisition. This is 5 db above the required hardware acquisition level of -108 dbm. Just after burn-out, which should have occurred at about 43 sec after main retro ignition, the signal would have been about 18 db above acquisition threshold. The above-5-db margin would have been increased an additional 5 db because of decreased range and an additional 8 db because of the improvement in acquisition level after burnout. Acquisition apparently occurred as soon as the beam frequency was within the sweep range. Acquisition was, therefore, not limited by received signal level. This also was the case on all the previous missions.

Velocity component (V_x and V_y) data is presented in Fig. IV-32. It should be noted again that beam acquisition did not occur until about 32 sec after main retro ignition. After acquisition, at least a second is allowed

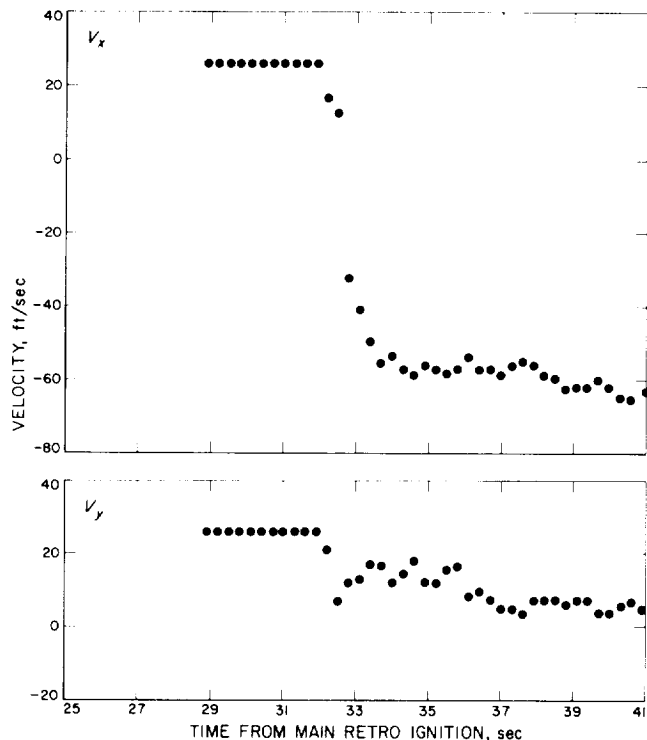


Fig. IV-32. RADVS lateral velocity components during descent

before the data can be considered reliable. The lateral velocities were well within the accuracy and noise requirements, but suggest a possible spacecraft attitude oscillation up to perhaps ± 0.1 deg. The low-amplitude, semiperiodic oscillation is observable in both of these velocity components, particularly in V_x . This characteristic was not noted in the lateral velocities on previous missions. The component V_z was not plotted since, as expected, the telemetry was saturated during the observable period.

H. Telecommunications

The *Surveyor* telecommunications subsystem contains radio, signal processing, and command decoding equipment to provide (1) a method of telemetering information to the earth, (2) the capability of receiving and processing commands to the spacecraft, and (3) angle-tracking one- or two-way doppler for orbit determination.

1. Radio Subsystem

The radio subsystem utilized on the *Surveyor* spacecraft is shown schematically in Fig. IV-33. Dual receivers, transmitters, and antennas were originally meant to provide redundancy for added reliability. As presently mechanized, this is not completely true owing to switching limitations. Each receiver is permanently connected to its corresponding antenna and transmitter. The transmitters, which are capable of operation in two different power modes (100-mW low power, and 10-W high power), can each be commanded to transmit through any of the three antennas. The *Surveyor* radio system operates at S-band, 2295-MHz down-link, and 2113-MHz up-link.

a. Receivers. Both receivers are identical, crystal-controlled, double-conversion units, which operate continuously as they cannot be commanded off. Each unit is capable of operation in an automatic frequency control (AFC) mode, or an automatic phase control (APC) mode. The receivers provide two necessary spacecraft functions; the detection and processing of commands from the ground stations for spacecraft control (AFC and APC modes), and the phase-coherent spacecraft-to-earth signal required for doppler tracking (APC mode).

b. Transmitters. Transmitters A and B are identical units which provide the spacecraft-to-earth link for telemetry and doppler tracking information. The transmitters are commanded on, one at a time, from the ground stations. Each unit contains two crystal-controlled oscillators, wideband for TV and scientific information,

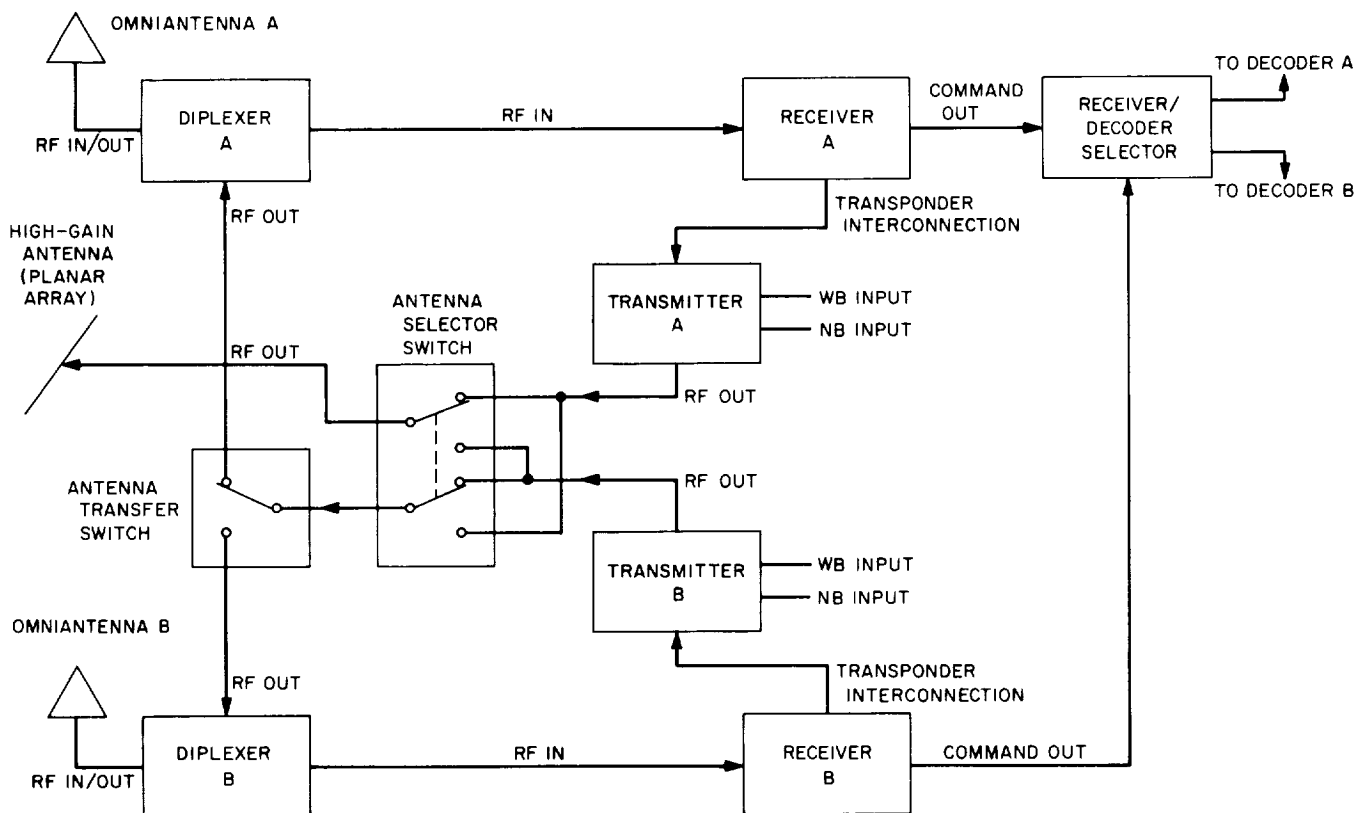


Fig. IV-33. Radio subsystem block diagram

narrowband for engineering data. Either unit can be commanded on at will, and, in addition, can operate from the receiver voltage-controlled oscillator (transponder mode) when coherent signals are required for two-way doppler tracking. The transmitters may be commanded to operate through any one of the spacecraft antennas as desired, and both are capable of providing either 100 mW or 10 W of output power.

c. Transponders. Two identical transponder interconnections permit each transmitter to be operated, on command, in a transponder mode. In the transponder mode, a transmitter is operated with the corresponding receiver voltage-controlled oscillator to provide coherent signals when two-way doppler tracking data is required.

d. Antennas. Three antennas are utilized on the *Surveyor* spacecraft. Two antennas are omnidirectional units which provide receive-transmit capability for the spacecraft. The third antenna is a high-gain, 27-db directional planar array used for transmission only of wide-band information.

e. Radio subsystem performance. The radio subsystem performed well during the *Surveyor IV* mission and gave no indication of abnormal behavior prior to loss of RF carrier power. The transmitter went to high power upon command from the *Centaur* shortly before spacecraft separation. The transmitter operated in high power for about 28 min until commanded to low power by DSS 72, Ascension, after that station had established good two-way lock with the spacecraft about 28 min after liftoff.

The RF frequencies of the receivers and transmitters remained well within the specified limits during the mission. However, about 35½ hr after launch, while the spacecraft was being tracked by DSS 51 and DSS 11, both tracking stations reported a drop of lock. The spacecraft was then in transponder operation with two-way lock between DSS 51 and the spacecraft. DSS 51 was then in the process of changing the up-link frequency as indicated by the station log and spacecraft telemetry. It is believed that the up-link frequency was changed too fast for the spacecraft to follow. Loss of up-link lock would result in transfer of the down-link frequency from transponder voltage-controlled crystal oscillator (VCXO) to transmitter

narrow band VCXO. The sudden change in down-link frequency would then cause the DSS receivers to lose lock. The momentary drop of lock is still being investigated, but no further significant information appears to be available.

The Canopus acquisition roll maneuver was initiated about 6 hr after liftoff. The up-link signal level of Omniantenna A/Receiver A during the roll is shown in Fig. IV-34. The signal strength varied about 25 db during the roll maneuver, and the measured and predicted antenna patterns followed each other within the expected tolerance except for a 120-deg section of the roll. During the 120-deg section, the measured signal averaged about 3 db below the predicted signal. Peaks and nulls of the predicted and measured signal strength did not correspond exactly and resulted in a maximum deviation of a little less than 6 db. Although the deviations from predicted levels are not understood at this time, Omniantenna A displayed the same characteristics during the Canopus roll maneuver on the *Surveyor III* mission.

Receiver A/Omniantenna A performance for the mission is plotted in Fig. IV-35. In general, the signal strength to Receiver A was above the predicted level. Although the signal level varied up and down, the larger variations can be identified with gyro drift checks and were expected because of the operating region within the antenna pattern. By observing the operating region indicated in Fig. IV-34 by the point at which Canopus lock occurred, the effect of slight spacecraft variations on signal strength is revealed. About 5-deg variation in angle produced 15-db difference in signal strength.

Receiver B/Omniantenna B performance is plotted in Fig. IV-36. The signal to Receiver B was below the predicted level during the entire mission. Prior to Canopus lock, the predicted signal strength is not expected to be valid, and the large deviation between predicted and measured values is of no concern. After Canopus lock, the received signal strength remained about 5 db below the expected level. The 5-db difference is not understood at this time and is being investigated. The received signal

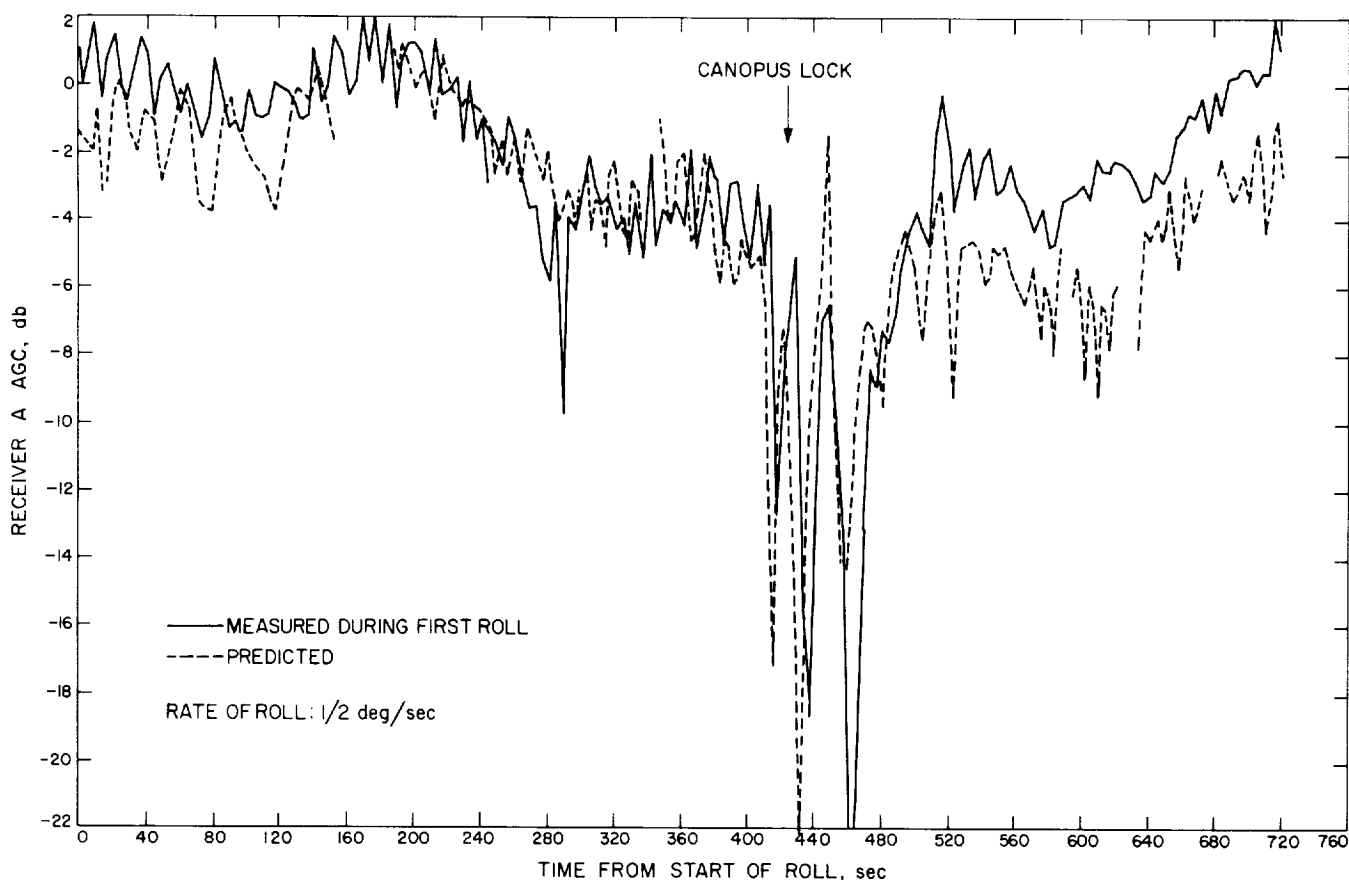


Fig. IV-34. Omniantenna A/Receiver A signal level during Canopus acquisition roll

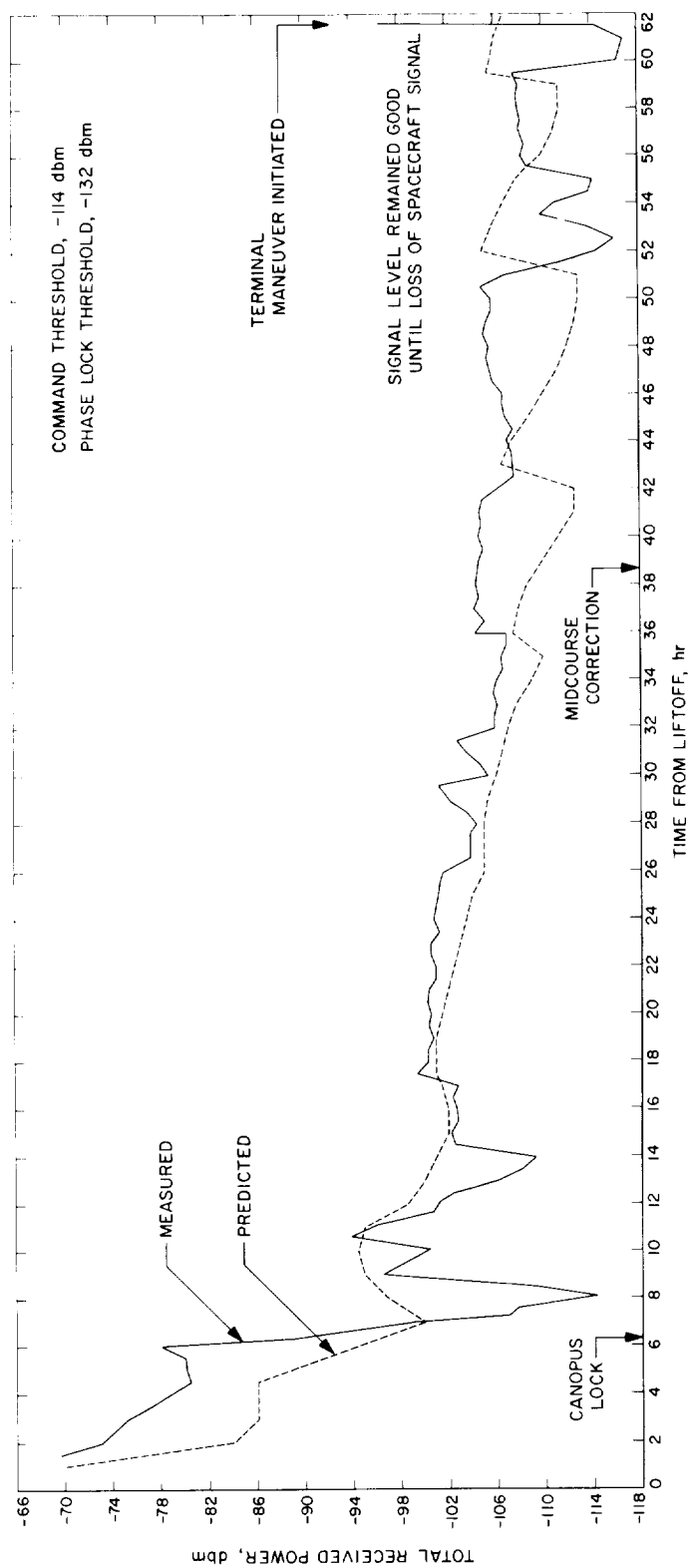


Fig. IV-35. Omniantenna A/Receiver A total received power during transit

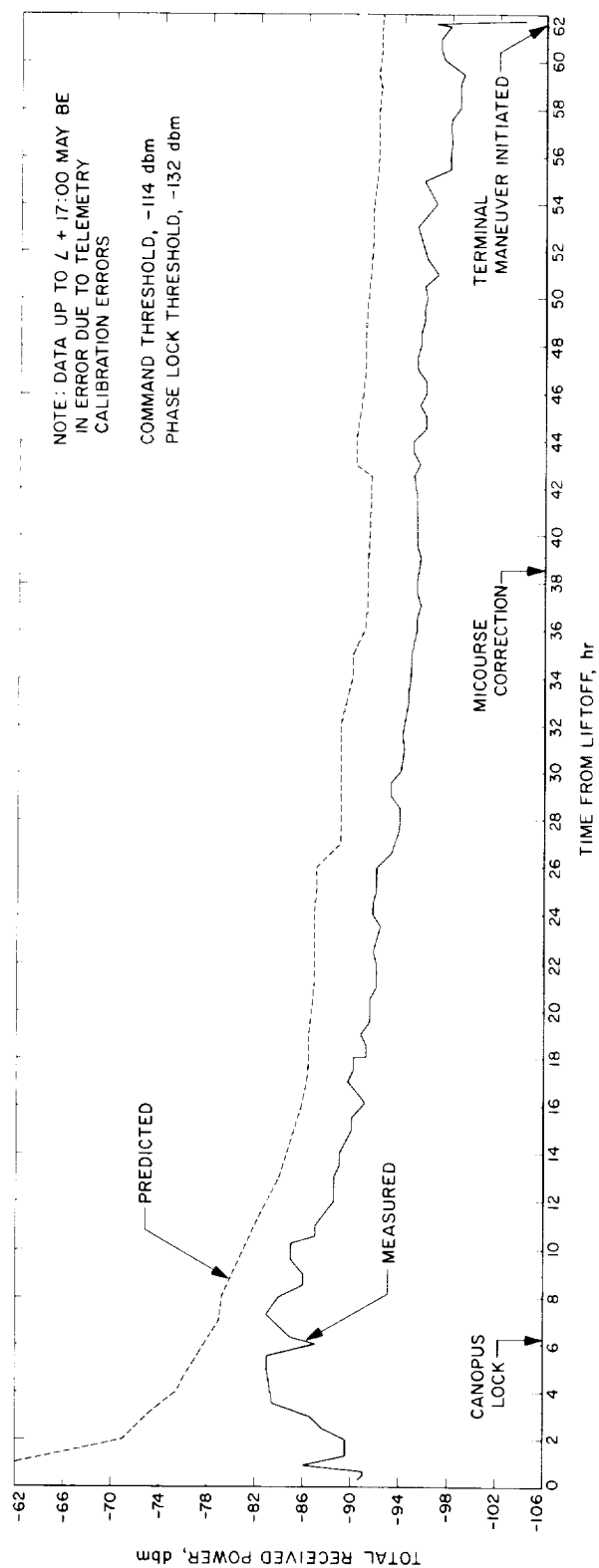


Fig. IV-36. Omniantenna B/Receiver B total received power during transit

level remained well above the command threshold level of -114 dbm, and no difficulty was experienced in commanding the spacecraft prior to the loss of spacecraft signal during terminal descent.

Measured and predicted down-link signal strengths are shown in Fig. IV-37. The down-link signal followed the predicted signal strength well during the mission. After Canopus lock, the measured signal strength remained within 2 db of the predicted signal strength. Toward the end of the mission, the down-link signal strength was greater than predicted.

At loss of spacecraft signal during terminal descent, the RF carrier and data subcarrier signals disappeared within less than 1 msec of each other, as illustrated in the DSIF recordings presented in Fig. IV-38. The signal loss closely followed the AGC circuit time constant, which would indicate that there was no evidence of subcarrier loss before carrier loss.

2. Signal Processing Subsystem

The *Surveyor* signal processing subsystem accepts, encodes, and prepares for transmission voltages, currents and resistance changes corresponding to various spacecraft parameters such as events, voltages, temperatures, accelerations, etc.

The signal processor employs both pulse code modulation and amplitude-to-frequency modulation telemetry techniques to encode spacecraft signals for frequency- or phase-modulating the spacecraft transmitters and for recovery of these signals by the ground telemetry equipment. A simplified block diagram of the signal processor is shown in Fig. IV-39.

The input signals to the signal processor are derived from various voltage or current pickoff points within the other subsystems as well as from standard telemetry transducing devices such as strain gages, accelerometers, temperature transducers, and pressure transducers. These signals generally are conditioned to standard ranges by the originating subsystem so that a minimum amount of signal conditioning is required by the signal processor.

As illustrated in Fig. IV-39, some of the signal inputs are commutated to the input of the analog-to-digital converter (ADC) while others are applied directly to subcarrier oscillators. The measurements applied directly are accelerometer and strain gage measurements which require continuous monitoring over the short intervals in which they are active.

The commutators apply the majority of telemetry input signals to the ADC, where they are converted to a digital word. Binary measurements such as switch closures or contents of a digital register already exist in digital form and are therefore routed around the ADC. In these cases, the commutator supplies an inhibit signal to the ADC and, by sampling, assembles the digital input information into 10-bit digital words. The commutators are comprised of transistor switches and logic circuits which select the sequence and number of switch closures. There are six engineering commutator configurations (or modes) used to satisfy the telemetry requirements for the different phases of the mission and one TV commutator configuration located in the TV auxiliary. The content of the telemetry modes is presented in Appendix C.

The ADC generates an 11-bit digital word for each input signal applied to it. Ten bits of the word describe the voltage level of the input signal, and the eleventh bit position is used to introduce a bit for parity checking by the ground telemetry equipment. The ADC also supplies commutator advance signals to the commutators at one of five different rates. These rates enable the signal processor to supply telemetry information at 4400, 1100, 550, 137.5, and 17.2 bit/sec. The bit rates and commutator modes are changed by ground commands.

The subcarrier oscillators are voltage-controlled oscillators used to provide frequency multiplexing of the telemetry information. This technique is used to greatly increase the amount of information transmitted on the spacecraft carrier frequency.

The summing amplifiers sum the outputs of the subcarrier oscillators and apply the composite signal to the spacecraft transmitters. Two types of summing amplifiers are employed because of the transmitter's ability to transmit either a phase-modulated or a frequency-modulated signal.

The signal processing subsystem employs a high degree of redundancy to insure against loss of vital spacecraft data. Two ADC's, two independent commutators—the engineering signal processor (ESP) and auxiliary engineering signal processor (AESP)—and a wide selection of bit rates (each with the ADC driving a different subcarrier oscillator) provide a high reliability of the signal processing subsystem in performing its function.

The signal processing subsystem behaved normally during the *Surveyor IV* mission. From launch to the loss of spacecraft signal, 151 commands effecting changes in the signal processor were received and properly executed by

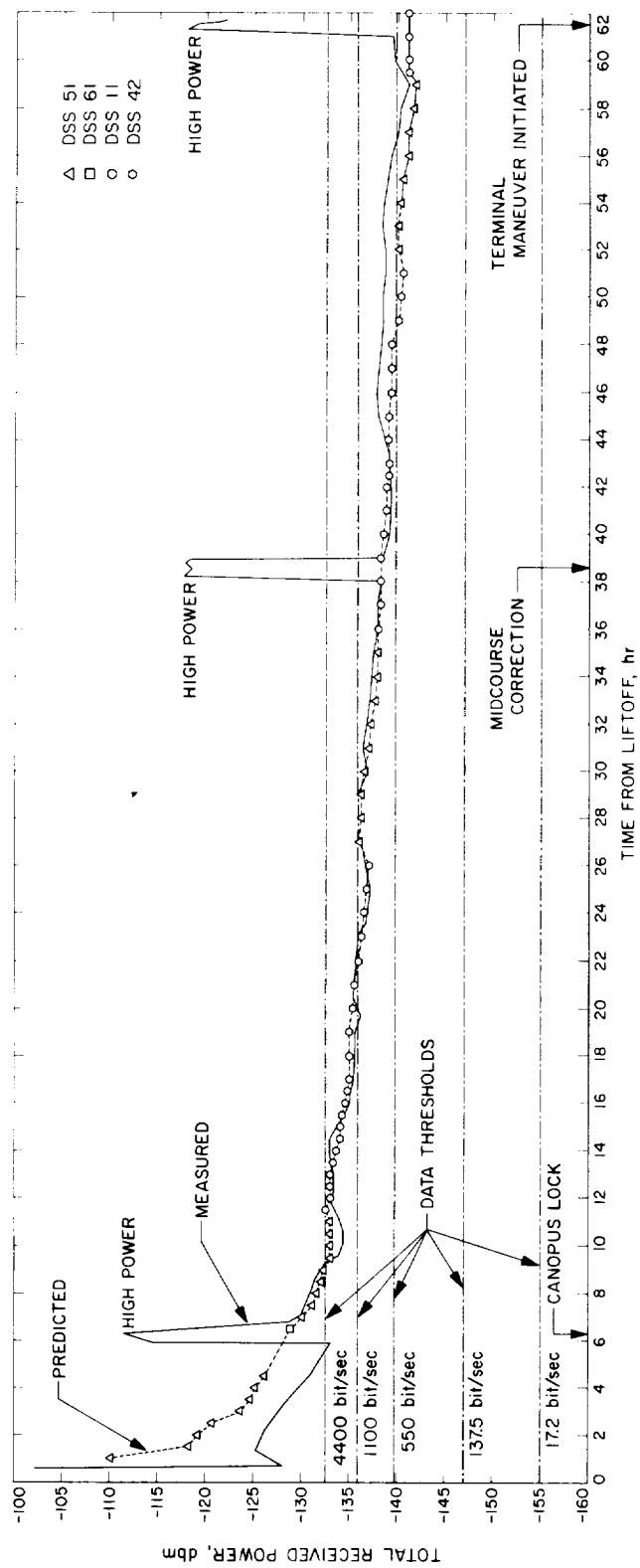


Fig. IV-37. DSIF total received power during transit

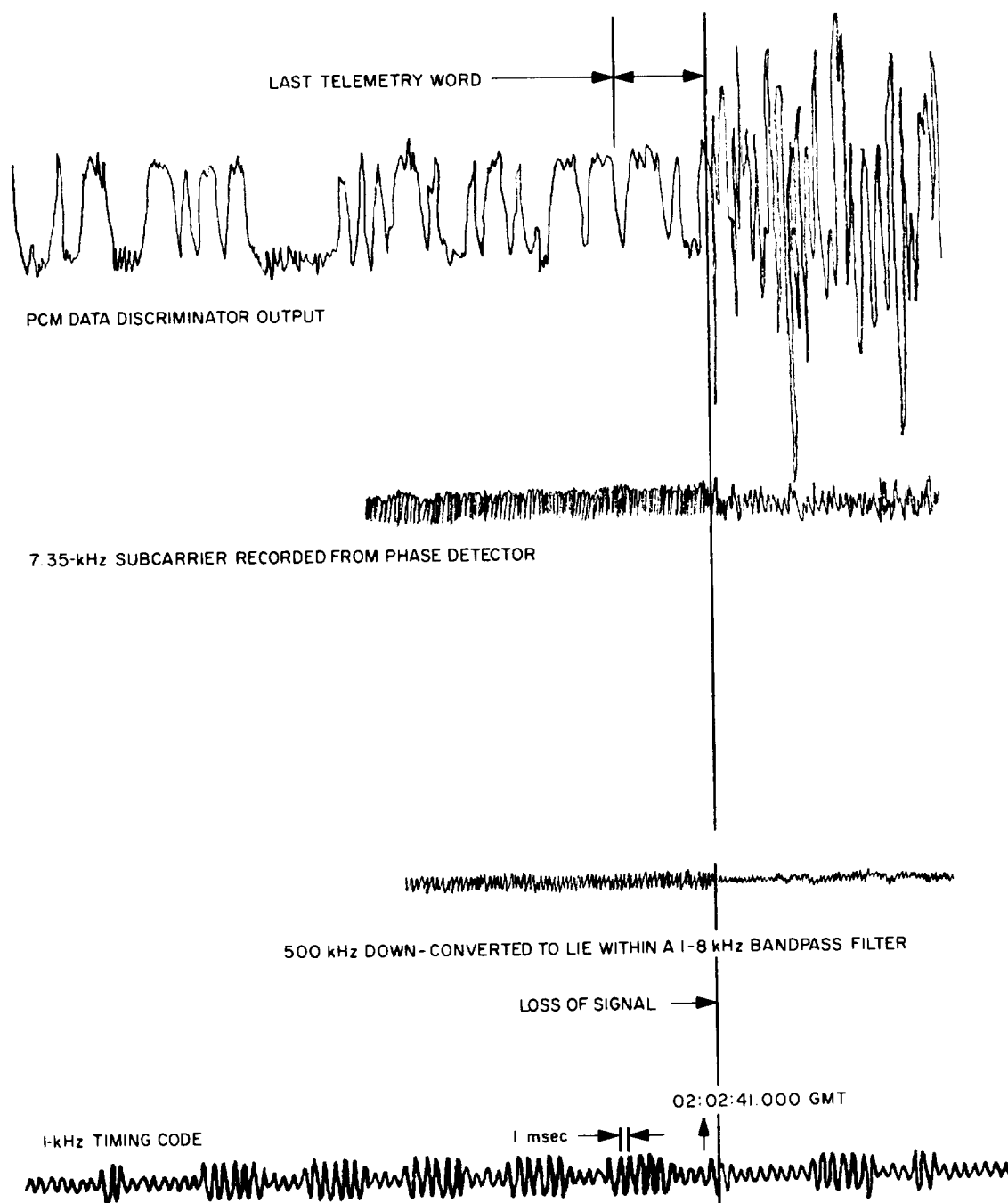


Fig. IV-38. DSS II recordings at time of loss of spacecraft signal

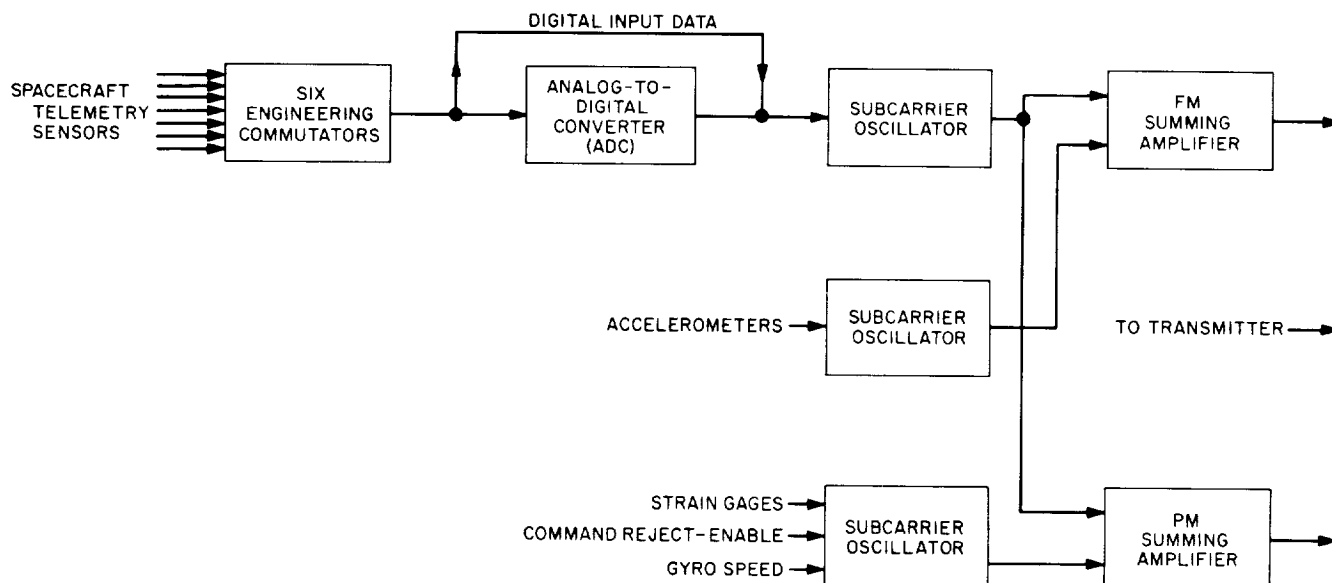


Fig. IV-39. Simplified signal processing functional block diagram

Table IV-16. Typical signal processing parameter values

Parameter	Prelaunch	Flight
ESP reference volts (Mode 2), V	4.812	4.851
ESP reference volts (Mode 4), V	4.870	4.861
ESP reference return, V	0.000	0.000
ESP unbalance current (Mode 2), μ A	-3.070	2.779
ESP unbalance current (Mode 4), μ A	-1.713	-1.713
ESP full-scale current calibration, % error from nominal	0.464	0.569
ESP mid-scale current calibration, % error from nominal	0.229	0.229
ESP zero-scale current calibration, % error from nominal	0.575	0.575
AESP full-scale current calibration, % error from nominal	0.105	0.300
AESP mid-scale current calibration, % error from nominal	0.094	0.288
AESP zero-scale current calibration, % error from nominal	0.293	0.391
AESP unbalance current, μ A	-2.814	-2.814

the signal processor. Table IV-16 shows representative prelaunch and flight values of the telemetered signal processing parameters.

3. Command Decoding Subsystem

These commands were received, detected, and decoded by one of the four receiver/central command decoder (CCD) combinations possible in the *Surveyor* command subsystem. The selection of the combination is accom-

plished by stopping the command information from modulating the up-link radio carrier for 0.5 sec. Once the selection is made, the link must be kept locked up continuously by either sending serial command words or unaddressable command words (referred to as fill-ins) at the maximum command rate of 2 word/sec.

The command information is formed into a 24-bit Manchester-coded digital train and is transmitted in a PCM/FM/PM modulation scheme to the spacecraft. When picked up by the spacecraft omniantennas, the radio carrier wave is stripped of the command PCM information by two series FM discriminators and a Schmitt digitizer. This digital output is then decoded by the CCD for word sync, bit sync, the 5-bit address and its complement, and the 5-bit command and its complement—this latter only for DC's (direct commands) since the QC's (quantitative commands) contain 10 bits of information rather than 5 command bits and their complements. The CCD then compares the address with its complement and the command with its complement on a bit-by-bit basis. If the comparisons are satisfactory, the CCD then selects that one of the eight subsystem decoders (SSD's) having the decoded address bits as its address, applies power to its command matrix, and then selects that one of the 32 matrix inputs having the decoded command bits as its address to issue a 20-msec pulse which initiates the desired single action.

Those DC commands that are irreversible or extremely critical are interlocked with a unique command word.

Ten of the DC's and all of the QC's are in this special category. None of these commands can be initiated if the interlock command word is not received immediately prior to the critical command.

The QC's, besides being interlocked, are also treated somewhat differently by the command subsystem. The only differences between the DC and QC are: (1) a unique address is assigned the QC words; (2) the QC word contains 10 bits of quantitative information in place of the 5 command and 5 command complement bits. Therefore, when this unique QC address is recognized, the CCD selects the flight control sensor group (FCSG) SSD and shifts the 10 bits of quantitative information into the FCSG magnitude register. Hence, the QC quantitative bits are loaded as they are decoded.

The command decoding subsystem performed properly throughout the *Surveyor IV* mission. No substandard behavior was evidenced through loss of the spacecraft signal. From liftoff to loss of signal, the *Surveyor IV* mission required a total of 295 earth commands. Nine of these were quantitative commands which provided the spacecraft with the quantitative information necessary for attitude and trajectory correction maneuvers; the other 285 were direct commands which initiated single actions such as *AMR power on*, *A/D clock rate 1100 bit/sec*, etc.

I. Television

The television subsystem is designed to obtain photographs of the lunar surface, lunar sky, and portions of the landed spacecraft. For the *Surveyor IV* mission, the subsystem consisted of a survey camera capable of panoramic viewing and a television auxiliary for processing commands and telemetry data.

1. Survey Camera

The survey television camera is shown in Fig. IV-40. The camera provides images over a 360-deg panorama and from +40 deg above the plane normal to the camera Z-axis to -60 deg below this same plane. The camera Z-axis is inclined 16 deg from the spacecraft Z-axis. Each picture, or frame, is imaged through an optical system onto a vidicon image sensor whose electron beam scans a photoconductive surface, thus producing an electrical output proportional to the conductivity changes resulting from the varying reception of photons from the subject. The camera is designed to accommodate scene luminance levels from approximately 0.008 ft-lamberts to

2600 ft-lamberts, employing both electromechanical mode changes and iris control. Camera operation is totally dependent upon reception of the proper commands from earth. Commandable operation allows each frame to be generated by shutter sequencing preceded by appropriate lens settings and mirror azimuth and elevation positioning to obtain adjacent views of the subject. Functionally, the camera provides a resolution capability of approximately 1 mm at 4 meters and can focus from 1.23 meters to infinity.

Figure IV-41 depicts a functional block diagram of the survey camera and television auxiliary. Commands for the camera are processed by the telecommunications command decoder, with further processing by the television auxiliary decoder. Identification signals, in analog form, from the camera are commutated by the television auxiliary, with analog-to-digital conversion being performed within the signal processing equipment of the telecommunications subsystem. The ID data in PCM form is mixed in proper time relationship with the video signal in the TV auxiliary and subsequently sent to the telecommunications system for transmission to earth.

The survey camera contains a mirror, filters, lens, shutter, vidicon, and the attendant electronic circuitry.

The mirror assembly is comprised of a 10.5×15 cm elliptical mirror supported at its minor axis by trunnions. This mirror is formed by vacuum-depositing a Kanogen surface on a beryllium blank, followed by a deposition of aluminum with an overcoat of silicon monoxide. The mirrored surface is flat over the entire surface to less than $\frac{1}{4}$ wavelength at $\lambda = 550 \text{ m}\mu$ and exhibits an average specular reflectivity in excess of 86%. The mirror is positioned by means of two drive mechanisms, one for azimuth and the other for elevation.

The mirror assembly contains three filters (red, green, and blue), in addition to a fourth section containing a clear element for nonmonochromatic observations. The filter characteristics are tailored such that the camera responses, including the spectral response of the image sensor, the lens, and the mirror match as nearly as possible the standard CIE tristimulus value curves (Fig. IV-42). Color photographs of any given lunar scene can be reproduced on earth by combining three video photographs, each made with a different monochromatic filter element in the field of view.

The optical formation of the image is performed by means of a variable-focal-length lens assembly placed

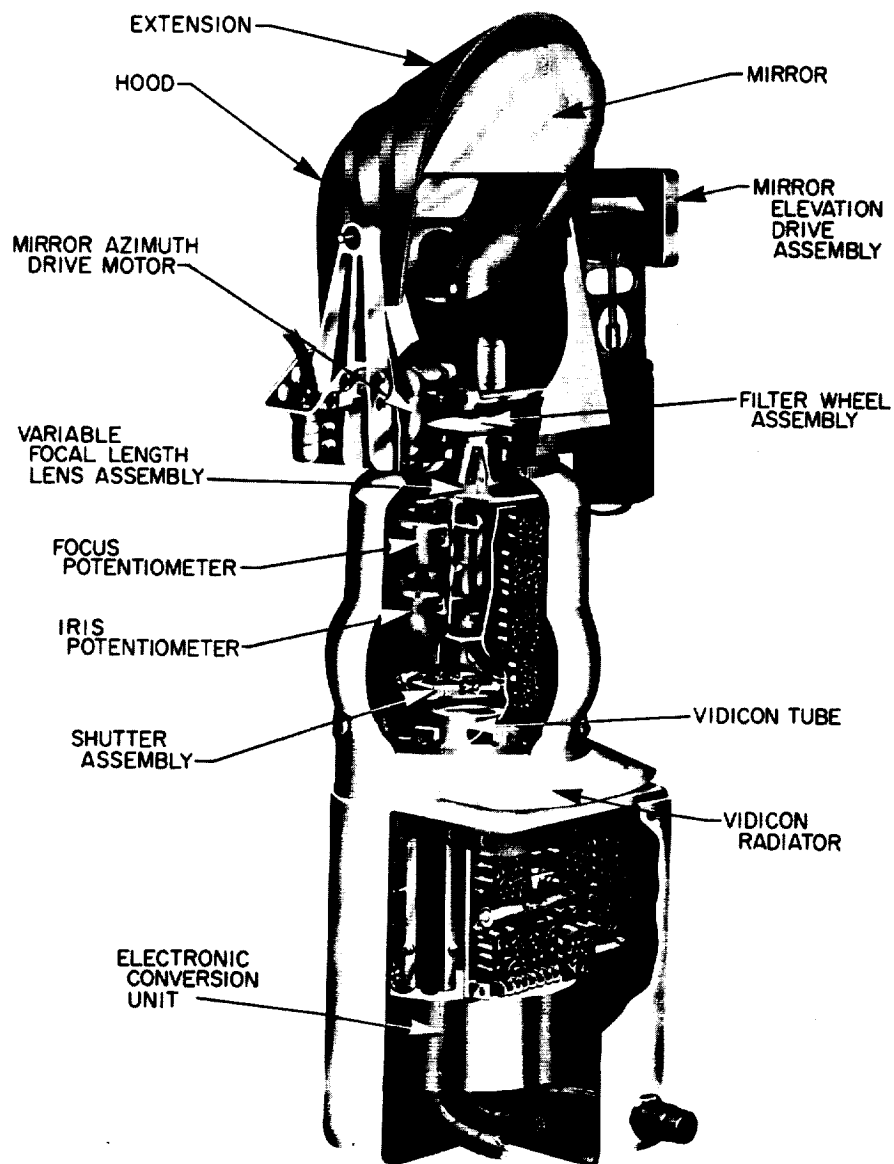


Fig. IV-40. Survey TV camera

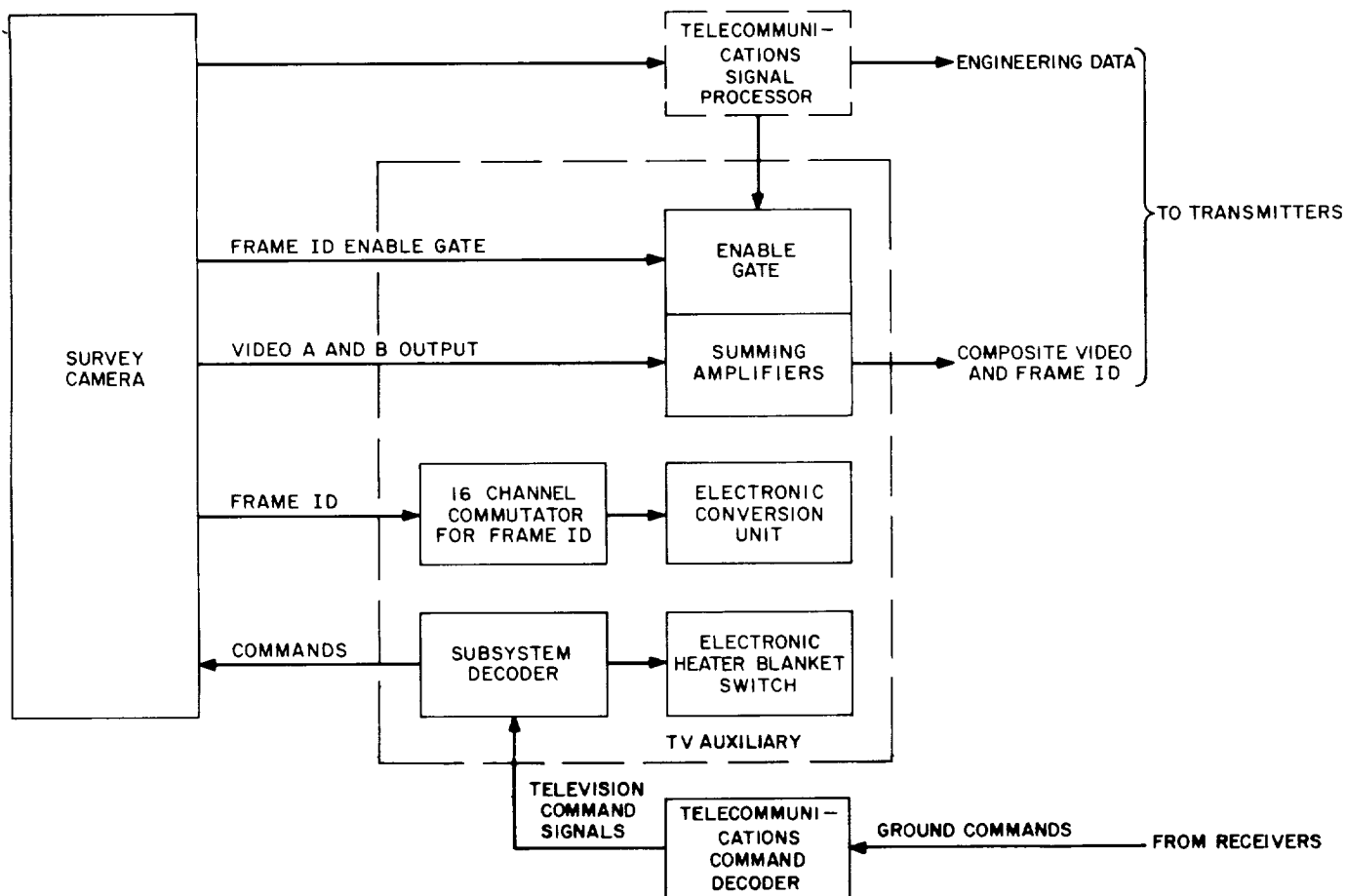


Fig. IV-41. Simplified survey TV camera functional block diagram

between the vidicon image sensor and the mirror assembly. The lens is capable of providing a focal length of either 100 or 25 mm, which results in an optical field of view of approximately 6.43 or 25.3 deg, respectively. Additionally, the lens assembly may vary its focus by means of a rotating focus cell from 1.23 meters to infinity, while an adjustable iris provides effective aperture changes of from $f/4$ to $f/22$, in increments which result in an aperture area change of 0.5. While the most effective iris control is accomplished by means of command operation, a servo-type automatic iris is available to control the aperture area in proportion to the average scene luminance. As in the mirror assembly, potentiometers are geared to the iris, focal length, and focus elements to allow readout of these functions. A beam splitter, integral to the lens assembly, provides the necessary light sample (10% of incident light) for operation of the automatic iris.

Three modes of exposure control are afforded the camera by means of a mechanical focal plane shutter

located between the lens assembly and the vidicon image sensor. In the *normal shutter* mode, upon earth command, the shutter blades are sequentially driven by solenoids across an aperture in the shutter base plate, thereby allowing light energy to reach the image sensor. The time interval between the initiation of each blade determines the exposure interval, nominally 150 msec.

In the second shutter mode (*open shutter* mode) the blades are positioned to leave the aperture open, thereby providing continuous light energy to the image sensor. This mode of operation is useful in the imaging of scenes exhibiting extremely low luminance levels, including star patterns.

A third exposure mode, used for stellar observations and lunar surface observation under earthshine illumination conditions, is referred to as the *integrate* mode. This mode is implemented by turning off the vidicon electron beam, opening the shutter, and then closing it

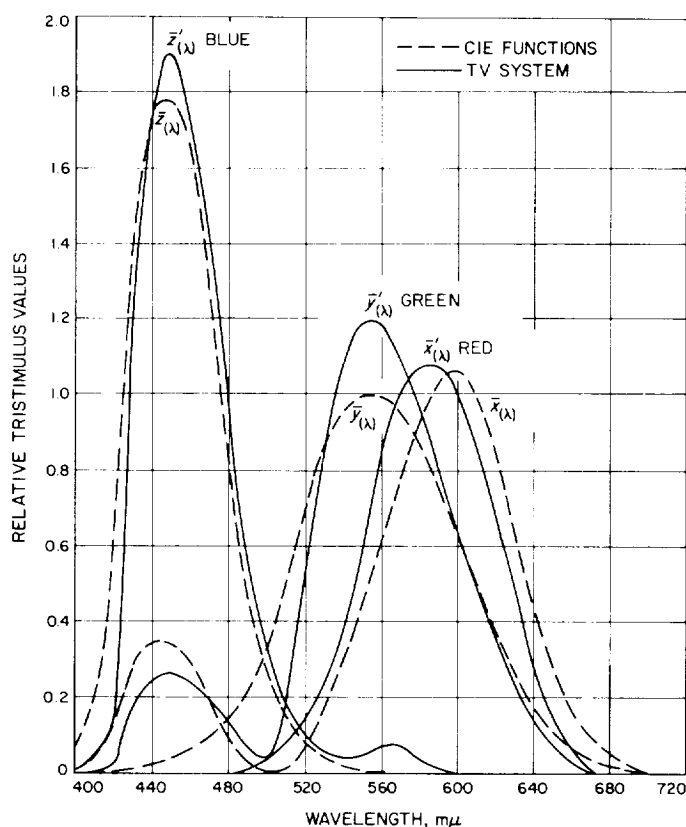


Fig. IV-42. Camera response functions compared with CIE color matching functions

after the desired exposure time. Scene luminances on the order of 0.008 ft-lamberts are reproduced in this mode of operation, thereby permitting photographs under earth-shine conditions.

The transducing process of converting light energy from the object space to an equivalent electrical signal in the image plane is accomplished by the vidicon tube. A reference mark is included in each corner of the scanned format, which provides, in the video signal, an electronic level of the scanned image.

In the normal, or 600-line scan mode, the camera provides one frame every 3.6 sec. Each frame requires nominally 1 sec to be read from the vidicon and utilizes a bandwidth of 220 kHz, requiring transmission over the high-gain (planar array) antenna.

A second scan mode of operation provides one 200-line frame every 61.8 sec. Each 200-line frame requires 20 sec to complete the video transmission and utilizes a bandwidth of 1.2 kHz. This 200-line mode is used for transmission over one of the omniantennas.

Integral to the spacecraft and within the viewing capability of the camera are two photometric/colorimetric reference charts (Fig. IV-43). These charts, one on Omni-antenna B and the other adjacent to Footpad 3, are located such that the line of sight of the camera when viewing the chart is normal to the plane of the chart. Each chart is identical and contains a series of 13 gray wedges arranged circumferentially around the chart. In addition, three color wedges, whose CIE chromaticity coordinates are known, are located radially from the chart center. A series of radial lines is incorporated to provide a gross estimate of camera resolution. Finally, the chart contains a centerpost which aids in determining the solar angles after lunar landing by means of the shadow information. Prior to launch, each chart is calibrated gonio-photometrically to allow an estimation of postlanding camera dynamic range and to aid photometric and colorimetric data reduction.

The survey camera incorporates heaters to maintain proper thermal control and to provide a thermal environment in which the camera components operate. The heater elements are designed to provide a sustaining operating temperature during the lunar night if energized. These consume 36 W of power when activated. A temperature of -20°F must be achieved prior to camera turn-on.

The camera used on the *Surveyor IV* spacecraft was fitted with a hood extension like that used on *Surveyor III* in order to reduce the possibility of direct sunlight striking the camera lens (through the filter elements). This served

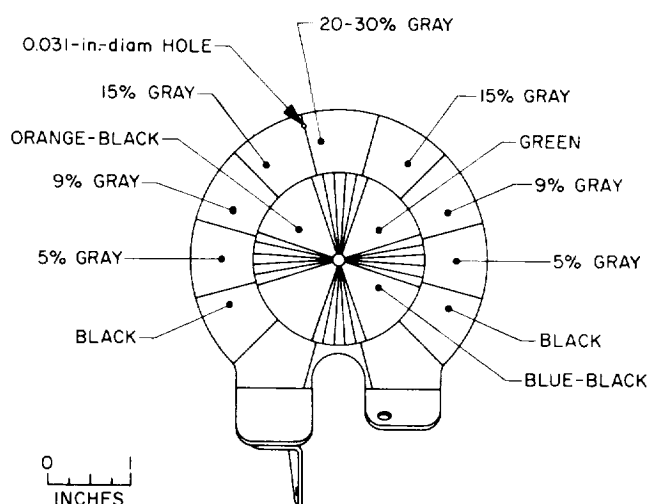


Fig. IV-43. TV photometric/colorimetric reference chart

to reduce the cases where image glare could be caused by multiple reflections within the lens assembly.

2. Performance Characteristics

A premission calibration was performed on the survey camera with the camera mounted on the spacecraft. Each calibration utilized the entire telecommunication system of the spacecraft, thereby including those factors of the modulator, transmitter, etc., which influence the overall image transfer characteristics. The calibration data, in FM form, was recorded on magnetic tape for playback through the ground support equipment (GSE) at Goldstone and Pasadena. Thus the final calibration data recorded on the real-time mission film and tape equipment provides a complete system calibration.

The parameters which were calibrated included light transfer characteristics, color response, sine wave response, erasure characteristics, automatic iris tracking, geometric linearity, and camera pointing accuracy. Data were taken in both 600- and 200-line scan modes and in normal shutter, open shutter, and integrate exposure modes.

A sampling of the calibration results using Transmitter A, at the point of initial recording (i.e., not including the GSE), is shown in Figs. IV-44 through IV-48. The ordinate in these graphs is scaled in frequency units at the output of the spacecraft transmitters with sync tip frequency deviation set to the nominal values of 1.25 MHz for 600-line scan mode and 5.0 kHz for 200-line

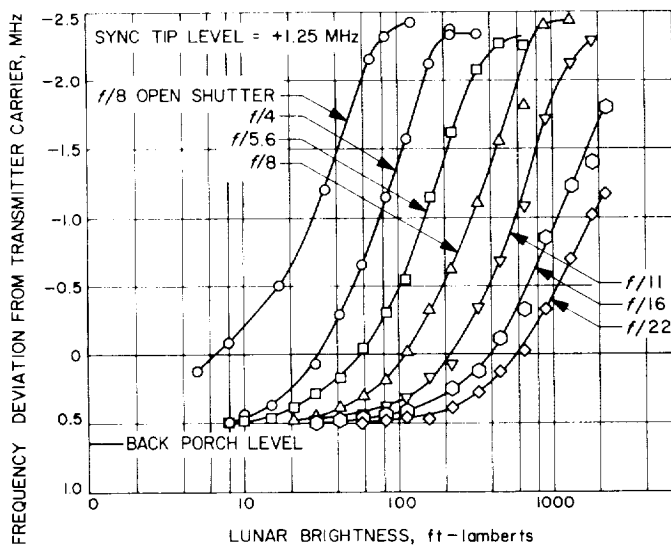


Fig. IV-44. Surveyor IV camera 600-line light transfer characteristic for center of frame

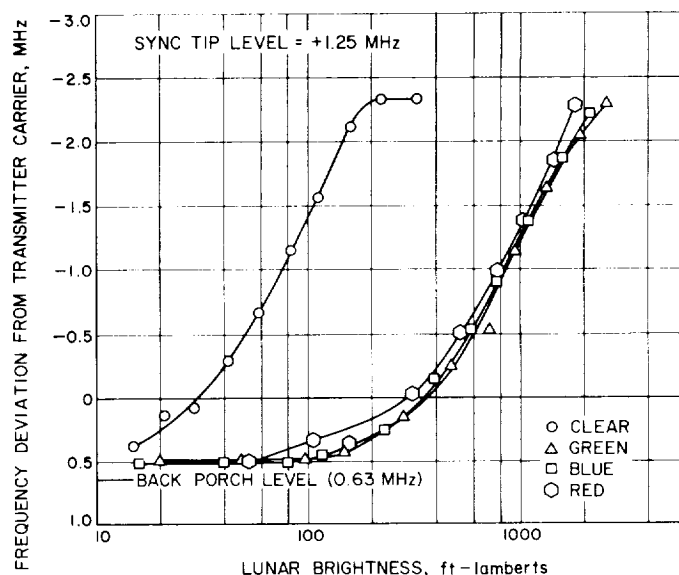


Fig. IV-45. Surveyor IV camera 600-line light transfer characteristic at $f/4$ for all filter wheel positions

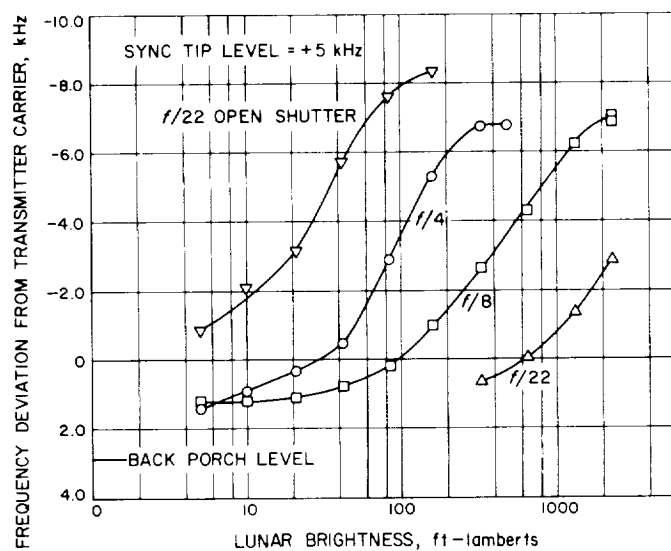


Fig. IV-46. Surveyor IV camera 200-line light transfer characteristic for center of frame

scan mode. The ordinate scale can therefore be viewed as a measure of relative video voltage.

Figures IV-44 through IV-46 show the individual curves that were obtained for various f /stops and color filters for the 200- and 600-line scan modes. The curves depict the sensitivity of the camera system at the central portion of the frame to scenes of constant or static light level. The camera system, however, did not respond the same over the entire frame. This nonuniform response,

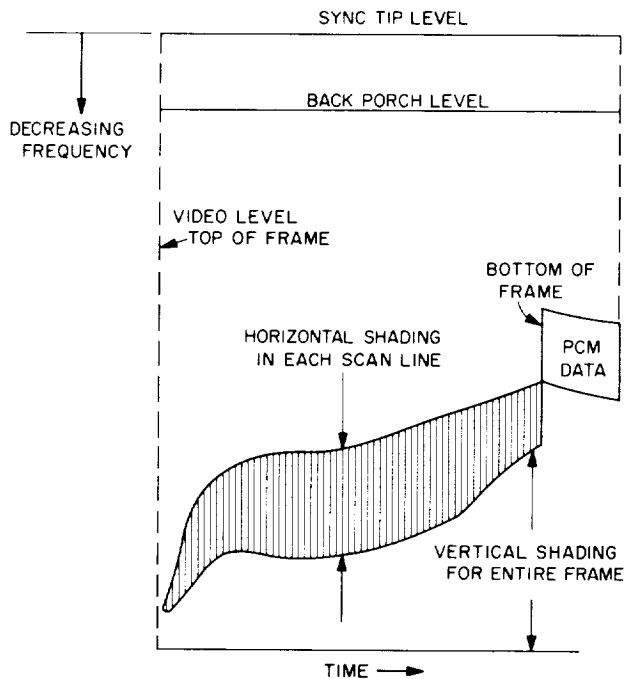


Fig. IV-47. Surveyor IV camera 600-line shading near saturation (diagram measured from Polaroid of composite frame)

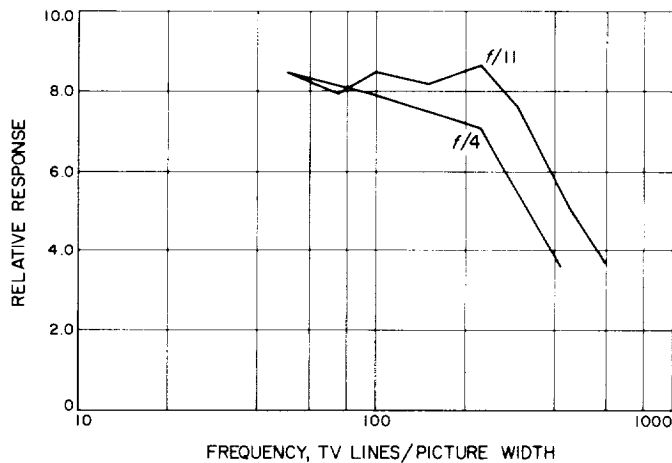


Fig. IV-48. Surveyor IV camera 600-line frequency response for center of frame

called "shading," is depicted in Fig. IV-47 for 600-line scan mode.

The data in Fig. IV-45 shows that the light transfer characteristics for the three color filters are almost identical. This provides the capability of taking a set of color

pictures without the necessity of changing iris position. Reduction of color data is then independent of accuracy or repeating limitations in iris control.

The response of the spacecraft camera system to sinusoidally varying brightness scenes is shown by Fig. IV-48. Here, the sinusoidal nature of the test scene is given by the abscissa in terms of frequency, and the relative attenuation of the sine wave amplitude by the camera system is given at the ordinate. From these curves it is seen that the spacecraft system has a 40% horizontal response at about 600 TV lines in the 600-line scan mode.

J. Soil Mechanics/Surface Sampler (SM/SS)

The SM/SS is an electromechanical device which is remotely operated by ground command to pick, dig, scrape, trench, and handle lunar surface material. The SM/SS was originally planned for later model *Surveyor* spacecraft. However, after the complete success of *Surveyor I*, the decision was made to fly the instrument on the *Surveyor III* and *IV* missions. The SM/SS was adapted to the mounting location and interface of the approach television camera and electronics which it replaced. It was necessary also to simplify the instrument to suit the reduced telemetry and commanding capability of the *Surveyor III* and *IV* spacecraft.

The SM/SS subsystem consists of a mechanism and an electronics auxiliary, with the necessary supporting substructure and interconnecting wire harnesses.

The instrument mechanism is located below the survey television camera, between the auxiliary battery and Leg 2 as shown in Fig. IV-49. The mechanism has an extension/retraction arm which can also be pivoted in azimuth or elevation to permit operations within the surface area indicated in the figure. The arm is locked in the folded position until it is to be deployed after lunar landing, at which time it is unlocked by the firing of a squib. Attached to the end of the arm is a scoop having a sharpened blade and a door. The scoop is capable of holding solid material up to about 1.25 in. (3.2 cm) in diameter and granular material up to about 6 in.³ (100 cm³) in volume. A small footpad is attached to the scoop door to present a flat surface to the lunar surface when the door is closed. Four electric motors are used to manipulate the SM/SS: one each for extension/retraction, azimuth, and elevation motions, and one located at the scoop to open or close the door. An electromechanical clutch can be operated by earth command to disengage the elevation drive train, allowing the scoop to be impelled

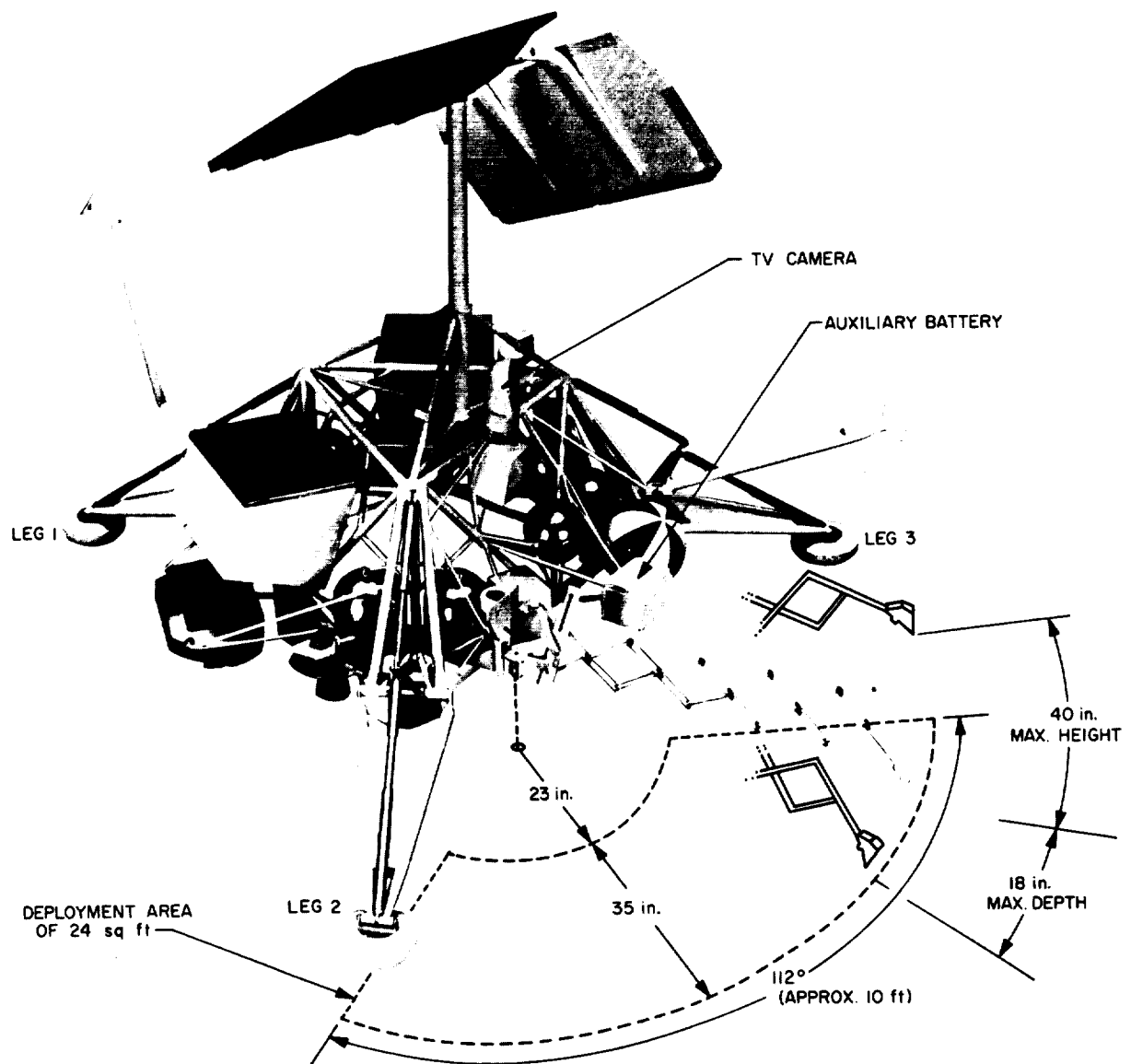


Fig. IV-49. SM/SS deployment envelope

downward by a pretensioned elevation torque spring to strike the lunar surface.

The electronics auxiliary provides command decoding, data buffering, power management, squib firing, and switch control of the mechanism motors and clutch. Either a 2-sec or a 0.1-sec period of operation of any of the motors can be selected by earth command. The angle or distance through which the SM/SS moves by these commands depends on the motor involved, its condition, temperature, voltage, and the working load. To adapt

the SM/SS to the *Surveyor III* and *IV* spacecraft design, the strain-, acceleration-, and position-measuring systems originally planned were removed, and a means was provided within the auxiliary to measure the current drawn by the motors. It is possible to make rough determinations of lunar surface mechanical properties from motor current data by using the relationship between motor current and operating loads. However, motor current data is commutated, so it is necessary to transmit data at the higher bit rates to obtain current measurements during the short periods of motor operation.

Since SM/SS direct instrumentation is limited to motor current, the primary means of obtaining SM/SS data is through the coordinated operation of the television camera, wherein television frames are commanded at selected intervals between SM/SS movements. Sequences and priorities of SM/SS tests are therefore dependent upon viewing conditions, spacecraft shadow patterns, and the performance of the television system. The azimuth axes of the SM/SS mechanism and camera are not collinear; therefore, the television viewing angle of the scoop varies with scoop position. When the scoop is positioned near Footpad 2, the camera looks directly down the extension arm, which largely obscures the scoop itself. When positioned near the auxiliary battery, a slight side view of the scoop is afforded.

A static bearing test is performed by exercising the extension and azimuth motions until the scoop is positioned above the desired surface point. Then the scoop is driven downward with the elevation motor until the desired penetration is achieved, or until the motor is stalled. The static test is normally performed with the scoop door closed to provide a flat surface for contact. However, an open scoop static test can also be carried out. As the SM/SS is extended, the angle that the scoop makes with the test surface varies. At contact with a

smooth surface, the flat face of the scoop door is normal to the tangential elevation motion, when the arm is fully extended.

For an impact test, the scoop is also positioned first above the desired surface area. Then the elevation drive clutch is released, allowing the scoop to drop to the surface, accelerated by gravity and the elevation torque spring. Impact tests are also performed with the scoop door open or closed, as desired.

A trenching operation is performed by driving the scoop down into the surface with the door open, then drawing it toward the spacecraft by repeated commanding of the retraction motor. Material can be removed from the trench either by retracting the scoop until it is clear of the surface, forming a pile at the foot of the trench, or by closing the scoop and lifting the material out of the trench.

During the transit phase of the *Surveyor IV* mission, the SM/SS electronics auxiliary temperature profile was similar to that which was experienced on *Surveyor III*. Heater power was applied to maintain the temperature well above the survival temperature of -67°F .

V. Tracking and Data System

The TDS (Tracking and Data System) for the *Surveyor IV* mission included selected resources of the AFETR (Air Force Eastern Test Range), the MSFN (Manned Space Flight Network), the DSN (Deep Space Network) and the NASCOM (NASA Communications System). This section summarizes the mission preparation, flight support, and performance evaluation of each element of the TDS.

The TDS support for the *Surveyor IV* mission was considered good. The problems experienced by elements of the TDS did not significantly affect the overall support. All requirements were met and in most cases exceeded.

A. Air Force Eastern Test Range

The AFETR performs TDS supporting functions for *Surveyor* missions during the countdown, launch and near-earth phase of the flight.

The *Surveyor* mission requirements for near-earth-phase tracking and telemetry coverage are classified as follows, in accordance with their relative importance to successful mission accomplishment:

Class I requirements consist of the minimum essential needs to ensure accomplishment of first-priority flight

test objectives. These are mandatory requirements which, if not met, may result in a decision not to launch.

Class II requirements define the needs required to accomplish all stated flight test objectives.

Class III requirements define the ultimate in desired support, and would enable the range user to achieve the flight test objectives earlier in the test program.

The AFETR configuration for the *Surveyor IV* mission is presented in Table V-1. The configuration is similar to the *Surveyor III* configuration, except that the only Range Instrumentation Ship (RIS) supporting the mission was the *Coastal Crusader*.

Figure V-1 illustrates the test support position of the *Coastal Crusader* and the planned coverage for the *Surveyor IV* on launch day. AFETR preparations for *Surveyor IV* consisted of routine testing of individual facilities, followed by several Operational Readiness Tests. All *Surveyor IV* mission requirements were met by AFETR.

1. Tracking Data (Metric)

The AFETR tracks the C-band beacon of the *Centaur* stage to provide metric data. This data is required during

Table V-1. AFETR configuration

Station		C-band tracking		Telemetry	
No.	Location	Capability	Antenna type	Capability	Antenna type
0	Patrick AFB	Beacon/skin	FPQ-6		
1	Cape Kennedy (Tel 2)	Beacon/skin	FPS-16	VHF	TLM-18
19	Kennedy Space Center, Merritt Island (Tel 4)	Beacon/skin	TPQ-18	S-band	3-ft parabola
3	Grand Bahama	Beacon	FPS-16	VHF	TAA-2A
7	Grand Turk	Beacon/skin	TPQ-18	S-band	TAA-3A
91	Antigua	Beacon/skin	FPQ-6	VHF	LH tri-helix
40	Trinidad	Beacon/skin	TPQ-18	S-band	TAA-2
WHI	RIS Coastal Crusader	Skin	FPS-43	VHF	TLM-18
12	Ascension	Skin	FPS-43	S-band	TAA-3A
13	Pretoria	Beacon	FPS-16	VHF	TAA-1
		Beacon	TPQ-18	S-band	TAA5-24
		Beacon	MPS-25	VHF	TLM-18
				S-band	3-ft parabola

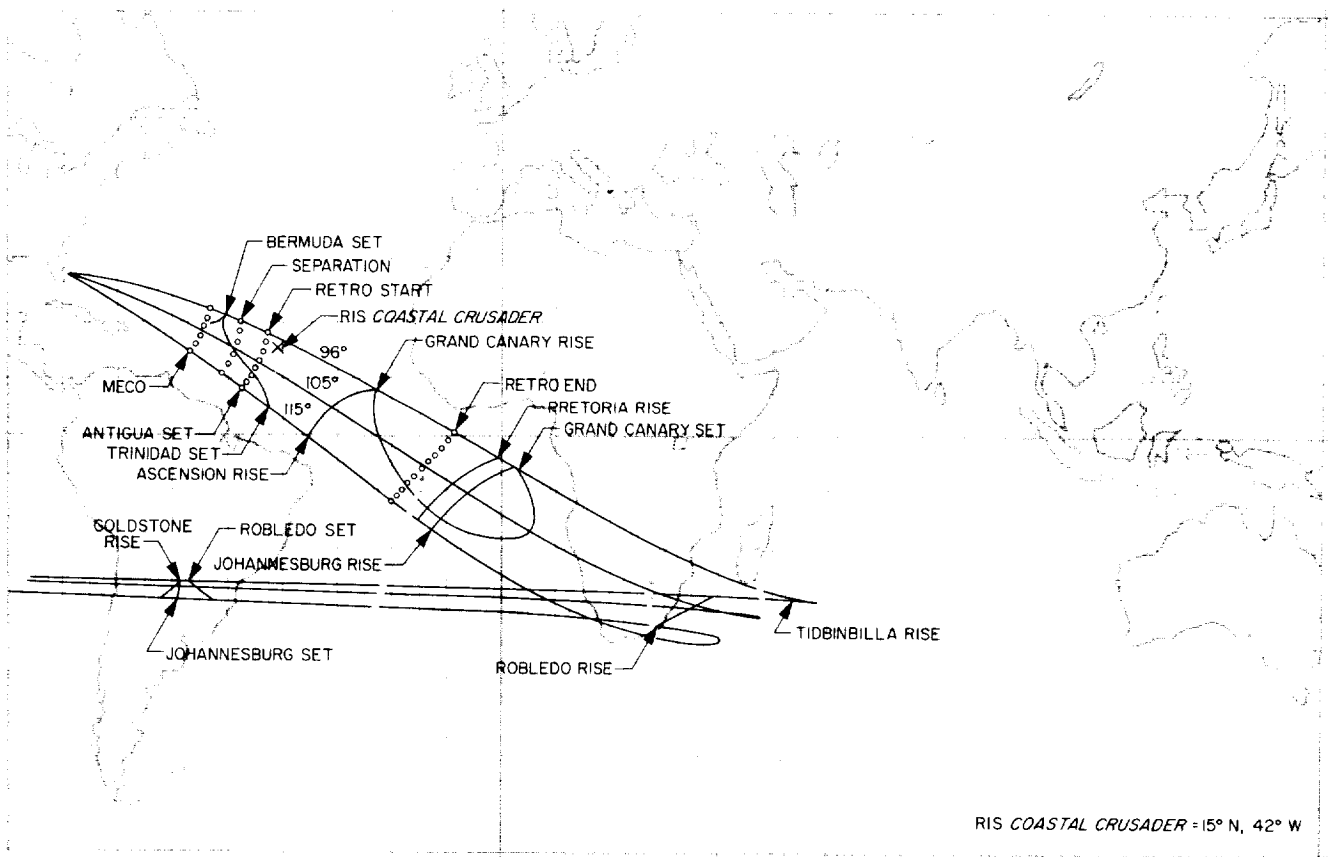


Fig. V-1. Earth tracks and TDS station coverage for July 14, 1967

intervals of time before and after separation of the spacecraft for use in calculating the *Centaur* orbit, which can be used as a close approximation of the postseparation spacecraft orbit. The *Centaur* orbit calculations are used to provide DSN acquisition information (in-flight predicts).

Estimated and actual radar coverages are shown in Figs. V-2 and V-3. The Class I requirements were met and exceeded, with AFETR stations downrange to Antigua providing continuous coverage to $L + 779$ sec and with Ascension and Pretoria providing continuous coverage from $L + 1142$ to $L + 2976$ sec.

The TPQ-18 radar at Grand Bahama experienced a failure with the azimuth servo valve on the antenna pedestal during the countdown. The radar remained down through the launch and did not support. Redundant coverage during the Grand Bahama interval was provided by other stations (see Fig. V-2).

The FPS-16 radar at Cape Kennedy experienced a 13-sec dropout at $L + 464$ sec. However, this occurred 114 sec after the end of the estimated coverage interval. Following the dropout, Cape Kennedy provided another 73 sec of data. The Grand Turk TPQ-18 radar also experienced a short dropout toward the end of its coverage interval. The radar was off track from $L + 579$ to $L + 600$ sec, then provided data until loss of signal (LOS) at $L + 675$ sec. Redundant data from other stations were provided during both of the above dropout periods.

2. Atlas/Centaur Telemetry (VHF)

To meet the Class I telemetry requirements, the AFETR must continuously receive and record *Atlas* telemetry (229.9-MHz link) from before liftoff until shortly after *Atlas/Centaur* separation, plus *Centaur* telemetry (225.7-MHz link) until shortly after spacecraft separation. Thereafter, *Centaur* telemetry is to be recorded as station coverage permits, until completion of the *Centaur* retro maneuver. In addition to the land stations, AFETR provided the RIS *Coastal Crusader*.

Estimated and actual VHF telemetry coverages are shown in Figs. V-4 and V-5. All requirements were met, since continuous and substantially redundant VHF telemetry data was received beginning with the countdown and through Pretoria LOS at $L + 3570$ sec. Coverage was greater than predicted.

3. Surveyor Telemetry (S-Band)

The AFETR is required to receive, record and retransmit *Surveyor* S-band (2295-MHz) telemetry in real-time from spacecraft transmitter *high power on* until 2 min after continuous view by DSIF stations begins. The AFETR S-band telemetry resources assigned to meet this requirement are shown in Table V-1. All S-band resources committed were on a "best effort" basis, since the *Centaur* vehicle is not roll-attitude-stabilized, and the aspect angle cannot be predicted.

Estimated and actual S-band coverages and receiver phase-lock times are shown in Figs. V-6 and V-7. Continuous coverage was obtained from liftoff to Ascension LOS at $L + 2444$ sec. Tel-4 dropped receiver phase-lock between $L + 197$ and $L + 270$ sec. However, Grand Bahama maintained lock throughout this period and provided redundant coverage.

Antigua's coverage interval was quite a bit in excess of the estimated coverage, but phase-lock was maintained for only 30% of the time. Coverage from Grand Bahama and the *Coastal Crusader* overlapped most of the Antigua view. However, during the interval from $L + 495$ to $L + 673$ sec, no station other than Antigua was in receiver phase-lock.

Receiver phase-lock was maintained continuously by the *Coastal Crusader* and then Ascension from $L + 673$ to $L + 2197$ sec. Pretoria provided redundant coverage during this interval, with receiver phase-lock from $L + 1377$ to $L + 1698$ sec.

4. Surveyor Real-Time Telemetry Data

AFETR retransmits *Surveyor* data (VHF or S-band) to Building AO, Cape Kennedy, for display and for retransmission to the SFOF. In addition, downrange stations monitor specific channels and report events via voice communication.

For the *Surveyor IV* mission, existing hardware and software facilities were utilized to meet the real-time data requirements.

All requirements were met. Spacecraft telemetry data via the VHF telemetry link were transmitted in real-time to the SFOF from liftoff to spacecraft *high-power-on*. At *high-power-on*, AFETR switched as planned to real-time transmission of spacecraft telemetry data received via the S-band link. Real-time data flow was very good.

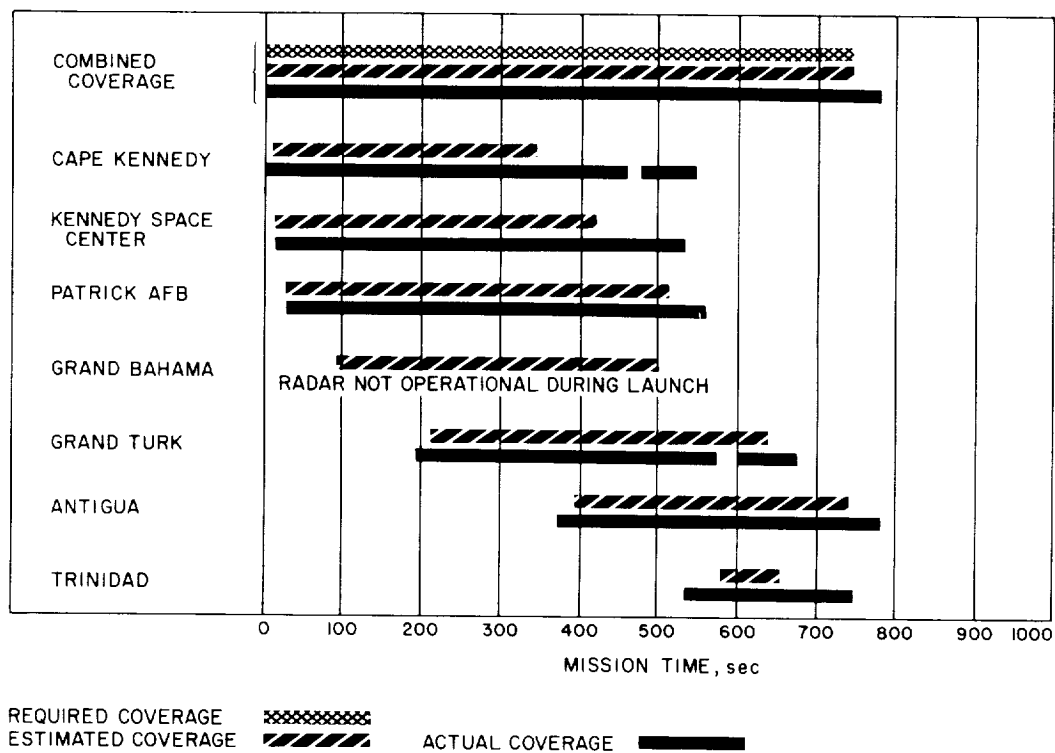


Fig. V-2. AFETR C-band radar coverage: liftoff through Trinidad

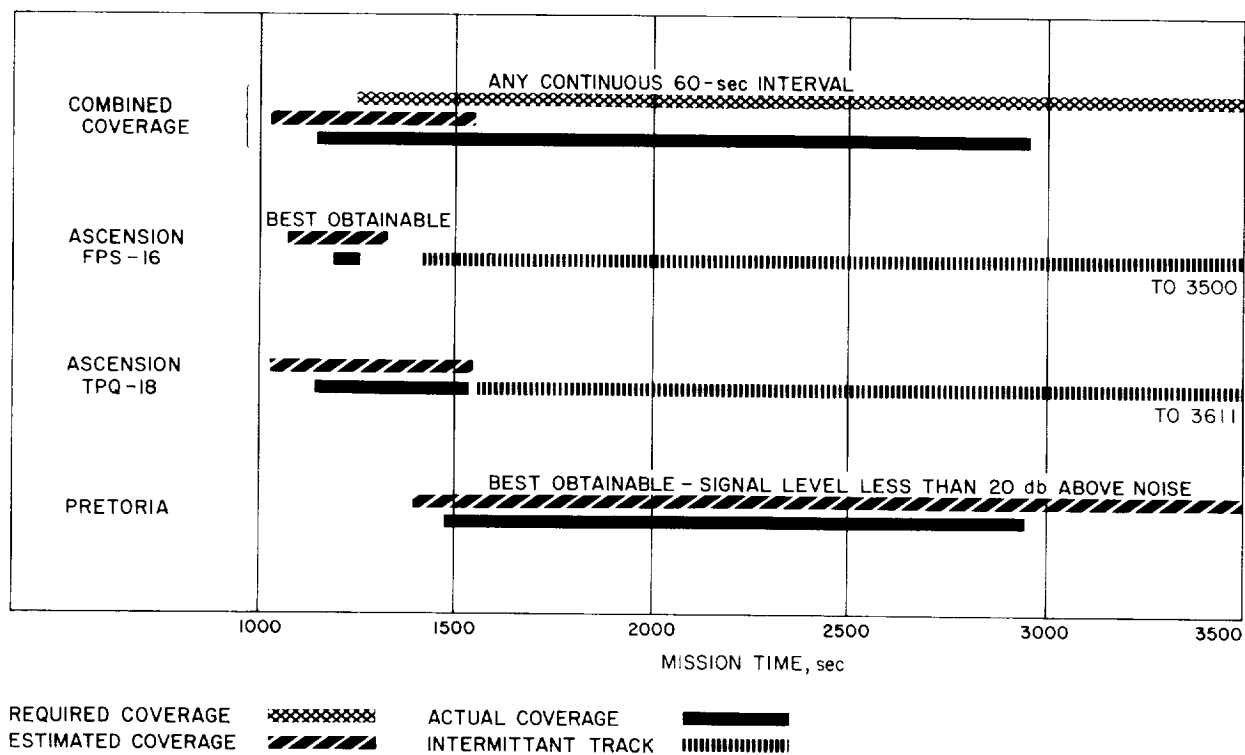


Fig. V-3. AFETR C-band radar coverage: Ascension through Pretoria

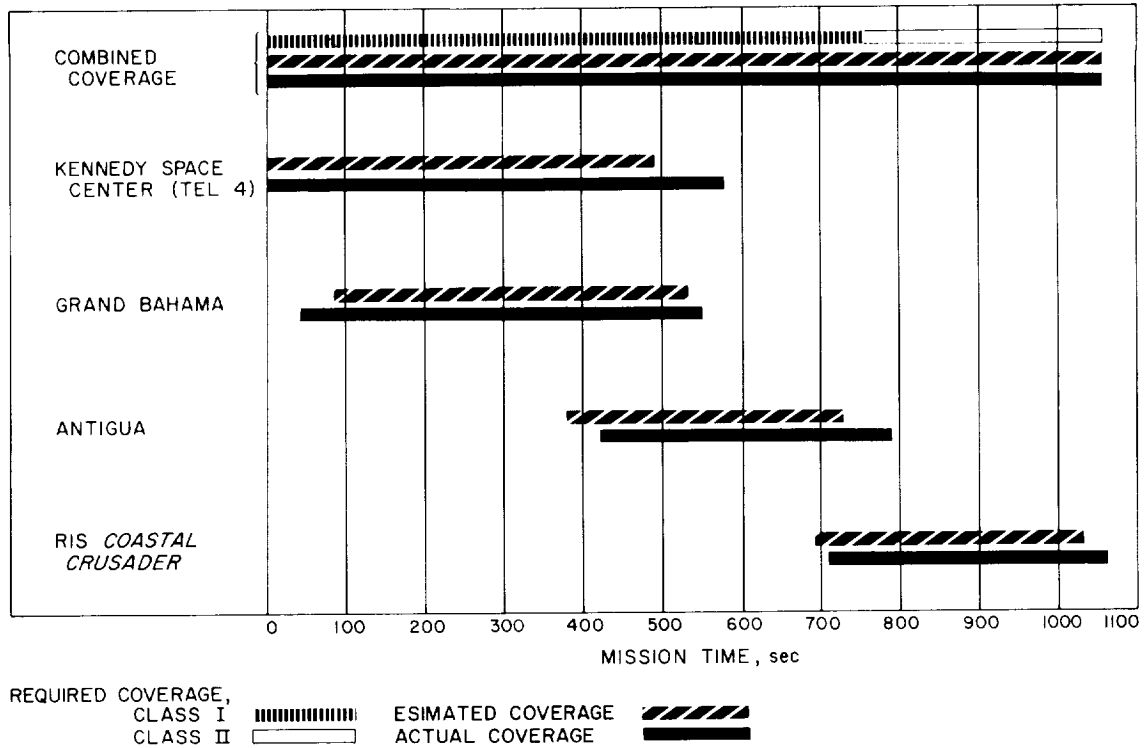


Fig. V-4. AFETR VHF telemetry coverage: liftoff through RIS Coastal Crusader

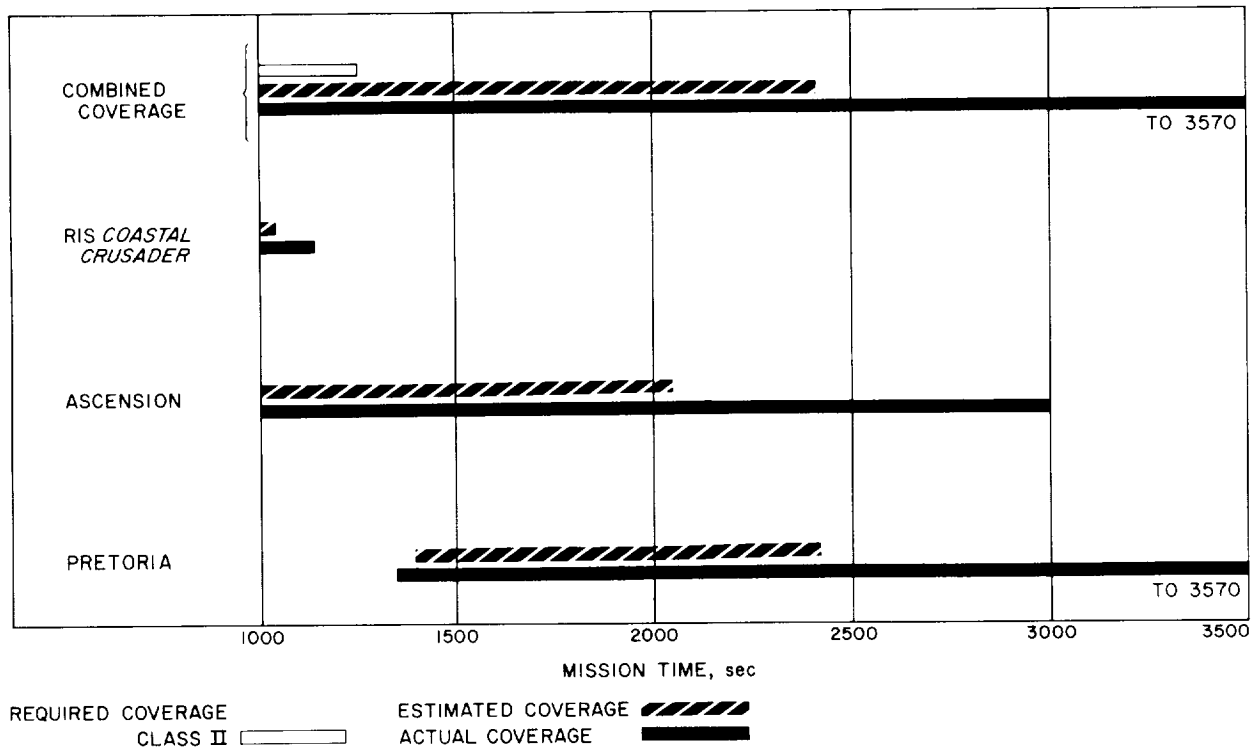


Fig. V-5. AFETR VHF telemetry coverage: RIS Coastal Crusader through Pretoria

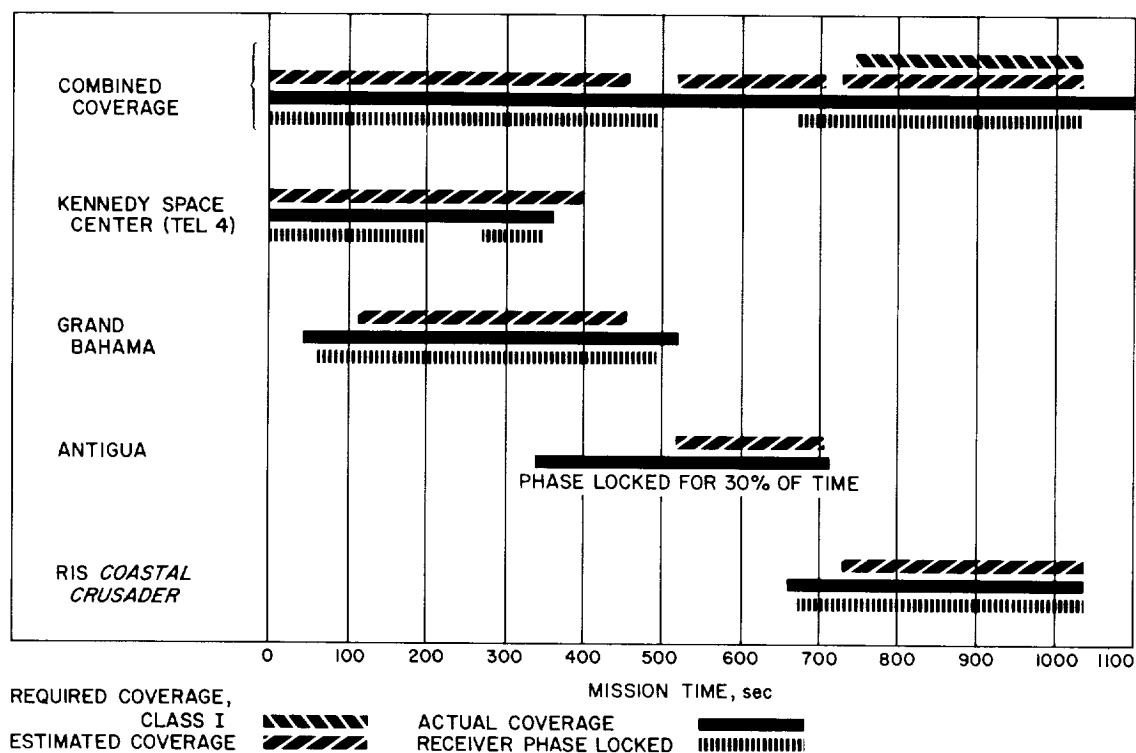


Fig. V-6. AFETR S-band telemetry coverage: liftoff through RIS Coastal Crusader

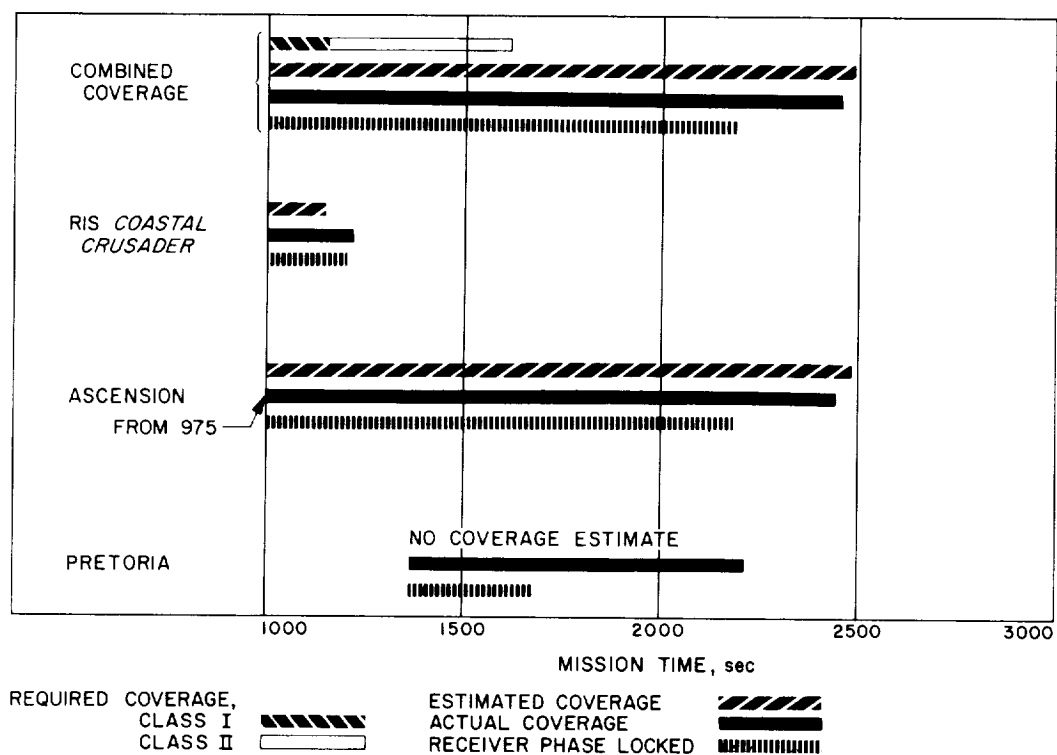


Fig. V-7. AFETR S-band telemetry coverage: RIS Coastal Crusader through Pretoria

In addition, all Mark Events except *mark 14* were read out and reported. The Mark Event times read out by AFETR and MSFN stations are shown in Table V-2. (See Appendix A, Table A-1, for a list of the Mark Events and event times determined postflight.)

5. Real Time Computer System (RTCS)

For the launch and near-earth phase of the mission, the RTCS provides trajectory computations based on tracking data and telemetered vehicle guidance data. The RTCS output includes:

- (1) The interrange vector (IRV), the standard orbital parameter message (SOPM), and orbital elements and injection conditions.
- (2) Predicts, look angles, and frequencies for acquisition use by downrange stations.
- (3) Injection conditions mapped to lunar encounter and I-matrices defining orbit determination accuracies for early trajectory evaluation prior to the highly refined orbits generated by the Flight Path Analysis and Command (FPAC) group.

A total of six orbits were computed by the RTCS, including a preretro orbit from Antigua data, a second preretro orbit from *Centaur* guidance telemetry data, a postretro orbit using Ascension and Pretoria data, two spacecraft orbits from DSS 72 data and a spacecraft orbit using DSS 72 and DSS 51 data. This last orbit was a very good solution, which compared favorably with the final pre-midcourse computation generated by the SFOF. (Also refer to Sections II-D and VII.)

B. Goddard Space Flight Center

The MSFN, managed by Goddard Space Flight Center (GSFC), supported the *Surveyor IV* mission by performing the following functions:

- (1) Tracking of the *Centaur* beacon (C-band).
- (2) Receiving and recording *Centaur*-link telemetry.
- (3) Providing real-time confirmation of certain Mark Events.
- (4) Providing NASCOM support to all NASA elements for simulations and launch, and extending this communications support as necessary to interface with the combined worldwide network.

The GSFC tracking and telemetry facilities and equipment used in support of *Surveyor IV* are listed in Table V-3. GSFC also supported the ORT prior to launch.

Table V-2. Atlas/Centaur Mark Event readouts

Mark Event	Time (GMT) (July 14, 1967)	Readout from
Liftoff	1153:29.215	Cape Kennedy
1	1155:51.100	Cape Kennedy
2	1155:54.600	Cape Kennedy
3	1156:25.400	Cape Kennedy
4	1156:52.600	Cape Kennedy
5	1157:28.900 1157:27.2	Cape Kennedy Bermuda
6	1157:31.950 1157:30.8	Cape Kennedy Bermuda
7	1157:41.000 1157:41.1	Cape Kennedy Bermuda
8	1204:57.100 1204:57.2	Cape Kennedy Antigua
9	1205:25.000 1205:24.6 1205:24.5	Cape Kennedy Antigua Coastal Crusader
10	1205:34.600 1205:34.5	Antigua Coastal Crusader
11	1206:00.100 1205:55.2	Antigua Coastal Crusader
12	1206 00.100 1206:00.5	Antigua Coastal Crusader
13	1206:06.100	Coastal Crusader
14	Not reported	
15	1210:06.100 1210:00.6	Coastal Crusader Ascension
16	1214:00.800 1214:16.8	Ascension Grand Canary
17	1214:00.800 1214:16.8	Ascension Grand Canary

1. Acquisition Aids

Stations at Bermuda and Grand Canary are equipped with acquisition aids to track the vehicle and provide RF inputs to the telemetry receivers from AOS to LOS. Performance recorders are used to record AGC and angle errors for postmission analysis. The acquisition aid systems performed their required functions during the *Surveyor IV* mission.

2. Telemetry Data

Bermuda and Grand Canary are also equipped to receive, record, and decommutate telemetry. The telemetry requirements placed on the MSFN were:

- (1) Bermuda was to receive and record the *Centaur* 225.7-MHz link from AOS to LOS.

Table V-3. GSFC network configuration

Location	Acquisition aid	VHF telemetry	C-band radar	SCAMA	Radar high-speed data	Real-time readouts
Bermuda	X	X	X	X	X	X
Grand Canary ^a	X	X		X		X
GSFC				X	X	

^aGrand Canary was not scheduled to support. However, the station was called up on a "best-obtainable" basis on launch day.

- (2) Bermuda was to receive and record the *Atlas* 229.9-MHz link from AOS to LOS.
- (3) *Centaur* Mark Event readouts were required in real-time or as near real-time as possible, after the vehicle was in view of the station.
- (4) Bermuda was to display range safety parameters on the *Atlas* and *Centaur* links.
- (5) Bermuda was to provide magnetic tape recordings, strip chart recordings, and Post Launch Instrumentation Message (PLIM) data sheets.

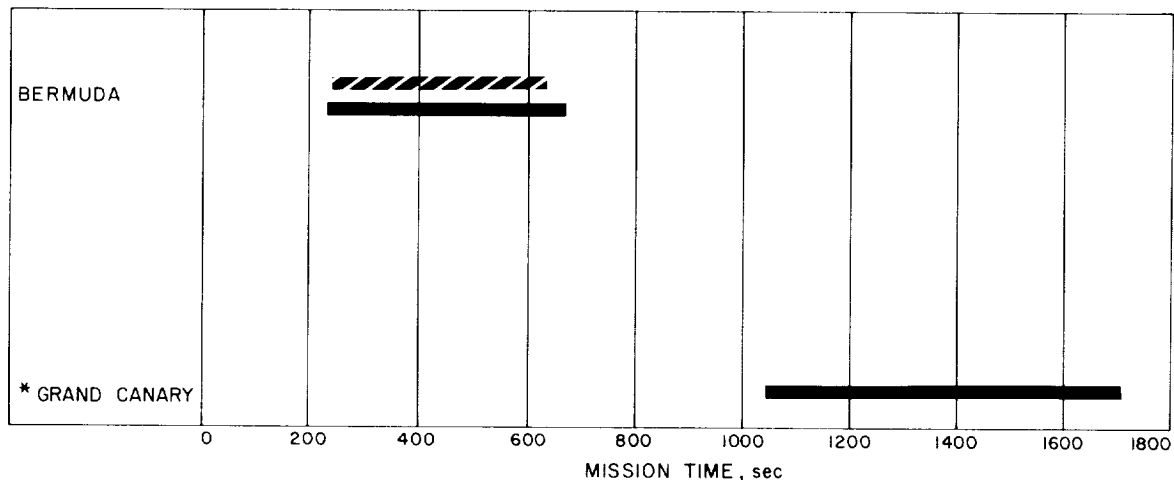
The telemetry systems at Bermuda performed all required functions. Bermuda received and recorded range safety parameters and reported Mark Events 5, 6 and 7 (see Table V-2). Canary reported Mark Events 16 and 17, attitude rates and propellant ullages.

No problems were encountered, although Grand Canary reported a maximum signal strength of -103 dbm, which was just above threshold. Numerous drop-outs occurred during the last 2 min of track. However, the decommutator maintained lock long enough to confirm *mark 16*. The predicted vs actual coverage is shown in Fig. V-8.

3. Metric Tracking Data (C-band)

The radar requirements placed on the MSFN for the *Surveyor IV* mission were:

- (1) Bermuda was to provide C-band beacon tracking of the *Centaur* from AOS to LOS and range safety backup support to AFETR.
- (2) Bermuda was to provide real-time transmission of high-speed and low-speed radar data to GSFC and RTCS.



* PREDICTS NOT PROVIDED FOR GRAND CANARY; COVERAGE ON "BEST OBTAINABLE" BASIS

PREDICTED COVERAGE 
ACTUAL COVERAGE 

Fig. V-8. MSFN VHF telemetry coverage

- (3) Bermuda was to provide magnetic tape recordings (at a minimum of 10 points/sec), strip chart recordings, and PLIM data sheets.

The Bermuda FPQ-6 radar achieved 402 sec of valid autotrack data. However, 2 sec of FPQ-6 data was lost at 12:01:08 GMT owing to phasing separation. The FPS-16 radar tracked passively, with no data taken.

The range safety impact prediction plot became erratic at approximately $L + 8$ min. Investigation revealed a possible problem in the 4101 computer program. This problem may have resulted in improper smoothing of the elevation data, thereby causing the rough impact prediction plot.

The predicted vs actual coverage is shown in Fig. V-9.

4. Computer Support, Data Handling and Ground Communications

The GSFC DOB (Data Operations Branch) was to provide computing support for the MSFN stations during the prelaunch, launch, and orbital phases of the mission. Computer requirements were to provide MSFN station view periods for mission planning purposes, and post-flight reformatting of magnetic tape recordings of the radar data received from AFETR and MSFN.

The GSFC DOB provided all required support. Because Grand Canary was not scheduled for support and was called up for support on a "best-obtainable" basis on launch day, the DOB generated and transmitted nominal pointing data to Canary during the minus count on launch day.

The NASCOM Network provided 22 teletype, 8 voice, and 6 high-speed data circuits to the DSN, and 4 tele-

type, 8 voice, and 1 high-speed data circuits to the MSFN in support of the mission. Special coverage was implemented at $L - 6$ hr, and special radio propagation forecasts were provided for all HF radio circuits commencing at $L - 8$ hr. Both voice and teletype circuits were activated via the AFETR. The voice was used to back-feed "Voice of *Surveyor*" to DSS 51. There was no requirement for the teletype circuit, although it was available if needed.

No communication problems were encountered except for a 4 min outage on all DSS 72 teletype circuits, which occurred at liftoff. This outage was due to a power dip at Ascension, which caused a loss of sync on AFETR equipment.

C. Deep Space Network

The DSN supports *Surveyor* missions with the integrated facilities of the Deep Space Instrumentation Facility (DSIF), the Ground Communications Facility (GCF), and the Space Flight Operations Facility (SFOF). The DSN provides a command and telemetry link with the spacecraft upon initial acquisition of spacecraft signals by a DSIF station, enabling the DSIF station to control the spacecraft and furnish range rate, angular tracking, and real-time telemetry data to the SFOF. Continuous tracking and control are then provided throughout the remainder of the mission by the prime DSIF stations designated to support each *Surveyor* mission.

Following the accumulation of sufficient tracking data by the SFOF, an orbit is determined that predicts the future path of the spacecraft. This data allows the computation of a midcourse maneuver to compensate for injection errors. The DSIF commands the midcourse maneuver, after which engineering telemetry and tracking data is gathered and transmitted via the GCF to the

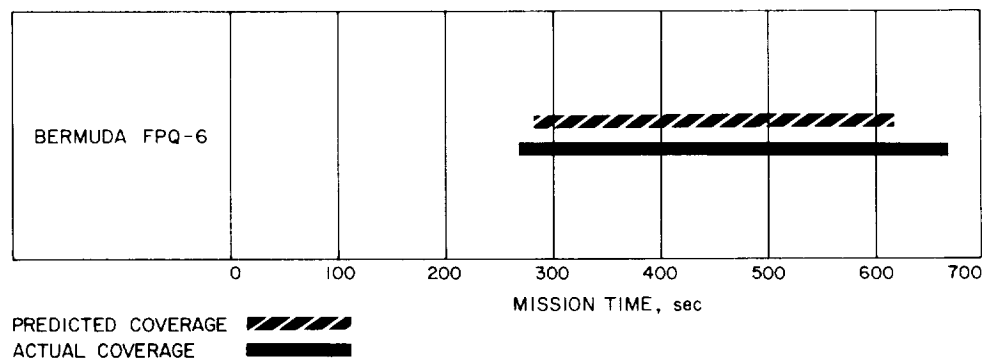


Fig. V-9. MSFN radar coverage

SFOF, where the midcourse maneuver is evaluated and appropriate commands for the terminal maneuver are computed. After touchdown, DSIF stations receive video and engineering and scientific telemetry data and command the spacecraft during lunar operations.

1. The DSIF

The following Deep Space Stations (DSS) were committed as prime stations for support of the *Surveyor IV* mission:

DSS 11 Pioneer, Goldstone Deep Space Communications Complex (DSCC), Barstow, California

DSS 42 Tidbinbilla, Australia, near Canberra

DSS 51 Johannesburg, South Africa (transit phase coverage only)

DSS 61 Robledo, Spain, near Madrid

DSS 72 Ascension Island (Fig. V-10) (initial acquisition to DSS 11 acquisition plus 1 hr)

For the July 14 launch date, DSS 72 was designated the initial two-way acquisition station as *Surveyor IV* used a direct ascent trajectory.

In addition to the basic support provided by prime stations, the following support was provided for the *Surveyor IV* mission:

- (1) DSS 71, Cape Kennedy, provided facilities for spacecraft/DSIF compatibility testing and also received and recorded telemetry data after liftoff. In addition, DSS 71 used its Command and Data Handling Console (CDC) and Telemetry and Command Processor (TCP) computer to process AFETR range telemetry data for transmission to JPL.
- (2) DSS 14 Mars, Goldstone DSCC, Barstow, California, provided midcourse and terminal phase backup tracking and command support using its 210-ft-diameter antenna. At predicted touchdown the baseband telemetry output of the DSS 14 prime receiver was transmitted to the SFOF.
- (3) DSS 12 Echo, Goldstone DSCC, Barstow, California, provided backup telemetry coverage during the terminal descent phase.

The DSN was required to track the spacecraft and provide doppler and telemetry data as shown in Table V-4.

Table V-4. DSN tracking data requirements

Coverage and sampling rate	Data required
1. Track spacecraft from separation to first midcourse at 1-min sample rate (from initial DSIF acquisition to $L + 1$ hr, the sample rate is 1 sample per 10 sec).	Doppler (two- and three-way), antenna pointing angles, and telemetry
2. Track spacecraft from first midcourse to touchdown at 1-min sample rate.	Doppler (two- and three-way), antenna pointing angles and telemetry
3. Track spacecraft during midcourse maneuver and terminal maneuver executions at 1-sec sample rate, and transmit data at 10-sec sample rate.	Doppler (two- and three-way or one-way), antenna pointing angles and telemetry
4. Track spacecraft from touchdown to end of mission at 1-min sample rate during 1 hr following 10-deg elevation rise, during 1 hr centered around maximum elevation, and during 1 hr prior to 10-deg elevation set for DSS 11, 42, and 61.	Doppler (two- and three-way), telemetry



Fig. V-10. DSS 72 30-ft antenna system at Ascension

Data is handled by the prime DSIF stations as follows:

- (1) Tracking data, consisting of antenna pointing angles and doppler (radial velocity) data, is supplied in near-real-time via teletype to the SFOF and postflight in the form of punched paper tape. Two- and three-way doppler data is supplied full-time during the lunar flight, and also during lunar operations when requested by the *Surveyor* Project

Office. The two-way doppler function implies a transmit capability at the prime stations.

(2) Spacecraft telemetry data is received and recorded on magnetic tape. Baseband telemetry data is supplied to the CDC for decommutation and real-time readout. The DSIF also performs precommunication processing of the decommutated data, using an on-site data processing (OSDP) computer. The data is then transmitted to the SFOF in near-real-time over high-speed data lines (HSDL).

(3) Video data is received and recorded on magnetic tape. This data is sent to the CDC and, at DSS 11 only, to the spacecraft TV Ground Data Handling System (TV-GDHS, TV-11) for photographic recording. In addition, video data from DSS 11 is sent in real-time to the SFOF for magnetic and photographic recording by the TV-GDHS, TV-1. After lunar landing, the two DSS 11 receivers are used for different functions. One provides a signal to the CDC, the other to the TV-GDHS. (Signals

for the latter system are the prime *Surveyor* Project requirement during this phase of a mission.)

(4) Command transmission is another function provided by the DSIF. Approximately 280 commands are sent to the spacecraft during the nominal sequence from launch to touchdown. Confirmation of the commands sent is processed by the OSDP computer and transmitted by teletype to the SFOF.

The characteristics of S-band tracking systems are shown in Table V-5.

The maximum doppler tracking rate depends on the loop noise bandwidth. For phase error of less than 30 deg and strong signal (greater than -100 dbm), tracking rates are as follows:

Loop noise bandwidth, Hz	Maximum tracking rate, Hz/sec
12	100
48	920
152	5000

Table V-5. Characteristics for S-band tracking systems

Antenna, tracking		Transmitter	
Type	85-ft parabolic	Frequency (nominal)	2113 MHz
Mount	Polar (HA-Dec)	Frequency channel	14b
Beamwidth ± 3 db	-0.4 deg	Power	10 kW, max
Gain, receiving	53.0 db, +1.0, -0.5	Tuning range	± 100 kHz
Gain, transmitting	51.0 db, +1.0, -0.5	Modulator	
Feed	Cassegrain	Phase input impedance	$\geq 50 \Omega$
Polarization	LH ^b or RH circular	Input voltage	≤ 2.5 V peak
Max. angle tracking rate ^a	51 deg/min ≈ 0.85 deg/sec	Frequency response (3 db)	DC to 100 kHz
Max. angular acceleration	5.0 deg/sec/sec	Sensitivity at carrier output frequency	1.0 rad peak/V peak
Tracking accuracy (1 σ)	0.14 deg	Peak deviation	2.5 rad peak
Antenna, acquisition		Modulation deviation stability	$\pm 5\%$
Type	2 \times 2-ft horn	Frequency, standard	
Gain, receiving	21.0 db ± 1.0	Stability, short-term (1 σ)	Rubidium
Gain, transmitting	20.0 db ± 2.0	Stability, long-term (1 σ)	1×10^{-11}
Beamwidth ± 3 db	~ 16 deg	Doppler accuracy at F_{1c} (1 σ)	5×10^{-11}
Polarization	RH circular	Data transmission	0.2 Hz ≈ 0.03 m/sec
Receiver			TTY and HSDL
Typical system temperature			
With paramp	270 $\pm 50^\circ$ K		
With maser	55 $\pm 10^\circ$ K		
Loop noise bandwidth threshold (2B _{L0})	12, 48 or 152 Hz		
	+0, -10%		
Strong signal (2B _{L0})	120, 255, or 550 Hz		
	+0, -10%		
Frequency (nominal)	2295 MHz		
Frequency channel	14a		

^aBoth axes.

^bGoldstone only.

The angle tracking parameters for the DSS 72 30-ft antenna are as follows:

- (1) Maximum azimuth tracking rate: 6 deg/sec.
- (2) Maximum elevation angle tracking: 3 deg/sec.
- (3) Tracking accuracy: 0.01 deg.
- (4) The system doppler tracking accuracy and doppler tracking rates are the same as for 85-ft antennas.

a. DSIF preparation testing. Configuration verification, compatibility, and Operational Readiness Tests are conducted for each mission to verify that all prime stations, communication lines, and the SFOF are fully prepared to meet mission responsibility.

Configuration verification tests, with all participating stations, were conducted in June and confirmed that the DSIF was in a functional configuration to meet mission requirements. An RF compatibility test verifying the compatibility of the spacecraft with the DSIF was also conducted in June at DSS 71. Additional training and acquisition tests were conducted at DSS 72 as this was the first time DSS 72 was committed as a prime DSS initial acquisition station.

An Operational Readiness Test was conducted 5 days prior to launch and involved all DSIF-committed stations, including DSS 11, 51, 61, 71 and 72. DSS 42 participated during the prelaunch countdown only, and DSS 14 was exercised during the test to back up DSS 11 during midcourse and terminal descent phases. Selected portions of the sequence of events were followed during the ORT, using both standard and nonstandard procedures.

Surveyor on-site computer program (SOCP) integration tests are conducted to check out the SOCP and to verify that data can be transmitted from a DSIF station to the SFOF and then processed. Such tests were run on a regular basis with each prime station (DSS 11, 42, and 61). These tests were concluded with a checkout of the final SOCP program in July, 1967. Operational tests continued up until 4 days prior to launch to provide additional training for operational personnel. An evaluation of station and net control support during the ORT indicated the readiness of the TDS.

b. DSIF flight support. The DSIF stations supported the *Surveyor IV* mission with a high level of performance. Continuous tracking and telemetry coverage was provided from $L + 16$ min until complete loss of contact

with the *Surveyor IV* spacecraft during terminal descent. High-quality angular tracking and two-way doppler data was received throughout the mission with the exception of minor outages, which did not adversely affect the conduct of the flight or result in any mission objectives not being met. A number of minor equipment anomalies and procedural problems occurred, but were readily corrected by station personnel without affecting the mission.

All of the DSIF prime stations reported "go" status during the countdown. All measured station parameters were within nominal performance specifications, and communications circuits were up.

During the countdown, DSS 11 experienced minor magnetic tape recorder problems but these did not impose a launch constraint. From liftoff until the spacecraft was acquired by the initial DSIF acquisition station (DSS 72), AFETR telemetry was received, computer processed, and retransmitted in real-time to the SFOF by DSS 71.

Figure V-11 is a profile of the DSIF mission activity from liftoff until mission termination. This figure shows the periods each station tracked the spacecraft and the numbers of commands transmitted by each DSS during each pass. (Also refer to the station view periods indicated in Fig. VII-2.)

Sixteen minutes after liftoff, initial acquisition of the spacecraft was made by DSS 72, which provided early two-way tracking data for orbit determination. Two-way acquisition by DSS 72 was accomplished within the committed period. However, during initial acquisition of the spacecraft signal, the DSS 72 antenna drove off track in azimuth causing a loss of up-link and 10 min of two-way tracking data.

The signal levels received at the DSIF stations are shown in Fig. V-12 and correspond very closely to the predicted levels. The predicted levels for the tracking period prior to star acquisition are not given, as the spacecraft was not fixed in a known roll position during this period. Therefore, the received signal level could vary over a wide range owing to variations in spacecraft antenna patterns. During star acquisition, midcourse correction, and retro maneuver, the spacecraft was in high-power mode, which provides a signal level 20 db above the low-power mode. Data bit rate changes were commanded within 2 db of the predicted thresholds. The periods during which gyro drift tests were conducted

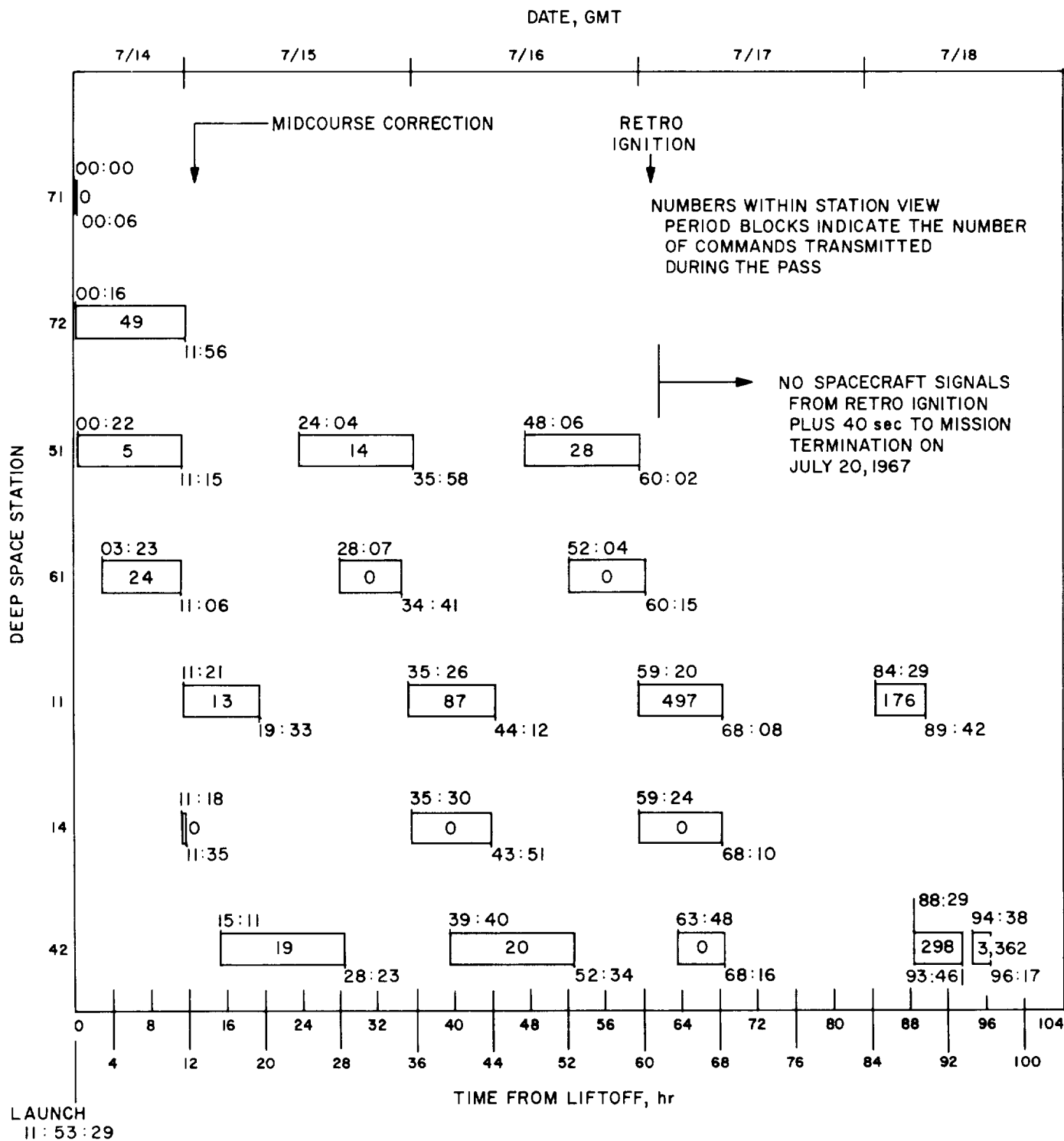
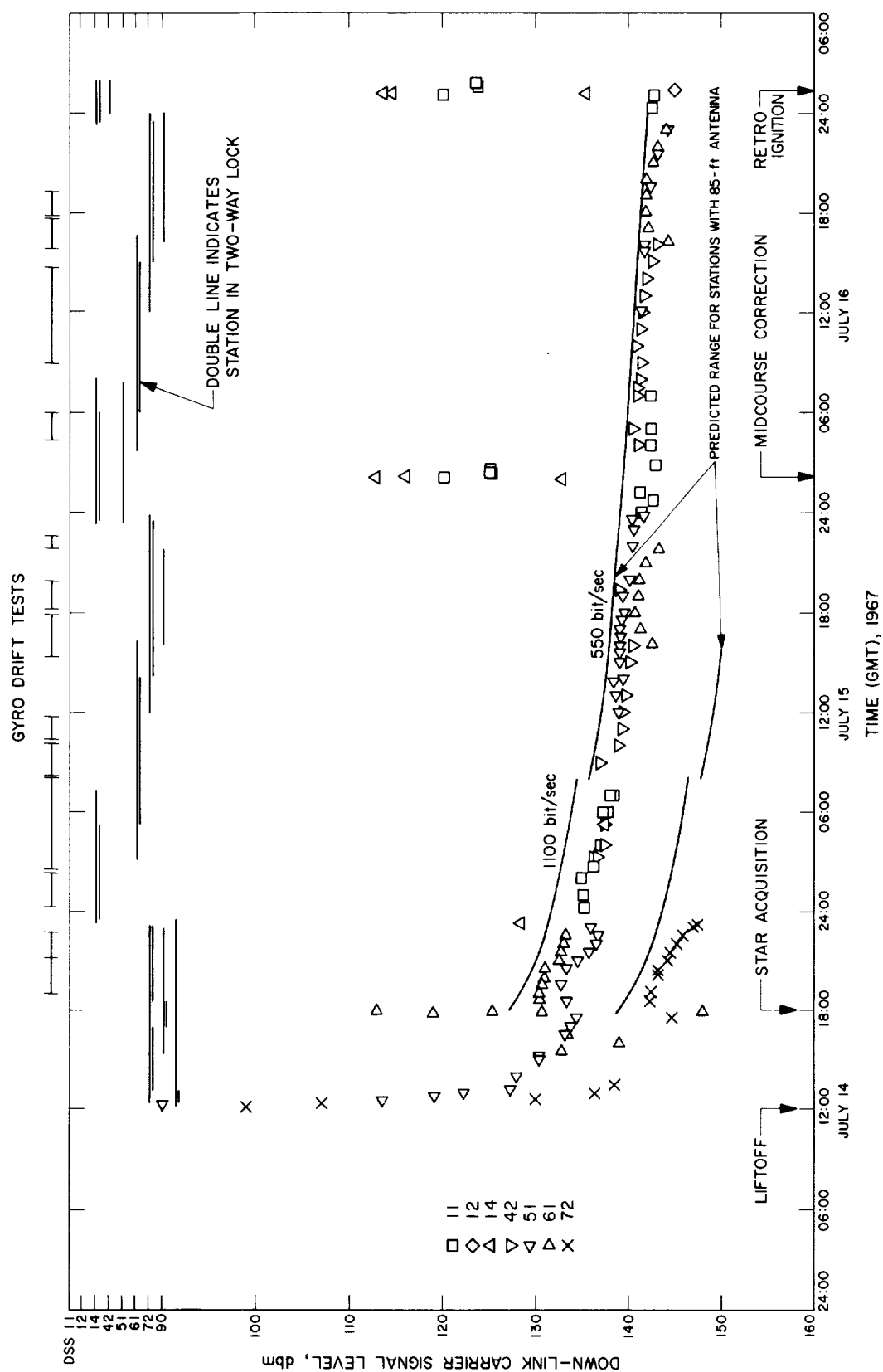


Fig. V-11. Station tracking periods



are shown at the top of the figure. The random gyro drift and subsequent antenna pattern variations produced a spread in the received signal levels of ± 3 db. Consistent with its 30-ft antenna, DSS 72 signal levels were approximately 10 db below signal levels received by the stations with 85-ft antennas.

The two-way acquisition at DSS 11 was delayed 20 min due to a tuning error, resulting in the loss of 15 min of two-way doppler data. Tracking and Data Handling (TDH) system anomalies at DSS 11 resulted in intermittent doppler data during the second and third passes. Also at DSS 11, a video recorder head malfunction of the FR 800 recorder caused the loss of the predetection telemetry signal from TV-11.

The second pass at DSS 61 was prematurely terminated due to an antenna hydraulic leak, causing a loss of three-way doppler data and backup telemetry. DSS 61 also experienced TDH problems during the first pass, losing approximately 1½ hr of two-way doppler data. However, DSS 51 took over two-way tracking and provided the required support while DSS 61 repaired its TDH system.

The midcourse maneuver was performed by DSS 11 during its second pass on July 15 and was reported as a successful event. DSS 11 also commanded and tracked the retro maneuver during its third pass. During the midcourse maneuver and terminal phases, the 210-ft antenna of DSS 14 provided recording and command backup coverage. DSS 12 also provided backup coverage during the terminal phase owing to the video recorder head malfunction at DSS 11.

About 40 sec after retro motor ignition, during terminal descent, all tracking and telemetry signals from the spacecraft ceased abruptly. At the time the *Surveyor IV* signal was lost, five receivers utilizing three different antennas were monitoring the spacecraft at the Goldstone complex. This provided immediate and positive indication that the loss of signal was not due to a DSIF system failure. Despite repeated attempts by DSS 11, 42, and 61, contact with *Surveyor IV* was not regained. Owing to premature termination of the mission, no video was received from the spacecraft.

2. GCF/NASCOM

For *Surveyor* missions, the GCF transmits tracking, telemetry, and command data from the DSIF to the SFOF, and control and command functions from the SFOF to the DSIF by means of NASCOM facilities. The GCF also transmits simulated tracking data to the DSIF

and video data and base-band telemetry from DSS 11, Goldstone DSCC, to the SFOF. The links involved in the system are shown in Fig. V-13.

The GSF/NASCOM demonstrated a high degree of reliability during the Operational Readiness Tests conducted before the mission. The performance of the NASCOM facilities in support of the *Surveyor IV* mission was considered excellent, demonstrating a high degree of reliability.

a. Teletype (TTY) circuits. Teletype circuits (four available to prime stations) are used for transmitting tracking data, telemetry, commands and administrative traffic. The teletype circuits were exceptionally reliable, the weakest circuits (DSS 51) showing approximately 95% reliability.

A teletype circuit, via satellite to Ascension, then by HF radio through Pretoria to DSS 51, was activated during the ORT but did not prove satisfactory due to propagation problems from Ascension to Pretoria.

During the mission and the final ORT, DSS 72 tracking data and operational message circuits were routed via satellite with excellent results.

b. Voice circuits. The voice circuits are shared between the DSIF and the *Surveyor* Project for administrative, control, and commanding functions. The NASCOM voice circuits provided for the *Surveyor IV* mission performed well except for several minor outages.

A voice circuit, via satellite to Ascension, then by HF radio through Pretoria to DSS 51, was activated as a backup during the mission launch phase. This circuit provided coverage during periods when the normal voice circuits failed.

The DSS 72 voice circuit was routed via satellite during both the ORT and the mission and performed exceptionally well.

c. High-speed data lines. One HSDL is provided to each prime site for telemetry data transmission to the SFOF in real-time. This part of the communications system performed well during both the prelaunch testing and mission phases.

The lines were used during testing to transmit simulation data to the stations and during the mission to back-feed various voice nets as required. The DSS 72 data circuit was routed via satellite during both the ORT and the mission. Performance was excellent.

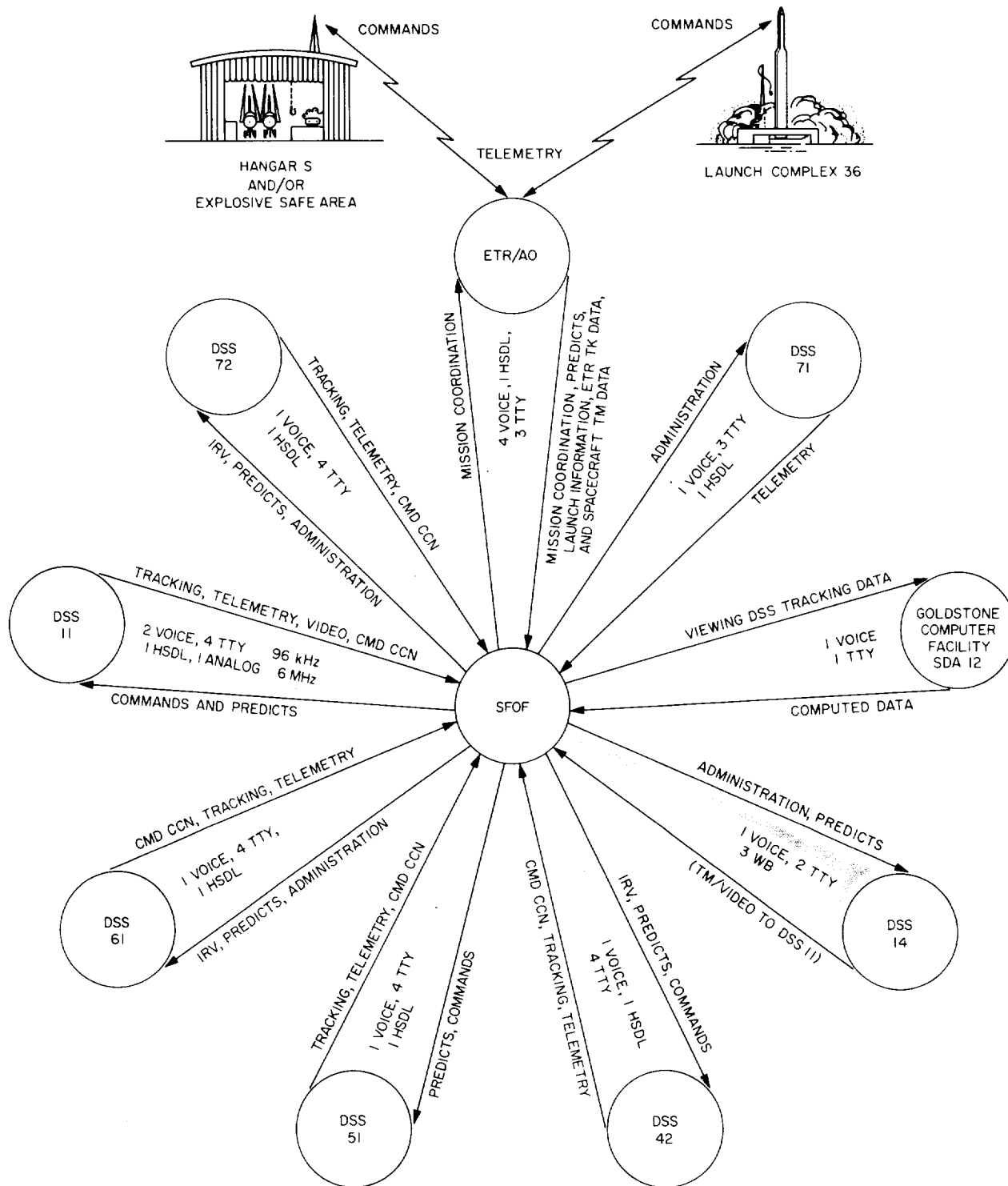


Fig. V-13. DSN/GCF communications links

d. Wideband microwave system. The wideband microwave link between DSS 11, Goldstone DSCC, and the SFOF consists of one 6-MHz simplex (one-way) channel for video, and one 96-kHz duplex (two-way) data channel. The link performed with 100% reliability during the *Surveyor IV* mission.

3. DSN in the SFOF

The DSN supports the *Surveyor* missions by providing mission control facilities and performing special functions within the SFOF.

a. Data Processing System (DPS). The SFOF DPS performs the following functions for *Surveyor* missions.

- (1) Computation of acquisition predictions for DSIF stations (antenna pointing angles and receiver and transmitter frequencies).
- (2) Orbit determinations.
- (3) Midcourse maneuver computation analysis.

(4) On-line telemetry processing.

(5) Command tape generation.

(6) Simulated data generation (telemetry and tracking data for tests).

The DPS general configuration for the *Surveyor IV* mission is shown in Fig. V-14 and consists of two PDP-7 computers in the telemetry processing station (TPS), two strings of IBM 7044/7094 computers in the Central Computing Complex (CCC), and a subset of the input/output (I/O) system.

For *Surveyor IV*, the translunar portion of the mission utilized the existing 7044 computer configuration with manually switched teletype lines. After touchdown, a redesigned computer configuration in conjunction with a communication processing system was to be implemented. This was to allow computer sharing in support of other concurrent space program missions. However,

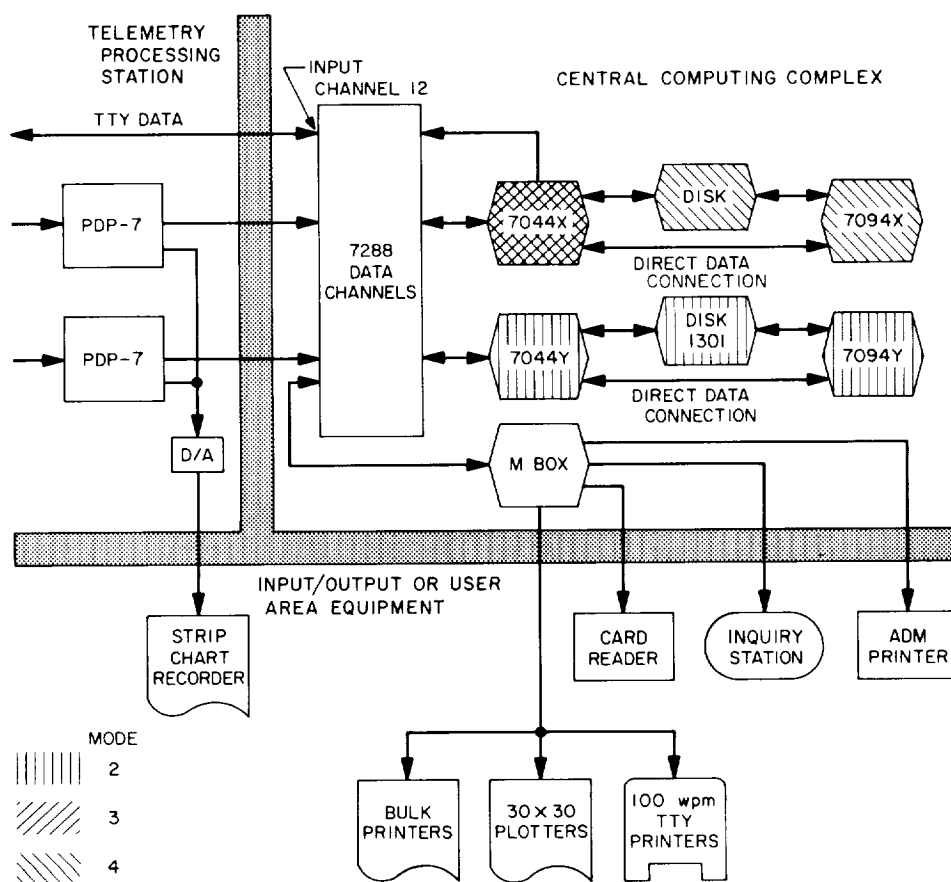


Fig. V-14. General configuration of SFOF data processing system

owing to the abbreviated mission this new data processing system was not exercised.

The DPS performed in a nominal manner, with only minor hardware problems which did not detract from mission support. The two PDP-7 computers were used extensively to process high-speed telemetry data for the *Surveyor IV* mission. This processing consisted of decommutating and transferring the data to the 7044 computer via the 7288 data channels, generating a digital tape for non-real-time processing, and supplying digital-to-analog converters with discrete data parameters to drive analog recorders in both the Spacecraft Analysis Area and the Space Science Analysis Area.

The IBM 7044/7094 computer string dual configuration successfully processed all high-speed data received from the TPS and all teletype data received from the communications center, as well as all input/output requests from the user areas.

The input/output system provides the capability for entering data control parameters into the 7044/7094 computers and also for displaying computed data in the user areas via the various display devices. The input/output system performed adequately, with only a few problems reported.

b. DSN Intracomunications System (DSN/ICS). The DSN/ICS provides the capability of receiving, switching, and distributing all types of information required for spaceflight operations and data analysis to designated areas or users within the SFOF. The system includes facilities for handling all voice communications, closed circuit television, teletypes, high-speed data, and data received over the microwave channels. The DSN/ICS performed in an exceptional manner, with only minor anomalies.

Both modem* types (NASCOM and Hallicrafter) were required during the *Surveyor IV* mission. NASCOM modems were used for sending high-speed data from all

stations except DSS 51, and reliability was very high. DSS 51 used the Hallicrafter modem, which performed reliably, the only circuit problems being due to propagation. Minor problems occurred during launch when several stations were active and modem switching was required in order for each station to perform data transfer tests.

The television communications subsystem experienced minor equipment problems that were resolved in real-time. During the launch phase there was a shortage of TV monitors used for viewing teletype lines.

4. DSN/AFETR Interface

The DSN/AFETR interface provides real-time data transmission capability for both VHF and S-band down-range telemetry from Building AO at Cape Kennedy to the SFOF. The nominal switchover time is after the spacecraft S-band transmitter high-power turn-on. The interface with the *Surveyor* Project is at the input to the CDC, Building AO, where it is sent to DSS 71 for processing by the CDC and the telemetry and command processor (TCP) computer. The output of the CDC is transmitted to the SFOF via the GCF/NASCOM. During the *Surveyor IV* mission, this configuration was established as the prime link between the SFOF and AFETR to provide an interface similar to the data transmission links with prime DSIF stations. The previously used link between Building AO and SFOF, via Bell modems, was retained as backup.

In-flight spacecraft telemetry was received from the AFETR stations and relayed to the SFOF until approximately $L + 40$ min.

Both the prime DSS 71 and the Bell modem backup systems provided good data during the mission, but due to the high quality of the DSS 71 data, the backup data was not processed. However, the backup system was used during the ORT to provide simulated telemetry data from the SFOF to Building AO and performed well.

DSIF tracking data for early orbit determination was successfully back-fed to the Real Time Computer Facility at the AFETR.

*A modem (modulator-demodulator) is a device for converting a digital signal to a signal which is compatible with telephone line transmission (i.e., a frequency-modulated tone).

VI. Mission Operations System

A. Functions and Organization

The basic functions of the Mission Operations System (MOS) are the following:

- (1) Continual assessment and evaluation of mission status and performance, utilizing the tracking and telemetry data received and processed.
- (2) Determination and implementation of appropriate command sequences required to maintain spacecraft control and to carry out desired spacecraft operations during transit and on the lunar surface.

The *Surveyor* command system philosophy introduces a major change in the concept of unmanned spacecraft control: virtually all in-flight and lunar operations of the spacecraft must be initiated from earth. In previous space missions, spacecraft were directed by a minimum of earth-based commands. Most in-flight functions of those spacecraft were automatically controlled by an on-board sequencer which stored preprogrammed instructions. These instructions were initiated by either an on-board timer or by single direct commands from earth. For example, during the *Ranger VIII* 67-hr mission, only 11 commands were sent to the spacecraft; whereas for a standard *Surveyor* mission, approximately 280 commands

must be sent to the spacecraft during the transit phase, out of a command vocabulary of 256 different direct commands. For *Surveyor IV*, 322 commands were sent during transit up to loss of spacecraft signal.

Throughout the space flight operations of each *Surveyor* mission, the command link between earth and spacecraft is in continuous use, transmitting either fill-in or real commands every 0.5 sec. The *Surveyor* commands are controlled from the SFOF and are transmitted to the spacecraft by a DSIF station.

The equipment utilized to perform MOS functions falls into two categories: mission-independent and mission-dependent equipment. The former is composed chiefly of the *Surveyor* TDS equipment described in Section V. It is referred to as mission-independent because it is general-purpose equipment which can be utilized by more than one NASA project when used with the appropriate project computer programs. Selected parts of this equipment have been assigned to perform the functions necessary to the *Surveyor* Project. The mission-dependent equipment (described in Section VI-B, following) consists of special equipment which has been installed at DSN facilities for specific functions peculiar to the project.

The *Surveyor* Project Manager, in his capacity as Mission Director, is in full charge of all mission operations. The Mission Director is aided by the Assistant Mission Director and a staff of mission advisors. During the mission, the MOS organization was as shown in Fig. VI-1.

Mission operations are under the immediate, primary control of the Space Flight Operations Director (SFOD) and supporting *Surveyor* personnel. Other members of the team are the TDS personnel who perform services for the *Surveyor* Project.

During space flight and lunar surface operations, all commands are issued by the SFOD or his specifically delegated authority. Three groups of specialists provide technical support to the SFOD in the flight path, spacecraft performance, and science areas.

1. Flight Path Analysis and Command Group

The Flight Path Analysis and Command (FPAC) group handles those space flight functions that relate to the location of the spacecraft. The FPAC Director maintains control of the activities of the group and makes specific

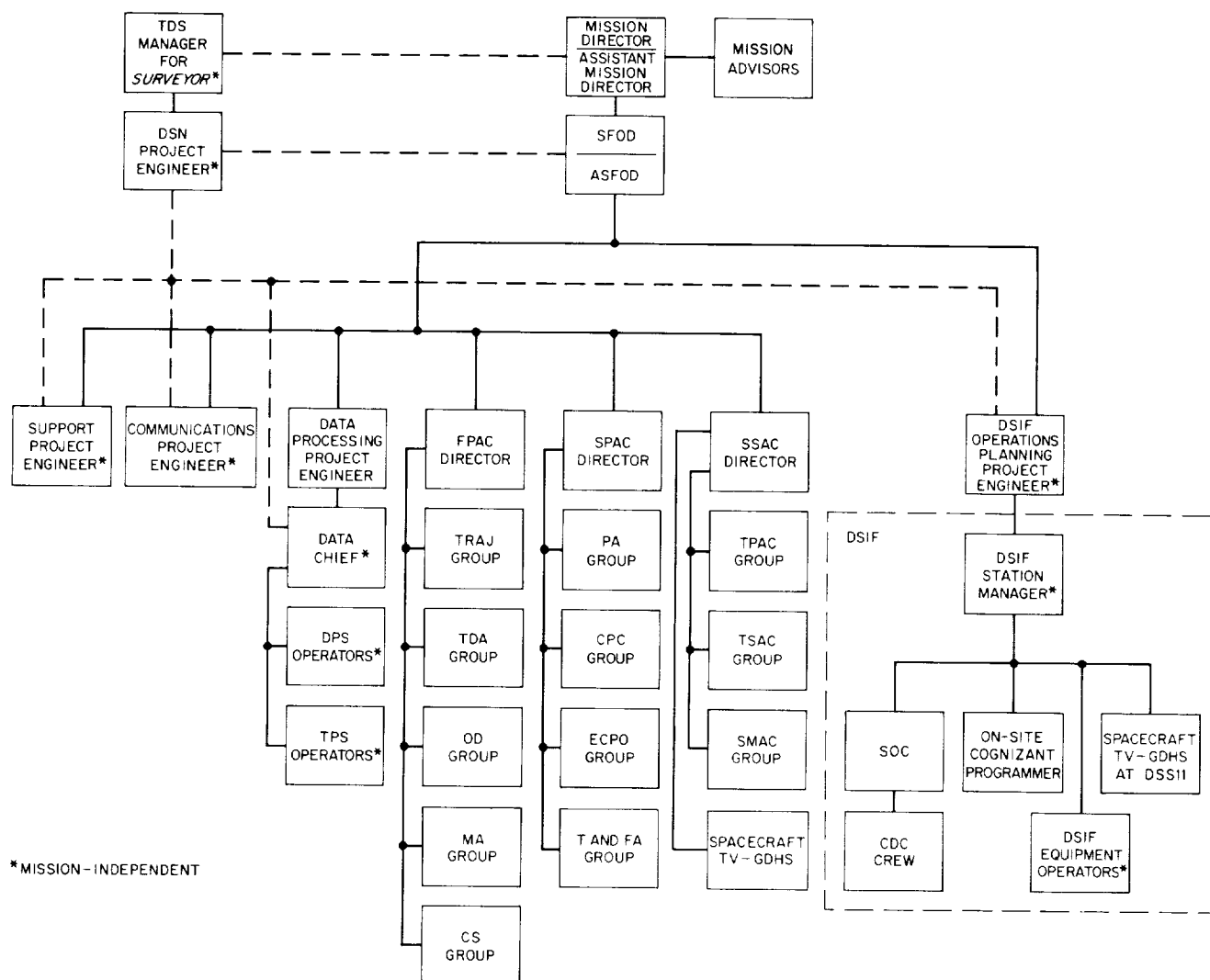


Fig. VI-1. Organization of MOS

recommendations for maneuvers to the SFOD in accordance with the flight plan. In making these recommendations, the FPAC Director relies on five subgroups of specialists within the FPAC group.

- (1) The Trajectory (TRAJ) group determines the nominal conditions of spacecraft injection and generates lunar encounter conditions based on injection conditions as reported by AFETR and computed from tracking data by the Orbit Determination group. The actual trajectory determinations are made by computer.
- (2) The Tracking Data Analysis (TDA) group makes a quantitative and descriptive evaluation of tracking data received from the DSIF stations. The TDA group provides 24-hr/day monitoring of incoming tracking data. To perform these functions the TDA group takes advantage of the Data Processing System (DPS) and of computer programs generated for their use. The TDA group acts as direct liaison between the data users (the Orbit Determination group) and the DSIF and provides predictions to the DSIF.
- (3) The Orbit Determination (OD) group, during mission operations, determines the actual orbit of the spacecraft by processing the tracking data received from the DSN tracking stations by way of the TDA group. Also, statistics on various parameters are generated so that maneuver situations can be evaluated. The OD group generates tracking predictions for the DSIF stations and recomputes the orbit of the spacecraft after maneuvers to determine the success of the maneuver.
- (4) The Maneuver Analysis (MA) group is the subgroup of FPAC responsible for developing possible mid-course and terminal maneuvers for both standard and nonstandard missions in real-time during the actual flight. In addition, once the decision has been made as to what maneuver should be performed, the MA group generates the proper spacecraft commands to effect these maneuvers. These commands are then relayed to the Spacecraft Performance Analysis and Command group to be included with other spacecraft commands. Once the command message has been generated, the MA group must verify that the calculated commands are correct.
- (5) The Computer Support (CS) group acts in a service capacity to the other FPAC subgroups, and is responsible for ensuring that all computer programs used in space operations are fully checked out

before mission operations begin and that optimum use is made of the Data Processing System facilities.

2. Spacecraft Performance Analysis and Command Group

The Spacecraft Performance Analysis and Command (SPAC) group, operating under the SPAC Director, is basically responsible for the operation of the spacecraft itself. The SPAC group is divided into four subgroups:

- (1) The Performance Analysis (PA) group monitors incoming engineering data telemetered from the spacecraft, determines the status of the spacecraft, and maintains spacecraft status displays throughout the mission. The PA group also determines the results of all commands sent to the spacecraft. In the event of a failure aboard the spacecraft, as indicated by telemetry data, the PA group analyzes the cause and recommends appropriate nonstandard procedures.
- (2) The Command Preparation and Control (CPC) group is basically responsible for preparing command sequences to be sent to the spacecraft. In so doing they provide inputs for computer programs used in generating the sequences, verify that the commands for the spacecraft have been correctly received at the DSS, and then ascertain that the commands have been correctly transmitted to the spacecraft. If nonstandard operations become necessary, the group also generates the required command sequences. The CPC group controls the actual transmission of commands at the DSS by the *Surveyor* operations chief.
- (3) The Engineering Computer Program Operations (ECPO) group includes the operators for the DPS input/output (I/O) console and related card punch, card reader, page printers, and plotters in the spacecraft performance analysis area (SPAA). The ECPO group handles all computing functions for the rest of the SPAC group, including the maintenance of an up-to-date list of parameters for each program.
- (4) The Trend and Failure Analysis (T&FA) group consists of spacecraft design and analysis specialists who provide in-depth, near-real-time spacecraft performance analysis (in contrast to the PA group's real-time analysis). The group also manages the interface for the SCCF computer facility at Hughes Aircraft Company. The SCCF 1219 is used mainly

for premission spacecraft ground testing, but during the mission the T&FA group is provided two data lines to the SCCF 1219 (via the TPS) which will accommodate bit rates up to 4400 bit/sec, and eight incoming lines terminating at seven teleprinters and one line printer in the SPAC area. The T&FA group uses the system to process and display engineering data transmitted from the spacecraft. The group also includes draftsmen who perform wall chart plotting and maintain wall displays of spacecraft condition and performance.

3. Space Science Analysis and Command Group

The Space Science Analysis and Command (SSAC) group performs those space flight functions related to the operation of the survey TV camera and the SM/SS. SSAC is divided into three operating subgroups:

- (1) The Television Performance Analysis and Command (TPAC) group analyzes the performance of the TV equipment and is responsible for generating standard and nonstandard command sequences for the survey TV camera.
- (2) The Television Science Analysis and Command (TSAC) group analyzes and interprets the TV pictures for the purpose of ensuring that the mission objectives are being met. The TSAC group is under the direction of the Project Scientist and performs the scientific analysis and evaluation of the TV pictures.
- (3) The Soil Mechanics Analysis and Command (SMAC) group prepares and recommends the commands to be sent to the SM/SS. This group is also responsible for operating the SM/SS and analyzing its performance.

The portion of the spacecraft TV Ground Data Handling System (TV-GDHS) in the SFOF provides direct support to the SSAC group in the form of processed electrical video signals and finished photographic prints. The TV-GDHS operates as a service organization within the MOS structure. Documentation, system checkout, and quality control within the system are the responsibility of the TV-GDHS Operations Manager. During operations support the TV-GDHS Operations Manager reports to the SSAC Director.

4. Data Processing Personnel

The use of the Data Processing System (DPS) by *Surveyor* is under the direction of the Assistant Space Flight Operations Director (ASFOD) for Computer Pro-

gramming. His job is to direct the use of the DPS from the viewpoint of the MOS. He communicates directly with the Data Chief, who is in direct charge of DPS personnel and equipment. Included among these personnel are the I/O console operators throughout the SFOF, as well as the equipment operators in the DPS and Telemetry Processing Station (TPS) areas.

Computer programs are the means of selecting and combining the extensive data processing capabilities of electronic computers. By means of electronic data processing, the vast quantities of mission-produced data are assembled, identified, categorized, processed and displayed in the various areas of the SFOF where the data are used. Their most significant service to the MOS is providing knowledge, in real-time, of the current state of the spacecraft throughout the entire mission. This service is particularly important to engineers and scientists of the technical support groups since, by use of the computer programs, they can select, organize, compare and process current-status data urgently needed to form their time-critical recommendations to the SFOD. (See Section V-C-3 for a description of the DPS.)

5. Other Personnel

The Communications Project Engineer (PE) controls the operational communications personnel and equipment within the SFOF, as well as the DSN/GCS lines to the DSIF stations throughout the world.

The Support PE is responsible for ensuring the availability of all SFOF support functions, including air conditioning and electric power; for monitoring the display of *Surveyor* information on the Mission Status Board and throughout the facility; for directing the handling, distribution, and storage of data being derived from the mission; and for ensuring that only those personnel necessary for mission operations are allowed to enter the operational areas.

The DSIF Operations Planning PE is in overall control of all DSIF stations; his post of duty is in the SFOF in Pasadena. At each station, there is a local DSIF station manager, who is in charge of all aspects of his DSIF station and its operation during a mission. The *Surveyor* personnel located at each station report to the station manager.

B. Mission-Dependent Equipment

Mission-dependent equipment consists of special hardware provided exclusively for the *Surveyor* Project to

support the Mission Operations System. Most of the equipment in this category is contained in the Command and Data Handling Consoles (CDC) and spacecraft Television Ground Data Handling System (TV-GDHS), which are described below.

1. Command and Data Handling Console

a. CDC equipment. The Command and Data Handling Console comprises that mission-dependent equipment located at the participating Deep Space Stations. It is used to:

- (1) Generate commands for control of the *Surveyor* spacecraft by modulation of the DSS transmitter.
- (2) Process and display telemetered spacecraft data and relay telemetry signals to the on-site data processor (OSDP) for transmission to the SFOF.
- (3) Process, display, and record television pictures taken by the spacecraft.

The CDC consists of four major subsystems:

- (1) The command subsystem, which generates FM digital command signals from punched tape or manual inputs for the DSS transmitter, and prints a permanent record of the command sent. The major units of the command subsystem, which can accommodate 1024 different commands, are the command generator, the command subcarrier oscillator, the punched tape reader, and the command printer. Outgoing commands are logged on magnetic tape by the DSS and are relayed to the SFOF.
- (2) The FM demodulator subsystem, which accepts the FM intermediate-frequency signal of the DSS receiver and derives from it a baseband signal. The baseband signal consists of either video data or a composite of engineering subcarrier signals. Depending upon the type of data constituting the baseband signal, the CDC processes the data in either the TV data subsystem or the telemetry data subsystem.
- (3) The TV data subsystem, which receives video data from the FM demodulator and processes it for real-time display at the CDC and for 35-mm photographic recording. In addition, telemetered frame-identification data is displayed and photorecorded. A long-persistence-screen TV monitor is mounted in the CDC. The operator, when requested, can thus evaluate the picture and, upon the SFOF's direction, initiate corrective commands during lunar television surveys.

- (4) The telemetry data subsystem of the CDC, which separates the various data channels from the baseband signal from either the FM demodulator or the DSS receiver phase-detected output and displays the desired data to the operators. Discriminators are provided for each subcarrier channel contained in the baseband signal. In the case of time-multiplexed data, the output of each discriminator is sent to the pulse code modulation (PCM) demodulator and then relayed to both the OSDP computer for subsequent transmission to the SFOF and to meters for evaluation of spacecraft performance. In the case of continuous data transmissions, the output of the discriminator is sent to an oscilloscope for recording and evaluation.

The CDC contains built-in test equipment to ensure normal operations of its subsystems. A CDC tester, consisting of a spacecraft transponder with the necessary modulation and demodulation equipment, ensures day-to-day compatibility of the CDC and DSIF stations.

Table VI-1. CDC mission-dependent equipment support of *Surveyor IV* at DSIF stations

DSS 11, Goldstone	Prime station with command, telemetry, and TV
DSS 42, Canberra	Prime station with command, telemetry, and TV
DSS 51, Johannesburg	Prime station for telemetry during cislunar phase
DSS 61, Madrid	Prime station with command, telemetry, and TV
DSS 71, Cape Kennedy	Station used for spacecraft compatibility tests and pre- and postlaunch telemetry data processing
DSS 72, Ascension	Prime station with command and telemetry
DSS 14, Goldstone	Station configured for command backup and telemetry reception via both the DSS 11 CDC and SFOF. Also used to record terminal descent and landing phase

b. CDC operations. Table VI-1 lists the CDC mission-dependent equipment provided for support of *Surveyor IV* at the DSIF stations. CDC's were located at DSS 11, 42, 51, 61, 71, and 72 and, during the mission, CDC operations were conducted at each of these stations. Table VI-2 lists the number of commands transmitted by each station prior to the loss of the spacecraft signal. (Also refer to Fig. V-11.)

Table VI-2. Surveyor IV command activity prior to loss of spacecraft signal

Station	Commands Transmitted
DSS 11	166
DSS 42	39
DSS 51	44
DSS 61	24
DSS 71	0
DSS 72	49

- (1) DSS 11, Goldstone. The Pioneer station at Goldstone participated in four passes during the mission. Midcourse maneuver and terminal descent were the two major events to be commanded from Goldstone. The midcourse maneuver was delayed from the first Goldstone view period to the second view period in order to improve the accuracy of the final trajectory. Terminal descent occurred during the third pass. After the spacecraft signal was lost, additional commands were sent in an unsuccessful attempt to reacquire a signal from the spacecraft. DSS 11 participated in a fourth pass in an attempt to revive the spacecraft.

An interface was established with DSS 14, Mars station, for command backup and telemetry reception. During the second pass, the CDC input was transferred to DSS 14 and the signal level increased 8.5 db.

Two dataphone links were established with Hughes Aircraft Company (HAC), El Segundo, California. One line carried the reconstructed telemetry PCM waveform to HAC from the CDC demultiplexer. The second line carried the command waveform obtained at the CDC system tester.

There were no failures or anomalies in the CDC at DSS 11 during the mission.

- (2) DSS 42, Canberra. Canberra participated in four passes during the mission. The last two were in an attempt to revive the spacecraft. No significant problems with the CDC were encountered during the tracking periods.
- (3) DSS 51, Johannesburg. DSS 51 participated in three passes from 24 min after liftoff to approximately 2 hr before spacecraft retro. Voice communications with DSS 51 were fairly good for the first two

passes but were quite bad for part of the third pass. Communications via teletype worked well, however, and considerable commanding was accomplished using this means for instructions. There were no equipment problems in the CDC during the mission.

- (4) DSS 61, Madrid. DSS 61 tracked *Surveyor IV* for the three transit-phase view periods. The station was in two-way lock with the spacecraft for slightly less than 2 hr. For the major portion of the transit phase, DSS 61 was in three-way lock in conjunction with DSS 51. No problems were experienced with the CDC equipment during the mission.

Prior to the mission, a computer program was written by one of the DSS 61 personnel to allow converting spacecraft telemetry counts directly to engineering units utilizing the backup TCP computer and outputting this to a teletype page printer for immediate analysis. This program was successfully utilized and, during the third pass, this data was routed to the SFOF for review and comment rather than transmitting "average alarm data."

- (5) DSS 71, Cape Kennedy. The support provided for *Surveyor IV* consisted of one operational readiness test and the spacecraft countdown and launch. During the spacecraft countdown and launch, support included the processing of telemetry data from the station and from various downrange stations via TEL-2,* using the CDC and the telemetry and command processor (TCP) computer, and transmitting the data to the SFOF via the high-speed data line. The TEL-2 data was continued until approximately 38 min after liftoff. However, there were numerous parity errors at times and occasional demultiplexer out-of-lock conditions.

- (6) DSS 72, Ascension. DSS 72 was committed as the initial acquisition station for *Surveyor IV*. The spacecraft was acquired and two-way lock was established. For the first time in any mission this station transmitted commands to the spacecraft. The CDC telemetry data became unusable 38 min, 47 sec after initial acquisition. However, the station continued to track the spacecraft through station transfers to DSS 51, DSS 61, DSS 71, and DSS 11, and was released from track at approximately 12 hr after liftoff. There were no CDC problems during DSS 72 participation in the mission.

*AFETR telemetry processing facility at Cape Kennedy.

2. The Spacecraft Television Ground Data Handling System

The spacecraft Television Ground Data Handling System (TV-GDHS) was designed to record, on film, the television images received from *Surveyor* spacecraft. The principal guiding criterion was photometric and photogrammetric accuracy with negligible loss of information. This system was also designed to provide display information for the conduct of mission operations, and the production of user products, such as archival negatives, prints, enlargements, duplicate negatives, and a digital tape of the TV ID information for use in production of the ID catalogs.

The system is in two parts—TV-11 at DSS 11, Goldstone, and TV-1 at the SFOF, Pasadena. At DSS 11 is an on-site data recovery (OSDR) subsystem and an on-site film recorder (OSFR) subsystem. These subsystems are duplicated in the media conversion data recovery (MCDR) subsystem and the media conversion film recorder (MCFR) subsystem at the SFOF. The portion of the system used in real-time at the SFOF is comprised of the MCDR, the MCFR, the media conversion computer, the video display and driver subsystem (VDDS), and the FR-700 and FR-1400 magnetic tape recorders. Equipment used in near-real-time are the strip contact printer and strip contact print processor. The photographic subsystem used in non-real-time is comprised of several enlargers, a copy camera, the identity copier, two film processors, a film chip file, other photographic equipment, and film storage areas.

a. TV-GDHS at DSS 11 (TV-11). Data for the TV-GDHS is injected into the system at the interface between the DSS 11 receiver and the OSDR. In both the 200- and 600-line modes, the OSDR provides to the film recorder subsystem: (1) the baseband video signal, (2) the horizontal sync signal, (3) the vertical frame gate, (4) the resynchronized raw ID telemetry information, and (5) the time code. In 200-line mode, the OSDR also supplies a 500-kHz predetection signal to the DSS 11 FR-800 and FR-1400 magnetic tape recorders and to the SFOF via the microwave communication link. In 600-line mode, the OSDR also provides: (1) a 4-MHz predetection signal to the DSS 11 FR-800 and to the SFOF via the microwave communication link, and (2) a baseband video signal to the DSS 11 FR-1400 magnetic tape recorder.

The OSFR records the following on 70-mm film: the video image, the raw ID telemetry in bit form, the "human readable" time and record number, and an internally gen-

erated electrical gray scale. The film is then sent to the SFOF for development.

Owing to the early termination of the *Surveyor IV* mission prior to landing, TV-11 made no recordings other than those made during normal countdown. The only problems which TV-11 experienced during these countdowns related to setting up the interfaces to the station. These problems were found and corrected prior to the pretouchdown countdown.

b. TV-GDHS at the SFOF (TV-1). The signal presented to the microwave terminal at DSS 11 is transmitted to the SFOF, where it is distributed to the MCDR and to the VDDS. The MCDR processes the signal in the same manner as the OSDR. In addition, the MCDR passes the raw ID information to the media conversion computer, which converts the data to engineering units. This converted data is used by: (1) the film recorder, where it is recorded as human readable ID, (2) the wall display board in the SSAC area, (3) the disc file where the film chip index file is kept, and (4) the history tape.

The VDDS produces the signals to drive the scan converter and the signals to drive the various display monitors and the paper camera in the SSAC area. The VDDS also supplies the signals recorded by the FR-700 and the FR-1400 video magnetic tape recorders in the same manner as the FR-800 and the FR-1400 recorders at DSS 11. The scan converter converts the slow scan information from the spacecraft to a standard RETMA television signal for use by the SFOF closed-circuit television and the public TV broadcasting stations.

The MCFR records on two different films. Both films are wet-processed off-line. One of the negatives is used to make strip contact prints, which are delivered to the users. Additionally, this negative is used to make a master positive for the production of a duplicate negative for the JPL Public Information Office and a preliminary duplicate negative for the science users. The negative is then cut into chips, which are entered into the chip file where they are available for use in making additional contact prints and enlargements.

With the early termination of the flight, TV-1 was not exercised in a real-time operation other than to make a real-time decision to attempt an FR-800 baseband recording as soon as signal loss was reported during terminal descent. Although the results of this did not provide any useful data, the act brought into focus a capability which could be useful in evaluation of the mission if this recording were made at each critical maneuver. Problems were

encountered in the scan converter driver system and in the film recorder prior to the terminal maneuver. However, at the time of terminal maneuver, all systems of TV-1 were operational.

C. Mission Operations Chronology

Inasmuch as mission operations functions were carried out on an essentially continuous basis throughout the *Surveyor IV* mission, only the more significant and special, or nonstandard, operations are described in this chronicle. Refer also to the sequence of mission events presented in Table A-1 of Appendix A.

1. Countdown and Launch Phase

The first attempt to launch *Surveyor IV* was delayed until the second day of the launch period in order to correct a problem with an electrical connector in the *Centaur* propellant utilization system. No significant problems were reported in the early phases of the countdown, which proceeded smoothly down to approximately $T - 40$ sec, when a 29-sec hold was called to complete liquid hydrogen topping of the *Centaur*. The countdown was resumed without recycling, and liftoff ($T = 0$, $L + 0$) occurred at 11:53:29.215 GMT on July 14, 1967, with all systems reported in a "go" condition.

Atlas/Centaur (AC-11) performance appeared nominal on the direct ascent launch. Following *Centaur* main engines cutoff, the spacecraft was injected into a very accurate lunar transfer trajectory. The required retro maneuver was successfully performed by the *Centaur*. A description of launch vehicle performance and the sequence of events from launch through injection are contained in Section III.

Following separation at 12:06:06 GMT ($L + 00:12:36$), the spacecraft executed the planned automatic sequences as follows. By using its cold-gas jets, which were enabled at separation, the flight control subsystem nulled out the small rotational rates imparted by the separation springs and initiated a roll-yaw sequence to acquire the sun. After a minus roll of 59 deg and a plus yaw of 44 deg, acquisition and lock-on to the sun by the spacecraft sun sensors were completed at 12:10:21 GMT. Concurrent with the sun acquisition sequence, the antenna/solar panel positioner (A/SPP) stepping sequence was initiated to deploy the solar panel and roll axes. At 12:11:59 and 12:16:06 GMT, the solar panel and A/SPP roll axes, respectively, were locked in the proper transit positions. All of these operations were confirmed in real-time from the spacecraft telemetry.

Following sun lock-on, the spacecraft coasted with its pitch and yaw attitude controlled to track the sun and with its roll attitude held inertially fixed.

2. DSIF and Canopus Acquisition Phase

DSS 72 (Ascension Island) achieved one-way lock (down-link) with the spacecraft at approximately 12:10:07 GMT, 16 min after liftoff; two-way communication was established by DSS 72 at 12:16:23 GMT and, after temporary loss of the up-link, was reestablished at 12:21:46 GMT to complete initial acquisition.

The first ground-controlled sequence ("initial spacecraft operations") was initiated at 12:29 GMT ($L + 00:36$) and consisted of commands for (1) increasing the telemetry sampling rate to 1100 bit/sec from 550 bit/sec, (2) turning off spacecraft equipment required only until DSIF acquisition, such as high-power transmitter and accelerometer amplifiers, (3) seating the solar panel and roll axis locking pins securely, and (4) performing the initial interrogation of commutator Modes* 1, 4, 2, 6, and 5, in that order. All spacecraft responses to the commands were normal.

Initial spacecraft operations were completed at 12:51:47 GMT, with *Surveyor IV* configured in low power, coast phase commutator on (Mode 5), and transmitting at 1100 bit/sec. A profile of telemetry rates and modes throughout the *Surveyor IV* mission is presented in Fig. VI-2. During the operations, it was determined from the star intensity telemetry signal that the earth was in the field of view of the Canopus sensor. Therefore, it was recommended that the roll axis be held in the sun mode and that the *cruise mode on* command, which at this time would have caused the roll attitude to be slaved to the high-intensity light source, not be sent to the spacecraft. (Cruise mode was commanded on a few hours later at 15:22:47 GMT, when the intensity signal had dropped to approximately 0.5 V.) It was also determined that there was no need to turn on Transponder A since the Receiver A AFC telemetry indicated only 6.2 kHz error.

The spacecraft continued to coast normally, with its pitch-yaw attitude controlled to track the sun and with its roll attitude held inertially fixed. Tracking and telemetry data were obtained by use of Transponder B and Transmitter B.

*See Section IV-A (Table IV-1) and Appendix C for data content of telemetry modes.

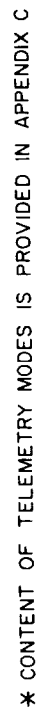


Fig. VI-2. Surveyor IV telemetry bit rate/mode profile

At 17:51 GMT ($L + 05:57$), DSS 61 (Robledo) commanded a positive spacecraft roll maneuver which initiated the star verification/acquisition sequence. This maneuver provides a measure of the intensity of light received from celestial objects passing through the Canopus sensor's field of view. This data is used for comparison with a precomputed star map for positive identification of the star Canopus. At the recommendation of SPAC, the following spacecraft configuration was used during the sequence: telemetry Mode 5 at 4400 bit/sec,* Omnia antenna B with Transmitter B in high-power, and the transponder on. The first revolution was used for the verification part of the sequence.

The roll maneuver proceeded smoothly as the stars Alkaid (Eta Ursa Majoris), Delta Velorum, Gamma Cassiopeiae, and Canopus (after 212 deg of roll), and the earth and moon were detected by the Canopus sensor and identified on the map in the SPAC area. The spacecraft continued to roll, and as the moon passed from the field of view the second time, the star acquisition mode was commanded on. When light from Canopus was sensed, *Surveyor IV* ended the maneuver by automatically locking onto the star. (In both the *Surveyor I* and *II* missions, the Canopus intensity was above the upper threshold of lock-on range, necessitating manual acquisition; *Surveyor III* locked on automatically.) Canopus acquisition occurred at 18:10:22 GMT ($L + 06:16:53$), after the spacecraft had rolled through 572 deg for 18 min, 57 sec. Both the star map prepared by the SPAC and used during this sequence and the spacecraft's predicted position relative to Canopus as computed by the FPAC group proved to have been very accurate.

At the end of the star verification/acquisition sequence, the spacecraft was coasting with pitch and yaw axes controlled to track the sun and the roll axis controlled to track Canopus. *Surveyor IV* was in a fixed attitude, a precise position from which midcourse maneuvers could be initiated.

3. Pre-midcourse Coast Phase

About 35 min after Canopus lock-on, the first gyro drift check was initiated by commanding the spacecraft to inertial mode. The vehicle continued to coast as before, but with its attitude held inertially so that the sun and star sensors continued to point at the sun and Canopus, respectively. At 20:54 GMT ($L + 09:00$), the gyro drift

check was terminated, but a second check was begun 3 min later. In fact, 13 gyro drift checks were performed during the mission, nine of which occurred during this coast phase. The first check had indicated drift slightly higher than specification. Therefore, other checks were desirable to increase confidence in the measured values so that drift could be compensated for accurately during retro maneuvers. Also, during the pre-midcourse coast phase, five standard engineering interrogations were performed in Modes 4, 2, and 5, two at 1100 bit/sec and three at 550 bit/sec.

During the pre-midcourse conference, the decision had been made to delay midcourse correction until $L + 39$ hr, during the second DSS 11 (Goldstone) pass. The midcourse sequences performed during the *Surveyor I*, *II*, and *III* missions had each occurred at about $L + 15$ or 20 hr, during the first Goldstone pass. However, based on the excellent injection conditions of *Surveyor IV* and the small velocity correction required, it was expected that landing site accuracy improvement could be better obtained by executing the maneuver at $L + 39$ hr.

Final computation of midcourse parameters was conducted following the selection of a midcourse correction plan from the alternatives which had been studied. (Refer to Section VII for a discussion of the factors considered in selecting the midcourse correction plan.)

The final pre-midcourse engineering interrogation was started at 00:11 GMT ($L + 36:18$) on July 16. This sequence was executed using low-power transmitter operation and indicated that the spacecraft was operating normally. As part of this sequence, the gyro speed outputs were measured and were found to be exactly nominal at 50 Hz.

4. Midcourse Maneuver Phase

The midcourse correction sequence was initiated at $L + 37:54$, with an engineering interrogation in commutator Modes 4, 2, and 1. The telemetry readings indicated that the spacecraft was in satisfactory condition for midcourse operations. The interrogation was followed by commands to turn on Transmitter B high power and increase the telemetry sampling rate from 1100 to 4400 bit/sec. Starting at 02:15 GMT ($L + 38:22$), the required roll (+72.45 deg) and yaw (-64.32 deg) maneuvers were executed to align the spacecraft axes in the desired direction for applying the midcourse thrust. The attitude maneuvers were initiated at limit cycle nulls in an attempt to reduce pointing errors. Following engineering interrogation in commutator Modes 2 and 1, the spacecraft was

*This nonstandard bit rate was selected to obtain a greater sampling rate of Canopus sensor signals than was possible at 1100 bit/sec. After the sequence, the rate was lowered to 1100 bit/sec.

prepared for thrusting, including sending commands to (1) turn on propulsion strain gage power, (2) turn on inertial mode, (3) pressurize the vernier propulsion system, and (4) load the desired thrust time (10.463 sec) in the flight control programmer magnitude register. Midcourse velocity correction was executed at 02:30:02 GMT ($L + 38:36:33$) on July 16 in accordance with the planned thrust time. All engines fired simultaneously, burned for 10.475 sec for a velocity change of 10.13 m/sec, then shut down automatically. The spacecraft remained stable throughout the thrusting period.

Following midcourse velocity correction (which corrected the miss distance to within 8.6 km of the final aiming point), commands were sent to turn off various power sources used during the thrusting phase and to execute attitude maneuvers in reverse order and opposite direction. The sun was reacquired at 02:35:03 GMT after a positive yaw, and Canopus was reacquired at 02:39:51 GMT at the end of a negative roll. Thus, confirmation was obtained that the gyros had retained inertial reference during vernier engine shutdown, eliminating the need for performing a post-midcourse star verification to insure lock-on to Canopus.

The spacecraft was returned to flight control cruise mode, and a high-power engineering interrogation was conducted in telemetry Modes 2, 4, and 5, after which the 550 bit/sec data rate and low-power transmission were established.

5. Post-midcourse Coast Phase

The second coast phase was relatively uneventful. As mentioned previously, extra gyro drift checks were performed. Six engineering interrogations at 550 bit/sec were also conducted during this period. As in the *Surveyor I* and *III* missions, power-mode cycling checks were made to help predict the percentage of electrical load that would be supplied by each spacecraft battery (main and auxiliary) during terminal descent, when both batteries are placed directly on the power bus. The spacecraft was also commanded to turn on Vernier Oxidizer Tank 2 heater and the survey television electronics temperature control.

The last gyro drift check was terminated at 19:12:57 GMT ($L + 55:19:28$), 6.5 hr before main retro ignition, and the accumulated error was nulled. About 1.5 hr later, in preparation for terminal descent, the spacecraft was commanded to switch to the *main battery* mode, in which both batteries are on-line.

Prior to the terminal maneuver conference, the SFOD held a preliminary internal mission operations conference to generate a list of alternate terminal maneuver plans and an outline of postlanding operations for presentation to the Mission Director.

In the terminal maneuver conference, the plan which was presented to and approved by the Mission Director contained the following items:

- (1) Use of a roll-yaw-roll maneuver sequence with Omnantenna B to optimize telecommunications performance.
- (2) Initiation of the three-maneuver sequence 38 min prior to retro ignition.
- (3) Transmission of 1100 bit/sec PCM data.
- (4) Attempt to obtain strain gage data only if the received signal level provides sufficient telemetry gain margin after terminal maneuvers are completed.
- (5) Turnoff of the transponder prior to start of the maneuvers.

The preterminal engineering interrogation of Modes 4, 2, 1, and 5 was started at 23:45 ($L + 59:52$) and was followed by the gyro speed check. The VCXO check was then performed by commanding off transponder power for 1½ min. Spacecraft telemetry confirmed that *Surveyor IV* was in good condition and ready for terminal descent.

6. Terminal Maneuver and Descent Phase

On July 17, at 00:59:29 ($L + 61:06$), about an hour before retro ignition, Mode 6 (thrust phase commutator) interrogation was started. Then the television camera vidicon temperature control was turned on, Transmitter B was commanded from low to high power, the telemetry rate was increased to 1100 bit/sec, and power was turned on as required for monitoring vernier propulsion and touchdown forces by means of strain gages. The spacecraft transponder was then turned off and DSS 11 and DSS 14 maintained one-way lock for the terminal maneuvers.

The terminal maneuvers were begun approximately 38 min prior to the predicted time of retro ignition. During the first maneuver the spacecraft rolled +80.85 deg. This was followed by a yaw maneuver of +92.68 deg. With the retro thrust axis oriented in the desired direction, the final roll maneuver (-25.24 deg) was initiated at 01:35:05 GMT, about 27 min before retro ignition.

This established optimum roll positioning of the spacecraft, within the RADVS constraints, for postlanding operations. The maneuvers were compensated for flight control sensor group deflections and gyro drift rates; they were successfully initiated on limit cycle nulls to effectively reduce errors in the thrust vector direction.

In the remaining time before the automatic retro sequence, final preparations were made for terminal descent. The thrust level of the vernier engines was set at 200 lb, a delay time of 2.725 sec between the AMR *mark* event and ignition of the vernier engines was stored in the spacecraft, and commutator Mode 6 was selected. The AMR was turned on and then enabled at 02:00:14 GMT, 1 min and 44 sec before main retro ignition.

The AMR *mark* signal occurred automatically at 02:01:54.8 GMT. (The spacecraft received the DSIF-commanded backup AMR signal at 02:01:55.3 GMT, i.e., 0.5 sec after automatic *mark*.) The vernier engines ignited and, 1.1 sec later, main retromotor ignition occurred at 02:01:58.6 GMT ($L + 62:08:29$). RADVS power came on automatically as planned. At 02:02:30 GMT, the RODVS (*reliable operate doppler velocity sensor*) signal was transmitted by *Surveyor IV*, indicating that the three doppler velocity sensor beams had automatically acquired the lunar surface at the proper altitude. The spacecraft was stable and operating properly.

At 02:02:39.7 GMT, 41.09 sec after main retro ignition and 1.4 sec before predicted retromotor burnout, *Surveyor IV* suddenly stopped transmitting. At this time the spacecraft was approximately 49,000 ft from the moon's surface and was traveling 1070 ft/sec. DSS 11 and DSS 14 simultaneously lost the spacecraft carrier

signal and all incoming spacecraft data at 02:02.40.9 GMT, the delay due to the time required for spacecraft signals to reach the earth from the vicinity of the moon. The final telemetry data received at DSS 11 was a signal from the flight control subsystem giving the status of the thrust being applied to Vernier Engine 3. The first 10 bits of this signal had routinely been received, when abrupt loss of signal and telemetry occurred.

Surveyor IV never resumed transmission, so, if a successful landing can be assumed, it is unknown whether or not the spacecraft received any of the 4255 commands sent from loss of signal to the end of the mission 34 hr later. Mission operations were conducted based on the premise that the spacecraft could receive and act upon commands and that it had performed automatic descent properly, landing at about 02:05 GMT as scheduled. The first "postlanding" sequence was initiated at 02:05:31 GMT. The philosophy followed was that of obtaining a workable spacecraft transmitting system by exercising all of the logical redundancy that is inherent in the spacecraft RF subsystem. Operations included selection of various combinations of transmitters, antennas, and transmitter power levels while in different battery modes and with the overload trip circuit both bypassed and enabled. These efforts were conducted until 08:07 GMT on July 17, just before the end of Goldstone visibility, and were resumed on July 18 at 00:50 GMT, following Goldstone rise.

After station transfer shortly before 06:00 GMT, DSS 42 continued in the attempt to restore spacecraft transmission. At 10:40 GMT, the station began antenna and solar panel positioning operations. Finally, since there still was no response from the spacecraft, the final command was sent to *Surveyor IV* at 12:16 GMT, and the mission was terminated.

VII. Flight Path and Events

Surveyor IV was injected very accurately into a lunar transfer trajectory which required only a small midcourse correction. The *Surveyor IV* mission profile was altered from previous missions to perform the midcourse correction during the second rather than first Goldstone pass to improve landing site accuracy. A midcourse correction of 10.27 m/sec was commanded about 38½ hr after lift-off to reduce the main retro burnout velocity in addition to providing for correction of the small injection errors and slight refinement of the aiming point. Although the spacecraft signal was permanently lost about 41 sec after main retro ignition during terminal descent, the current best estimate is that the spacecraft may have softlanded in Sinus Medii at 0.43 deg north latitude and 1.61 deg west longitude, 8.6 km from the midcourse aiming point.

A. Prelaunch

For *Surveyor IV*, the landing site selected prior to launch for targeting of the launch vehicle ascent trajectory was in Sinus Medii near the center of the *Apollo* zone of interest at 0.58 deg north latitude and 0.83 deg west longitude. This site was selected because it is of prime interest to the *Apollo* Program. Subsequently, NASA Headquarters directed a refinement of the aim point to 0.417 deg north and 1.333 deg west at the request of *Apollo*. The design unbraked impact speed was selected within the spacecraft capability such that the

Goldstone postarrival visibility would be maximized while still satisfying the prearrival visibility constraint for all launch days in the launch period.

B. Launch Phase

Surveyor IV was launched on the first attempt from AFETR Launch Pad 36A at Cape Kennedy, July 14, 1967, the second day of the launch period. (Launching was not attempted on the first day of the period owing to a connector problem in the propellant utilization system of the *Atlas/Centaur* second stage.) Liftoff occurred at 11:53:29.215 GMT, only 29.2 sec after opening of the launch window, the brief delay being required to complete liquid hydrogen topping of the *Centaur*. At 2 sec after liftoff, the *Atlas/Centaur* launch vehicle began a 13-sec programmed roll that oriented the vehicle from a pad-aligned azimuth of 105 deg to a launch azimuth of 103.82 deg. At 15 sec, a programmed pitch maneuver was initiated which was completed at *Atlas* booster engine cutoff (BECO). As this was a direct ascent flight, the *Centaur* stage burned only once to inject the spacecraft into the desired lunar transfer trajectory. All event times were well within the 3- σ tolerance. The countdown and launch phase sequences are discussed in greater detail in Sections II and III, respectively. Nominal and actual event times for all phases of the mission are summarized in Table A-1 of Appendix A.

C. Cruise Phase

Separation of *Surveyor IV* from the *Centaur* occurred at 12:06:06.1 GMT on July 14, 1967. Automatic sun acquisition began about 49 sec after separation and was completed after a maneuver of -59 deg roll and $+44$ deg yaw. The spacecraft never entered the earth's shadow during either the launch or transit phases of the mission.

Near-earth tracking coverage was provided by stations of the Air Force Eastern Test Range and Manned Space Flight Network as described in Section V. Initial DSIF two-way acquisition was accomplished quite smoothly by DSS 72, Ascension. DSS 72 reported one-way doppler data at 12:10:03 GMT (only a few seconds after predicted spacecraft rise over the station's horizon) and good two-way data at 12:16:23 (about $6\frac{1}{2}$ min after rise). DSS 72 acquisition was marred, however, by loss of the uplink at 12:17:03, which was subsequently reestablished at 12:21:46. The DSN continued tracking *Surveyor IV* in the two-way mode with few exceptions and, in general, returned high-quality two-way doppler data until loss of the spacecraft signal. (The station tracking periods are presented in Fig. V-11.) The most serious loss of two-way doppler data occurred during the first DSS 61 pass, when about $1\frac{1}{2}$ hr of data was lost due to a sticking doppler counter (this problem also occurred on *Surveyor III*). The loss of the uplink during initial acquisition by DSS 72 was responsible for loss of about 10 min of early prime data. Some DSS 11 data was also lost due to an unnecessarily long time (20 min) required for acquisition on the first pass and an intermittent loss of the most significant digit of the doppler counter over a 30-min period during the second pass. Computer monitoring in near-real-time of all *Surveyor IV* two-way doppler data resulted in the timely discovery of the DSS 61 and DSS 11 doppler counter problems.

A plot of the actual *Centaur* and *Surveyor IV* trajectories, projected on the earth's equatorial plane, is provided in Fig. VII-1. The *Centaur* passed above and behind the moon with a radius of closest approach to the moon of 22,300 km at about 8 hr after loss of the spacecraft signal. The earth track traced by *Surveyor IV* appears in Fig. VII-2. Specific events such as sun and Canopus acquisition and rise and set times for DSIF stations are also noted.

Prior to Canopus acquisition, the spacecraft was rolled to generate a star map. Then, Canopus was acquired automatically at $L + 06:17$ with a net spacecraft roll of $+212$ deg. In the normal cruise mode, the spacecraft $-Z$ axis is aligned to the sun and the $-X$ axis to the projec-

tion of Canopus in the spacecraft X-Y plane (refer to Fig. IV-3).

The uncorrected, unbraked impact point and the original target point are shown in Fig. VII-3. Based upon the current best estimate, the uncorrected, unbraked impact point is located just to the southwest of Sinus Medii at 1.99 deg south latitude and 5.9 deg west longitude. The original target point was 0.58 deg north latitude and 0.83 deg west longitude, which is within Sinus Medii. The two points are approximately 176 km (110 miles) apart on the surface of the moon. Also shown in Fig. VII-3 are the sites where *Surveyors I* and *III* softlanded and the location where *Surveyor IV* may have softlanded.

Figure VII-4 is an enlarged section of the lunar area containing the uncorrected impact point. A few selected pre-midcourse orbit computations mapped to the moon are indicated in the figure. The numerical data for these selected pre-midcourse computations is presented in Table VII-1. The first transfer orbit computed by the Real Time Computer System at about $L + 00:15$ was based upon Antigua data. The results of this orbit computation mapped to the moon were transmitted at about $L + 00:33$ and gave the initial indication that lunar encounter would be achieved without a midcourse correction. The results of this mapping are included in Table VII-1, but the lunar impact coordinates fall outside the area shown in Fig. VII-4. Included in Fig. VII-4 are three RTCS orbit determinations mapped to the moon, which were transmitted at $L + 01:44$, $L + 02:27$, and $L + 02:31$, based upon DSS 72 data, *Centaur* guidance data, and DSS 72 and 51 data, respectively. Each of these mapping computations was quite consistent and close to nominal values. The first orbit computed by the SFOF at JPL was based on AFETR data (Antigua) and confirmed lunar impact. The first SFOF orbit based on DSN data (PROR YA) was completed at $L + 02:00$ and confirmed that the correction required to achieve the prelaunch aiming point was well within the midcourse correction capability. These results were verified by the second (ICEV YA) and third (PREL XB) orbit computations completed at $L + 02:55$ and $L + 04:00$, respectively (shown in Fig. VII-4). Since the angle tracking data appeared to be biased, they were eliminated from the third computation (PREL), resulting in a change of 40 km in the B-plane. During the data consistency (DACO) orbit computation period, the first DSS 11 data was obtained and utilized. However, it was decided not to use any DSS 61 data because of an apparent bias and excessive noise. A total of eleven DACO orbits were computed which indicated the two-way doppler data from DSS 11, 51, and 72 was consistent. By the

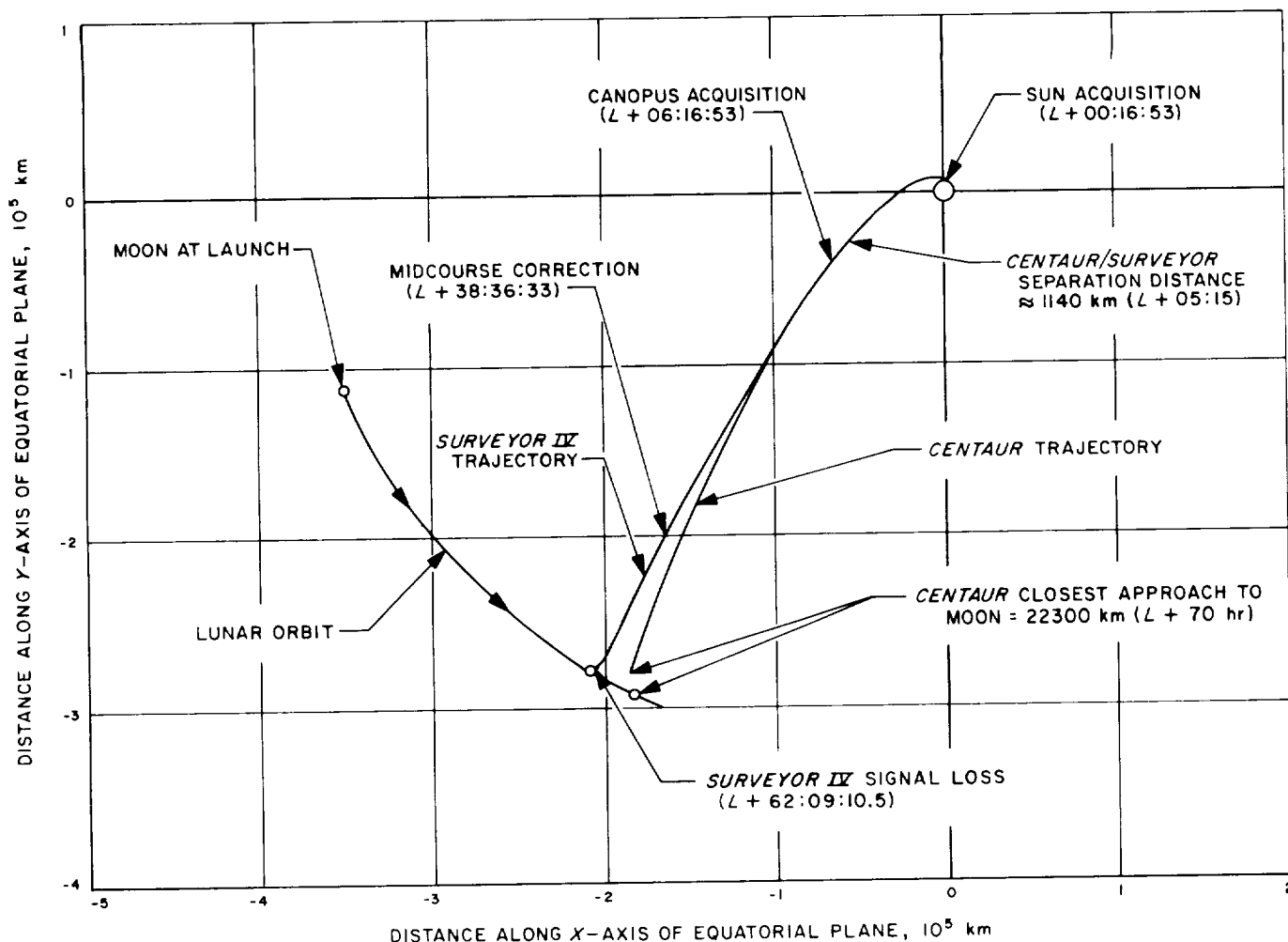


Fig. VII-1. Surveyor IV and Centaur trajectories in earth's equatorial plane

end of the DACO orbit computation period ($L + 10$ hr) it had been decided to delay the midcourse maneuver to approximately $L + 38$ hr. During the last pre-midcourse (LAPM) orbit computation period, calculations were run with all usable data from the DSIF stations (except DSS 61). The last of these orbits (LAPM YC) was used to determine the required midcourse correction. The current best estimate of the spacecraft uncorrected orbit (PRCL YB) includes additional DSIF data taken until the start of the midcourse maneuver.

D. Midcourse Maneuver Phase

The original target point was selected assuming the 99% (3σ) landing dispersions to be a 30-km-radius circle on the lunar surface. However, primarily because of the small midcourse correction required and high quality of the tracking data, the 99% dispersion computed in-flight from the assumed execution and tracking errors for a

midcourse correction during the Goldstone second pass (about $L + 38$ hr) was an ellipse having a semimajor axis of 10.8 km and a semiminor axis of 7.2 km as shown in Fig. VII-5. The original target point and final aim point are also shown in Fig. VII-5 together with the estimated landing site assuming a softlanding. The latitude and longitude for these locations as well as for the uncorrected impact point are given below:

	North latitude, deg	West longitude, deg
Original target point	0.58	0.83
Uncorrected impact point	-1.99	5.9
Final aim point	0.417	1.333
Estimated landing point	0.43	1.62

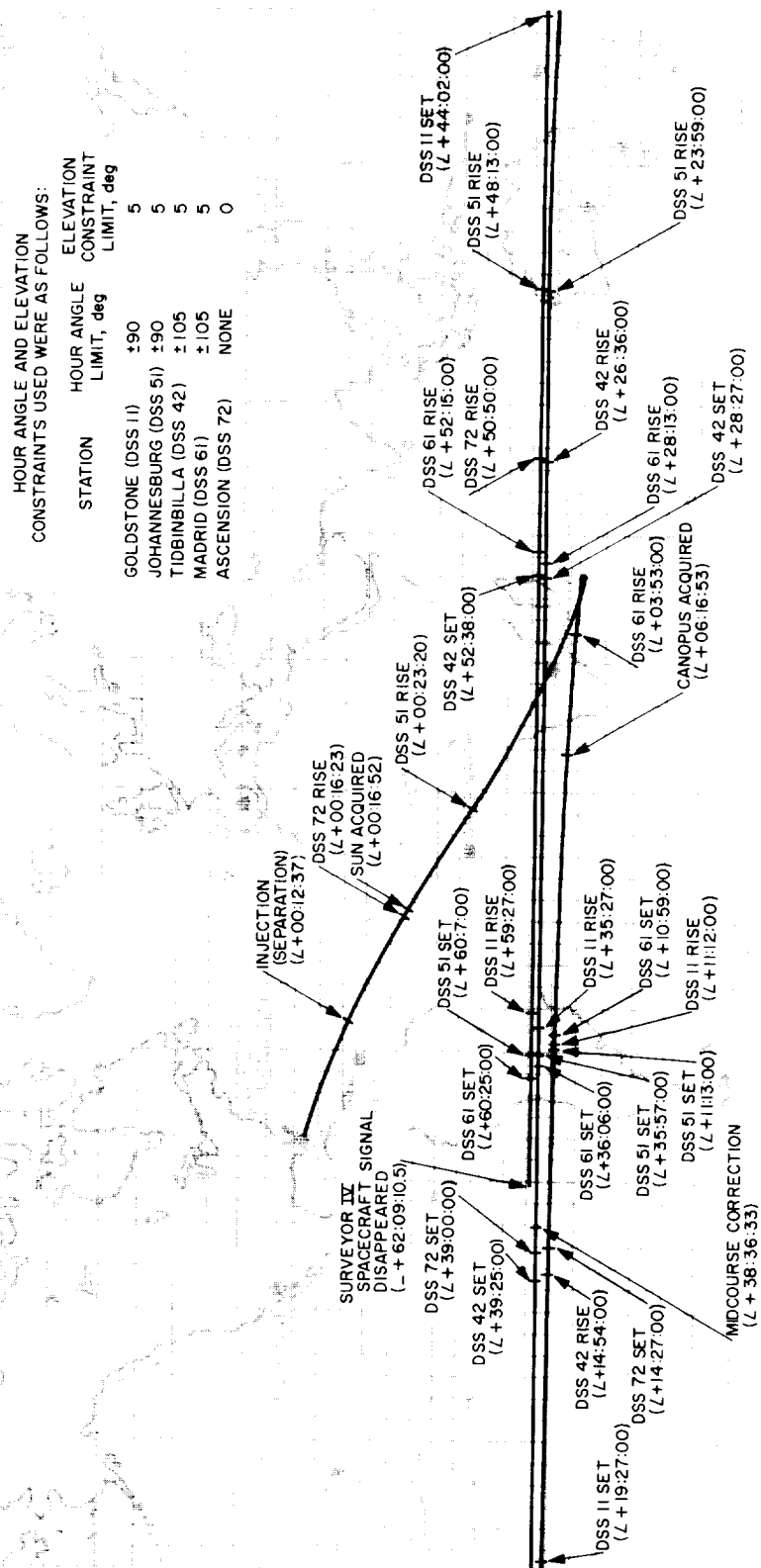


Fig. VII-2. Surveyor IV earth track

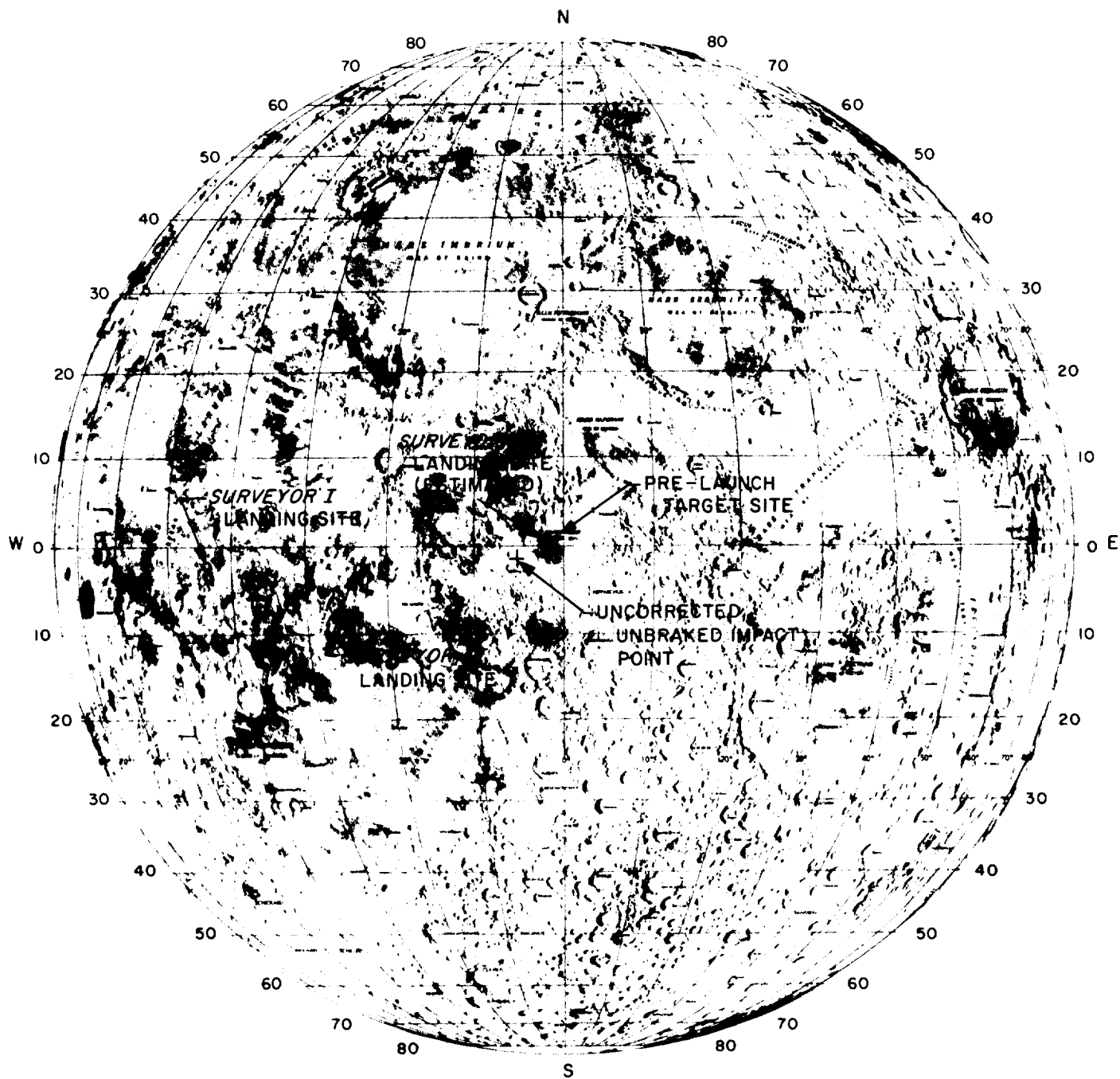


Fig. VII-3. Surveyor IV target and uncorrected impact points

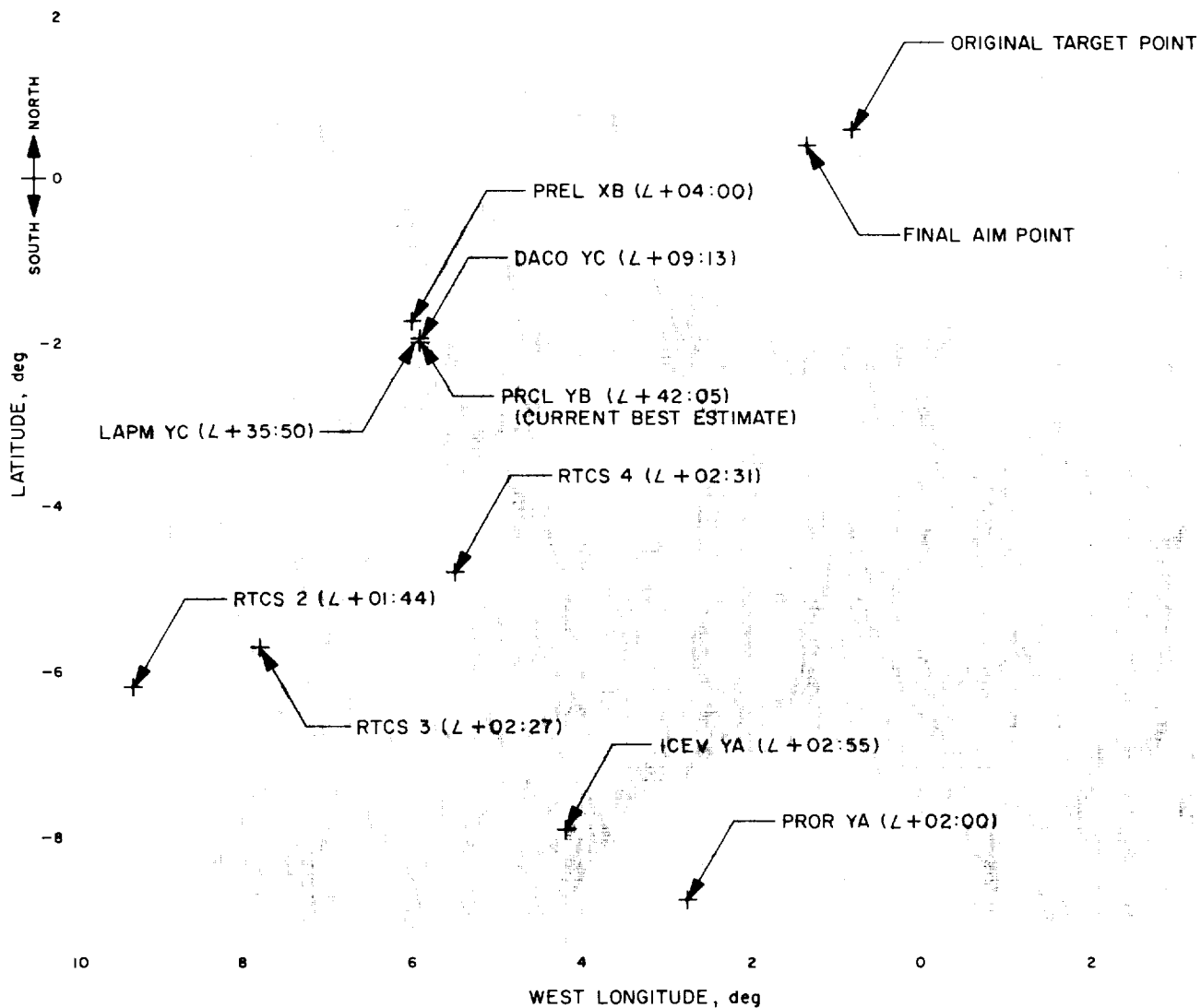


Fig. VII-4. Computed Surveyor IV pre-midcourse unbraked impact locations

Table VII-1. Surveyor IV enc

Orbit identification	Time computation completed (from liftoff)	Target statistics									
		B, km	B • TT, km	B • RT, km	TL, hr	SMAA (1 σ), km	SMIA (1 σ), km	Theta, deg	σ_T impact, (1 σ) sec	PHIP 99, deg	SVFIX R, (1 σ) km/sec
RTCS 1	00:33	768.04	586.93	-495.38	61.98						
SFOF (ETR)	12:42	3882.77	2498.0	2972.5	61.43	8224.0	1485.4	28.58	0.488×10^{11}	706.7	0.282
RTCS 2	01:44	1614.02	1613.38	-45.49	62.13						
PROR YA	02:00	1881.97	1878.4	115.33	62.19	93.42	35.80	97.31	60.93	3.14	0.000627
RTCS 3	02:27	1675.21	1673.88	-66.74	62.05						
RTCS 4	02:31	1781.10	1778.32	-98.51	62.10						
ICEV YA	02:55	1824.92	1823.7	66.86	62.20	89.48	6.80	99.19	36.45	1.835	0.000615
PREL XB	04:00	1785.30	1767.4	-251.9	62.17	55.82	5.78	104.1	17.24	1.044	0.000612
DACO YC	09:13	1786.40	1770.2	-240.1	62.17	5.01	3.93	55.76	1.501	0.103	0.000610
LAPM YC ^a	35:50	1784.01	1768.0	-238.7	62.17	2.07	1.22	35.00	0.8223	0.0626	0.000610
PRCL YB ^b	42:05	1785.9	1769.7	-239.4	62.18	48.14	9.12	83.05	16.80	1.163	0.000712

^aOrbit used for midcourse computations.^bCurrent best estimate.

SMAA = Semimajor axis of dispersion ellipse.

SMIA = Semiminor axis of dispersion ellipse.

Theta = Orientation angle of dispersion ellipse measured counterclockwise from T-T axis in B-plane.

 σ_T impact = Uncertainty in predicted unbraked impact time.

unter conditions based on premidcourse orbit determinations

Unbraked impact conditions			Data used
Lat, deg	Long, deg	GMT, July 17, 1967	
1.81	328.61	02:03:57.5	Antigua radar
-29.15	102.5	01:50:12.319	Antigua radar
-6.16	350.72	02:13:17.7	DSS 72
-8.75	357.2	02:12:59.134	DSS 72 and 51 angular and two-way doppler
-5.61	352.19	02:07:50.8	Centaur guidance telemetry
-4.78	354.48	02:11:06.4	DSS 72 and 51
-7.93	355.8	02:13:42.463	DSS 72 and 51 angular and two-way doppler
-1.74	354.0	02:11:39.209	DSS 72 and 51 two-way doppler
-1.97	354.1	02:11:43.937	DSS 72, 51 and 61 two-way doppler
-2.00	354.1	02:11:42.145	DSS 72, 11, 42, and 51 two-way doppler
-1.99	354.1	02:11:42.684	DSS 72, 11, 42, and 51 two-way doppler.
PHIP 99 = 99% velocity vector pointing error. SVFIX R = Uncertainty in magnitude of velocity vector at unbraked impact. TL = Flight time from injection.			

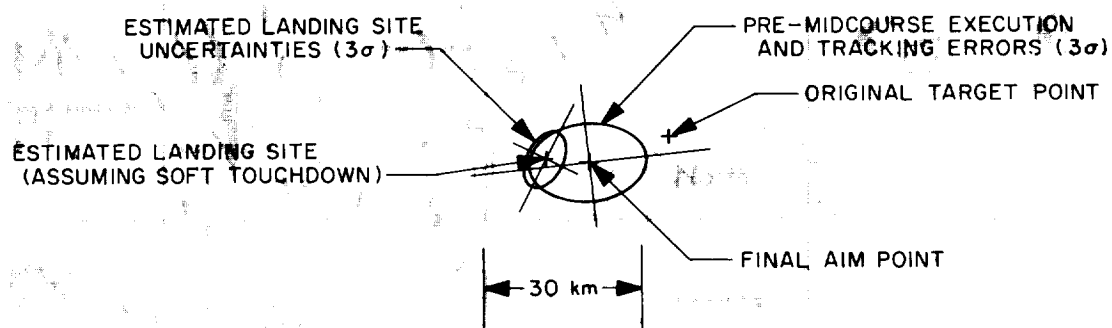


Fig. VII-5. Surveyor IV landing location

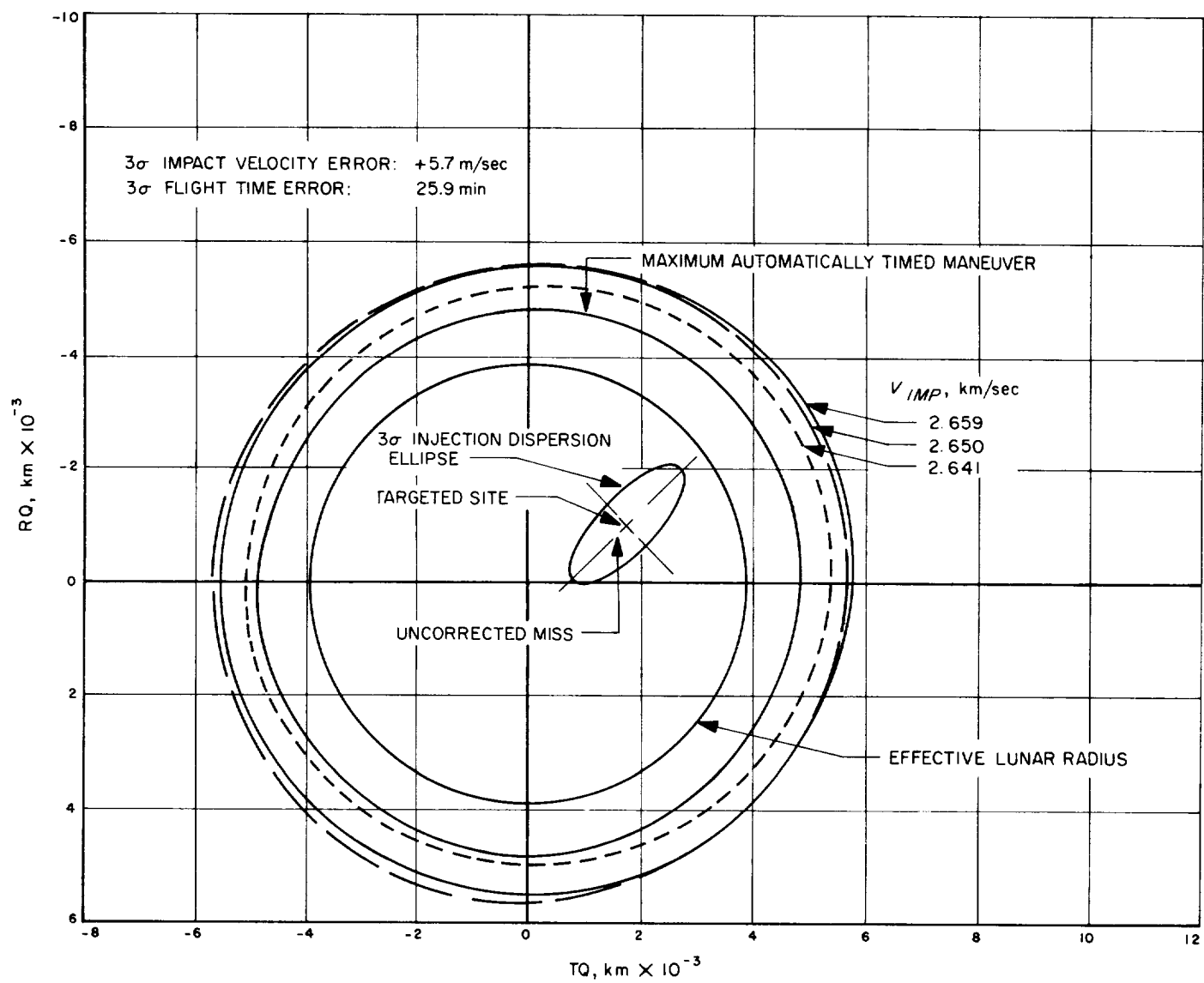


Fig. VII-6. Midcourse correction capability contours in B-plane (for a midcourse correction 40 hr after injection)

The maximum midcourse correction capability is shown in Fig. VII-6 for three values of unbraked impact speed V_{imp} . Also shown are the expected 3σ *Centaur* injection guidance dispersions, the effective lunar radius, and the maximum maneuver which could have been executed in the normal mode (i.e., thrusting terminated automatically by the spacecraft timer). The midcourse capability contours are in the conventional R-S-T coordinate system.*

A midcourse correction of 10.27 m/sec (equivalent to a burn time of 10.46 sec) was selected and executed upon ground command at $L + 38:36:33$ (02:30:02 GMT on July 16, 1967). The actual midcourse correction was 10.13 m/sec based upon post-midcourse orbit determinations. The velocity component in the critical plane, to correct "miss only," was 2.47 m/sec. This component is referred to as the critical component. The velocity component normal to the critical component is referred to as the noncritical component \dot{U}_3 since it does not effect miss to the first order. A midcourse execution time of about $L + 38$ hr was selected because, as shown in Fig. VII-7, significantly lower landing site uncertainty would be obtained compared with a 16-hr maneuver. Figure VII-8 presents the variations in flight time, main retro burnout velocity, vernier propellant margin, and landing site dispersions with the noncritical velocity component \dot{U}_3 for a midcourse execution time of about $L + 38$ hr. The vernier propellant margin and flight time were acceptable

within the limits shown. A noncritical component of -10.0 m/sec was selected because (1) landing uncertainties are fairly constant out to this value, (2) the main retro burnout velocity would be reduced to a more comfortable level of about 500 ft/sec, and (3) the Goldstone postarrival visibility time would be increased. If the maneuver strategy had been to correct "miss-plus-flight-time," the required noncritical component would have been $+3.19$ m/sec, giving a total correction of 4.15 m/sec.

Since the aiming point was changed during the flight, the above required correction does not properly evaluate the performance of the *Centaur* guidance system. Using the results of the last pre-midcourse orbit and correcting to the original aim point gives a miss only requirement of 1.51 m/sec and a miss-plus-time-of-flight requirement of 1.94 m/sec for a midcourse conducted 20 hr after injection.

The predicted results of the selected midcourse correction and other alternatives considered are given in Table VII-2. The possibility of not performing a midcourse correction was eliminated because it was required that the spacecraft land at a prime *Apollo* site. Execution of a midcourse correction during the first Goldstone pass (approximately 16 hr after injection) would have halved the magnitude of the critical velocity correction to 1.21 m/sec but would have increased the expected landing site dispersions as shown in Fig. VII-7 and Table VII-2. Therefore, the early midcourse correction was rejected owing to the small size of the *Apollo* landing

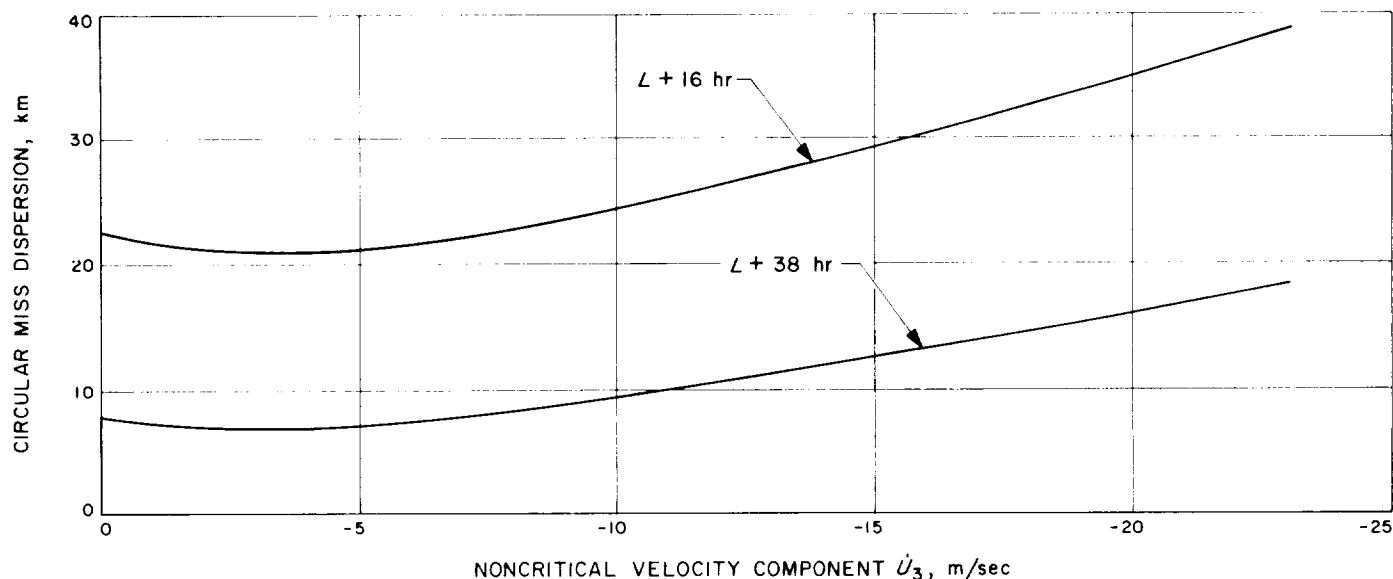


Fig. VII-7. Effect of midcourse correction magnitude and execution time on lunar surface miss

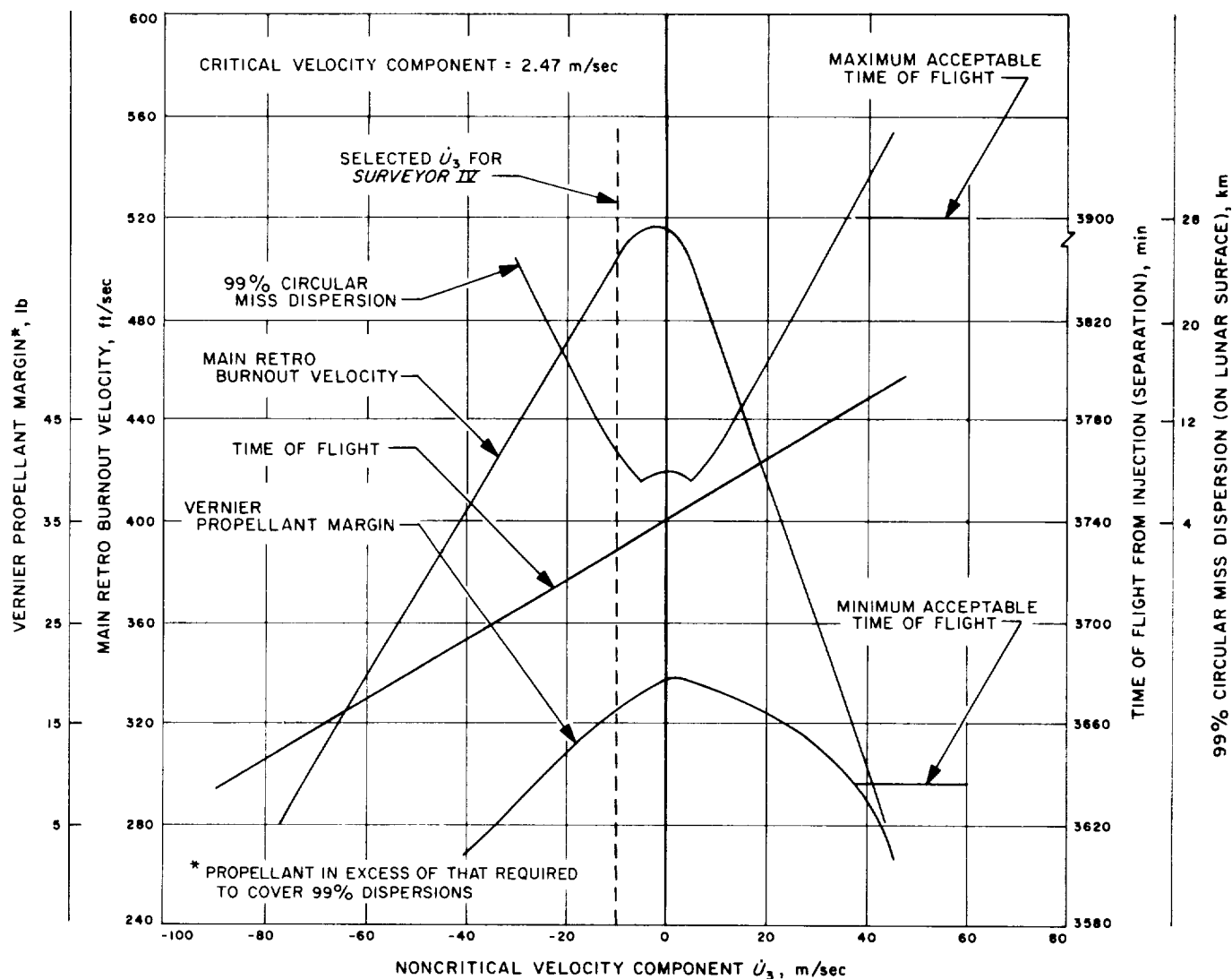


Fig. VII-8. Effect of noncritical velocity component on terminal descent parameters

site and surrounding rugged terrain. The possibility of performing a correction along the spacecraft-sun direction was investigated and eliminated because the desired site could not be reached.

An analysis was made of eight pairs of pre-midcourse attitude rotations, any pair of which would have correctly oriented the spacecraft for the midcourse velocity correction. A combination of +72.45 deg roll and -64.32 deg yaw was chosen because it maximized the probability of mission success by providing continuous high antenna gain, no antenna switching requirements, and maximum sun-lock time. The selected attitude rotations were compensated 0.3 deg to achieve alignment of the actual thrust axis (determined prior to launch) with the desired mid-

course vector. Also, the attitude maneuvers were initiated at limit cycle nulls in an attempt to further reduce pointing errors.

Table VII-3 presents the pre-midcourse and post-midcourse injection and encounter conditions.

E. Terminal Phase

A terminal attitude maneuver, consisting of +80.85 deg roll, +92.68 deg yaw, and -25.24 deg roll, was initiated approximately 38 min prior to retro ignition with a nominal 2-min allowance between rotations. This maneuver combination, using Omnantenna B, was selected to optimize telecommunications performance during the terminal

Table VII-2. Midcourse correction alternatives comparison

	Selected midcourse	Alternate considerations					
	38.4-hr ^a midcourse	No midcourse	16-hr midcourse			38.4-hr midcourse	
Midcourse Parameters							
Velocity magnitude, m/sec	10.27	0.00	1.21	10.06	22.02	2.47	20.18
Critical direction, m/sec	2.47	0.00	1.21	1.21	1.21	2.47	2.47
Noncritical direction, m/sec	-10.00	0.00	0.00	-10.00	-22.00	0.00	-20.00
Propellant weight, lb	8.83	0.00	1.04	9.1	18.95	2.13	17.37
Landing site dispersions (mechanization plus tracking), 3σ :							
Semimajor axis, km	10.8		26.1	28.2	43.8	9.3	18.6
Semiminor axis, km	7.2		5.1	12.6	26.1	2.8	13.5
Ellipse inclination, deg (positive TQ toward RQ)	-33.2		-48.1	-46.3	-40.0	-39.1	-32.1
Terminal Parameters							
Aim point: latitude, deg	0.417	-2.00	0.417	0.417	0.417	0.417	0.417
longitude deg	358.667	354.07	358.667	358.667	358.667	358.667	358.667
Incidence angle, deg	31.49	27.7	31.4	31.4	32.0	31.4	31.0
Unbraked impact speed, m/sec	2668.1	2663.5	2663.0	2668.0	2673.8	2663.0	2673.0
Main retro burnout velocity, ft/sec	504.4	530.0	532.0	504.5	463.0	525.0	470.0
Main retro burnout altitude, ft	40,896.1						
Propellant margin, lb	16	17	20	12	11	19	12
Postlanding visibility increase, min	10.4		0.0	21.4	47.1	0.0	20.8
^a Time from spacecraft separation.							

maneuver and terminal descent phases. The final roll maneuver was performed to achieve a spacecraft roll attitude at retro ignition to satisfy constraints of the radar altimeter and doppler velocity sensor (RADVS) and post-landing operations. The maneuver magnitudes included compensation for flight control sensor group deflection and gyro drift rates, and the maneuvers were successfully initiated on nulls in the limit cycles to effectively reduce errors in the thrust vector direction.

The terminal descent sequence is described in detail in Section IV-A. Table A-1 of Appendix A gives terminal phase event times. Sudden loss of spacecraft signal occurred about 41 sec after main retro ignition at 02:02:40 GMT on July 17, 1967, at a mission time of $L + 62:09:10$.

F. Landing Site

The current best estimate of the *Surveyor IV* landing site, assuming the spacecraft to have softlanded, is 0.43 deg north latitude and 1.62 deg west longitude. This location is 8.61 km (5.38 miles) from the final aim point and within the expected 3σ dispersion ellipse as shown in Fig. VII-5. If it is assumed the spacecraft proceeded along a ballistic path after loss of signal, the impact point is estimated to be 0.47 deg north latitude and 1.44 deg west longitude. The 3σ uncertainties associated with the soft landing or ballistic impact locations are the same: semimajor axis = 6.0 km, semiminor axis = 4.5 km, inclination of ellipse = 64.4 deg north of east. Loss of the spacecraft signal prevented a more refined estimate of the landing site.

Table VII-3. Pre-midcourse and post-midcourse injection and terminal conditions

Pre-midcourse injection conditions, July 14, 1967, 12:05:06.480 GMT							
Coordinate ^a system	Inertial cartesian	X = 3086.8903 km	Y = 5367.0375 km	Z = 2133.6793 km	DX = -8.0394318 km/sec	DY = 6.0570878 km/sec	DZ = -4.3609968 km/sec
	Inertial spherical	R = 6548.7839 km	DEC = 19.014840 deg	RA = 60.094330 deg	VI = 10.969917 km/sec	PTI = -1.2867137 deg	AZI = 114.38407 deg
	Earth-fixed spherical	R = 6548.7838 km	LAT = 19.014840 deg	LON = 307.14767 deg	VE = 10.560455 km/sec	PTE = -1.3366117 deg	AZE = 115.39569 deg
	Orbital elements	C3 = -1.3938430 km ² /sec ²	ECC = 0.97711166	INC = 30.559675 deg	TA = -2.6035793 deg	LAN = 275.80222 deg	APF = 142.75095 deg
Pre-midcourse encounter conditions, July 17, 1967, 02:11:42.684 GMT							
Coordinate system	Selenocentric	RAD = 1736.7998 km	LAT = -1.9887743 deg	LON = 354.11051 deg	VP = 2.6613657 km/sec	PTP = -62.400331 deg	AZP = 78.627148 deg
	Miss parameter earth equator	BTQ = 1555.2943 km	BRQ = -877.68785 km	B = 1785.8545 km			
	Miss parameter moon equator	B • TT = 1769.7410 km	B • RT = 239.36933 km	B = 1785.8558 km			
	Coordinate system	Post-midcourse injection conditions, July 16, 1967, 02:30:10.461 GMT					
Inertial cartesian	X = -163929.67 km	Y = -197931.44 km	Z = -107696.87 km	DX = -0.54574733 km/sec	DY = -1.0148226 km/sec	DZ = -0.36345851 km/sec	
	Inertial spherical	RAD = 278654.63 km	DEC = -22.736191 deg	RA = 230.36795 deg	VI = 1.2082248 km/sec	PTI = 78.125539 deg	AZI = 65.931236 deg
	Earth-fixed spherical	RAD = 278654.63 km	LAT = -22.736193 deg	LON = 259.57694 deg	VE = 18.551842 km/sec	PTE = 3.6541247 deg	AZE = 270.31378 deg
	Orbital elements	C3 = -1.4010910 km ² /sec ²	ECC = 0.97860993	INC = 32.636718 deg	TA = 167.87828 deg	LAN = 271.23665 deg	APF = 146.34440 deg
Post-midcourse encounter conditions, July 17, 1967, 02:02:30.238 GMT							
Coordinate system	Selenocentric	RAD = 1736.7997 km	LAT = 0.48414856 deg	LON = 358.62715 deg	VP = 2.6657373 km/sec	PTP = -58.802781 deg	AZP = 76.799493 deg
	Miss parameter earth equator	BTQ = 1686.0287 km	BRQ = -1042.7227 km	B = 1982.4135 km			
	Miss parameter moon equator	B • TT = 1952.3441 km	B • RT = -343.97969 km	B = 1982.4151 km			
	Coordinate system	Post-midcourse injection conditions, July 16, 1967, 02:30:10.461 GMT					

^aHoldridge, D. B., Space Trajectories Program for the IBM 7090 Computer, Technical Report 32-223, Jet Propulsion Laboratory, Pasadena, March 2, 1962.

^aHoldridge, D. B., Space Trajectories Program for the IBM 7090 Computer, Technical Report 32-223. Jet Propulsion Laboratory, Pasadena, March 2, 1962.

Appendix A
Surveyor IV Mission Events

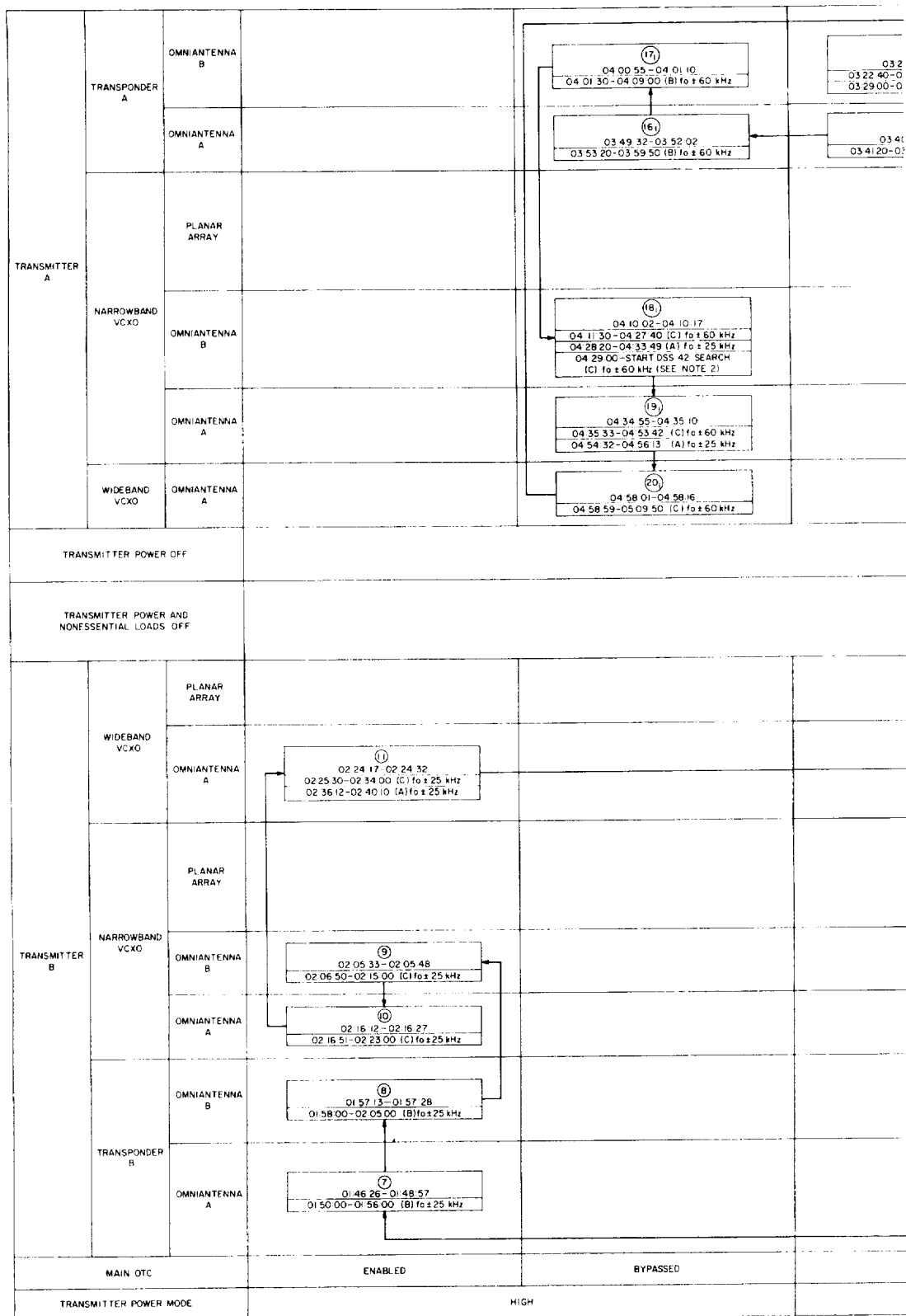
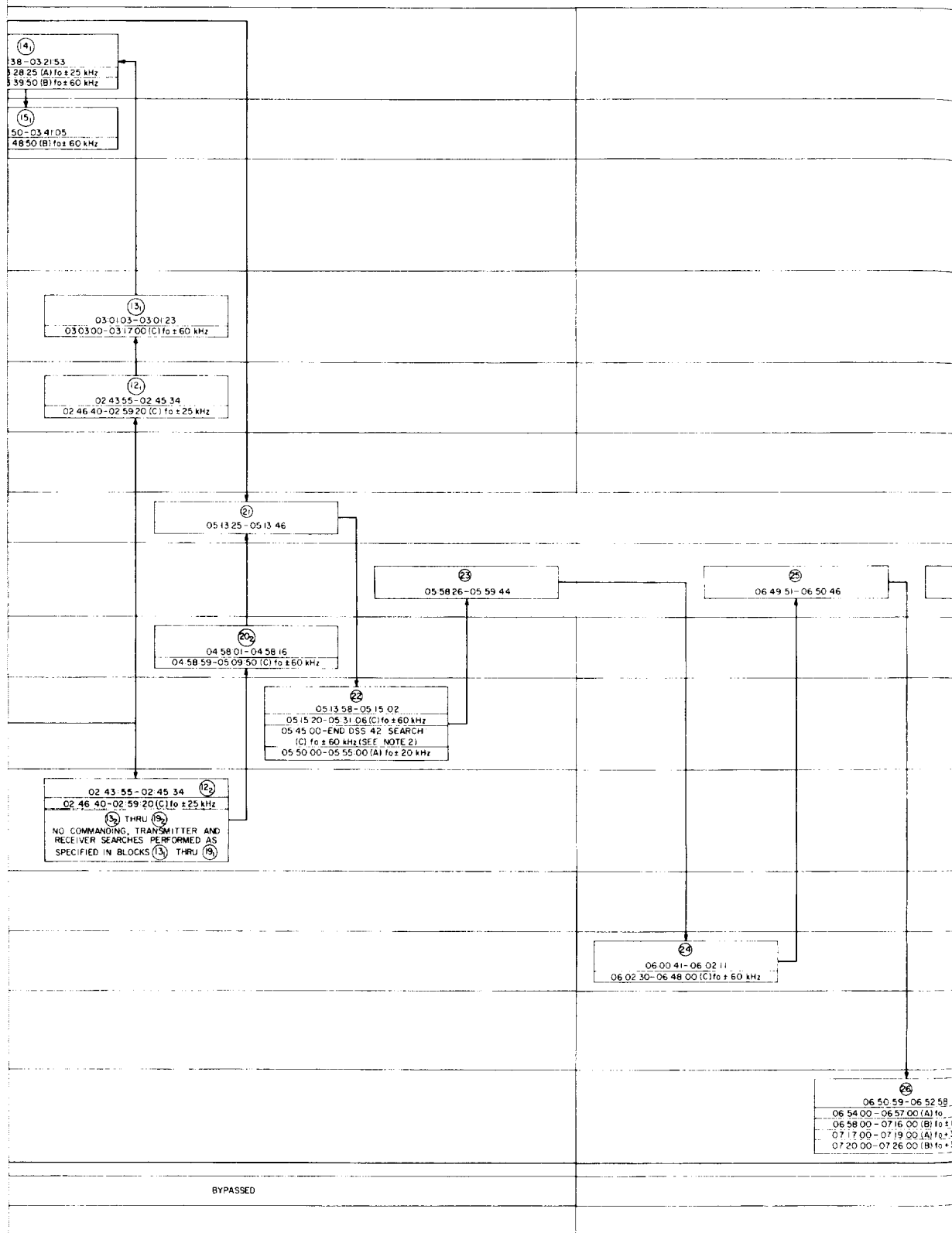
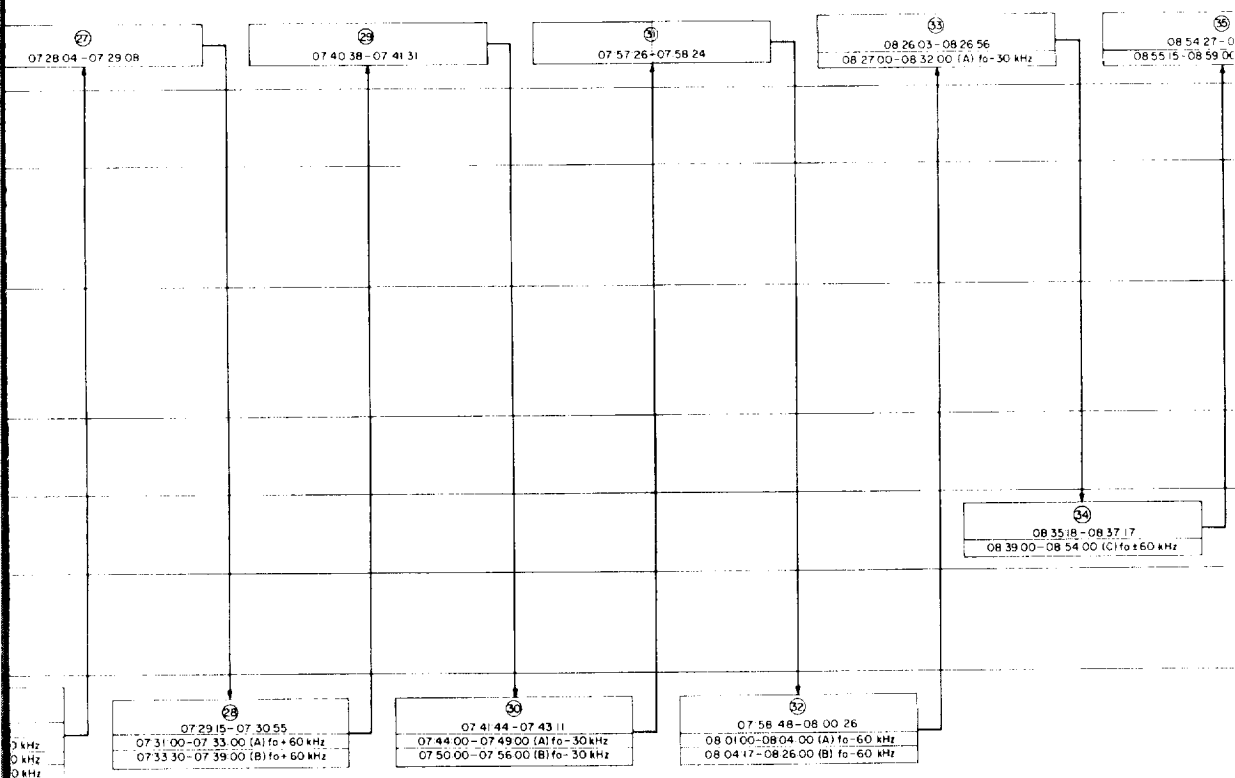


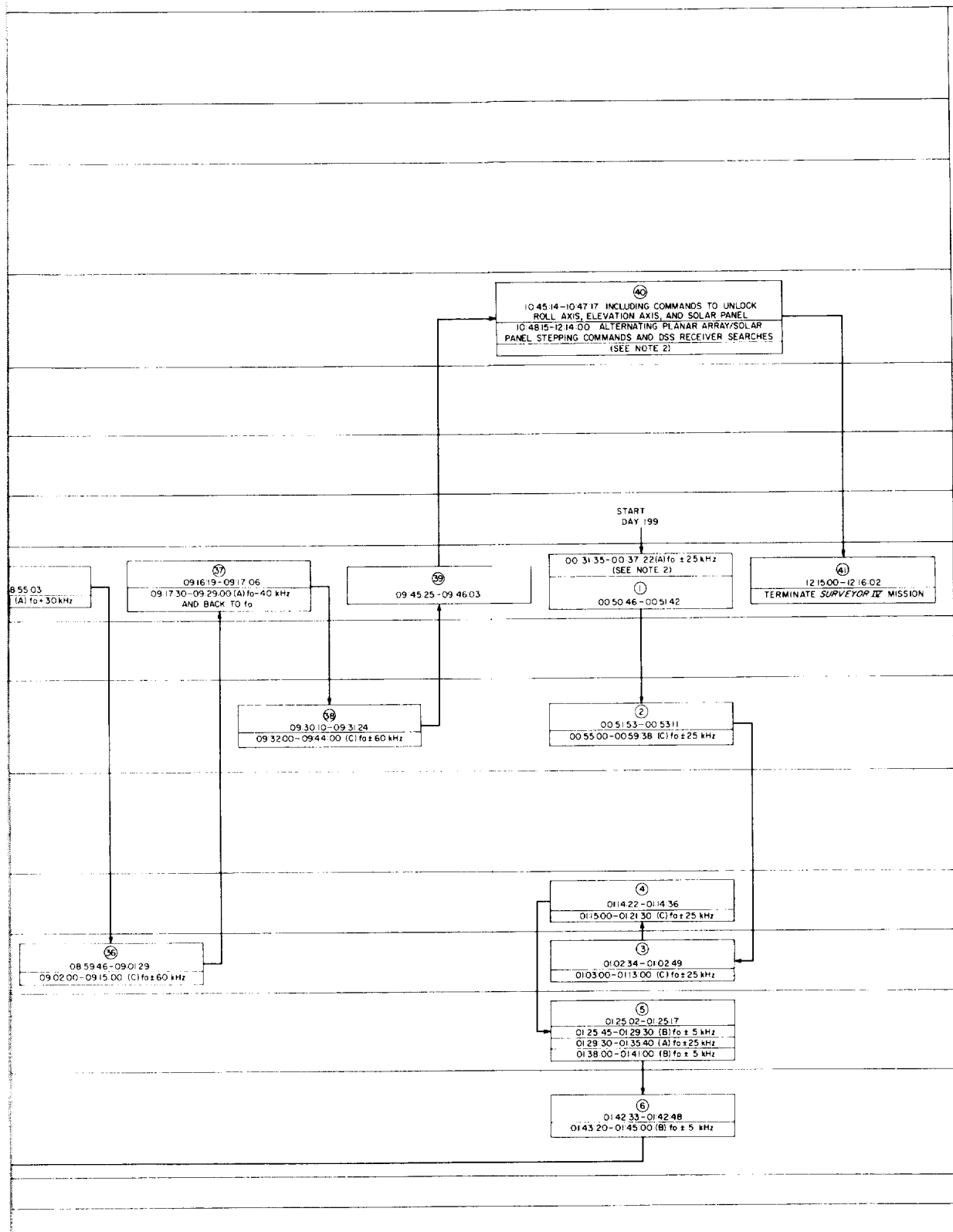
Fig. A-2. Operations conducted on July 18, 1967 (Day 199), in the attempt to reacquire Surveyor





ENABLE

LOW



NOTES

EACH NUMBERED BLOCK REPRESENTS A SPACECRAFT CONFIGURATION ATTEMPTED DURING THE COMMANDING PERIOD SHOWN IN THE BLOCK. EACH COMMAND OR COMMAND SEQUENCE WAS TRANSMITTED FOUR TIMES (ONCE ON EACH OF SURVEYOR'S FOUR POSSIBLE RECEIVER/DECODER COMBINATIONS). ALL TIMES GIVEN ARE IN GMT IN CHRONOLOGICAL ORDER FROM BLOCK (1) THRU BLOCK (4).

2. IN CONJUNCTION WITH COMMANDING PERIODS, DSS TRANSMITTER AND/OR RECEIVER SEARCHES WERE PERFORMED BY THE DSIF STATIONS. THE DURATION OF THESE SEARCHES AND THE FREQUENCIES AT WHICH THEY WERE PERFORMED ARE INCLUDED IN THE APPLICABLE BLOCKS. THE FOLLOWING STATIONS PARTICIPATED IN THE EXTENSIVE, BUT UNSUCCESSFUL ATTEMPT TO REACQUIRE SURVEYOR II ON JULY 18.

(1) THRU (22) 00:31:35 - 05:41:40
DSS 11 TRANSMITTING AND SEARCHING

(18) THRU (22) 04:29:00 - 05:45:00
DSS 42 SEARCHING (DOWNLINK) AT 2295 MHz \pm 60 kHz

(22) THRU (40) 05:50:00 - 12:14:00
DSS 42 TRANSMITTING AND SEARCHING

(41) 12:15:00 - 12:16:02
DSS 42 TRANSMITTING (12:17:00 TRANSMITTER OFF)

3. REFER TO TABLE A-1 FOR EVENTS PRECEDING AND IMMEDIATELY FOLLOWING LOSS OF SIGNAL, AND TO FIG A-1 FOR SPACECRAFT RECOVERY ATTEMPTS ON JULY 17 (DAY 198).

EXAMPLE:

(2)
00:51:53 - 00:53:11 } COMMANDING PERIOD, GMT
00:55:00 - 00:59:38 } DSS SEARCH PERIOD, GMT
(C) 10 \pm 25 kHz } DSS SEARCH FREQUENCY

LEGEND

(2) SPACECRAFT CONFIGURATION NUMBER

10 OPERATIONAL CENTER FREQUENCY (S-BAND)

NOMINAL 10'S ARE AS FOLLOWS

UP-LINK 10 = 2115 MHz (DSS TRANSMITTER/SPACECRAFT RECEIVER)

DOWN-LINK 10 = 2295 MHz (DSS RECEIVER/SPACECRAFT TRANSMITTER)

(A) UP-LINK SEARCH: DSS TRANSMITTER TUNED TO FREQUENCY SHOWN

(B) DOWN-LINK SEARCH (TRANSPONDER MODE): DSS RECEIVER SEARCH PERFORMED AT TRANSPONDER FREQUENCY CORRESPONDING TO FREQUENCY SHOWN

(C) DOWN-LINK SEARCH (NARROWBAND OR WIDEBAND VCXO MODE): DSS RECEIVER SEARCH PERFORMED AT FREQUENCY SHOWN

Table A-1. Mission flight events

Event	Mark No.	Mission time (predicted)	Mission time (actual)	GMT ^b (actual)
Liftoff to DSIF acquisition ^a				
			July 14, 1967 (Day 195)	
Liftoff (2-in. rise)		L + 00:00:00.00	L + 00:00:00.00	11:53:29.215
Initiate roll program			L + 00:00:02	11:53:31
Terminate roll, initiate pitch program			L + 00:00:15	11:53:44
Mach 1				
Maximum aerodynamic loading				
Atlas booster engine cutoff (BECO)	1	L + 00:02:23.66	L + 00:02:21.9	11:55:51.1
Jettison booster package	2	L + 00:02:26.76	L + 00:02:25.0	11:55:54.0
Admit guidance steering			L + 00:02:29.9	11:55:59.1
Jettison Centaur insulation panels	3	L + 00:02:57.66	L + 00:02:55.8	11:56:25.0
Jettison nose fairing	4	L + 00:03:24.66	L + 00:03:22.6	11:56:51.8
Start Centaur boost pumps		L + 00:03:25.66	L + 00:03:23.6	11:56:52.8
Atlas sustainer engine cutoff (SECO)	5	L + 00:03:57.73	L + 00:03:59.35	11:57:28.57
Atlas/Centaur separation	6	L + 00:03:59.63	L + 00:04:01.24	11:57:30.46
Prestart Centaur main engines (chilldown)		L + 00:04:01.23	L + 00:04:02.85	11:57:32.07
Centaur main engines start (MES)	7	L + 00:04:09.23	L + 00:04:10.8	11:57:40.0
Centaur main engines cutoff (MECO)	8	L + 00:11:20.99	L + 00:11:27.8	12:04:57.0
Extend Surveyor landing legs command	9	L + 00:11:53.2	L + 00:11:55	12:05:24
Extend Surveyor omniantennas command	10	L + 00:12:03.7	L + 00:12:05	12:05:34
Surveyor transmitter high power on command	11	L + 00:12:24.2	L + 00:12:26	12:05:55
Surveyor/Centaur electrical disconnect	12	L + 00:12:29.7	L + 00:12:31.35	12:06:00.57
Surveyor/Centaur separation	13	L + 00:12:35.2	L + 00:12:36.86	12:06:06.08
Start Surveyor solar panel stepping			L + 00:12:37.7	12:06:06.9
Start Centaur 180-deg turn	14	L + 00:12:40.2	L + 00:12:42.0	12:06:11.2
Start Centaur lateral thrust		L + 00:13:20.2	L + 00:13:21.9	12:06:51.1
Start Surveyor sun acquisition roll			L + 00:13:25.9	12:06:55.1
Cut off Centaur lateral thrust		L + 00:13:40.2	L + 00:13:41.9	12:07:11.1
Complete Centaur 180-deg turn			L + 00:14:30	12:07:59
Complete Surveyor roll; begin sun acquisition yaw turn			L + 00:15:23.9	12:08:53.1
Start Centaur tank blowdown (retro)	15	L + 00:16:35.2	L + 00:16:36.9	12:10:06.1
Surveyor primary sun sensor lockon			L + 00:16:52.7	12:10:21.9
Solar panel locked in transit position			L + 00:18:30.5	12:11:59.7
Start A/SPP roll axis stepping			L + 00:18:37.3	12:12:06.5
Cut off Centaur electrical power and end blowdown	16	L + 00:20:45.2	L + 00:20:46.9	12:14:16.1
Energize power changeover switch	17	L + 00:20:45.2	L + 00:20:46.9	12:14:16.1
A/SPP roll axis locked in transit position			L + 00:22:37.7	12:16:06.9
Initial DSIF acquisition in good two-way lock (for 40 sec) by DSS 72, followed by loss of up-link (one-way lock)			L + 00:22:54	12:16:23
Good two-way lock reestablished and initial DSIF acquisition completed			L + 00:28:17	12:21:46

Table A-1 (contd)

Event	Mission time (actual)	GMT ^b (actual)
Initial spacecraft operations to Canopus acquisition		
July 14, 1967 (Day 195) (contd)		
Initial spacecraft operations		
1. Command on 1100-bit/sec data rate	L + 00:36:29	12:29:58
2. Command Transmitter B from high to low power	L + 00:40:50	12:34:19
3. Command off basic bus accelerometer amplifiers, solar panel deployment logic, propulsion strain gage power, auxiliary accelerometer amplifiers, touchdown strain gage power, and Transmitter A high power	L + 00:44:45 to L + 00:45:02	12:38:14 to 12:38:31
4. Command step solar panel minus, then plus, to seat locking pin	L + 00:46:01 to L + 00:46:18	12:39:30 to 12:39:47
5. Command step roll axis plus, then minus, to seat locking pin	L + 00:47:04 to L + 00:47:19	12:40:33 to 12:40:48
6. Command on telemetry Modes 1, 4, 2, 6, and 5 for interrogation at 1100-bit/sec data rate	L + 00:48:04 to L + 00:58:18	12:41:33 to 12:51:47
Command on cruise mode	L + 03:29:18	15:22:47
Command on telemetry Modes 4, 2, 1, and 5 for interrogation at 1100-bit/sec data rate	L + 05:33:37 to L + 05:39:54	17:27:06 to 17:33:23
Star verification/acquisition		
1. Command Transmitter B from low to high power	L + 05:53:06	17:46:35
2. Command on 4400-bit/sec data rate	L + 05:54:30	17:47:59
3. Command on cruise mode and manual delay mode, then command roll direction (positive)	L + 05:56:35	17:50:04
4. Command execution of positive roll (light sources detected by Canopus sensor: eta Ursa Majoris, delta Velorum, gamma Cassiopeiae, Canopus, earth, moon)	L + 05:57:58	17:51:27
5. Command on star acquisition mode (after the moon passed field of view during second revolution)	L + 06:14:30	18:07:59
6. Automatic Canopus acquisition	L + 06:16:53	18:10:22
7. Command on cruise mode	L + 06:19:25	18:12:54
8. Command on 1100-bit/sec data rate	L + 06:20:20	18:13:49
9. Command Transmitter B from high to low power	L + 06:21:27	18:14:56
Pre-midcourse coast phase		
Command on inertial mode (start first gyro drift-check, all axes)	L + 06:52:32	18:46:01
Command on cruise mode (end first gyro drift check)	L + 09:00:45	20:54:14
Command on inertial mode (start second gyro drift check, all axes)	L + 09:04:14	20:57:43
Command on cruise mode (end second gyro drift check)	L + 10:43:55	22:37:24
Command on telemetry Modes 4, 2, and 5 for interrogation at 1100-bit/sec data rate	L + 12:05:40	23:59:09

Table A-1 (contd)

Event	Mission time (actual)	GMT ^b (actual)
Pre-midcourse coast phase (contd)		
	July 15, 1967 (Day 196)	
	to	to
Command on inertial mode (start third gyro drift check, all axes)	L + 12:14:23	00:07:52
Command on cruise mode (end third gyro drift check)	L + 12:15:56	00:09:25
Command on sun acquisition mode (start fourth gyro drift check, roll axis only)	L + 14:15:55	02:09:24
Command on telemetry Modes 4, 2, and 5 for interrogation at 1100-bit/sec data rate	L + 14:25:23	02:18:52
	L + 16:18:09	04:11:38
	to	to
Command on 550-bit/sec data rate	L + 16:24:48	04:18:17
Command on cruise mode (end fourth gyro drift check)	L + 19:59:18	07:52:47
Command on inertial mode (start fifth gyro drift check, all axes)	L + 20:01:27	07:54:56
Command on telemetry Modes 4, 2, and 5 for interrogation at 550-bit/sec data rate	L + 20:07:27	08:00:56
	L + 20:09:26	08:02:55
	to	to
Command on cruise mode (end fifth gyro drift check)	L + 20:14:54	08:08:23
Command on inertial mode (start sixth gyro drift check, all axes)	L + 22:04:58	09:58:27
Command on cruise mode (end sixth gyro drift check)	L + 22:26:43	10:20:12
Command on telemetry Modes 4, 2, and 5 for interrogation at 550-bit/sec data rate	L + 23:53:32	11:47:01
	L + 24:08:19	12:01:48
	to	to
Command on telemetry Modes 4, 2, and 5 for interrogation at 550-bit/sec data rate	L + 24:14:08	12:07:37
	L + 28:06:32	16:00:01
	to	to
Command on inertial mode (start seventh gyro drift check, all axes)	L + 28:13:53	16:07:22
Command on cruise mode (end seventh gyro drift check)	L + 28:15:04	16:08:33
Command on inertial mode (start eighth gyro drift check, all axes)	L + 29:45:04	17:38:33
Command on cruise mode (end eighth gyro drift check)	L + 30:09:48	18:03:17
Command on sun acquisition mode (start ninth gyro drift check, roll axis only)	L + 31:49:07	19:42:36
Command on cruise mode (end ninth gyro drift check)	L + 33:46:20	21:39:49
	L + 34:33:57	22:27:26
	July 16, 1967 (Day 197)	
Pre-midcourse interrogation and gyro speed check		
1. Command on telemetry Modes 4, 2, 1, and 5 for interrogation at 550-bit/sec data rate	L + 36:18:05	00:11:34
	to	to
	L + 36:24:06	00:17:35
2. Command on gyro speed signal processor and check angular rate of gyro spin in roll, pitch, and yaw axes; command off gyro speed signal processor and return to telemetry Mode 5	L + 36:24:57	00:18:26
	to	to
	L + 36:29:02	00:22:31

Table A-1 (contd)

Event	Mission time (actual)	GMT ^b (actual)
Midcourse maneuvers		
July 16, 1967 (Day 197) (contd)		
Command on telemetry Modes 4, 2, and 1 for interrogation at 550-bit/sec data rate	L + 37:53:59 to L + 37:58:00	01:47:28 to 01:51:29
Command Transmitter B from low to high power	L + 38:08:50	02:02:19
Command on 4400-bit/sec data rate	L + 38:09:49	02:03:18
Pre-midcourse attitude maneuvers		
1. Command on cruise mode, then command roll maneuver direction (positive) and store roll magnitude (145.0 sec)	L + 38:14:58	02:08:27
2. Command roll execution	L + 38:21:59.7	02:15:28.9
3. Roll maneuver completed (+72.45 deg)	L + 38:24:26.1	02:17:55.3*
4. Command on sun acquisition mode, then store yaw magnitude (128.6 sec)	L + 38:25:06	02:18:35
5. Command yaw execution	L + 38:27:40.7	02:21:09.9
6. Yaw maneuver completed (-64.32 deg)	L + 38:29:50.8	02:23:20.0*
Command on telemetry Modes 2 and 1 for interrogation at 4400-bit/sec	L + 38:30:32, L + 38:32:11	02:24:01, 02:25:40
Command on propulsion strain gage power and inertial mode	L + 38:32:41	02:26:10
Command off thermal control power to the surface sampler, to the AMR, and to vernier lines, Vernier Fuel Tank 2, and Vernier Oxidizer Tanks 2 and 3; then unlock Vernier Engine 1 roll actuator and pressurize the vernier system (helium)	L + 38:33:56	02:27:25
Command on flight control thrust phase power	L + 38:34:24	02:27:53
Midcourse correction		
1. Store magnitude of vernier engines burn time (10.463 sec, a velocity correction of 10.27 m/sec)	L + 38:34:48	02:28:17
2. Command execution of midcourse velocity correction	L + 38:36:33.1	02:30:02.3
3. Midcourse velocity correction completed	L + 38:36:44.8	02:30:14.0*
4. Command standard emergency terminate midcourse velocity correction	L + 38:36:45.5	02:30:14.7
Command off flight control thrust phase power, propulsion strain gage power, auxiliary accelerometer amplifiers, and touchdown strain gage power	L + 38:37:01 to L + 38:37:27	02:30:30 to 02:30:56
Command on telemetry Mode 5	L + 38:37:55	02:31:24
Command on vernier lines temperature control, AMR temperature control, and surface sampler heater power	L + 38:38:21	02:31:50
Post-midcourse attitude maneuvers		
1. Command reverse yaw maneuver direction (positive) and store yaw magnitude	L + 38:38:50	02:32:19
2. Command yaw execution	L + 38:39:24.2	02:32:53.4
3. Yaw maneuver completed (+64.32 deg) and sun reacquired	L + 38:41:34.3	02:35:03.5*
4. Command on sun acquisition mode, then store roll magnitude	L + 38:42:15	02:35:44
5. Command roll execution	L + 38:43:55.9	02:37:25.1
6. Roll maneuver completed (-72.45 deg) and Canopus reacquired	L + 38:46:22.3	02:39:51.5*
Command on cruise mode	L + 38:47:28	02:40:57
Command on telemetry Modes 2, 4, and 5 for interrogation at 4400-bit/sec data rate	L + 38:48:00 to L + 38:51:00	02:41:29 to 02:44:29
Command on 550-bit/sec data rate	L + 38:51:34	02:45:03
Command Transmitter B from high to low power	L + 38:52:41	02:46:10

Table A-1 (contd)

Event	Mission time (actual)	GMT ^h (actual)
Post-midcourse coast phase		
July 16, 1967 (Day 197) (contd)		
Command on inertial mode (start tenth gyro drift check, all axes)	L + 40:22:29	04:15:58
Command on cruise mode (end tenth gyro drift check)	L + 41:57:15	05:50:44
Command on telemetry Modes 4, 2, and 5 for interrogation at 550-bit/sec data rate	L + 43:17:17 to L + 43:24:58	07:10:46 to 07:18:27
Command on auxiliary battery mode, command on high current, then restore main battery mode (initial power mode cycling to determine load sharing of main and auxiliary batteries)	L + 44:04:48 to L + 44:17:08	07:58:17 to 08:10:37
Command on sun acquisition mode (start eleventh gyro drift check, roll axis only)	L + 44:57:30	08:50:59
Command on telemetry Modes 4, 2, and 5 for interrogation at 550-bit/sec data rate	L + 48:05:18 to L + 48:11:18	11:58:47 to 12:04:47
Command on auxiliary battery mode, command off high current, restore main battery mode, and command on high current (subsequent power mode cycling to determine battery load sharing and leave both batteries directly on line)	L + 49:09:03 to L + 49:27:35	13:02:32 to 13:21:04
Command on cruise mode (end eleventh gyro drift check)	L + 50:42:49	14:36:18
Command on Vernier Oxidizer Tank 2 thermal control power	L + 50:43:56	14:37:25
Command on telemetry Modes 4, 2, and 5 for interrogation at 550-bit/sec data rate	L + 51:22:51 to L + 51:29:22	15:16:20 to 15:22:51
Command on inertial mode (start twelfth gyro drift check, all axes)	L + 51:47:06	15:40:35
Command on cruise mode (end twelfth gyro drift check)	L + 53:37:02	17:30:31
Command on inertial mode (start thirteenth gyro drift check, all axes)	L + 53:46:13	17:39:42
Command on cruise mode (end thirteenth gyro drift check)	L + 55:19:28	19:12:57
Command on telemetry Modes 4, 2, and 5 for interrogation at 550-bit/sec data rate	L + 55:30:46 to L + 55:48:06	19:24:15 to 19:41:35
Command on auxiliary battery mode, command off high current, restore main battery mode, and command on high current (subsequent power mode cycling)	L + 56:20:26 to L + 56:48:58	20:13:55 to 20:42:27
Command on survey camera electronics temperature control	L + 57:15:20	21:08:49
Command on telemetry Modes 4 and 5 for interrogation at 550-bit/sec data rate	L + 57:42:21, L + 57:45:18	21:35:50, 21:38:47
Command on telemetry Modes 4, 2, and 5 for interrogation at 550-bit/sec data rate	L + 58:44:33 to L + 58:49:20	22:38:02 to 22:42:49
Preterminal interrogation, gyro speed check, and VCXO check		
1. Command on telemetry Modes 4, 2, 1, and 5 for interrogation at 550-bit/sec data rate	L + 59:52:16 to L + 60:00:21	23:45:45 to 23:53:50
2. Command on gyro speed signal processor and check angular rate of gyro spin in roll, pitch, and yaw axes; command off gyro speed signal processor and return to telemetry Mode 5	L + 60:01:21 to L + 60:04:34	23:54:50 to 23:58:03
July 17, 1967 (Day 198)		
3. Command off transponder power to perform VCXO check, then command Transponder B power back on	L + 60:07:28, L + 60:09:02	00:00:57, 00:02:31

Table A-1 (contd)

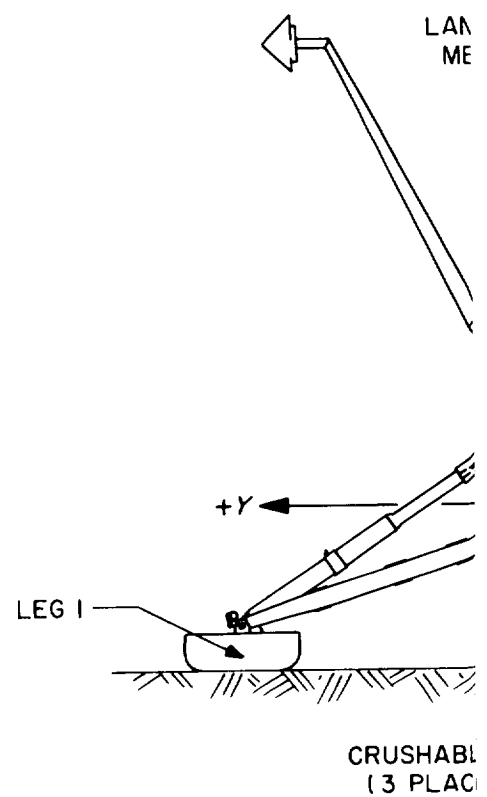
Event	Mission time (actual)	GMT ^b (actual)
Terminal maneuvers		
July 17, 1967 (Day 198) (contd)		
Command on telemetry Modes 6 and 4 for interrogation at 550-bit/sec data rate	L + 61:06:00, L + 61:11:22	00:59:29, 01:04:51
Command on survey camera vidicon temperature control	L + 61:12:45	01:06:14
Command Transmitter B from low to high power	L + 61:15:58	01:09:27
Command on 1100-bit/sec data rate	L + 61:16:27	01:09:56
Command off summing amplifiers and command on Phase Summing Amplifier B	L + 61:17:08	01:10:37
Command on telemetry Modes 2 and 5 for interrogation at 1100-bit/sec data rate	L + 61:18:09, L + 61:19:42	01:11:38, 01:13:11
Command on propulsion strain gage power, touchdown strain gage power, and touchdown strain gage data channels	L + 61:22:04	01:15:33
Command off transponder power (one-way lock)	L + 61:23:40	01:17:09
Terminal maneuvers		
1. Command on cruise mode, then command roll maneuver direction (positive) and store roll magnitude (161.71 sec)	L + 61:25:56	01:19:25
2. Command roll execution	L + 61:31:15.0	01:24:44.2
3. Roll maneuver completed (+80.85 deg)	L + 61:33:58.1	01:27:27.3*
4. Store yaw magnitude (185.36 sec)	L + 61:34:24	01:27:53
5. Command yaw execution	L + 61:36:05.0	01:29:34.2
6. Yaw maneuver completed (+92.68 deg) and retro thrust direction properly aligned	L + 61:39:11.5	01:32:40.7*
7. Command on inertial mode (positive maneuver off), then store roll magnitude (50.47 sec)	L + 61:39:40	01:33:09
8. Command roll execution	L + 61:41:35.4	01:35:04.6
9. Roll maneuver completed (-25.24 deg)	L + 61:42:27.2	01:35:56.4*

Table A-1 (contd)

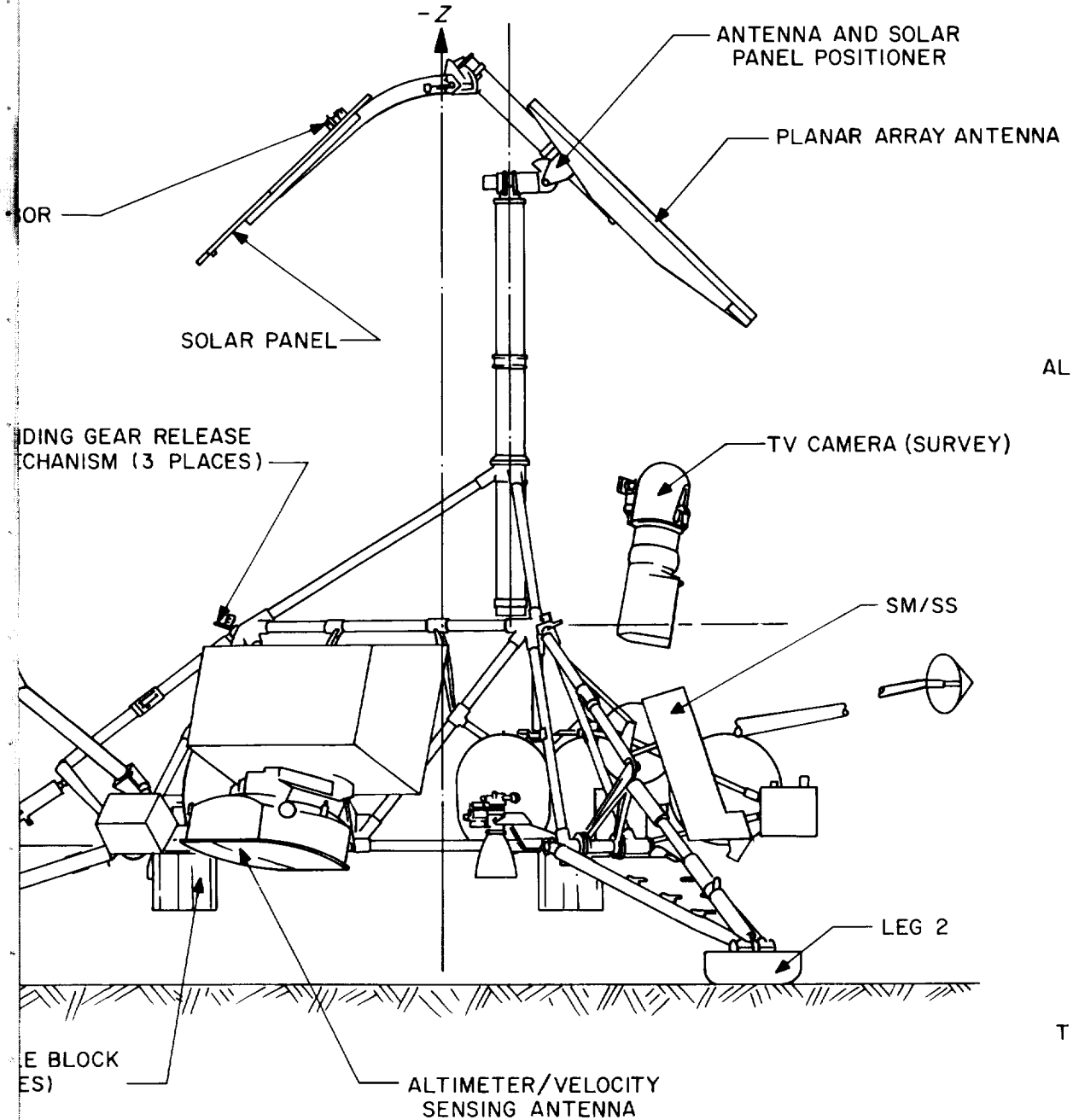
Event	GMT (predicted)	Mission time (actual)	GMT ^b (actual)
Terminal descent to predicted touchdown ^c			
		July 17, 1967 (Day 198) (contd)	
Command reset nominal thrust bias to increase vernier thrust to 200 lb		L + 61:47:20	01:40:49
Store retro sequence delay magnitude (2.725 sec between AMR mark and vernier engine ignition)		L + 61:48:24	01:41:53
Command on telemetry Mode 6 (thrust phase commutator)		L + 61:50:13	01:43:42
Command on retro sequence mode		L + 62:02:52	01:56:21
Command off thermal control power to vernier lines, Vernier Fuel Tank 2, and Vernier Oxidizer Tanks 2 and 3; to the surface sampler, survey camera vidicon, and survey camera electronics; and to the AMR		L + 62:03:12	01:56:41
Command on AMR power		L + 62:03:46	01:57:15
Command on thrust phase power		L + 62:04:46	01:58:15
Command AMR enable		L + 62:06:45.5	02:00:14.7
AMR mark at 60-mile altitude and start of delay quantity countdown	02:01:53.992	L + 62:08:25.569	*02:01:54.784
Command standard emergency AMR signal (3 times)	02:01:55.26	L + 62:08:26.070	*02:01:55.285
Vernier engine ignition	02:01:56.723	L + 62:08:28.278	*02:01:57.493
Main retro motor ignition and AMR ejection	02:01:57.823	L + 62:08:29.387	*02:01:58.602
RADVS power on	02:01:58.373	L + 62:08:30.249	*02:01:59.464
Reliable operation-doppler velocity sensor (RODVS) signal (following acquisition of lunar surface by Doppler Velocity Sensor Beam 3)		L + 62:09:00.952	*02:02:030.167
Loss of spacecraft carrier signal and loss of data			
1. At spacecraft: Surveyor IV stopped transmitting at main retro motor ignition + 00:00:41.09		L + 62:09:10.481	*02:02:39.696
2. At Goldstone: DSS 11 and DSS 14 simultaneously lost contact with the spacecraft		L + 62:09:11.703	02:02:40.918
(Since spacecraft transmission had ceased, it is unknown whether or not any of the following automatic and commanded events were actually performed by Surveyor IV): ^d			
Main retro burnout and increase in vernier thrust output	02:02:39.8		
Main retro case eject	02:02:51.8		
Command on presuming amplifier			02:03:27
Command emergency start programmed thrust			02:03:40
Command off presuming amplifiers to increase chance of carrier detection			02:04:46
10-ft/sec mark	02:05:04.1		
14-ft mark	02:05:09.6		
Touchdown	02:05:11.3		
^a The predicted values for this phase were computed postflight utilizing actual launch azimuth, tanked propellant weights, and atmospheric data which depend on day and time of liftoff. ^b An asterisk (*) in this column denotes time at spacecraft. ^c The predicted values for this phase are based upon the final post-midcourse computer run of the Terminal Guidance Program completed approximately 3 hr before retro ignition. ^d Refer to Figs. A-1 and A-2 for configurations attempted for spacecraft recovery from loss of signal to termination of mission on July 18.			

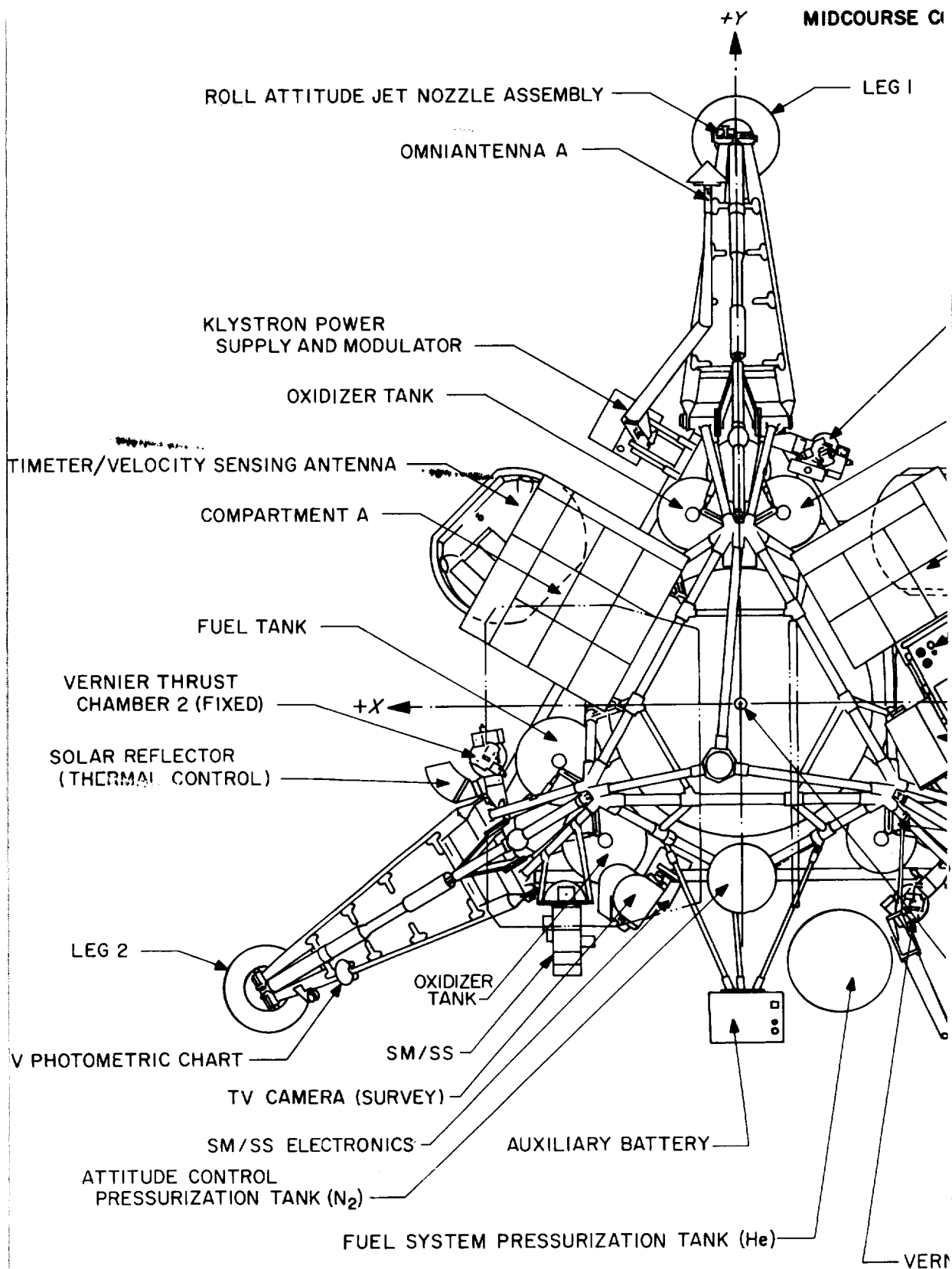
Appendix B
***Surveyor IV* Spacecraft Configuration**

SECONDARY SOLAR SENS



POSTLANDING CONFIGURATION





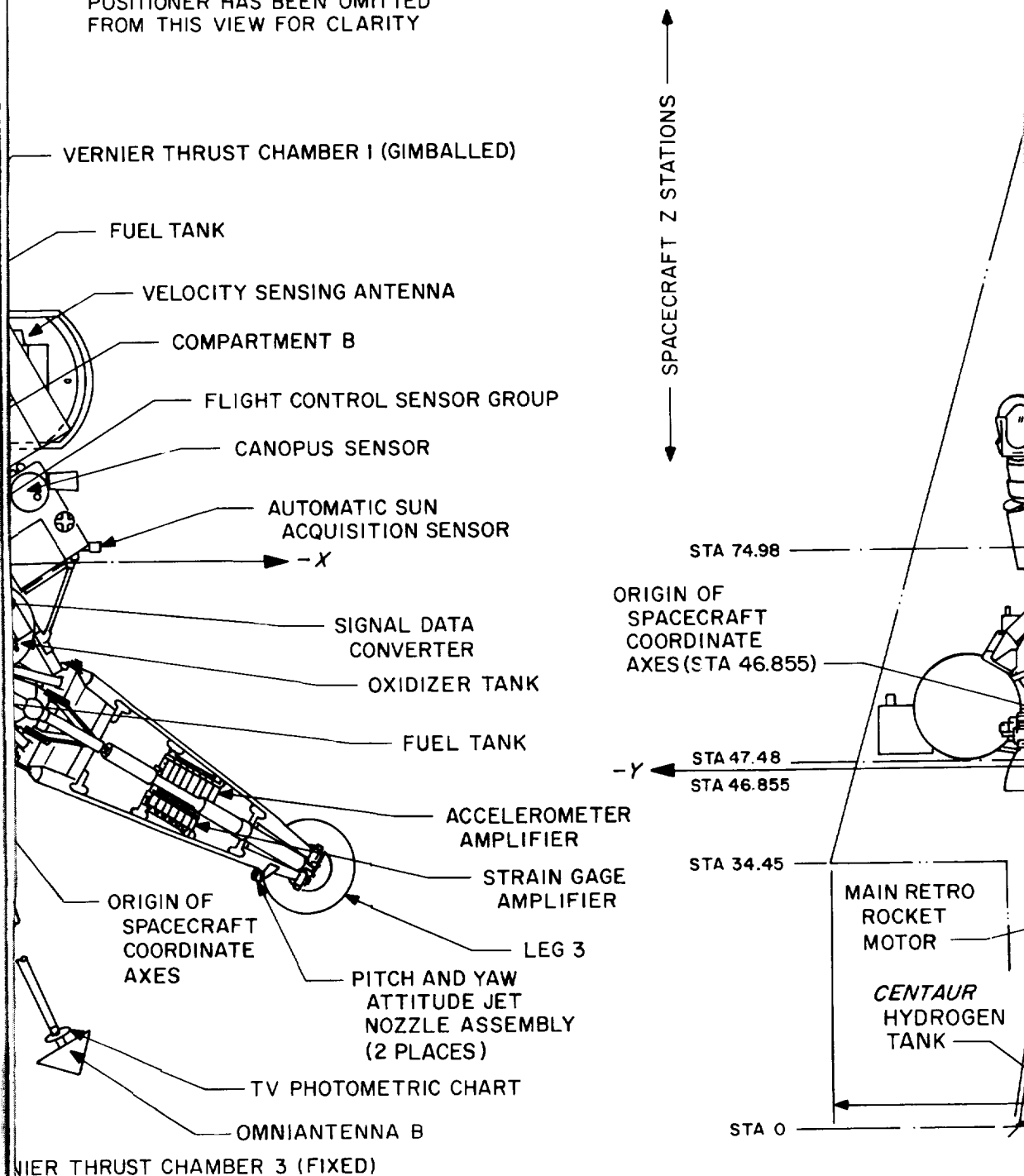
149-B

CONFIGURATION

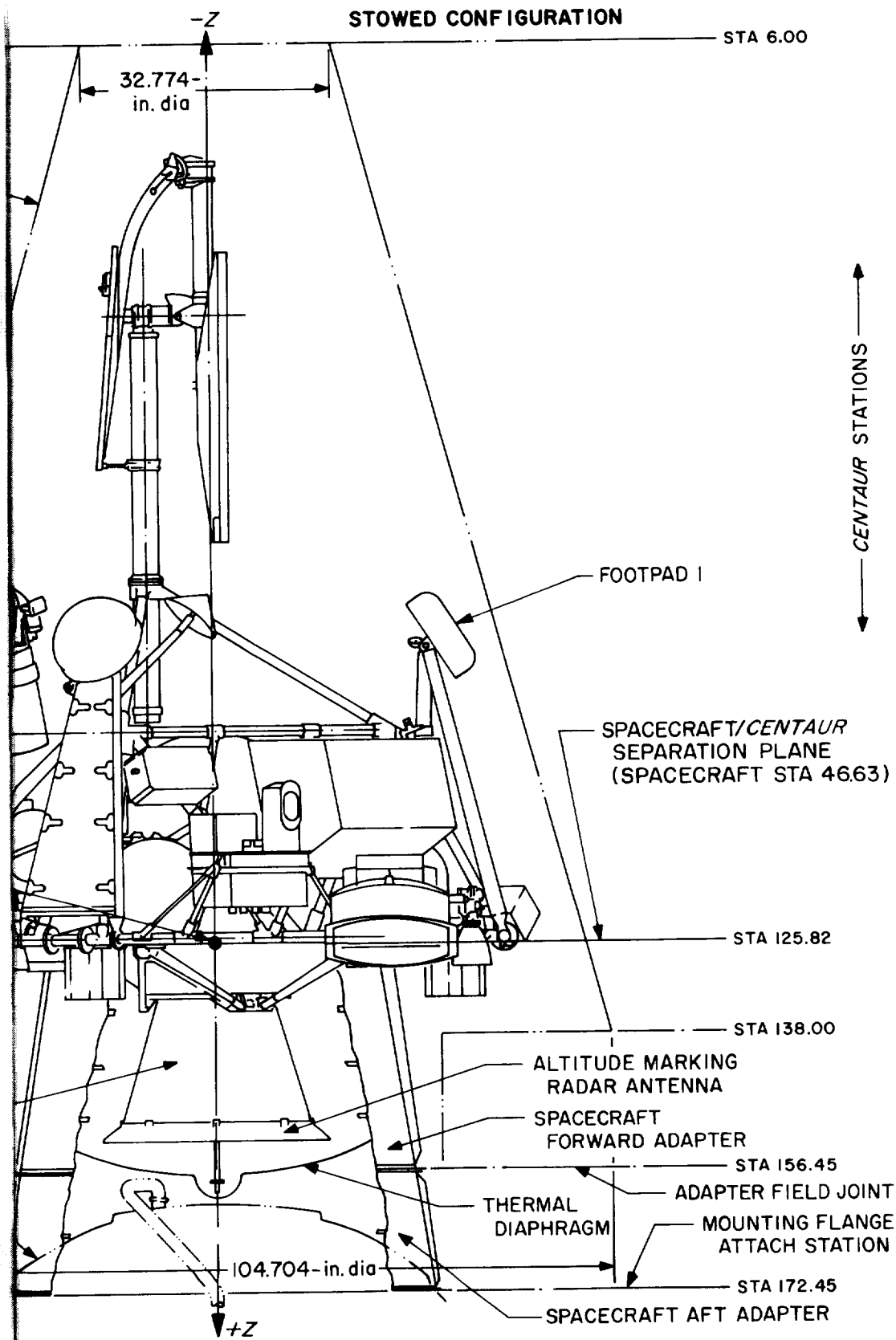
STA 166.45

NOTE:
ANTENNA AND SOLAR PANEL
POSITIONER HAS BEEN OMITTED
FROM THIS VIEW FOR CLARITY

SPACECRAFT
MAXIMUM
STATIC ENVELOPE



149-C



Appendix C
Surveyor IV Spacecraft Data Content of Telemetry Modes

RADIO AND COMMAND DECODING (DATA LINK)

CHAN	NAME	MODE 1 WORDS	MODE 2 WORDS	MODE 3 WORDS	MODE 4 WORDS	MODE C (5) WORDS	MODE T (6) WORDS
D-1	OWNI B TRANSMITTER POWER						
D-3	STATIC PHASE ERROR A				3,21,43,63,83	87	
D-6	RECEIVER B AGC				3,23,53,73,93	17	
D-10	TRANSMITTER A TEMPERATURE				5,25,45,65,85	27	
D-14	TRANSMITTER B TEMPERATURE				15,35,55,75,95	31	
D-17	RECEIVER B AGC				7, 2, 30, 30	6	30
					7, 2, 30, 30	30	41
ELECTRICAL POWER							
EP-1	29V NON-ESSENTIAL VOLTAGE						
EP-2	UNREGULATED BUS VOLTAGE	66	81		27	11	69
EP-3	MAIN BATT MANICOLD PRESS.				6	65	6
EP-5	MAIN BATTERY VOLTAGE	22	27		27	63	7
EP-6	BATTERY CHARGE CURRENT				27	75	75
EP-7	BOOST REG. DIFFERENCE CURRENT				49	45	
EP-8	BATTERY DISCHARGE CURRENT				69	45	
EP-9	SOLAR CELL ARRAY VOLTAGE				7	42	42
EP-10	SOLAR CELL ARRAY CURRENT				2	67	29
EP-11	BOOST REGULATOR TEMPERATURE				2	67	
EP-13	REGULATED OUTPUT CURRENT				35	23	
EP-16	RADIAND SQUB CURRENT				6	36	28
EP-17	ORT CHARGE REG OUTPUT CURR.				42	30	
EP-18	MID-SCALE CURR. CALIB. (LSP)				79	33	
EP-19	MID-SCALE CURR. CALIB. (LSP)				85	49	49
EP-20	ZERO SCALE CURR. CALIB. (LSP)				85	49	
EP-21	COMPARTMENT A WATER CURRENT				15	5	
EP-23	AUXILIARY BATTERY VOLTAGE				9		
EP-24	SOLAR CELL STRING 4 CURRENT				29		81
EP-25	SOLAR CELL STRING 6 CURRENT				37		
EP-27	AUXILIARY BATTERY TEMP. (ALSP)					81	
EP-28	MID-SCALE CURR. CALIB. (ALSP)				78	96	
EP-29	ZERO SCALE CURR. CALIB. (ALSP)					73	
EP-30	BOOST REG. REF. VOLTAGE	64	7			95	
EP-31	FLIGHT CONTROL UNREGULATED CURRENT	32	32			73	46
					78	46	19
FLIGHT CONTROL							
FC-4	NITROGEN GAS PRESSURE	35					
FC-5	PRIM. SUN SENSOR PITCH ERROR	1,7,9,4,6,8,11				7	
FC-6	SECONDARY SUN SENSOR PITCH ERROR	4,21,43,63,83				77	
FC-7	SECONDARY SUN SENSOR CELL A	20,70	35			77	
FC-9	SECONDARY SUN SENSOR CELL B	18,78	47			125	
FC-10	SECONDARY SUN SENSOR CELL C	38,86	55			107	
FC-12	CANOPUS ERROR SUN SENSOR CELL D	7,27,47,67				139	
FC-14	STAR INTENSITY SIGNAL	6,26,46,66,86				152	
FC-15	ACCELERATION ERROR	1,5,9,13,17,21	11				6,36,56,96
FC-16	PITCH GYRO ERROR	1,5,9,13,17,21,25	13,23			1	3,33,63,93
FC-19	THRUST CMD TO VERNIER ENG 1	1,5,9,13,17,21,25	17,27			3	3,33,63,93
FC-23	THRUST CMD TO VERNIER ENG 2	1,5,9,13,17,21,25	1,5			8	8,38,58,98
FC-27	THRUST CMD TO VERNIER ENG 3	1,5,9,13,17,21,25	2,8			16	16,46,76,106
FC-29	RADAR ALTITUDE RANGE SIGNAL	1,5,9,13,17,21,25	24			17,47,77,107	
FC-35	DOPPLER VELOCITY V _r	31,63	34			19,49,79,109	
FC-36	DOPPLER VELOCITY V _t	41,57	38			25,35,65,115	
FC-40	ROLL ACCELERATION SIGNAL	48,58				27,57,87,117	
FC-43	FLIGHT CONTROL E U TEMP 1	24				18	
FC-45	FLIGHT CONTROL E U TEMP 2	44				68	
FC-46	NITROGEN GAS TANK TEMP	4,34,54,74,94	13			82	3,33,63,93
FC-49	ROLL PRECISION COMMAND					48	
FC-50	PITCH PRECISION COMMAND					58	
FC-53	SEC. SUN SENSOR CENTER CELL					89	89
FC-54	PITCH GYRO TEMPERATURE					110	
FC-55	YAW GYRO TEMPERATURE					110	
FC-71	ROLL GYRO TEMPERATURE					124	
FC-77	FLT. CONTR. REFERENCE RETURN					124	
							99
MECHANISMS							
M-3	SOLAR PANEL POSITION						
M-4	POLAR AXIS POSITION						
M-6	ELEVATION AXIS POSITION						
M-8	ROLL AXIS POSITION						
M-9	SOLAR PANEL STEP. MOTOR TEMP.						
M-10	ELEV. AXIS STEP. MOTOR TEMP.						
CHAN	NAME	MODE 1 WORDS	MODE 2 WORDS	MODE 3 WORDS	MODE 4 WORDS	MODE C (5) WORDS	MODE T (6) WORDS

PROPULSION

CHAN	NAME	MODE 1 WORDS	MODE 2 WORDS	MODE 3 WORDS	MODE 4 WORDS	MODE C (5) WORDS	MODE T (6) WORDS
P-1	HELIUM PRESSURE	84	25			21	21
P-3	UPPER STRO CASI TEMPERATURE	66	41			51	51
P-4	VERNIER LINES 2 TEMPERATURE	2	66			86	86
P-5	VERNIER FUEL TANK 1 TEMP.						
P-7	VERNIER ENGINE 1 TEMPERATURE	26	74			36	36
P-8	VERNIER LINES 3 TEMPERATURE	52				90	90
P-9	VERNIER LINES 3 TEMPERATURE	82				100	100
P-10	VERNIER ENGINE 2 TEMPERATURE	80				50	50
P-11	VERNIER ENGINE 2 TEMPERATURE	46				86	86
P-12	LOWER RETRO CASE TEMPERATURE					4	
P-13	VERNIER FUEL TANK 1 TEMP.					56	56
P-14	VERNIER FUEL TANK 3 TEMP.					76	76
P-15	VERNIER FUEL TANK 2 TEMP.					82	82
P-16	VERNIER OXIDIZER TANK 2 TEMP.					84	
P-17	HELIUM TANK TEMP.				20	92	
P-18	VERNIER ENGINE 1 STRAIN GAGE					86	
P-20	VERNIER ENGINE 3 STRAIN GAGE	15,35,55,75,95					7,37,57,97
P-22	VERNIER ENGINE 3 STRAIN GAGE	6,36,56,76,96					11,41,71,101
P-23	RETRO NOZZLE TEMPERATURE	90					76,86
RADAR							
R-2	RADVS-P AMPLITUDE						4, 84
R-3	RADVS-D AMPLITUDE						14, 94
R-4	RADVS-D2 AMPLITUDE						34, 94
R-5	RADVS-D3 AMPLITUDE						
R-6	AMW ELECTRONICS TEMPERATURE						10
R-7	RADVS KLY. UNIT TEMP.						76
R-8	RADVS SIG. DATA CONVERT TEMP.						72
R-9	ADOPAR RADAR SENSOR TEMP.						94
R-10	ADOPAR RADAR SENSOR TEMP. (ALT)						76
R-11	ALTITUDE MARKING RADAR AGC						74
R-13	ALTITUDE MARKING RADAR AGC						84
R-27	AMW ANTENNA TEMPERATURE NO. 2						38
R-28	AMW LATE GATE SIGNAL						21
SIGNAL PROCESSING							
S-1	REFERENCE VOLTAGE						
S-2	COMPARATOR UNBAL. CURR. (LSP)						
S-3	COMPARATOR UNBAL. CURR. (LSP)						
S-5	COMPARATOR UNBAL. CURR. (ALSP)						
S-7	COMPARATOR UNBAL. CURR. (ALSP)						
TELEVISION							
TV-18	SURV. CAM. 3 ELECTRONICS TEMP						
TV-19	SURV. CAM. 3 MIRROR ASSY. TEMP.						
SURFACE SAMPLER EXPERIMENT							
SS-1	MOTOR CURRENT						
SS-12	AUX. ELECTRONICS TEMPERATURE						
STRUCTURES (VEHICLE)							
V-8	LANDING GEAR 2 DEFLECTION						
V-7	LANDING GEAR 3 DEFLECTION						
V-15	COMP. A TEMP. THERMAL RAY TOP						
V-16	COMP. A TEMP. LOWER SUPPORT						
V-17	COMP. A TEMP. LOWER TAILER						
V-18	COMP. A TEMP. CANISTER						
V-20	COMP. A TEMP. SW. 3 IN FAC. RAD.						
V-21	COMP. A TEMP. SW. 3 IN FAC. RAD.						
V-22	COMP. B TEMP. CANISTER						
V-23	COMP. B TEMP. LOWER SUPPORT						
V-24	COMP. B TEMP. SW. 3 IN FAC. RAD.						
V-25	COMP. B TEMP. SW. 3 IN FAC. RAD.						
V-26	UPPER SPACEFRAME TEMP. NO. 1						
V-27	UPPER SPACEFRAME TEMP. NO. 2						
V-28	SPACEFRAME TEMP. UNDER COMP. A						
V-29	SPACEFRAME TEMP. UNDER COMP. A						
V-30	LEG 2 UPPER WEB TEMP.						
V-31	SHOCK ABSORB 2 TEMPERATURE						
V-32	SHOCK ABSORB 3 TEMPERATURE						
V-33	UPPER SPACEFRAME TEMP. NO. 3						
V-34	SPACEFRAME TEMP. UNDER COMP. 3						
V-35	REFUG ATTACH POINT 1 TEMP.						
V-36	REFUG ATTACH POINT 2 TEMP.						
V-37	REFUG ATTACH POINT 3 TEMP.						
V-38	CELL SHIELD BLOCK TEMP.						
V-39	COMP. B TEMP. SW. 3 IN FAC. RAD.						
V-40	COMP. B TEMP. SW. 3 IN FAC. RAD.						
V-41	COMP. A TEMP. SW. 3 IN FAC. RAD.						
V-42	COMP. A TEMP. SW. 3 IN FAC. RAD.						

* BRACKETED SCO'S TURNED ON BY A SINGLE COMMAND

Appendix D
***Surveyor IV* Spacecraft Temperature Histories**

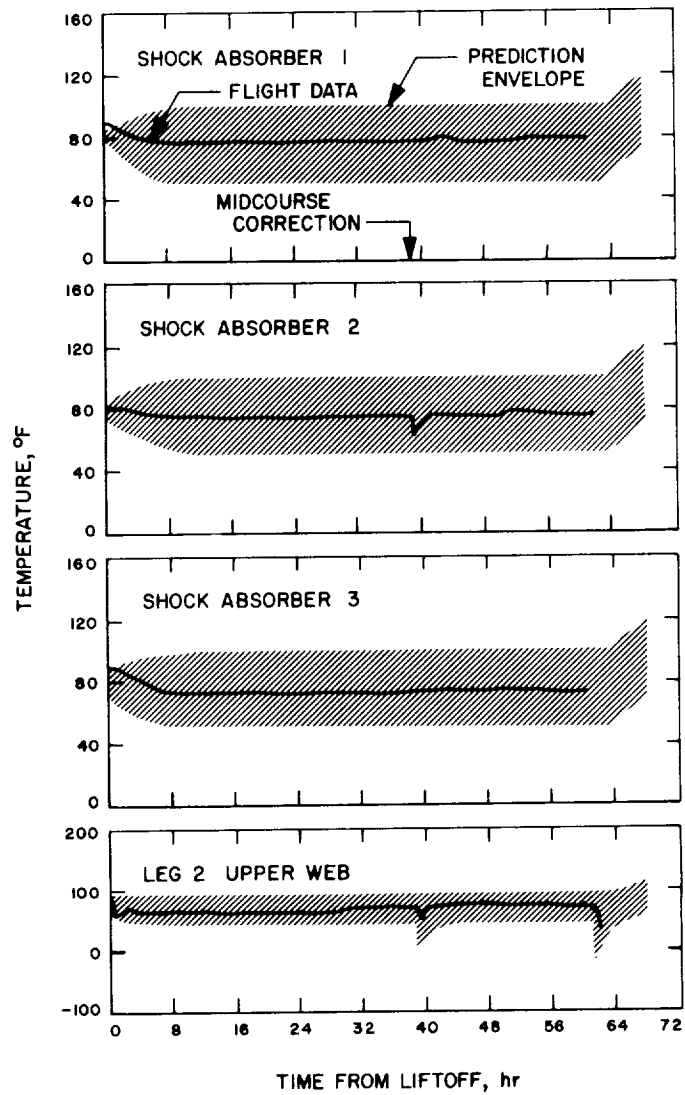


Fig. D-1. Landing gear temperatures

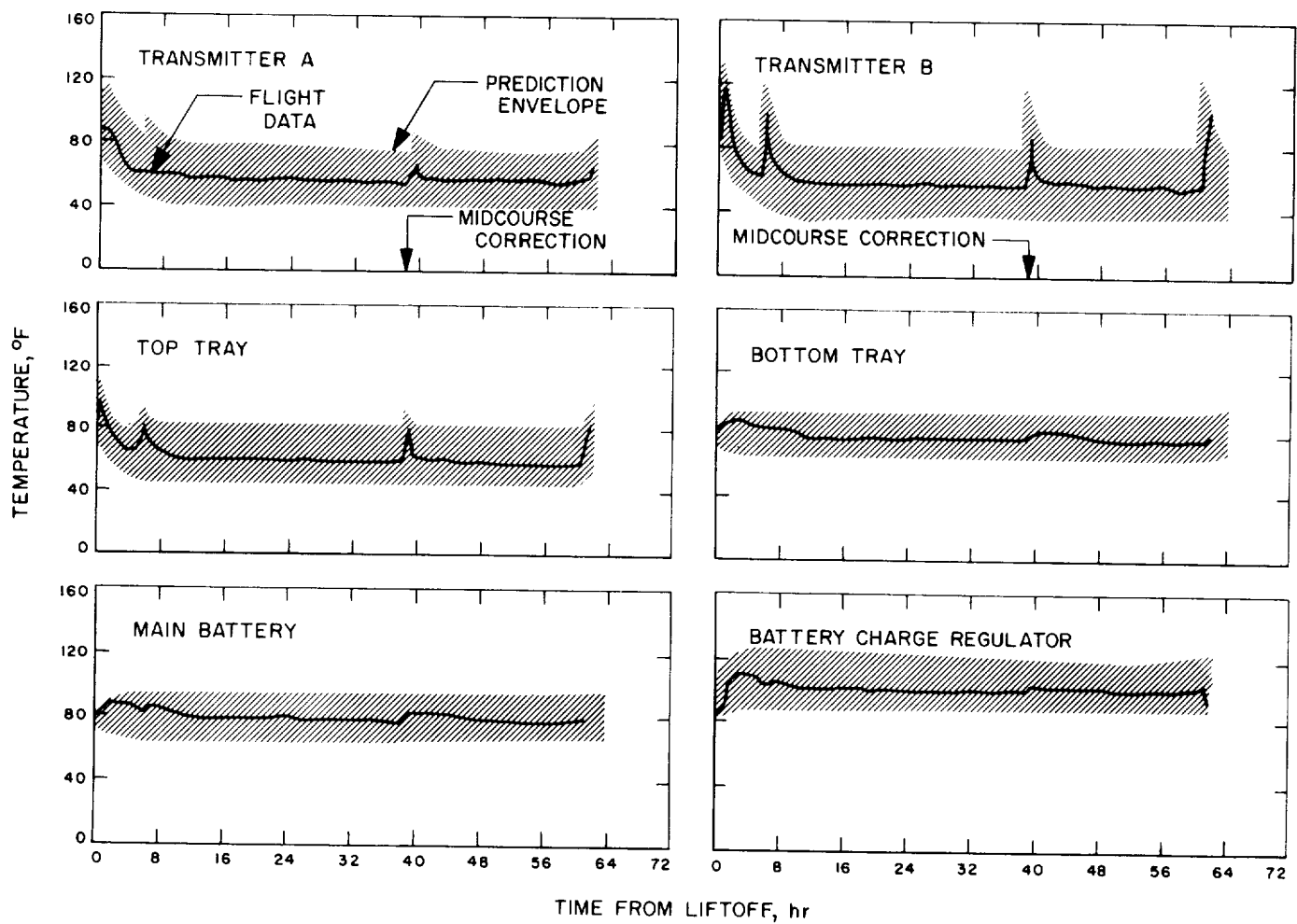


Fig. D-2. Compartment A temperatures

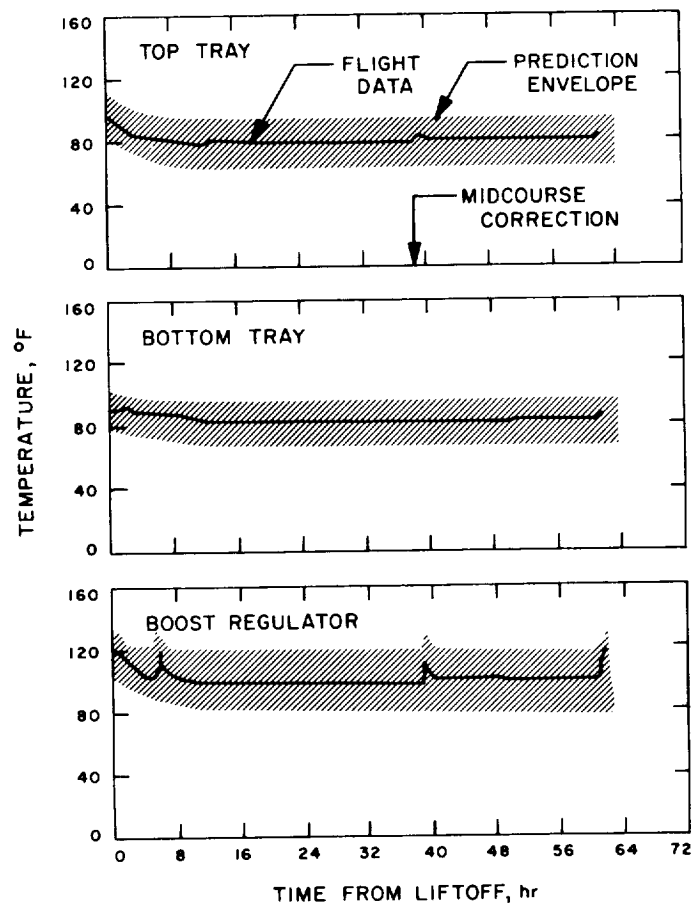


Fig. D-3. Compartment B temperatures

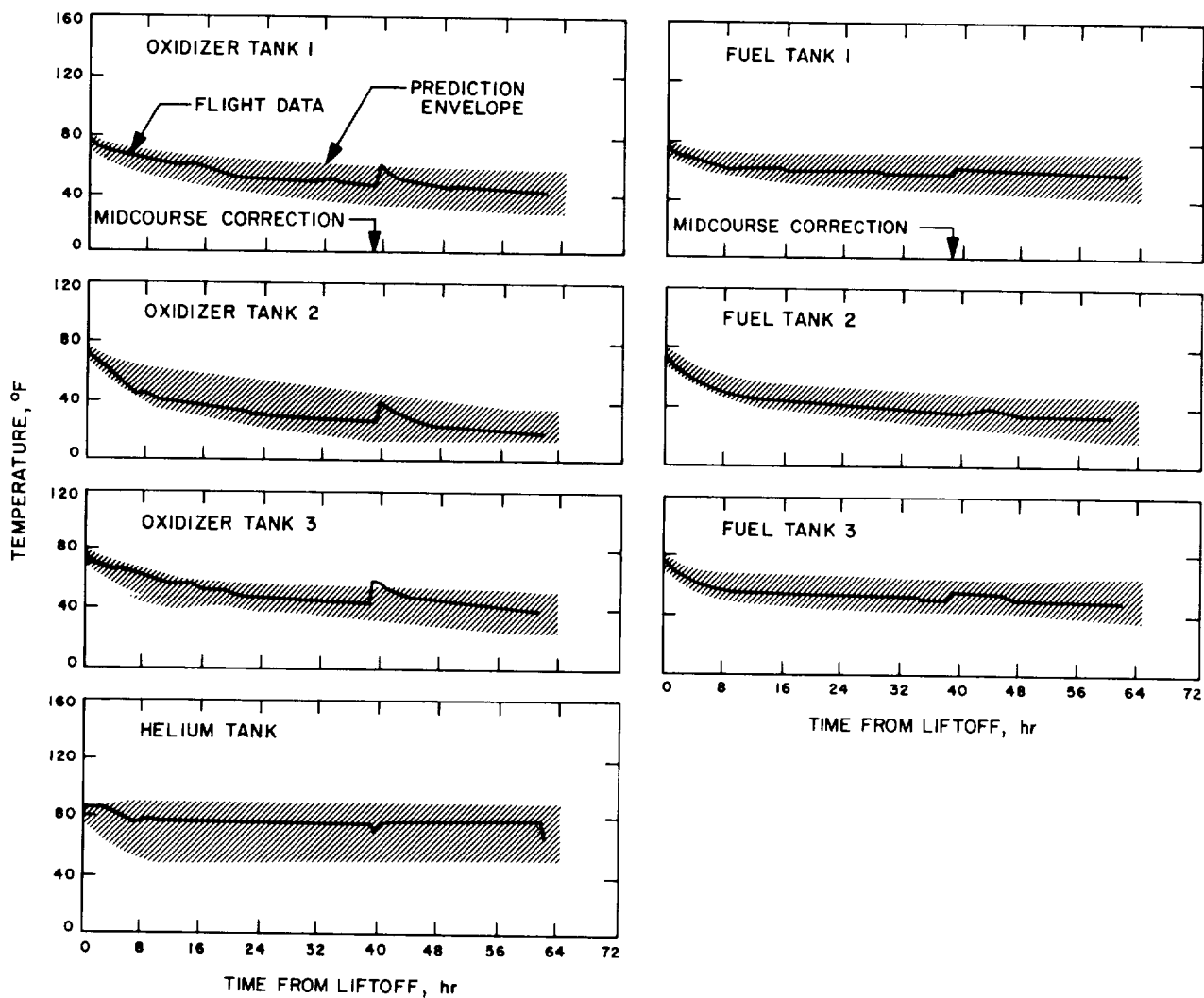


Fig. D-4. Vernier propulsion system temperatures

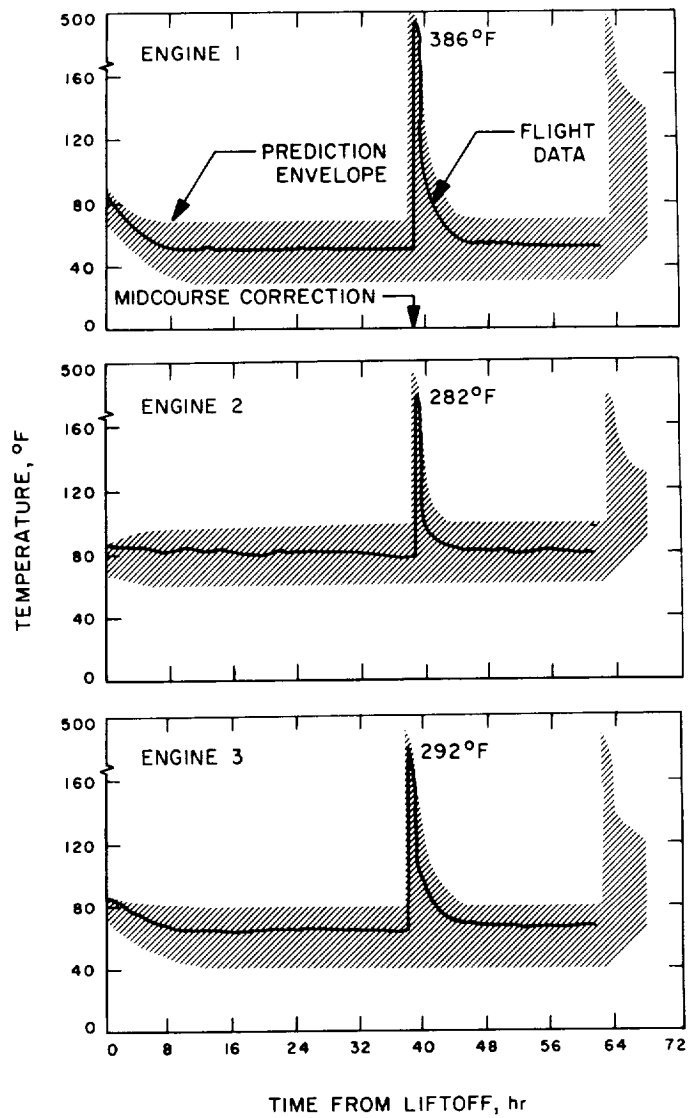


Fig. D-4 (cont)

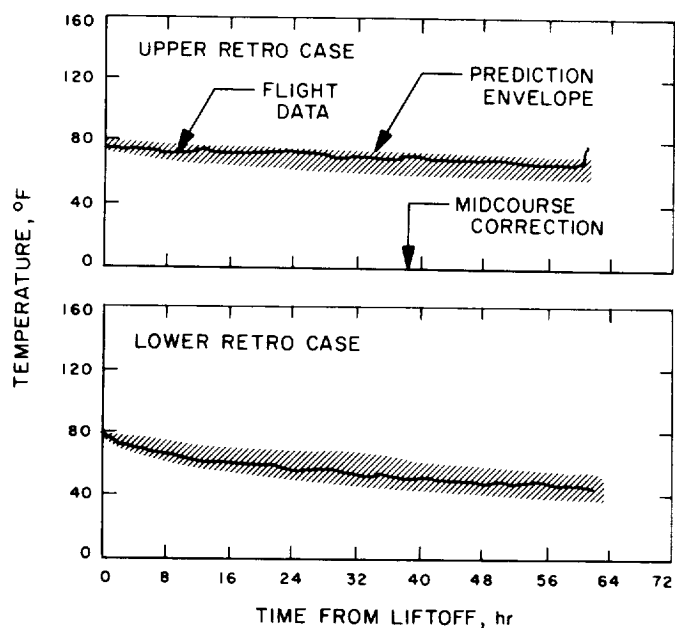


Fig. D-5. Main retromotor temperatures

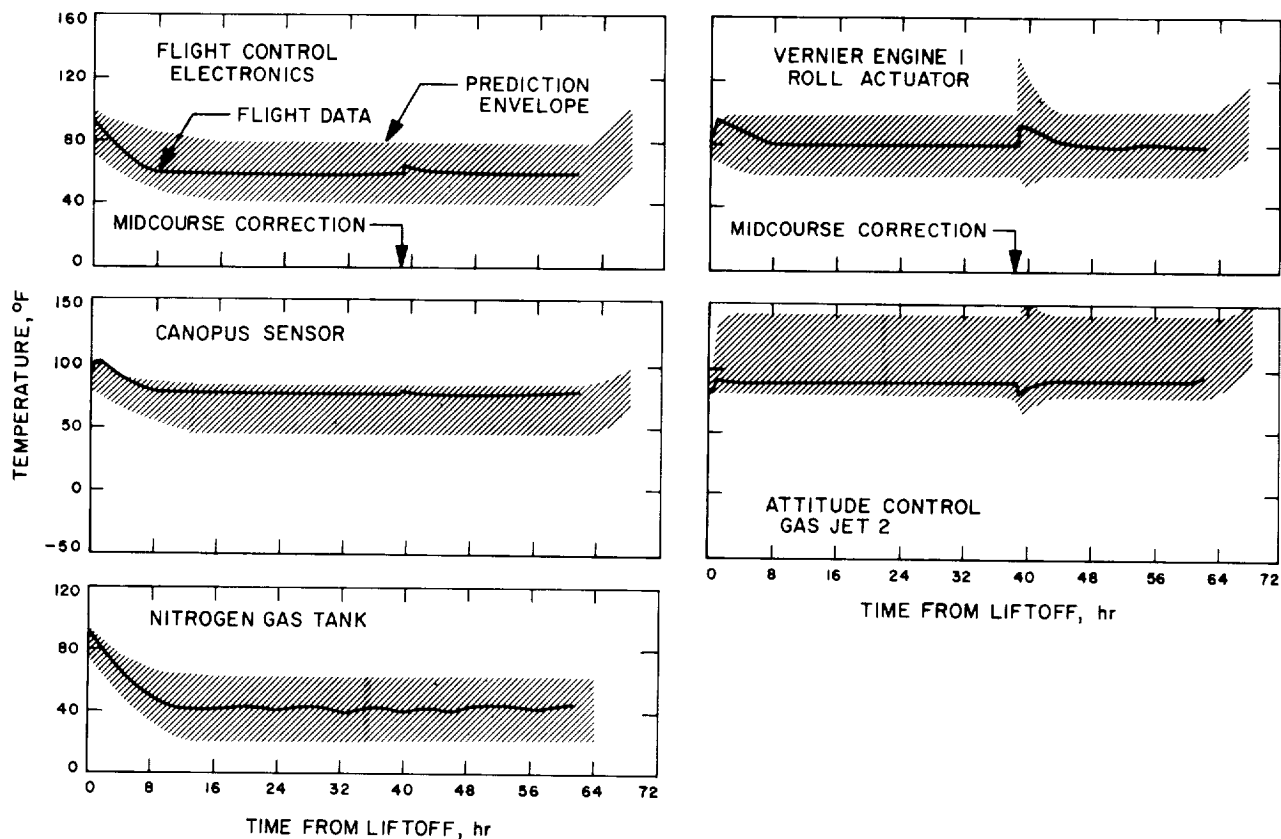


Fig. D-6. Flight control temperatures

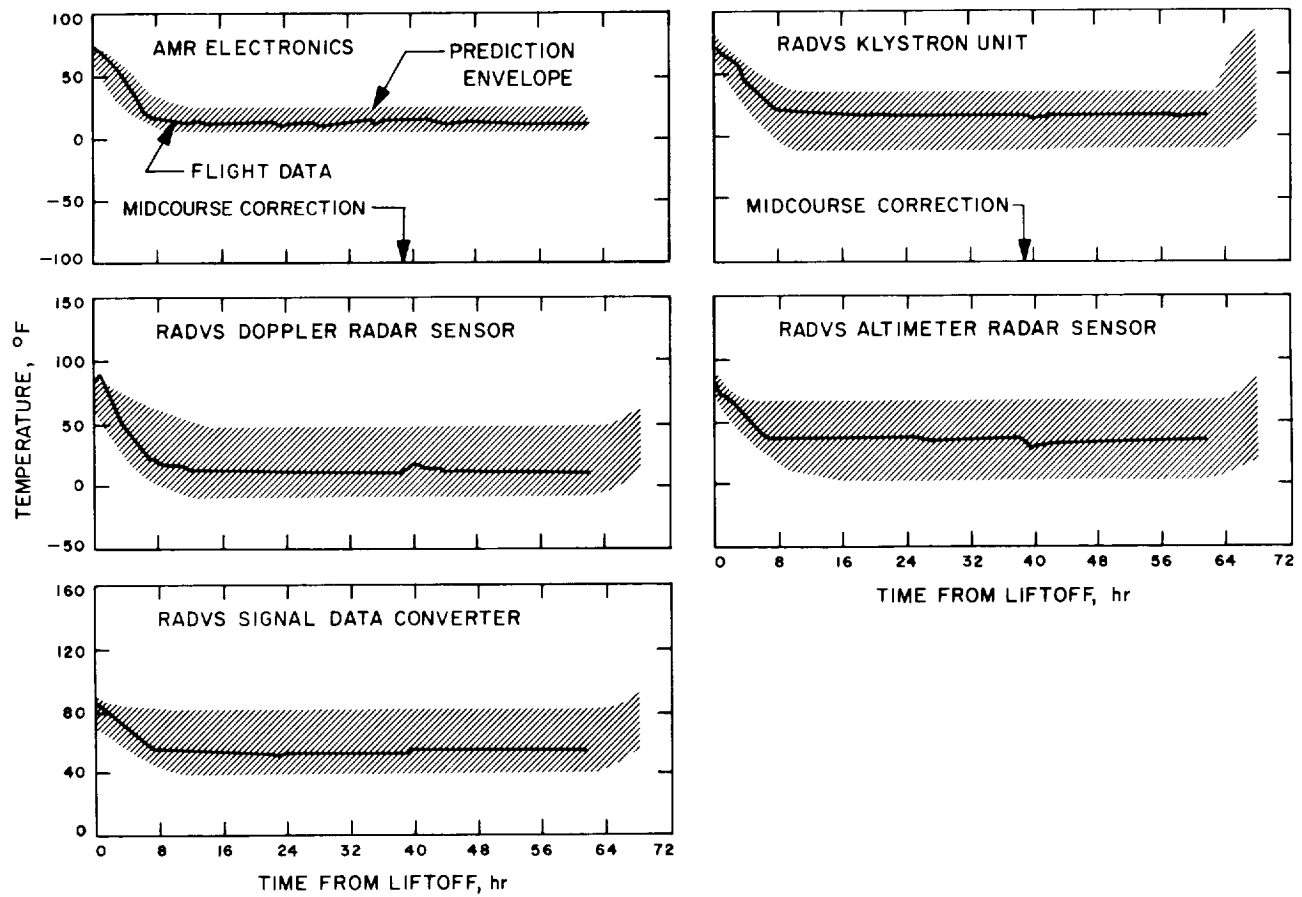


Fig. D-7. Radar temperatures

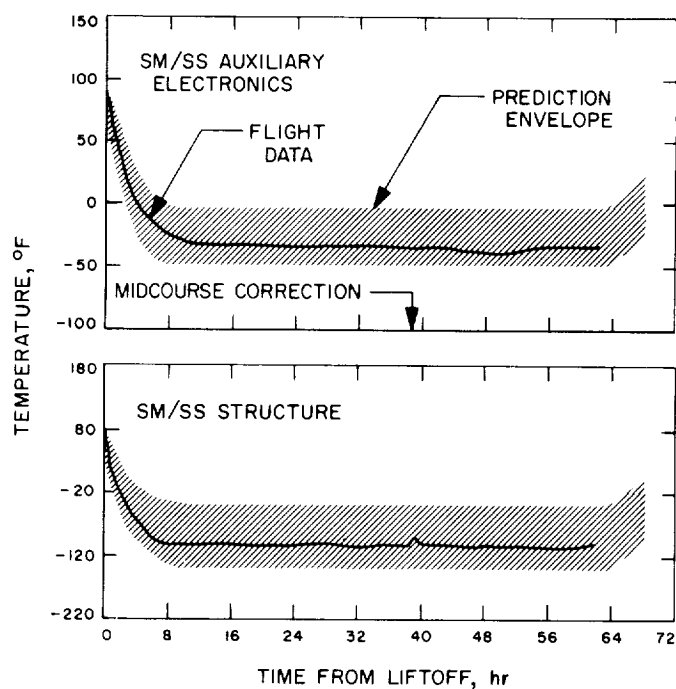


Fig. D-8. SM/SS temperatures

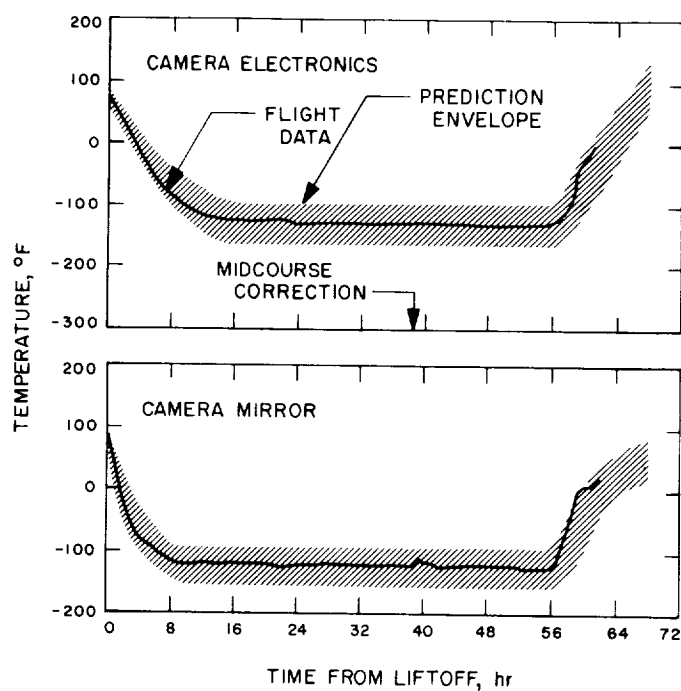


Fig. D-9. Television temperatures

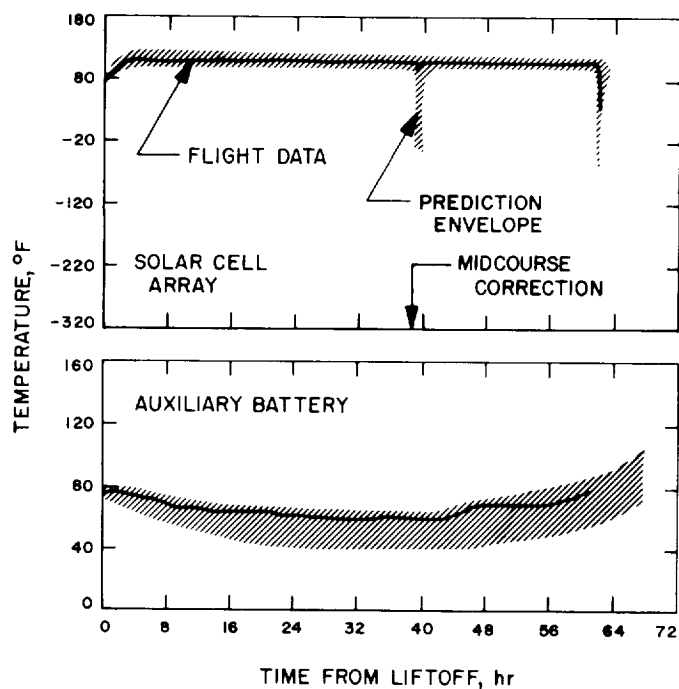


Fig. D-10. Miscellaneous temperatures

Glossary

ABC	auxiliary battery control	FRT	fine resolution tracking
AC	<i>Atlas/Centaur</i>	GCF	Ground Communications Facility
A/D	analog-to-digital	GSE	ground support equipment
ADC	analog-to-digital converter	GSFC	Goddard Space Flight Center
AESP	auxiliary engineering signal processor	HSDL	high-speed data line
AFC	automatic frequency control	ICS	Intracommunications System
AFETR	Air Force Eastern Test Range	IF	intermediate frequency
AGE	aerospace ground equipment	I/O	input/output
AOS	acquisition of signal	IRV	interrange vector
APC	automatic phase control	J-FACT	Joint Flight Acceptance Composite Test
A/SPP	antenna and solar panel positioner	KPSM	klystron power supply modulator
BCD	binary coded digital	KSC	Kennedy Space Center
BECO	booster engine cutoff	LOS	loss of signal
BR	boost regulator	MAG	Maneuver Analysis Group
CCC	Central Computing Complex	MCDR	media conversion data recovery (subsystem)
CDC	command and data (handling) console	MCFR	media conversion film recorder (subsystem)
CDS	computer data system	MECO	main engine cutoff
CP	Command Preparation (Group)	MES	main engine start
CRT	Composite Readiness Test	MSFN	Manned Space Flight Network
CSP	central signal processor	NASCOM	NASA World-Wide Communication Network
CSTS	Combined Systems Test Stand		
DC	direct command	OCR	optimum charge regulator
DOD	Department of Defense	ODG	Orbit Determination Group
DPS	Data Processing System	ORT	Operational Readiness Test
DSCC	Deep Space Communications Complex	OSDP	on-site data processing
DSIF	Deep Space Instrumentation Facility	OSDR	on-site data recovery (subsystem)
DSS	Deep Space Station	OSFR	on-site film recorder (subsystem)
DVS	doppler velocity sensor	OTC	overload trip circuit
ECPO	Engineering Computer Program Operations (Group)	OVCS	operational voice communication system
EM	electromagnetic	PA	Performance Analysis (Group)
EMA	engineering mechanism auxiliary	PCM	pulse code modulation
ESF	Explosive Safe Facility	PLIM	postlaunch instrumentation message
ESP	engineering signal processor	PU	propellant utilization
FC	flight control	PUVEP	propellant utilization valve electronics package
FCSCG	Flight Control Sensor Group	PVT	Performance Verification Tests
FPAC	Flight Path Analysis and Command	QC	quantitative command
FRB	Failure Review Board		

Glossary (contd)

RA	radar altimeter	SSAC	Space Science Analysis and Command
RADVS	radar altimeter doppler velocity sensor	SSD	subsystem decoder
RETMA	Radio Electronics Television Manufacturing Association	SSE	Standard Sequence of Events
RFI	radio frequency interference	STEA	system test equipment assembly
RIS	range instrumentation ship	STV	solar-thermal-vacuum
RODVS	reliable operate doppler velocity sensor	TCP	telemetry and command processor
RORA	reliable operate radar altimeter	TDA	Tracking Data Analysis (Group)
RTCS	Real Time Computer System, Cape Kennedy	TDS	Tracking and Data System
SDC	signal data converter	T&DA	tracking and data acquisition
SECO	sustainer engine cutoff	TelPAC	Television Performance Analysis and Command (Group)
SFOD	Space Flight Operations Director	TPS	Telemetry Processing Station
SFOF	Space Flight Operations Facility	TSAC	Television Science Analysis and Command (Group)
SOCP	<i>Surveyor</i> on-site computer program	TTY	teletype
SOPM	standard orbital parameter message	TV-GDHS	TV Ground Data Handling System
SOV	solenoid-operated valves	VCXO	voltage controlled crystal oscillator
SRT	System Readiness Test	VECO	vernier engine cutoff
SCAT	Spacecraft Analysis Team	VPS	vernier propulsion system
SPAC	Spacecraft Performance Analysis and Command (Group)		

Bibliography

Project and Mission

Surveyor A-G Project Development Plan, Project Document 13, Vol. 1, Jet Propulsion Laboratory, Pasadena, January 3, 1966.

Clarke, V. C., Jr., *Surveyor Project Objectives and Flight Objectives for Missions A through D*, Project Document 34, Jet Propulsion Laboratory, Pasadena, March 15, 1965.

Travers, E. S., *Surveyor D Mission Plan*, Project Document 129 (602-5), Jet Propulsion Laboratory, Pasadena, June 5, 1967.

Surveyor I Mission Report. Part I. Mission Description and Performance, Technical Report 32-1023, Jet Propulsion Laboratory, Pasadena, August 31, 1966.

Surveyor II Mission Report. Mission Description and Performance, Technical Report 32-1086, Jet Propulsion Laboratory, Pasadena, April 1, 1967.

Surveyor III Mission Report. Part I. Mission Description and Performance, Technical Report 32-1177, Jet Propulsion Laboratory, Pasadena, September 1, 1967.

Bibliography (contd)

Launch Operations

- Macomber, H. L., *Surveyor Launch Constraints Document*, Project Document 43, Rev. 1, Jet Propulsion Laboratory, Pasadena, March 6, 1967.
- Travers, E. S., *Surveyor Launch Constraints, Mission D—July 1967 Launch Opportunity*, Project Document 43, Rev. 1, Addendum No. 4, Jet Propulsion Laboratory, Pasadena, June 26, 1967.
- Centaur Unified Test Plan, AC-11/SC-4 Launch Operations and Flight Plan (Surveyor Mission D)*, Section 8.11B, Report AY62-0047, Rev. B, General Dynamics/Convair, San Diego, June 21, 1967.
- Test Procedure Centaur/Surveyor Launch Countdown Operations*, AC-11/SC-4 Launch (CTP-INT-0004M), Report AA63-0500-004-03M, General Dynamics/Convair, San Diego, June 30, 1967.
- Atlas/Centaur-11 Surveyor-D, Operations Summary*, TR-550, Centaur Operations Branch, KSC/ULO, Cape Kennedy, July 7, 1967.
- Barnum, P. W., *JPL/ETR Field Station Launch Operations Plan, Surveyor Mission D*, JPL/ETR Field Station Document 690-1, Jet Propulsion Laboratory, ETR Field Station, Cape Kennedy, July 5, 1967.
- Atlas/Centaur-11 Surveyor-D, Flash Flight Report*, Report TR-558, Centaur Operations Branch, KSC/ULO, Cape Kennedy, July 19, 1967.
- Travers, E. S., *Surveyor IV Launch Phase Mission Analysis Report*, Section Technical Memorandum 312-842, Jet Propulsion Laboratory, Pasadena, August 24, 1967.

Launch Vehicle System

- Galleher, V. R., and Shaffer, J., Jr., *Surveyor Spacecraft/Launch Vehicle Interface Requirements*, Project Document 1, Rev. 2, Jet Propulsion Laboratory, Pasadena, December 14, 1965.
- Atlas Space Launch Vehicle Systems Summary*, Report GDC-BGJ67-001, General Dynamics/Convair, San Diego, February, 1967.
- Centaur Systems Summary*, Report GDC-BGJ67-003, General Dynamics/Convair, San Diego, April 1967.
- Centaur Technical Handbook*, Convair Division, Report GD/C-BPM64-001-1, Rev. B, General Dynamics/Convair, San Diego, January 24, 1966.
- Centaur Monthly Configuration, Performance and Weight Status Report*, Report GDC63-0495-48, General Dynamics/Convair, San Diego, June 21, 1967.
- Preliminary AC-11 Atlas-Centaur Flight Evaluation* (by staff of Lewis Research Center, Cleveland, Ohio), NASA Technical Memorandum X-52339, NASA, Washington, D.C., 1967.
- Atlas/Centaur AC-11 Flight Evaluation Report*, GDC-BNZ67-055, General Dynamics/Convair, San Diego, October 6, 1967.

Bibliography (contd)

Spacecraft System

Surveyor Spacecraft A-21 Functional Description, Document 239524 (HAC Pub. 70-93401), 3 Vols., Hughes Aircraft Co., El Segundo, Calif., November 1, 1964 (with revision sheets).

Surveyor Spacecraft A-21 Model Description, Document 224847B, Hughes Aircraft Co., El Segundo, Calif., March 1, 1965 (with revision sheets).

Surveyor Spacecraft Monthly Performance Assessment Report, SSD68252-9, Hughes Aircraft Co., El Segundo, Calif., April 21, 1967.

Surveyor IV Mission—Preliminary Post Flight Data Analysis, Hughes Aircraft Co., El Segundo, Calif., August 1, 1967.

Surveyor IV Flight Performance Final Report, SSD 68189-4, Hughes Aircraft Co., El Segundo, Calif., September 1967.

Tracking and Data Acquisition

Program Requirements No. 3400, Surveyor, Revision 14, Air Force Eastern Test Range, Patrick Air Force Base, Fla., April 25, 1967.

Operations Requirement No. 3401, Surveyor Launch, Air Force Eastern Test Range, Patrick Air Force Base, Fla., May 11, 1967.

Operations Directive No. 3401, Surveyor Launch, Direct Ascent, Air Force Eastern Test Range, Patrick Air Force Base, Fla., March 13, 1967.

Project Surveyor—Support Instrumentation Requirements Document, Rev. 3, prepared by JPL for NASA, March 24, 1967.

Surveyor Project/Deep Space Network Interface Agreement, Engineering Planning Document 260, Rev. 2, Jet Propulsion Laboratory, Pasadena, November 22, 1965.

DSIF Tracking Instruction Manual (TIM), Surveyor Mission B (4 volumes), Engineering Planning Document 391, Jet Propulsion Laboratory, Pasadena, August 1966 (with revision sheets for Mission D).

Barnum, P. W., and Elliott, C. F., *Preflight Readiness Review of Tracking and Data System, Near Earth Phase, for Surveyor Mission D*, JPL/ETR Field Station Document 690-2, Jet Propulsion Laboratory ETR Field Station, Cape Kennedy, July 7, 1967.

Barnum, P. W., and Elliott, C. F., *Post-Flight Review of Tracking and Data System, Near-Earth Phase, for Surveyor D*, JPL/ETR Field Station Document 690-12, Jet Propulsion Laboratory ETR Field Station, Cape Kennedy, September 1, 1967.

Bibliography (contd)

Mission Operations System

- Surveyor Mission Operations System*, Technical Memorandum 33-264, Jet Propulsion Laboratory, Pasadena, April 4, 1966.
- Space Flight Operations Plan—Surveyor Mission D*, Engineering Planning Document 180-S/MD, Jet Propulsion Laboratory, Pasadena, November 5, 1966 (and revision sheets through June 26, 1967).
- Goble, M. E., *Surveyor Lunar Operations Plan—Mission D*, Engineering Planning Document 486-MD (Project Document 602-1), Revision 1, Jet Propulsion Laboratory, Pasadena, July 1, 1967.
- Surveyor Mission D Space Flight Operations Report*, Report SSD 74109, Hughes Aircraft Company, El Segundo, Calif., August 1967.
- Callan, R., *Surveyor Mission Operations System Space Flight Operations Memorandum—Surveyor IV*, Project Document 602-24, Jet Propulsion Laboratory, Pasadena, September 1, 1967.

Flight Path

- Davids, L., Meredith, C., and Ribarich, J., *Midcourse and Terminal Guidance Operations Programs*, SSD 4051R, Hughes Aircraft Co., El Segundo, Calif., April 1964.
- Cheng, R. K., Meredith, C. M., and Conrad, D. A., *Design Considerations for Surveyor Guidance*, IDC 2253.2/473, Hughes Aircraft Co., El Segundo, Calif., October 15, 1965.
- Surveyor Spacecraft/Launch Vehicle Guidance and Trajectory Interface Schedule*, Project Document 14, Rev. 3, Jet Propulsion Laboratory, Pasadena, November 30, 1966 (and revision sheet of December 7, 1966).
- Surveyor/Centaur Target Criteria—Surveyor Mission D*, Specification LS501480, Revision B, Jet Propulsion Laboratory, Pasadena, May 8, 1967.
- Fisher, J. N., and Gillett, R. W., *Surveyor Direct Ascent Trajectory Characteristics*, SSD 56028R, Hughes Aircraft Co., El Segundo, Calif., December 1965.
- Surveyor Station View Periods and Direct Ascent Trajectory Coordinates—Launch Dates August, September, October, November 1967*, SSD 68266R, and supplement for July 1967 launch dates, SSD 78015R, Hughes Aircraft Co., El Segundo, Calif., February 1967.
- O'Connel, H. P., *Pre-Injection Trajectory Characteristics Report—AC-11*, GDC-BKM67-023, General Dynamics/Convair, San Diego, May 1967.
- Dunn, H. S., *Surveyor Mission D Post-Injection Standard Trajectories*, SSD 68169-3 and Appendix A (SSD 78071), Hughes Aircraft Co., El Segundo, Calif., June 1967.
- Gans, J. F., *Surveyor Mission D Final Preflight Maneuver Analysis Report*, SSD 68230-2 and Appendix A (SSD 78070), Hughes Aircraft Co., El Segundo, Calif., May 1967.

Bibliography (contd)

Flight Path (contd)

Seiley, R. E., Nelsen, H. D., and Winkler, M. K., *Final Guidance Equations and Performance Analysis for AC-11*, GDC-BKM67-036, General Dynamics/Convair, San Diego, May 26, 1967.

Flight Path and Mission Requirements—Surveyor Mission D, Specification LS503672, Revision A, Jet Propulsion Laboratory, Pasadena, May 23, 1967.

Firing Tables—AC-11, July Opportunity, GDC-BKM67-031, and Appendix A, General Dynamics/Convair, San Diego, June 15, 1967.

Surveyor IV Flight Path Analysis and Command Operational Report, SSD 74108, Hughes Aircraft Co., El Segundo, Calif., August 10, 1967.